COMPUTATIONAL STUDIES ON OLEFIN METATHESIS REACTIONS

Ph.D. THESIS

by

JAY SINGH MEENA

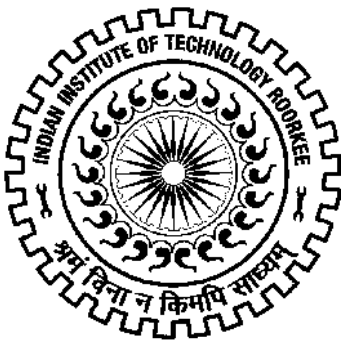

DEPARTMENT OF CHEMISTRY
INDIAN INSTITUTE OF TECHNOLOGY ROORKEE
ROORKEE-247 667 (INDIA)
APRIL, 2014

COMPUTATIONAL STUDIES ON OLEFIN METATHESIS REACTIONS

A THESIS

Submitted in partial fulfilment of the requirements for the award of the degree of

DOCTOR OF PHILOSOPHY

in

CHEMISTRY

by

JAY SINGH MEENA

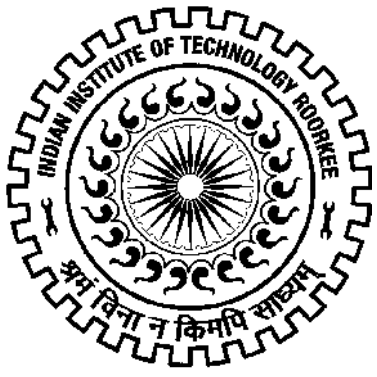

DEPARTMENT OF CHEMISTRY
INDIAN INSTITUTE OF TECHNOLOGY ROORKEE
ROORKEE-247 667 (INDIA)
APRIL, 2014

INDIAN INSTITUTE OF TECHNOLOGY ROORKEE
ROORKEE

CANDIDATE'S DECLARATION

I hereby certify that the work which is being presented in the thesis entitled **"COMPUTATIONAL STUDIES ON OLEFIN METATHESIS REACTIONS"** in partial fulfilment of the requirements for the award of the Degree of **Doctor of Philosophy** and submitted in the **Department of Chemistry** of the Indian Institute of Technology Roorkee, Roorkee is an authentic record of my own work carried out during a period from **July, 2009 to April, 2014** under the supervision of **Dr. P. P. Thankachan,** Associate Professor, Department of Chemistry, Indian Institute of Technology Roorkee, Roorkee.

The matter presented in this thesis has not been submitted by me for the award of any other degree of this or any other Institute.

(JAY SINGH MEENA)

This is to certify that the above statement made by the candidate is correct to the best of my knowledge.

(P. P. Thankachan)
(Supervisor)

Dated: _____

The Ph.D. Viva-Voce Examination of **Mr. JAY SINGH MEENA**, Research Scholar, has been held on.....

Signature of Supervisor **Chairman, SRC** **Signature of External Examiner**

Head of the Department/Chairman, ODC

CONTENTS

ABSTRACT

Olefin metathesis is a unique carbon skeleton redistribution in which unsaturated carbon-carbon bonds are rearranged in the presence of metal carbene complexes. With the advent of efficient catalysts, this reaction has emerged as a powerful tool for the formation of C-C bonds. The number of applications of this reaction has dramatically increased in the past few years. The broad applicability of olefin metathesis has attracted attention from both academic and industrial scientists.

In the last several years, computational studies on olefin metathesis reactions have proliferated. Treatment of the reactions with quantum chemical methods involves calculation of geometries and energetics of reactants, intermediates, transition states, and products.

In the present work we investigate computationally some olefin metathesis reactions catalyzed by tungsten (W), molybdenum (Mo) and ruthenium (Ru) alkylidene. The mechanistic studies of tungsten catalyzed ring opening metathesis (ROM) and molybdenum catalyzed ring opening metathesis polymerization (ROMP) are carried out using the highly strained 3,3-dimethyl cyclopropene (DMCP) moiety. The stereochemistry of ring opening of asymmetric 3-methyl-3-phenylcyclopropene (MPCP) is also studied and the effect of substituents on ROM is explored. The ruthenium catalyzed ring opening-cross metathesis (ROCM) is investigated using trisubstituted cyclopentene and methyl vinyl ketone as model compounds. All calculations have been performed using the Gaussian 09W suite of programs.

The thesis has been divided into six chapters:

The first chapter presents a general introduction to olefin metathesis reactions and a review of the relevant literature. Emphasis is placed on the different types of metathesis in olefins and metathesis reaction mechanism. Acyclic diene metathesis (ADMET), cross metathesis (CM), ring opening metathesis (ROM), ring closing metathesis (RCM) and ring opening metathesis polymerization (ROMP) are discussed along with the mechanisms. The Schrock and Grubbs catalysts used in olefin metathesis are also described. A critical review of the available literature on computational studies of olefin metathesis reactions is presented and comparisons with relevant experiments are also made wherever possible.

The second chapter outlines the computational methods used. A brief introduction to ab initio SCF and Density Functional methods and of the location and characterization of stationary points on the potential energy surface is presented.

The third chapter deals with the computational studies of the ring opening metathesis of 3,3-dimethyl cyclopropene using tungsten model catalyst $W(NH)(CH_2)(OCH_3)_2$. Two different faces of the catalyst namely COO face and CNO face have been investigated for their involvement in the cycloaddition step of ROM of the DMCP. syn and anti orientations of cyclopropene are also explored for the reaction. Optimization of the geometry of all species has been done at DFT/B3LYP level using LANL2DZ basis set. The critical geometrical parameters are also reported. Relative energies of the stationary species are presented. Frequency analyses were also performed to confirm that the structures obtained were true minima on the PES or saddle points as the case may be. IRC calculations are done from each transition state, to verify the structure moving towards the reactant and product sides.

The fourth chapter incorporates computational studies on the molybdenum model catalyst $Mo(NH)(CH_2)(OCH_3)_2$ mediated ring opening metathesis polymerization reaction of 3,3-dimethylcyclopropene. The COO and CNO faces of molybdenum catalyst as well as syn and anti orientations of cyclopropene are discussed for ROMP reaction. The geometries of the stationary structures are obtained at the DFT/B3LYP level using LANL2DZ basis set in each case and the nature of each stationary point was probed by frequency calculations. IRC calculations have also been performed.

The fifth chapter of the thesis presents the investigation of the stereochemistry of the ring opening metathesis of asymmetric 3-methyle-3-phenylcyclopropene (MPCP). DFT/B3LYP calculations have been performed with LANL2DZ basis sets. The calculations revealed ring opening of MPCP with parallel and perpendicular conformers. Effect of substituents on ring opening metathesis of cyclopropene is also explored by substituting the phenyl group of MPCP with NH_2, OH, CN and CF_3 groups. The viability of reaction has been verified using energy barriers calculated for the reaction path.

The sixth chapter presents the computational modeling of the whole catalytic cycle of ruthenium catalyzed tandem ring opening cross metathesis reaction to obtain end-differentiated product. The dissociative mechanism was explored in a detailed study of the ROCM of trisubstituted cyclopentene with methyl vinyl ketone. Distal and proximal orientations of trisubstituted cyclopropene are discussed for the first catalytic cycle (ROM). In subsequent catalytic cycle (Cross metathesis) of ROCM, cis and trans orientations of methyl vinyl ketone are studied and the catalytic cycle is investigated using cis orientation to obtain end-differentiated olefin through tandem ROCM. All calculations are performed

using B3LYP and M06-L functional. Ruthenium atom is treated with LANL2DZ basis set and 6-31G(d) basis set applied for all other atoms. Stationary points located on potential energy surface were characterized by frequency calculations as minima or transition state.

ACKNOWLEDGEMENTS

*Foremost, my greatest regards to the almighty **GOD** for bestowing upon me the courage to face the complexities of life and complete this thesis successfully.*

*I would like to record my gratitude to my supervisor **Dr. P. P. Thankachan** for his supervision, advice and guidance throughout this research. He provided me unflinching encouragement and support in various ways. He is a constant oasis of ideas and full of knowledge. His guidance helped me in all the time of research and writing of this thesis. I could not have imagined having a better advisor and mentor for my Ph.D. study.*

*I wish to express my warm and sincere thanks to the present Head, **Prof. Anil Kumar**, and the former Head, **Prof. Kamaluddin** and **Prof V. K. Gupta,** Department of Chemistry, IIT Roorkee, Roorkee, for providing the basic infrastructural facilities for carrying out the research work.*

*I am thankful to the **Ministry of Human Resource and Development** (**MHRD**), Government of India for providing Junior Research Fellowship (JRF) and Senior Research Fellowship (SRF) during the period of research.*

I am thankful to all the non-teaching staff of the Department of Chemistry for their help and support.

For writing this thesis I have consulted several books and journals. I would like to express my sincere thanks to the Departmental Library and the Central Library staff for providing one of the most state-of-art library facilities in India.

*I wish to thank my respected seniors **Dr. Vibha Kumar, Dr. Neeraj Naithani, Dr. Hitendra**, **Dr. Vipin Bansal and Dr**. **Neeraj Uppadhyay**. They were always with me for mental support.*

*I wish to thank everybody with whom I have shared experiences in life. Specially those who played a significant role in my life, and those which with the gift of their company made my days more enjoyable and worth living. This work would not have been possible without the support and encouragement of my seniors and friends **Dr. Neeraj Upadhyaya, Dr. Rajeev, Dr. Sushil Vashisth, Dr. Sujata, Dr. Rajesh, Dr. Uma Shankar, Dr. Brij Bhushan, Dr. Arunima Nayak, Dr. Anand Kumar Haldua, Dr. Sheshi Reddi, Dr. Dhirendra Kumar, Dr. Arvind Bharti, Dr. Varun Rawat, Kamal Prakash, Varun Kundi, Sapna Bondwal**, **Shrinivas Rao Atchuta, Mainak Roy, Manish Yadav, Seema Singh, Shriom, Himanshu Gupta, Vinod Vashisth, Nishant Gautam.** A would like to extend my special thanks to **Nisha Jarwal and Er. Praveen Kumar Toni** for helping me with thesis corrections and helpful discussions.*

I am fortunate to have a circle of friends whose support and encouragement I shall cherish through life. I would like to warm thanks ***Dr. Satya Prakash Singh, Dr. Goverdhan, Dr. Vivek Acharya, Dr. Ajay Kushwaha, Abhishek Baheti, Vinod Sonkar, Prafull Bhati, Rajesh Fatrod.*** *Though some of them were not with me during the last phase of my thesis but they have always encouraged me and they are always remembered. Especially I would like to thanks* ***Hariom Nagar and his wife Rakeshi Devi*** *as well as* ***Rajiv Sachdeva and his wife Ruchika*** *for their selfless and unconditional cooperation and mental support they provide during the research work. I also express my deep gratitude to* ***Rinki Didi and Mr. Akhilesh Soni*** *for being there for me always and showing me the right path in life.*

My deepest gratitude goes to my family for their unflagging love and support throughout my life, this thesis is simply impossible without them. They have always supported and encouraged me to do my best in all matters of life. I am indebted to my ***father (Shri Joharee Lal Meena)*** *for his care and love. He provided the best possible environment for me to grow up and the best available education. He never complained in spite of all the hardships in his life. I cannot ask for more from my* ***mother (Smt. Rampati Meena****) as she is simply perfect. I have no suitable words that can fully describe her everlasting love to me. My brothers* ***Mr. Laxmi Chand, Mr.Vishamver, Mr. Amar Singh and Mr. Mahesh*** *have always been there for me to provide a joyful environment and helped to keep my strains off.*

I cannot end without thanking my loving ***Rashmi****, who came in my life in the year April, 2009 and on whose constant encouragement and love I have relied thought my time. She had never let down and has always been a constant source of inspiration, patience and moral encouragement to me.*

Finally I would like to thank everybody who contributed to the successful realization of this thesis, and wish express my apology for not mention by them all by name.

Roorkee

April, 2014 ***JAY SINGH MEENA***

LIST OF ABBREVIATIONS

AC	Active Catalyst
ACTS	anti Cycloaddition Transition State
ADMET	Acyclic Diene Metathesis
AMCP	3-Amino-3- Methylcyclopropene
AO	Atomic Orbital
APr	anti Product
AROP	anti Ring Opening Product
ARTS	anti Ring Opening Transition Structure
ASP	anti Square Pyramidal
ATBP	anti Trigonal Bipyramidal
B3LYP	Becke-style 3-Parameter Density Functional Theory (using the Lee-Yang-Parr correlation functional)
C	Complex
CASSCF	Complete Active Space Self-Consistent Field
CC	Coupled Cluster
CCSD	Coupled-Cluster Singles and Doubles
CCSD(T)	Coupled-Cluster Singles, Doubles and Triples
CGTO	Contracted Gaussian Type Orbitals
CI	Configuration Interaction
CM	Cross Metathesis
CMCP	3-Cynaide-3- Methylcyclopropene
COM	Center of Mass
CSF	Configuration State Function
DFT	Density Functional Theory
DMCP	3,3-Dimethyl cyclopropene
DSCP	Disubstituted Cyclopropene
DTS	Distal Transition State
DZ	Double Zeta
ECP	Effective Core Potential
EDP	End-Differentiated Product
E_e	Electronic Energy
EVE	Ethyl Vinyl Etheer

FORS	Full Optimized Reaction Space
G	Gibbs Free Energy
GTF	Gaussian Type Function
GTO	Gaussian Type Orbitals
H	Enthaly
HF	Hartree Fock
HMCP	3-Hydoxyl-3-Methylcyclopropene
IRC	Intrinsic Reaction Coordinate
LCAO	Linera Combination of Atomic Orbitals
MBPT	Many-Body Perturbation Theory
MCB	Metallacyclobutane Intermediate
MCSCF	Multi Configuration Self -Consistent Field Method
MINDO	Modified Intermediate Neglect of Differential Overlap
MNDO	Modified Neglect of Differential Overlap
MO	Molecular Orbital
MPCP	3-Methyl-3-Phenylcyclopropene
MPPT	Moller-Plesset Perturbation Theory
MTCP	3-Methyle-3-Trifluromethylcyclopropene
MVK	Methyl Vinyl Ketone
$NBDF_6$	2,3-bis(trifluoromethyl) Norbornadiene
NEDP	Non End-Differentiated Product
PES	Potential Energy Surface
Pr	Product
PRDDO	Partial Retention of Diatomic Differential Overlap
PTS	Propagation Transition State
PTS	Proximal Transition State
QCISD	Quadratic Configuration Interaction Single and Double
QCISD(T)	Quadratic Configuration Interaction Single, Double and Triples
RASSCF	Restricted Active Space Self-Consistent Field
RCM	Ring Closing Metathesis

RHF	Restricted Hartree -Fock
RMP2	Restricted Møller-Plesset Second Order
ROCM	Ring Opening –Cross Metathesis
ROHF	Restricted Open Shell Hartree -Fock
ROM	Ring Opening Metathesis
ROMP	Ring Opening Metathesis Polymerization
SCF	Self Consistent Field
SCTS	syn Cycloaddition Transition State
SHOP	Shell Higher Olefin Process
SP	Square Pyramidal
SPr	syn Product
SROP	syn Ring Opening Product
SRTS	syn Ring Opening Transition Structure
SSP	syn Square Pyramidal
STBP	syn Trigonal Bipyramidal
STF	Slater Type Functional
SV	Split Valence
TBP	Trigonal Bipyramidal
TCP	Trisubstituted Cyclopentene (1-Methyl Cyclopentene)
TS	Transition State
TZ	Triple Zeta
UHF	Unrestricted Hartree -Fock
ZDO	Zero Differential Overlap

LIST OF SCHEMES AND FIGURES

SCHEMES

FIGURES

LIST OF TABLES

RESEARCH PAPERS

1. Meena J S and Thankachan P P (**2013**) "Theoretical Studies of the Ring Opening Metathesis Reaction of 3,3-Dimethyl Cyclopropene with Molybdenum Catalyst" *Comp. Theor. Chem.* **1024**: 1-8.

2. Meena J S and Thankachan P P (**2014**) "Ring Opening of Monocyclic Dimethyl Cyclopropene via Metathesis by Tungsten Catalyst- A Computational Study" *J. Chem. Sci. (In Press).*

1 Introduction

1.1 OLEFIN METATHESIS

Metathesis is the exchange of parts of two substances. The metathesis reactions in olefins (alkenes) have become one of the most spectacular recent improvements in synthetic strategies for organic synthesis and polymer sciences [Anderson-Wile and Coates, 2012; Furstner, 2000; Grubbs, 2004; Grubbs and Chang, 1998; Haigh et al., 2004; Hoveyda and Zhugralin, 2007; Kotha and Dipak, 2012; Mol, 2004; Matsuda and Sato, 2013; Schrock, 2011]. Yves Chauvin, Robert H. Grubbs and Richard R. Schrock shared the 2005 Nobel prize in Chemistry for "the development of the metathesis methods in organic synthesis" [Advanced information, 2005].

Metathesis in olefins is a metal-catalyzed transformation, which acts on carbon-carbon double bonds (C = C) and rearranges them via cleavage and reassembly [Grubbs, 2003; Ivin and Mol, 1997; Trnka and Grubbs, 2001]. The reaction is catalyzed by transition metals such as titanium, tungsten, molybdenum, rhenium, osmium and ruthenium. The general nature of olefin metathesis is outlined in Scheme 1.1, wherein carbene (alkylidene) exchange between the two starting olefins has resulted in two new olefins.

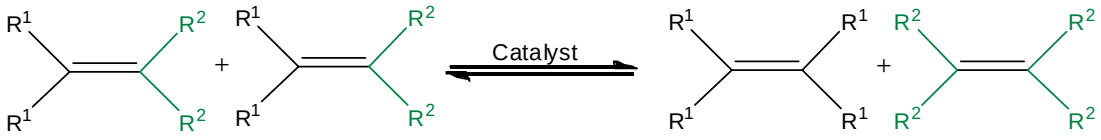

Scheme 1.1: General nature of olefin metathesis

The name metathesis was given to this reaction by Calderon (1967). In fact, the first observation of the metathesis of propene at high temperature was reported in 1931[Schneider and Frolich, 1931]. The first catalyzed metathesis reactions were found in the 1950's when industrial chemists at Du Pont, Standard oil and Phillips Petroleum (H. S. Eleuterio, E. F. peters, B. L. vering, R. L. Banks and G. C. Bailey) reported that propene on heating with molybdenum (in the form of the metal, oxide or $[Mo(CO)_6]$ on alumina) yielded ethylene and 2-butenes [Banks and Bailey, 1964]. The first notable description of the polymerization of norbornene by the system $WCl_6/AlEt_2Cl$ was independently reported in 1960 by Eleuterio (1991) and Truett *et al.* (1960). But it took years to be recognized that the ring-opening metathesis polymerization and the disproportionation of acyclic olefins were based on similar reactions. Olefin metathesis reaction was first used commercially in petroleum reformation for the synthesis of higher olefins from the products (α-olefins)

from the shell higher olefin process (SHOP) with nickel catalyst under high pressure and high temperatures [Keim et al., 1979].

Olefin metathesis is a unique carbon skeleton redistribution in which unsaturated carbon-carbon bonds are rearranged in the presence of a metal carbene complex [Grubbs, 2003; Ivin and Mol, 2001]. With the advent of efficient catalysts, this reaction has emerged as a powerful tool for the formation of carbon-carbon bonds in chemistry. Particularly significant is the fact that this reaction utilizes no additional reagent beyond a catalytic amount of metal carbene and in most cases releases only a volatile olefin as by product [Schuster and Blechert, 1997]. In the presence of certain transition-metal compounds, including various metal carbenes, olefins exchange groups around the double bonds, resulting in several outcomes such as straight swapping of groups between two acyclic olefins (cross metathesis-CM) [Chatterjee et al., 2002], closure of large rings (ring-closing metathesis-RCM) [Yoshida et al., 2006], formation of dienes from acyclic and cyclic olefins (ring-opening metathesis-ROM) [Peter and Tam, 2002], polymerization of cyclic olefins (ring-opening metathesis polymerization-ROMP) [Hejl et al., 2005] and polymerization of acyclic dienes (acyclic diene metathesis polymerization-ADMET) [Marsico et al., 2012]. Olefin metathesis is catalytic and is reversible. It is applicable to small molecules and there is a high level of chemo-, regio-, and stereo selectivity. Minimal substrate protection is required and it is applicable to diversity-oriented synthesis. Olefins which are used in commercial olefin metathesis are usually cheap and available in bulk quantities. Functional groups play an important role in olefin metathesis; they can promote the reaction by providing conformational bias *i.e.* bringing the “hands” together.

1.2 MECHANISM OF OLEFIN METATHESIS

The breakthrough in olefin metathesis chemistry came in 1971 with a publication by Yves Chauvin [Harrison and Chauvin, 1971]. Chauvin and his student Jean-Louis Herrison proposed that the catalyst was a metal carbene. The mechanism was further supported by the work of Katz et al [Ketz et al., 1976; Katz and Mcginnis 1975] later Schrock’s work published in 1980 [Schrock et al. 1980] clearly established the validity of the Chauvin mechanism, which remains the generally accepted mechanism today (Scheme 1.2).

In later literature metal carbene came to be termed metal alkylidene. Other metal carbenes had been discovered some years earlier by Ernst Otto Fischer (Noble prize in

Chemistry, 1973). Chauvin presented an entirely new mechanism to explain how the metal compound functions as a catalyst in the reaction. His experimental results tallied with this mechanism and could not be explained by any previously proposed mechanism.

The Chauvin mechanism (Scheme 1.2) involves the [2+2] cycloaddition of an olefin to a metal carbene catalytic species (or more precisely transition metal-alkylidene) leading to the reversible formation of a metallocyclobutane intermediate. This intermediate then undergoes cycloreversion via either of the two possible paths: (1) non-productive- resulting in the re-formation of the initial olefins or (2) product-forming -yielding a new olefin that has exchanged a carbene carbon from the metal catalyst and a new metal alkylidene that contains one carbon of the two carbenes of the initial olefin. This new metal alkylidene re-enters into a new catalytic cycle of the same type as the first one (initiation). The new metal alkylidene reacts with a new olefin molecule to yield another metallacyclobutane intermediate. On decomposition in the forward direction this intermediate yields the product internal olefin and metal carbene. This metal alkylidene is now ready to enter another catalytic cycle. Thus each step in the catalytic cycle involves exchange of alkylidenes-metathesis.

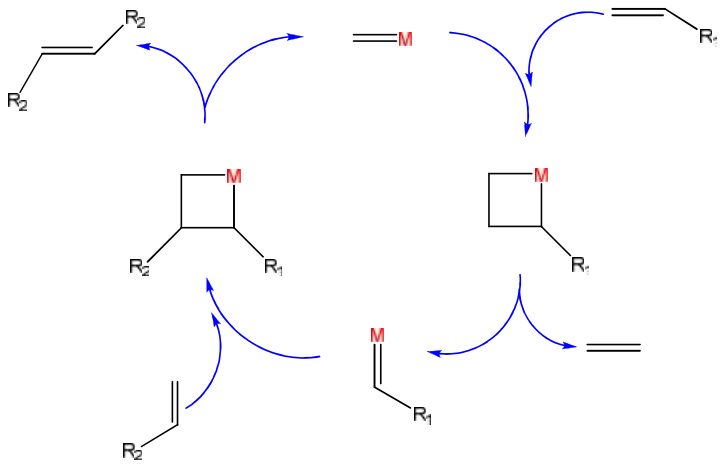

Scheme 1.2: Chauvin Mechanism for Olefin Metathesis

The new catalytic cycle, depending on the orientation of the coordinated olefin, can give two different metallocyclobutanes, one leading to the symmetrical olefin and the other one leading the initial olefin. This latter cycle is said to be degenerate olefin metathesis (Scheme 1.3). Hence, the catalytic cycles alternatively involve both metal-alkylidene

species resulting from the combination of the metal with each of the two carbenes from the initial olefin.

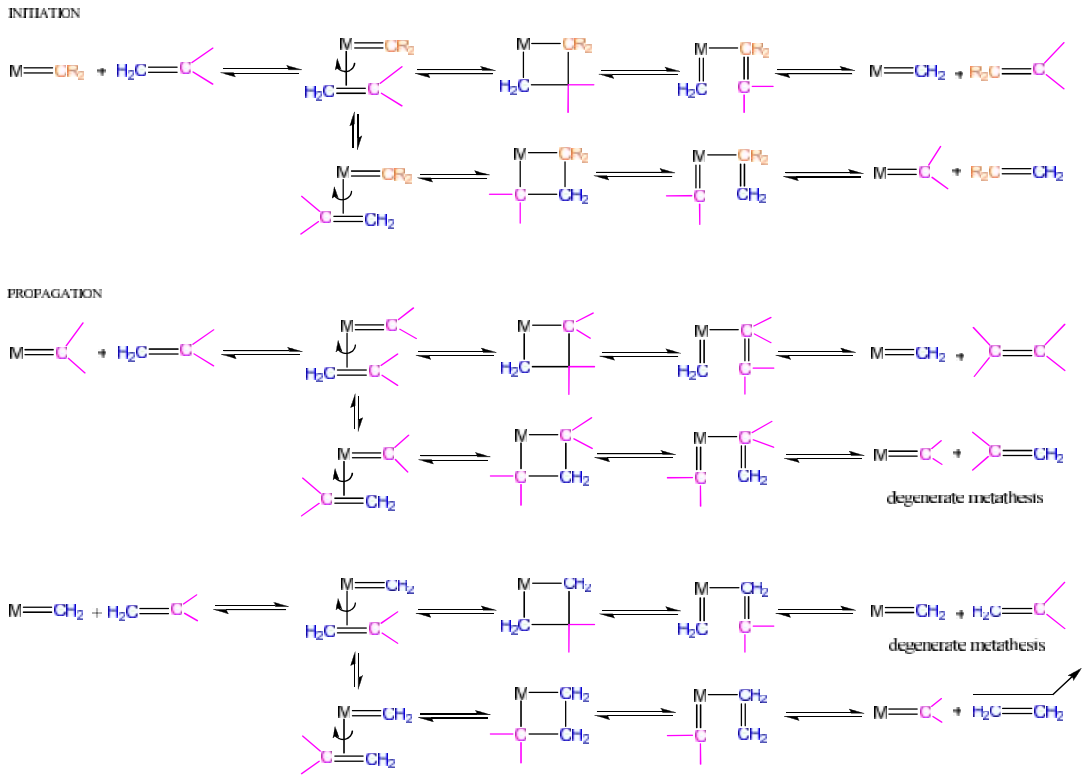

Scheme 1.3. Degenerate metathesis of propagation step

Interaction with the d-orbital on the transition metal alkylidene catalyst lowers the activation energy adequately for the reaction to proceed rapidly at modest temperatures. Since all of these processes are fully reversible only statistical mixtures of initial materials (olefins) as well as all of possible rearrangement products are produced in the absence of thermodynamic driving forces.

Chauvin's Metallocyclobutane

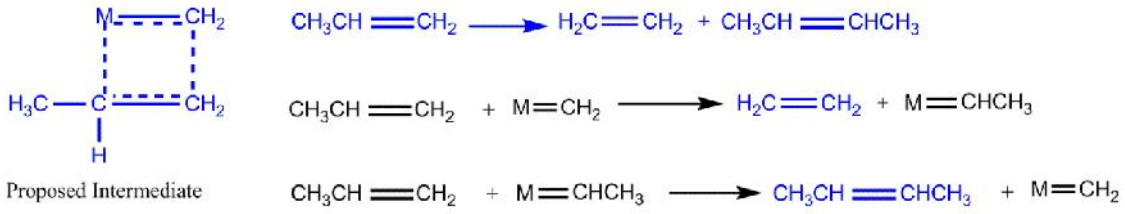

N. Calderon, E.A. ofstead, J.P. Ward, W. A. Judy, K. W. Schott. J. Am. Chem. Soc. 1968, 90,4133

Fortunately for the organic and polymer chemistry communities, thermodynamic equilibrium of the olefin metathesis reaction can be easily influenced. There are two most important approaches that are generally employed to drive the reaction towards the desired products. One tactic is to rely on Le Chatelier's principle by continuously removing one of the products from the reaction system in order to shift the equilibrium in favor of the other product. This method is particularly successful in the case of cross metathesis (CM) [Connon and Blechert, 2003] involving terminal olefins, ring-closing metathesis (RCM) [Deiters and Martin, 2004; Mcreynolds et al., 2004] and acyclic diene metathesis polymerization (ADMET) [Baughman and Wagener, 2005; Lehman and Wagener, 2002]. The other approach capitalizes on the ring strain of cyclic olefins such as norbornenes and cyclooctenes. The energy released during the ring opening of these cyclic compounds is sufficient to drive forward reactions such as ring opening-cross metathesis (ROCM) [Mayo and Tam 2002; Morgan et al. 2002] and ring-opening metathesis polymerization (ROMP) [Frenzel and Nuyken, 2002; Schrock, 1990]. In addition, in some instances, substrate concentration (which often distinguishes ADMET from RCM) or the sensitivity of the catalysts to olefin substitution can also be taken advantage of to influence product selectivity. All of these methods are currently productively employed in the synthesis of a large variety of small, medium, and polymeric molecules, as well as novel materials [Gorodetskaya et al., 2007; Guidry et al., 2007; Matson and Grubbs 2008].

1.3 TYPES OF OLEFIN METATHESIS

Different fundamental types of olefin metathesis reactions are shown in Scheme 1.4. Two types of olefin metathesis acyclic diene metathesis (ADMET) and ring opening metathesis polymerization (ROMP) have tended to polymerize the olefins, but each of which requires a different set of conditions for successful polymerization.

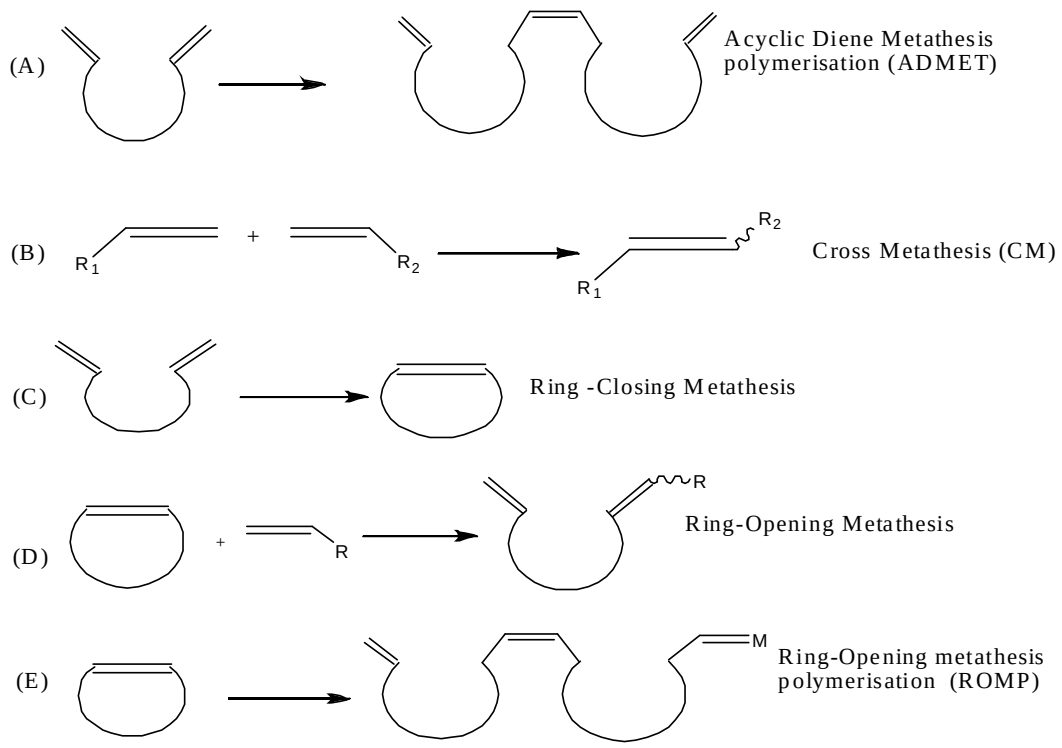

Scheme 1.4: Different types of metathesis

1.3.1 ACYCLIC DIENE METATHESIS (ADMET)

Acyclic diene metathesis polymerization is a special type of olefin metathesis pioneered by Wagener [Wagener and Patton, 1993; Patton et al., 1991; Wageneret al., 1991] using alpha-omega dienes (terminal dienes) to produce macromolecules by polymerization. It is considered to be a step-growth [O'Gara et al., 1993] polycondensation-type polymerization which produces strictly linear chains from acyclic diolefins. This type of metathesis reaction requires very high monomer conversion rates to produce polymer chains of considerable size. The reaction is driven by the removal of ethylene (volatile product) from the system. The new double bonds formed can be in cis or trans configuration.

Acyclic diene metathesis Polymerization

1.3.2 CROSS METATHESIS (CM)

This reaction is very versatile in its use and the scrambling of the mutual alkylidene fragments between two alkenes is promoted by the metal carbene complexes [Furstner, 2000; Trnka and Grubbs, 2001; Roy and Das, 2000]. The cross metathesis reaction has various problems as such as low product selectivity, the fact that mixtures of homodimers and copolymers can be formed, poor selectivity in the olefins produced and that there is no large driving force such as in ring opening metathesis polymerization and ring closing metathesis. But at present various examples exist in which two olefins with dissimilar reactivity give cross-coupled product with excellent yields and excellent selectivity [Benjamin et al., 2011; Mazoyer et al., 2012].

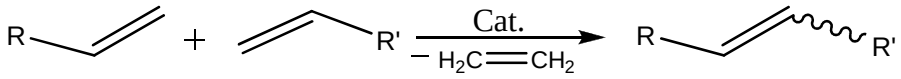

1.3.3 RING CLOSING METATHESIS (RCM)

RCM is basically an intramolecular olefin metathesis reaction. This metathesis reaction (RCM) allows synthesis of medium or large sized cyclic alkene from an α,ω-diolefin [Deiters and Martin, 2004; Armstrong , 1998; Fu and Grubbs, 1993], which can be achieved under ambient conditions in air using the first generation Grubbs alkylidene catalyst. It is the reverse of a ring opening metathesis reaction. The limitation in the use of ring closing metathesis is that it cannot be used to form highly-strained rings but it is entropically driven because a molecule is released. The driving force for this reaction is the removal of highly volatile ethylene from the reaction mixture and if the thermodynamics of the ring closure reaction is unfavorable, substrate can lead to polymerization of the substrate [Collins, 2006]. The efficiency of ring closing metathesis depends on the extent to which the competing acyclic diene metathesis polymerization can be suppressed [Xinyao et al., 2013]. However substrate concentration helps to reduce the occurrence of ADMET [Burt et al., 2010]. However, the success of ring-closing reaction of cyclic olefin via olefin metathesis is influenced to a large number of factors: (1) efficiency of the active metal catalyst, (2) size of the rings to be formed, (3) nature of the resulting rings and (4) functional groups/substituents present in the substrate [Ghosh et al., 2006; Deshmukh and Blechert, 2007].

The initiation of ring closing metathesis and its catalytic cycle is shown in Scheme1.5. The initiation step produces a metal alkylidene having terminal double bond at terminal which initiates the formation of metal carbene and this metal carbene continues the catalytic cycle of RCM.

Initiation:

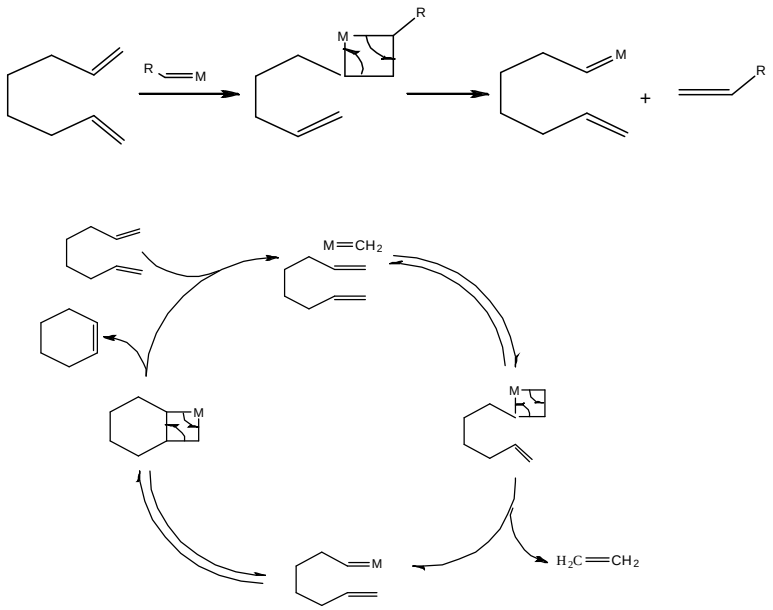

Scheme 1.5: Catalytic cycle of RCM

1.3.4 RING OPENING METATHESIS (ROM)

This type of reaction is typically useful for strained cyclic olefins and the driving force is the relief of strained rings i.e. it is thermodynamically favored in such systems [Mol, 2004; Ivin and Mol, 1997].In the absence of excess of a second reaction partner, polymerization (ROMP) occurs. The ROM reaction is similar to the ROMP reaction but the only difference is that in the ROM reactions, double bonds of the monomers are not preserved in the final product whereas; in ROMP reactions, the double bonds of the monomers are present both in the monomer and final polymer. Strained rings may be opened by a transition metal carbene catalyzed reaction as shown in Scheme 1.6.

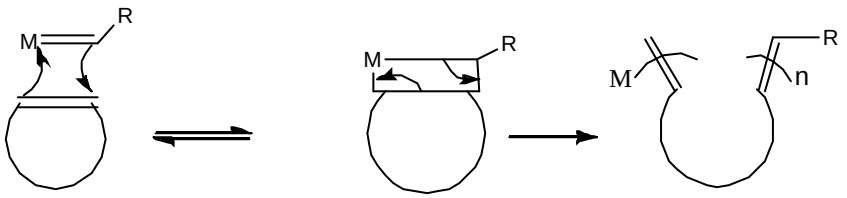

Scheme 1.6: ROM and ROMP

1.3.5 RING OPENING METATHESIS POLYMERIZATION (ROMP)

Ring opening metathesis polymerization is a chain-growth type polymerization process in which a mixture of cyclic alkenes is converted to a polymer. ROMP is thermodynamically favored in strained ring systems such as 3-, 4-,8- and larger membered compounds. In many cases, the ROMP of strained cyclic olefins initiated by metal carbene complexes shows the characteristic features of a living polymerization and therefore block copolymers can be made by sequential addition of different monomers [Bielawski and Grubbs, 2007; Frenzel et al., 2005; Sanford and Love, 2003]. When bridging groups are present, e.g. in bicyclic olefins, the Gibbs free energy of polymerization is typically more negative as a result of increased strain energy in the monomers. The ring opening metathesis polymerization mechanism involves an alkylidene catalyst and is identical to the olefin metathesis mechanism (Chauvin) with two important differences. First, as the reaction involves a cyclic-alkene substrate, "the new" alkene that is generated remains unattached to the metal catalyst as part of a growing polymer chain with a generic strained cyclic alkene. The second difference is that the driving force for ROMP is the relief of the ring strain and the second step, shown in Scheme 1.6, is irreversible [Bielaswki and Grubbs, 2007].

1.4 CATALYSTS FOR OLEFIN METATHESIS

The number of catalyst systems that initiate olefin metathesis is very large [Kress and Blechert, 2012; Kotha and Depak 2012]. Most early work in olefin metathesis was done using ill-defined multi component catalyst systems [Warwel and Siekermann, 1983; Leymet et al., 1989; Liaw and Lin, 1993]. In recent years well-defined single component metal carbene complexes of tungsten, molybdenum and ruthenium have been utilized in olefin metathesis. The molybdenum and ruthenium based metal alkylidenes are known as Schrock [Schrock, 2005] and Grubbs [Samojlowicz et al., 2009; Schwab et al., 1995] catalysts respectively and these are quite efficient and widely used as olefin metathesis catalysts. The basic structure of a Schrock-type catalyst Mo(NAr)(CHR) $(OR')_2$ and Grubbs first generation [Nguyen and Grubbs, 1993; Schwab et al., 1996] catalyst $L_2Cl_2Ru{=}CHR$ (where L is a phosphine ligand as well as Grubbs second generation [Schrodi and Pederson, 2007; Scholl et al., 1999] catalyst $(L)(L')Cl_2Ru{=}CHR$ (where L is a phosphine ligand and L' a saturated N-heterocyclic carbene or NHC ligand) are shown,

.

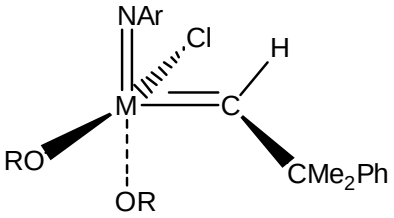

General formula of the family of Schrock's catalyst (M=Mo or W; R and Ar are bulky substituents

Schrock Catalyst

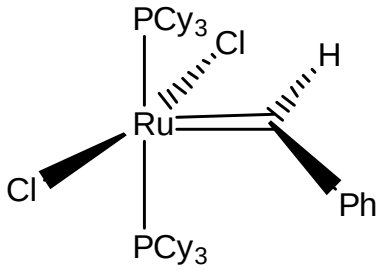

Grubbs 1st Generation catalyst

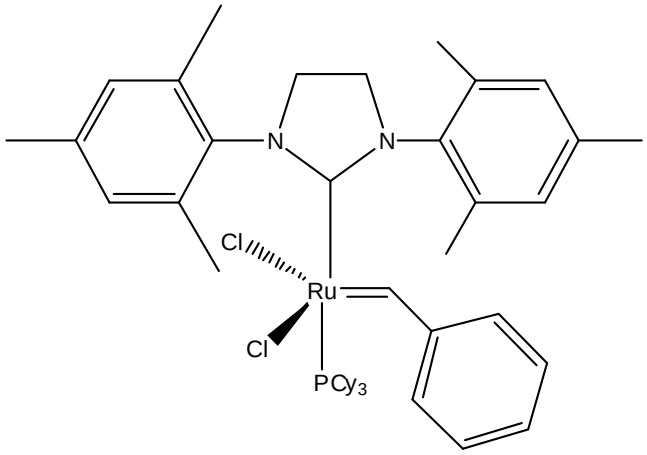

Grubbs 2nd Generation catalyst

Schrock's Mo catalyst is air sensitive and generally more active than the air-stable Grubbs Ru based catalysts which, in contrast to other olefin metathesis catalysts, tend to have a higher functional group tolerance and are more robust under some laboratory conditions [Heppekausen and Furstner, 2011; Malcolmson et al., 2008; Schrock, 2002; Schrock and Hoveyda, 2003]. The Grubbs second generation catalyst has the same uses in organic synthesis as the first generation catalyst, but has a higher activity. The Grubbs second generation (NHC) catalysts are also more thermally stable than the first generation catalyst [Samojłowicz et al., 2009; Vougioukalakis and Grubbs 2010].

1.5 LITERATURE REVIEW

During the last two decades, the metathesis reaction of olefins has been widely used as an efficient and versatile method for the formation of carbon-carbon double bonds. Olefin metathesis has a variety of applications, including ring opening metathesis polymerization (ROMP), ring Closing Metathesis (RCM), acyclic diene metathesis (ADMET), ring opening metathesis (ROM), and cross metathesis. Olefin metathesis opens up new industrial routes to important polymers, petrochemicals, oleochemicals and other commercial applications.

Olefin metathesis has also been the subject of number of experimental and theoretical studies. Eisenstein et al. (1981) have carried out extended Huckel and *ab initio* Hartree-Fock [Dediu and Eisenstein, 1982] studies on such reactions. Generalized valence bond (GVB) calculations [Rappe and Goddard, 1982] of the reaction between $Cl_4Mo{=}CH_2$ and ethylene have been reported by Rappe and Goddard, in which the formation of the metallacycle was found to be endothermic. However, it was found to be exothermic when recalculated using fully optimized geometries [Anslyn and Goddard, 1989; Sodupe et al., 1991]. Rappe and Goddard (1982) have used the results of an *ab initio* mechanistic study to suggest that the high valent Mo, W, and Re oxo-alkylidene complex $Cl_2(O)M{=}CH_2$ would favor formation of metallacycles. Cundari and Gordon performed an ab initio analysis of high-valent transition metal alkylidenes as models for olefin metathesis catalysts and found that greater polarization in $M^{+}{=}C^{-}$ for tungsten methylidene than for the molybdenum methylidene analogue and concluded that higher polarization correlates with greater metathesis activity [Cundari and Gordon, 1992].

Floga and Ziegler (1993) have been carried out a theoretical study on the structure of the metal carbene $L_2Mo(X)CH_2$ and metallacycle $L_2Mo(X)C_3H_6$ (X = O, NH and L = Cl,OCH_3, OCF_3). This study suggested the existence of two conformations square-pyramidal (SP) and trigonal-bipyramidal (TBP) for metallacycle. The decomposition energy of SP conformation was found more stable than the TBP conformation for $L_2Mo(O)C_3H_6$. In case of $L_2Mo(NH)C_3H_6$, the TBP conformation was preferred for the electron withdrawing ligand L = OCF_3 and SP for L = C1, OCH_3.

Crow and Goldberg (1995) reported the first examples of productive cross metathesis reactions of acrylonitrile. They found that troublesome functional groups are

tolerated by the catalyst system and that the reaction was useful due to cis selectivity. In the same year, Miller et al. (1995) investigated catalytic ring closing metathesis of dienes to prepare eight-membered rings. Their results indicated that a number of eight-membered ring substrate classes are amenable to synthesis in reasonable yield by RCM. Crowe et al. (1996) prepared allylsilanes by simple metathetical cross-coupling of terminal olefins with allyltrimethylsilane.

Various reports [Brzezinska and Deming, 2001; Brzezinska et al., 1999; Nubel et al., 1994; Wagener and Brzezinska, 1991] have appeared on olefin metathesis leading to polymerization and copolymerization of a variety of acyclic dienes via acyclic diene metathesis polymerization (ADMET). Wagener et al. (1997)] studied the kinetics of ADMET polymerization of oxygen and sulfur containing dienes using both Schrock's $Mo(=CHCMe_2Ph)(\textit{N}\text{-}2,6\text{-}C_6H_3\text{-}\textit{i}\text{-}Pr_2)(OCMe(CF_3)_2)_2$ and Grubbs $RuCl_2(=CHPh)(PCy_3)_2$ metathesis catalyst. Their results showed that the Mo catalyst produces linear diene polymers while Ru catalyst leads to formation of cyclic compounds rather than linear polymers. The negative neighboring group effect (NNGE) is more pronounced for the ruthenium catalyst.

Zhang et al. (1998) polymerized norbornene and dicylopentadiene using Cp TiCl2/ RMgX as a catalytic system (Cp= η^5-cyclopentadienyl and R= CH_3, C_2H_5, i-C_3H_7, C_6H_5, X=Cl, Br, I) for ring opening metathesis polymerization. The formation of challenging tetrasubstituted cycloalkenes by ring closing metathesis was investigated by Ackermann et al. (1999).

The cross-metathesis of styrene with various vinylsilanes $H_2C=C(H)SiR_3$ have been carried out using a complex of the type $Cl_2(PCy_3)_2Ru=CHPh$ as catalyst. Very high conversions are observed when R =OEt, $OSiMe_3$. The conversion significantly decreases with increasing substitution of Me for OR [Pietraszuk et al., 2000].Gas-phase mechanistic studies, by electrospray ionization tandem mass spectrometry, of the olefin metathesis by ruthenium carbene complexes suggested that metallacyclobutane structure is a transition structure rather than an intermediate [Aldhart et al., 2000].

Handzlik and Ogonowski conducted studies on ethene metathesis occurring on molybdenamethylidene centres of molybdena-alumina catalyst [Handzlik and Ogonowski, 2001]. The thermodynamics of the reactions of ethene with Mo^{VI} and Mo^{IV} carbene centres

were calculated. It was concluded that active centres of ethene metathesis do not contain Mo^{IV} because of high energy barriers of some elementary steps of the process. The formation of trigonal bipyramidal molybdacyclobutane with Mo^{VI} carbene is an endothermic reaction with low activation enthalpy while with Mo^{IV} the molybdacyclobutane is very exothermic and irreversible. Their results suggested that active centres of ethene metathesis do not contain Mo^{IV}.

Cavallo has carried out a study of the ruthenium catalyzed olefin metathesis reaction using density functional theory and found that metallacyclic structures represents minimum energy situations along the reaction coordinate, and are of slightly higher energy with respect to the corresponding olefin-bound intermediates in the case of the phosphane-based systems, while they are slightly more stable than the olefin adducts in the case of the NHC-based systems [Cavallo, 2002].

In 2003, Bernardi et al. studied olefin metathesis mechanism using the Grubbs complexes, $Cl_2(PH_3)_2Ru{=}CH_2$ and $Cl_2(PPh_3)_2Ru{=}CH_2$ at the B3LYP level of theory and found that the primary active species is the metal-carbene $(PH_3)_2Cl_2Ru{=}CH_2$ and not the carbenoid complex $(PH_3]_2Cl\text{-}Ru\text{-}CH_2Cl$ which is significantly higher in energy and that cyclopropanation is disfavored compared to metathesis since the former involves larger activation barriers than those found for the latter [Bernardi et al. 2003]. They also demonstrated that the ruthenacyclobutane is not a transition state, but a real intermediate on the reaction potential energy surface.

Kim and coworkers have reported experimental and theoretical studies on the olefin metathesis from alkenyl Baylis-Hillman adducts catalyzed by Grubbs second generation catalyst [Lee et al., 2004]. A detailed experimental study of the ROMP of low stain monomers cyclopentene and cycloheptene with several ruthenium catalysts has been reported by Hejl et al. (2005). They explored the effects of monomer concentration and catalyst dependence for unsubstituted cycloolefins. The ring opening metathesis polymerization of low-strain olefins with polar substituents is also examined with Grubbs olefin metathesis catalyst.

Poater et al. (2006) carried out gas phase DFT/B3PW91 calculations on the reactivity of ethylene with model systems M(NR)(CHtBu)(X)(Y) (M=Mo,W; R=CPh_3, 2,6-iPr-C_6H_3; X and Y = CH_2tBu, OtBu, OSi(OtBu)$_3$). Ring closing metathesis to form

tetrasubstituted olefins is reported by Grubbs et.al. They used N-heterocyclic carbene ligated ruthenium catalysts for RCM [Berlin et al., 2007].

A computational study on ring opening of cyclohexene using second-generation ruthenium alkylidene catalysts $(IMesH_2)(PCy_3)CI_2Ru{=}CHPh$ and $(IMesH_2)$-$(PCy_3)CI_2Ru{=}CHCOOMe$ and the first-generation $(PCy_3)_2$-$CI_2Ru{=}CHCOOMe$ catalyst (where $IMesH_2$ is 1,3-dimethyl-4,5-dihydroimidazol-2-ylidene) was carried out by Fomine and Tlenkopathev (2007). Torker et al. (2008) reported the experimental measurement of the activation energies for phosphine dissociation and ring closing metathesis for Grubbs catalyst in the gas phase. The absolute binding energy of the olefinic substrate to the 14-elelctron active species is about 18 kcal/mol.

The monitoring and evaluation of the crossover reaction in ring opening metathesis polymerization (ROMP) via MALDI mass spectrometry methods is reported by Binder et al. (2009). Fomine and Tlenkopatchev (2009) have carried out a computational study (B3LYP/LACVP* level of theory) on metathesis of halogenated olefins by ruthenium carbene. They calculated the free activation energies (2.5, -2.0, -11.9 and -31.6 kcal/mol) for the cross-metathesis reaction of ethylene, trans-1,2-dichloro-ethylene and fluorinated trans-1,2-difluro ethylene and tetrafluro-ethylene with norbornene respectively. The calculations also show that the natural charge at a ruthenium (Ru) center is strongly dependent on the nature of substitution and can be a measure of carbene stability. The stabilization of a metallacarbene is due to the stabilization of the metal center and not of a carbene carbon itself.

Sampson and coworkers investigated the ring opening metathesis polymerization reaction of 1-substituted cyclobutene derivatives (carboxylate esters, carboxamides, and carbinol esters). They also analyzed regio and stereochemical outcomes of these ROMP and ROM reactions at the B3LYP/6-31G* and LANL2DZ levels of theory (Song et al., 2010). Flook et al. (2010) have been reported Z-selective and syndioselective polymerization of 2,3-bis(trifluoromethyl)-bicyclo[2.2.1] hepta-2,5-diene (NBDF6) and 3-methyl-3-phenylcyclopropene (MPCP) by monoaryloxidemonopyrrolide imido alkylidene (MAP) catalyst of Molybdenum. In 2010, Density functional theory studies were performed to investigate the cross-metathesis reaction of ethylene and 2-butylene over heterogeneous Mo/HBeta catalyst [Li et al., 2010].

Hillier et al. (2011) have explored the potential energy surfaces for ring-closing metathesis reactions of a series of simple α,ω-dienes which lead to 5-10 membered cyclic products. The authors investigated the conformational aspects of the hydrocarbon chain during the course of the reactions, as well as the stationary structures on the corresponding potential energy surfaces. They also studied the structural variations along the pathway for the reactant hydrocarbons of differing chain length to identify points at which cyclisation events may begin to affect reaction rates. This work provides an excellent starting point from which to begin to learn about the way RCM reaction outcomes are controlled by diene structure.

A computational study of mechanistic aspects of olefin metathesis reactions involving metal oxo-alkylidene complexes was carried out at B3LYP/LACVP* and M06/LACVP * level of theory by Tia and Adei (2011). In the reaction of $Cl_2(O)MCH_2$ (M=Cr, Mo, W, Ru, Re) with ethylene they found that formation of the metallacyclobutane is a low-barrier process for each of the complexes studied. The highest barrier occurred in Ru (13.78 kcal/mol and 4.74 kcal/mol by B3LYP and M06 level respectively) and the lowest barrier occurring in W (0.38 kcal/mol and 0.28 kcal/mol by B3LYP and M06 calculations respectively). In the case of Re and Ru complexes, the metallacyclobutane was found to be very stable and cycloreversion does not proceed easily. They showed that metathesis occurs on use of molybdenum (Mo) and tungsten (W) but not of Cr, Ru or Re.

Keitz et al. (2011) experimentally demonstrate the first example of Z-selective homodimerization of terminal olefins using a ruthenium based catalyst. They also showed dimerization via metathesis of several challenging substrates, including alcohols, with good selectivity for the Z-olefin.

Mechanistic details of the ring opening metathesis polymerization of cyclic olefins using the second-generation Grubbs catalyst have been investigated at the M06-2X level of theory by Martinez et al. (2012). They have showed that the ROMP of Z-cyclooctene by Grubbs catalyst has a different rate-limiting step than that for smaller rings such as cyclopentene. For smaller rings metallacyclobutane intermediate formation via a [2+2] cycloaddition is the rate limiting step, while for larger rings it is the breakdown of that same intermediate via a retro-[2+2] step that is rate limiting. These authors also explored the factors that can be tuned to control stereo and regioselectivity in the design of future ROMP substrates and olefin metathesis catalysts.

In 2012, Density functional theory studies have been performed to explore the mechanism and origins of Z-selectivity of the metathesis homodimerization of terminal olefins catalyzed by chelated ruthenium complexes [Dang et al., 2012]. The results have shown that the active complex (Ru-benzylidene), formed by the Chauvin mechanism, leads to both the (Z-) and (E) olefin products (homodimers) and Z-selectivity arises from different kinetic barriers in the key transition states.

The ring opening metathesis reaction of (-)-α-pinene catalyzed by the second generation Grubbs catalyst, tungsten based Schrock and Fischer type metallacarbenes has been studied at PBE0/LACVP*//PBE0/LACVP* level of theory [Fomine and Tlenkopatchev, 2012). The result demonstrated the importance of steric factors in both metathesis catalyst and the monomer substrate. A successful catalyst for (-)-α-pinene metathesis should have small substituents at metal and carbene atoms. The lowest activation and reaction energies were found for methylene metallacarbenes. The oxidation state of the metal center plays an important role in the reactivity of tungsten containing carbene complexes.

Olefin metathesis of ethyl vinyl ether catalyzed by ruthenium catalyst $L(PCy_3)(X)_2Ru=CHPh$ (where L = PCy_3, IMes (1,3-dimesitylimidazol-2-ylidene), H_2IMes (1,3-dimesityl-4,5-dihydroimidazol-2-ylidene); X = Cl, Br, I) in toluene was carried out at the density functional theory level by Jensen [Minenkov et al. 2013]. Dispersion, thermochemical and continuum solvent effects have been studied for the metathesis of ethyl vinyl ether (EVE). In this study a complete set of intermediates and transition state of the EVE metathesis reaction has been obtained, allowing comparison with the experimental kinetic data [Sanford et al., 2001]. The calculations show that, from the active 14-electron complex, olefin coordination proceeds over a barrier involving contributions from entropy and solute-solvent interactions.

Park et al. (2013) experimentally investigated the tandem ring opening /ring closing metathesis polymerization (ROM/RCM) for various monomers including cyclo-olefins and terminal alkynes. These authors found that the reactivity was heavily influenced not only by the ring size of the cyclo-olefins but also by the length of the alkynes and the linker moieties. The mechanistic details for the tandem polymerization were studied by conducting end-group analysis using ^{1}H NMR, and it was concluded that the polymerization occurred exclusively by the alkyne-first pathway. They proposed that the

stability of the metallacyclobutane intermediates or the accessibility of the newly generated alkylidenes toward the cycloalkenes caused the dramatic structure-reactivity relationship of the monomers for the tandem polymerization. Authors also demonstrated a powerful tandem polymerization of monomers containing functional groups that were otherwise sterically and thermodynamically inactive for the conventional ROMP.

A comprehensive computational study on the regioselectivity in the nucleophilic ring opeining of epoxides has been carried out [Xinyao et al., 2013]. The less substituted side of alkyl epoxides was found to be favorable for regioselective ring opening and regulated by steric effect. Whereas aryl/alkenylepoxides show alterable regioselectivities, controlled by a combined action of the steric hindrance and the electronic effect of aryl and alkenyl groups, impacted by nucleophiles, solvents, and catalysts as well.

1.6 STATEMENT OF OBJECTIVE

In this thesis we present our computational studies on olefin metathesis reactions mediated by Schrock (tungsten, molybdenum alkylidenes) and Grubbs (ruthenium alkylidene) catalysts. The mechanistic path of Ring opening metathesis (ROM) and ring opening metathesis polymerization (ROMP) of strained 3,3-dimethyl cyclopropene is investigated. The stereochemical ring opening of asymmetric disubstituted cyclopropene is studied and effect of the substituents on the ring opening of cyclopropene has also been investigated. Ring opening-cross metathesis (ROCM) reaction of trisubstituted cyclopentene with methyl vinyl ketone is also investigated. The computational methods are briefly discussed in the next chapter.

1.7 REFERENCES

Ackermann L, Furstner A, Weskamp T, Kohl F J and Herrmann W A (**1999**) "Ruthenium carbene complexes with imidazolin-2-ylidene ligands allow the formation of tetrasubstituted cycloalkenes by RCM" *Tetrahedron Lett.* **40**: 4787-4790.

Adlhart C, Hinderling C, Baumann H and Chen P (**2000**) "Mechanistic studies of olefin metathesis by ruthenium carbene complexes using electrospray ionization tandem mass spectrometry" *J. Am. Chem. Soc.* **122**: 8204-8214.

Advanced information on the Nobel Prize in Chemistry (**2005)**, The Royal Swedish Academy of Sciences: http://nobelprize.org/chemistry/laureates/2005/chemadv05.pdf (accessed Nov 2010).

Anderson-Wile A M and Coates G W (**2012**) "Synthesis and ring-opening metathesis polymerization of norbornene-terminated syndiotactic polypropylene" *Macromolecules* **45**: 7863-7877.

Anslyn E V, and Goddard III W A (**1989**) "Structures and reactivity of neutral and cationic molybdenum methylidene complexes" *Organometallics* **8**: 1550-1558.

Armstrong S K (**1998**) "Ring closing diene metathesis in organic synthesis" *J. Chem. Soc., Perkin Trans.* **1**: 371-388.

Banks R L and Bailey G C (**1964**) "Olefin disproportionation: A new catalytic process" *Ind. Eng. Chem. Prod. Res. Dev.* **3**: 170-173.

Baughman T W and Wagener K B (**2005**) "Recent advances in ADMET polymerization" *Adv. Polym. Sci.* **76**: 1-42.

Benjamin K K, Endo K, Herbert M B and Grubbs R H (**2011**) "Z-Selective Homodimerization of Terminal Olefins with a Ruthenium Metathesis Catalyst" *J. Am. Chem. Soc.* **133**: 9686-9688.

Berlin J M, Campbell K, Ritter T, Funk T W, Chlenov A and Grubbs R H (**2007**) "Ruthenium-catalyzed ring-closing metathesis to form tetrasubstituted olefins" *Org. Lett.* **9**: 1339-1342.

Bernardi V, Bottoni A and Miscione G P (**2003**) "DFT study of the olefin metathesis catalyzed by ruthenium complexes" *Organometallics* **22**: 940-947

Bielawski C W and Grubbs R H (**2007**) "Living ring-opening metathesis polymerization" *Prog. Polym. Sci.* **32**: 1-29.

Binder W H, Pulamagatta B, Kir O, Kurzhals S, Barqawi H and Tanner S (**2009**) "Monitoring block-copolymer crossover-chemistry in ROMP:Catalyst evaluation via mass-spectrometry (MALDI)" *Macromolecules* **42**: 9457-9466.

Brzezinska K R and Deming T J (**2001**) "Synthesis of ABA triblock copolymers via ccyclic diene metathesis polymerization and living polymerization of α-amino acid-N-carboxyanhydrides" *Macromolecules* **34**: 4348-4354.

Brzezinska K R, Wagener K B and Burns G T (**1999**) "Silicon-terminated telechelic oligomers by ADMET chemistry: Synthesis and copolymerization" *J. Polym. Sci. Part A: Polym. Chem.* **37**: 849-856.

Burt M B, Crane A K, Su N, Rice N and Poirier R A (**2010**) "Ring-chain equilibria of R-but-3- enoate esters; a quantum mechanical study of ADMET and RCM pathways" *Can. J. Chem.* **88**(11):1-3.

Calderon N, Chen H Y and Scott K W (**1967**) "Olefin metathesis - A novel reaction for skeletal transformations of unsaturated hydrocarbons" *Tetrahedron Lett.* **34**: 3327-3329.

Cavallo L (**2002**) "Mechanism of ruthenium-catalyzed olefin metathesis reactions from a theoretical perspective" *J. Am. Chem. Soc*. **124**: 8965-8973.

Chatterjee A K, Sanders D P and Grubbs R H (**2002**) "Synthesis of symmetrical trisubstituted olefins by cross metathesis" *Org. Lett.* **11**: 1939-1942.

Collins S K (**2006**) "Preparation of cyclic molecules bearing "strained" olefins using olefin metathesis" *J. Organomet. Chem.* **691**: 5122-5128.

Connon S J and Blechert S (**2003)** "Recent developments in olefin cross-metathesis" *Angew. Chem. Int. Ed.* **42**: 1900-1923.

Crowe W E and Goldberg D R (**1995**) "Acrylonitrile Cross-metathesis: coaxing olefin metathesis reactivity from a reluctant substrate" *J. Am. Chem. Soc.* **117**: 5162-5163.

Crowe W E, Goldberg D R and Zhang Z J (**1996**) "Preparation of allylsilanes via cross-metathesis" *Tetrahedron Lett.* **37**: 2117-2120.

Cundari T R and Gordon M S (**1992**) "Theoretical investigations of olefin metathesis catalysts" *Organometallics* **11**: 55-63.

Dang Y, Wang Z X and Wang X (**2012**) "A thorough dft study of the mechanism of homodimerization of terminal olefins through metathesis with a chelated ruthenium catalyst: from initiation to Z-selectivity to regeneration" *Organometallics* **31**: 7222-7234.

Dediu A and Eisenstein O (**1982**) "Metallacyclobutanes: Are they distorted? A theoretical ab initio study" *Nouv. J. Chim.* **6**: 337-339.

Deiters A and Martin S F (**2004**) "Synthesis of Oxygen- and Nitrogen-containing heterocycles by ring-closing metathesis" *Chem. Rev.* **104**: 2199-2238.

Deshmukh P H and Blechert S (**2007**) "Alkene metathesis: the search for better catalysts" *Dalton Trans.* 2479-2491.

Eisenstein O, Hoffman R and Rossi A R (**1981**) "Some geometrical and electronic features of the intermediate stages of olefin metathesis" *J. Am. Chem. Soc.* **103**: 5582-5584.

Eleuterio H S (**1991**) "Olefin metathesis: chance favors those minds that are best prepared" *J. Mol. Catal.* **65**: 55-61.

Flook M M, Gerber L C H, Debelouchina G T and Schrock R R (**2010**) "Z-selective and syndioselective ring-opening metathesis polymerization (ROMP) initiated by monoaryloxidepyrrolide (MAP) catalysts" *Macromolecules* **43**: 7515-7522.

Folga E and Ziegler T (**1993**) "Density functional study on molybdacyclobutane and its role in olefin metathesis" *Organometallics* **12**: 325-331.

Fomine S and Tlenkopatchev M A (**2007**) "Ring-opening of cyclohexene via metathesis by ruthenium carbene complexes. A computational study" *Organometallics* **26**: 4491-4497.

Fomine S and Tlenkopatchev M A (**2009**) "Metathesis of fluorinated olefins by ruthenium alkylidene catalysts. Fluorine substituent effects on a Ru-carbene (alkylidene) complex stability: A computational study" *Applied Catalysis A: General* **355**: 148-155.

Fomine S and Tlenkopatchev M A (**2012**) "Metathesis transformations of terpenes. Computational modeling of (-)-α-pinene ring opening by ruthenium and tungsten carbene catalysts" *Comp. Theor. Chem* **701**: 68-74.

Frenzel U and Nuyken O (**2002**) "Ruthenium-based metathesis initiators: Development and use in ring-opening metathesis polymerization" *J. Polym. Sci. Part A: Polym. Chem.* **40**: 2895-2916.

Frenzel U, Müller B K M and Nuyken O (**2005**) "Metathesis polymerization of cycloolefins" In Handbook of polymer synthesis, 2nd Ed.; Kricheldorf H R, Nuyken O, Swift G, Eds; Marcel Dekker: New York, NY, USA, 381-426.

Fu G C and Grubbs R H (**1993**) "Synthesis of cycloalkenes via alkylidene-mediated olefin metathesis and carbonyl olefination" *J. Am. Chem. Soc.* **115**: 3800-3801.

Furstner A (**2000**) "Olefin metathesis and beyond" *Angew. Chem. Int. Ed.* **39**: 3012-3043.

Ghosh S, Ghosh S And Sarkar N (**2006**) "Factors influencing ring closure through olefin metathesis-A perspective" *J. Chem. Sci.* **118**: 223-235.

Gorodetskaya I A, Choi T L and Grubbs R H (**2007**) "Hyperbranched macromolecules via olefin metathesis" *J. Am. Chem. Soc.* **129**: 12672-12673.

Grubbs R H (**2003**) "Handbook of Metathesis" Wiley-VCH: Weinheim, Germany.

Grubbs R H (**2004**) **"**Olefin metathesis" *Tetrahedron* **60**: 7117-7140.

Grubbs R H and Chang S (**1998**) "Recent advances in olefin metathesis and its application in organic synthesis" *Tetrahedron* **54**: 4413-4450.

Guidry E N, Li J, Stoddart J F, Grubbs R H (**2007**) "Bifunctional [c2] daisy-chains and their incorporation into mechanically interlocked polymers" *J. Am. Chem. Soc.* **129**: 8944-8945.

Haigh D M, Kenwright A M and Khosravi E (**2004**) "Ring opening metathesis polymerisations of norbornene and norbornadiene derivatives containing oxygen: a study on the regeneration of Grubbs catalyst" *Tetrahedron* **60**: 7217-7224.

Handzlik J and Ogonowski J (**2001**) "Theoretical study on ethene metathesis proceeding on Mo^{VI} and Mo^{IV} methylidene centres of heterogeneous molybdena-alumina catalyst" *J. Mol. Catal. A: Chem.* **175**: 215-225.

Hejl A, Scherman O A and Grubbs R H (**2005**) "Ring-opening metathesis polymerization of functionalized low-strain monomers with ruthenium-based catalysts" *Macromolecules* **38**: 7214-7218.

Hejl A, Scherman O A and Grubbs R H (**2005**) "Ring-opening metathesis polymerization of functionalized low-strain monomers with ruthenium-based catalysts" *Macromolecules* **38**: 7214-7218.

Heppekausen J and Furstner A (**2011**) "Rendering Schrock-type molybdenum alkylidene complexes air stable: user-friendly precatalysts for alkene metathesis" *Angew. Chem. Int. Ed.* **50**: 7829-7832.

Hérisson J L and Chauvin Y (**1971**) "Catalyse de transformation des oléfines par les complexes du tungstène. II. Télomérisation des oléfines cycliques en présence d'oléfines acycliques" *Makromol. Chem.* **141**: 161-176.

Hillier I H, Pandian S, Percy J M and Vincent M A (**2011**) "Mapping the potential energy surfaces for ring-closing metathesis reactions of prototypical dienes by electronic structure calculations" *Dalton Trans.* **40**: 1061-1072.

Hoveyda A H and Zhugralin A R (**2007**) "The remarkable metal-catalyzed olefin metathesis reaction" *Nature* **450**: 243-251.

Ivin K J and Mol J C (**1997**) "Olefin Metathesis and metathesis polymerization" Academic Press: San Diego, CA.

Katz T J and McGinnis J (**1975**) "Mechanism of the olefin metathesis reaction" *J. Am. Chem. Soc.* **97**: 1592-1594.

Katz T J, Lee S J and Acton N (**1976**) "Stereospecific polymerizations of cycloalkenes induced by a metal-carbene" *Tetrahedron Lett.* **17**: 4247-4250.

Keim W, Hoffmann B, Lodewick R, Peuckert M, Schimtt G, Fleischhauer G, and Meir U (**1979**) "Linear oligomerization of olefins via nickel chelate complexes and mechanistic considerations based on semi-empirical calculations" *J. Mol. Catal.* **6**: 79-97.

Keitz B K, Endo K, Herbert M B and Grubbs R. H (**2011**) "Z-selective homodimerization of terminal olefins with a ruthenium metathesis catalyst" *J. Am. Chem. Soc.* **133**: 9686-9688.

Kotha S and Dipak M K (**2012**) "Strategies and tactics in olefin metathesis" *Tetrahedron* **68**: 397-421.

Kotha S and Dipak M K (**2012**) "Strategies and tactics in olefin metathesis" *Tetrahedron* **68**: 397-421.

Kress S and Blechert S (**2012**) "Asymmetric catalysts for stereo-controlled olefin metathesis reactions" *Chem. Soc. Rev.* **41**: 4389-4408.

Lee M J, Lee K Y, Lee J Y and Kim J N (**2004**) "Experimental and theoretical study on the olefin metathesis of alkenyl Baylis-Hillman adducts using second-generation Grubbs catalyst" *Org. Lett.* **6**: 3313-3316.

Lehman S E and Wagener K B (**2002**) "Comparison of the kinetics of acyclic diene metathesis promoted by Grubbs ruthenium olefin metathesis catalysts" *Macromolecules* **35**: 48-53.

Leymet I, Siove A, Parlier A, Rudler H and Fontanille M (**1989**) "Ring-opening polymerization of norbornene initiated by tungsten alkylidene complexes. Activation by $AlCl_3$" *Makromol. Chem.* **90**: 2397-2405.

Li X, Guan J, Zheng A, Zhou D, Han X, Zhang W and Bao X (**2010**) "DFT studies on the reaction mechanism of cross-metathesis of ethylene and 2-butylene to propylene over heterogeneous Mo/HBeta catalyst" *J. Mol. Catal A: Chem.* **330**: 99-106.

Liaw D J and Lin C L (**1993**) "Effect of lewis acid on the polymerization of *tert*-butylacetylene initiated by the new tungsten carbene complex: Geometric structure control with high cis content" *J. Polymer Sci. A Polym. Chem.* **31**: 3151-3154.

Malcolmson S J, Meek S J, Sattely E S, Schrock R R and Hoveyda A H (**2008**) "Highly efficient molybdenum-based catalysts for enantio selective alkene metathesis" *Nature* **456**: 933-937.

Marsico F, Wagner M, Landfester K and Wurm, F R. (**2012**) "Unsaturated polyphosphoesters via acyclic diene metathesis polymerization" *Macromolecules* **45**: 8511-8518.

Martinez H, Miro P, Charbonneau P, Hillmyer M A and Cramer C J (**2012**) "Selectivity in ring-opening metathesis polymerization of Z‑cyclooctenes catalyzed by a second-generation Grubbs catalyst" *ACS Catal.* **2**: 2547-2556.

Matson J B and Grubbs R H (**2008**) "Synthesis of Fluorine-18 functionalized nanoparticles for use as in vivo molecular imaging agents" *J. Am. Chem. Soc.* **130**: 6731-6733.

Matsuda T and Sato S (**2013**) "Synthesis of Dibenzoheteropines of Group 13-16 Elements via Ring-Closing Metathesis" *J. Org. Chem.***78**: 3329-3335.

Mayo P and Tam W (**2002**) "Ring-opening metathesis-cross-metathesis reactions (ROM-CM) of substituted norbornadienes and norbornenes" *Tetrahedron* **58**: 9513-9525.

Mazoyer E, Szeto K C, Basset J M, Nicholas C P and Taoufik M (**2012**) "High selectivity production of propylene from 2-butene: non-degenerate pathways to convert symmetric olefins via olefin metathesis" *Chem. Commun.* **48**: 3611-3613.

McReynolds M D, Dougherty J M and Hanson P R (**2004**) "Synthesis of phosphorus and sulfur heterocycles via ring-closing olefin metathesis" *Chem. Rev.* **104**: 2239-2258.

Miller S J, Kim S H, Chen Z R and Grubbs R H (**1995**) "Catalytic ring-closing metathesis of dienes: application to the synthesis of eight-membered rings" *J. Am. Chem. Soc.* **117**: 2108-2109.

Minenkov Y, Occhipinti G and Jensen V R. (**2013**) "Complete reaction pathway of ruthenium-catalyzed olefin metathesis of ethyl vinyl ether: kinetics and mechanistic insight from DFT" *Organometallics* **32**: 2099-2111.

Mol J C (**2004**) "Industrial applications of olefin metathesis" *J. Mol. Catal. A: Chem.* **213**: 39-45.

Morgan J P, Morrill C and Grubbs R H (**2002**) "Selective ring opening cross metathesis of cyclooctadiene and trisubstituted cycloolefins" *Org. Lett.* **4**: 67-70.

Nguyen S T and Grubbs R H (**1993**) "Syntheses and activities of new single-component, ruthenium-based olefin metathesis catalysts" *J. Am. Chem. Soc.* **115**: 9858-9859.

Nubel P O, Luthman C A and Yokelson H B (**1994**) "Acyclic diene metathesis polymerization using a modified WCl_6-SnR_4 olefin metathesis catalyst" *Macromolecules* **27**: 7000-7002.

O'Gara J E, Portmess J D and Wagener K B (**1993**) "Acyclic diene metathesis (ADMET) polymerization. Synthesis of unsaturated polythioethers" *Macromolecules* **26**: 2031-2041.

Park H, Lee H K and Choi T L (**2013**) "tandem ring-opening/ring-closing metathesis polymerization: relationship between monomer structure and reactivity" *J. Am. Chem. Soc.* **135**: 10769-10775.

Patton J T, Boncella J M and Wagener K B (**1992**) "Acyclic diene metathesis (ADMET) polymerization: the synthesis of unsaturated polyesters" *Macromolecules* **25**: 3862-3867.

Peter M and Tam W (**2002**) "Ring-opening metathesis-cross-metathesis reactions (ROM-CM) of substituted norbornadienes and norbornenes" *Tetrahedron* **58**: 9513-9525.

Pietraszuk C, Marciniec B, and Fischer H (**2000**) "Cross-metathesis of vinylsilanes with styrene catalyzed by ruthenium-carbene complexes" *Organometallics* **19**: 913-917.

Poater A, Monfort X S, Clot E, Coperet C. and Eisenstein O (**2006**) "DFT calculations of d^0 M(NR)(CHtBu)(X)(Y) (M =Mo, W; R = CPh_3,2,6-iPr–C_6H_3; X and Y = CH_2tBu, OtBu, OSi(OtBu)$_3$) olefin metathesis catalysts: structural, spectroscopic and electronic properties" *Dalton Trans.* 3077-3087.

Rappé A K, and Goddard III W A (**1982**) "Olefin metathesis-a mechanistic study of high-valent Group VI catalysts" *J. Am. Chem. Soc.* **104**: 448-456.

Roy R and Das S K (**2000**) "Recent applications of olefin metathesis and related reactions in carbohydrate chemistry" *Chem. Commun.* **7**: 519 -529.

Samojłowicz C, Bieniek M and Grela K (**2009**) "Ruthenium-based olefin metathesis catalysts bearing *N*-heterocyclic carbene ligands" *Chem. Rev.* **109**: 3708-3742.

Samojłowicz C, Bieniek M and Grela K (**2009**) "Ruthenium-based olefin metathesis catalysts bearing *N*-heterocyclic carbene ligands" *Chem. Rev.* **109**: 3708-3742.

Sanford M S and Love J A (**2003**) "Mechanism of ruthenium-catalysed olefin metathesis reactions" In Handbook of Metathesis, Grubbs R H, Ed., Vol. 1, Wiley: 112-131.

Sanford M S, Love J A and Grubbs R H (**2001**) "Mechanism and activity of ruthenium olefin metathesis catalysts" *J. Am. Chem. Soc.* **123**: 6543-6554.

Schneider V and Frolich P K (**1931**) "Mechanism of Formation of Aromatics from Lower Paraffins" *Ind. Eng. Chem.* **23**: 1405-1410.

Scholl M, Ding S, Lee C W and Grubbs R H (**1999**) "Synthesis and activity of a new generation of ruthenium-based olefin metathesis catalysts coordinated with 1, 3-dimesityl-4,5-dihydroimidazol-2-ylidene ligands" *Org. Lett.* **1**: 953-956.

Schrock R R (**1990**) "Living ring-opening metathesis polymerization catalyzed by well-characterized transition-metal alkylidene complexes" *Acc. Chem. Res.* **23**:158-165.

Schrock R R (2002) "High oxidation state multiple metal-marbon monds" *Chem. Rev.* **102**: 145-179.

Schrock R R **(2005**) "High oxidation state alkylidene and alkylidyne complexes" *Chem. Commun.* **22:** 2773-2777.

Schrock R R (**2011**) "Synthesis of stereoregular ROMP polymers using molybdenum and tungsten imido alkylidene initiators" *Dalton Trans.* **40**: 7484-7495.

Schrock R R and Hoveyda A H (**2003**) "Molybdenum and tungsten imido alkylidene complexes as efficient olefin-oetathesis catalysts" *Angew. Chem. Int. Ed.* **42**: 4592 -4633.

Schrock R R, Rocklage S, Wengrovius J, Rupprecht G and Fellmann J (**1980**) "Preparation and characterization of active niobium, tantalum and tungsten metathesis catalysts" *J. Mol. Catal*. **8:** 73-83.

Schrodi Y and Pederson R L (**2007**) "Evolution and applications of second-generation ruthenium olefin metathesis catalysts" *Aldrichemica ACTA* **40**: 45-52.

Schuster M and Blechert S (**1997**) "Olefin metathesis in organic chemistry" *Angew. Chem. Int. Ed. Engl.* **36**: 2036-2056.

Schwab P, France M B, Ziller J W and Grubbs R H (**1995**) "A series of well-defined metathesis catalysts-synthesis of $[RuCl_2(=CHR')(PR_3)_2]$ and its reactions" *Angew. Chem. Int. Ed. Engl.* **34**: 2039-2041.

Schwab P, Grubbs R H. and Ziller J W (**1996**) "Synthesis and applications of $RuCl_2(=CHR')(PR_3)_2$: The influence of the alkylidene moiety on metathesis activity" *J. Am. Chem. Soc.* **118**: 100-110.

Sodupe M, Lluch J M, Oliva A and Bertran J (**1991**) "Ab initio study of the reaction between methylenemolybdenum tetrachloride ($Cl_4Mo=CH_2$) and ethylene" *New J. Chem.* **15**: 321-325

Song A, Lee J C, Parker K A and Sampson N S (**2010**) "Scope of the ring-opening metathesis polymerization (ROMP) reaction of 1-substituted cyclobutenes" *J. Am. Chem. Soc*. **132**: 10513-10520.

Tia R and Adei E (**2011**) "Computational studies of the mechanistic aspects of olefin metathesis reactions involving metal oxo-alkylidene complexes" *Comp. Theor. Chem.* **971**:8-18.

Torker S, Merki D and Chen P (**2008**) "Gas-phase thermochemistry of ruthenium carbene metathesis catalysts" *J. Am. Chem. Soc.* **130**: 4808-4814.

Trnka T M and Grubbs R H (**2001**) "The Development of $L_2X_2Ru=CHR$ olefin metathesis catalysts: An organometallic success story" Acc. Chem. Res. **34**: 18-29.

Truett W L, Johnson D R, Robinson I M and Montague B A (**1960**) "Polynorbornene by Coordination Polymerization" *J. Am. Chem. Soc.* **82**: 2337-2340.

Vougioukalakis G C and Grubbs R H (**2010**) "Ruthenium-based heterocyclic carbene-coordinated olefin metathesis catalysts" *Chem. Rev.* **110**: 1746-1787.

Wagener K B and Brzezinska K (**1991**) "Acyclic diene metathesis (ADMET) polymerization. Synthesis of unsaturated polyethers" *Macromolecules* **24**: 5273-5277.

Wagener K B and Patton J T (**1993**) "Acyclic diene metathesis (ADMET) polymerization. Synthesis of unsaturated polycarbonates" *Macromolecules* **26**: 249-253.

Wagener K B, Boncella J M and Nel J G (**1991**) "Acyclic diene metathesis (ADMET) polymerization" *Macromolecules* **24**: 2649-2657.

Wagener K B, Brzezinska K, Anderson J D, Younkin T R, Steppe K and DeBoer W (**1997**) "Kinetics of acyclic diene metathesis (ADMET) polymerization. Influence of the negative neighboring group effect" *Macromolecules* **30**: 7363-7369.

Warwel S and Siekermann V (**1983**) "Olefin-Metathese, 12 Olefin-metathese mit homogenen rheniumcarben-komplexkatalysatoren" *Makromol. Chem. Rapid Commun.***4**: 423-427.

Xinyao L, Zuoyin Y, Jiaxi X (**2013**) "Comprehensive theoretical investigation on the regioselectivity in the nucleophilic ring opening of epoxides" *Curr. Org. Chem.* **10**: 169-177.

Yoshida K, Kawagoe F, Iwadate N, Takahashi H, and Imamoto T (**2006**) "Ring-closing olefin metathesis for the synthesis of benzene derivatives" *Chem. Asian J.* **1**: 611-613.

Zhang D, Huang J, Qian Y and Chan A S C (**1998**) "Ring-opening metathesis polymerization of norbornene and dicyclopentadiene catalyzed by Cp_2 TiCl /RMgX" *J. Mol. Catal. A: Chem.* **133**: 131-133.

Computational Methods 2

2.1 THEORETICAL BACKGROUND

In 1929 Dirac stated that the general theory of quantum mechanics is now almost complete, the imperfections that still remain being in connection with the exact fitting in of the theory with relativity ideas. Relativity gives rise to difficulties only when high-speed particles are involved, and so are of no great importance in the investigation of the structure of light atoms and molecules and of ordinary chemical reactions, in which it is usually sufficiently accurate if one neglects relativistic effects and assumes only Coulomb forces between the various electrons and atomic nuclei. The underlying physical laws necessary for the mathematical theory of a large part of physics and the whole of chemistry are thus well understood, and the difficulty is only that the exact application of these laws leads to equations much too complicated to be soluble. It thus becomes desirable that approximate practical methods of applying quantum mechanics should be developed, which can lead to an explanation of the main features of complex atomic systems without too much computation. This view of his defines the entire field of theoretical chemistry as it developed over the past eighty years or so. Early attempts to obtain meaningful theoretical results on organic molecules dealt with only π-electrons and later, treatments of all valence electrons become feasible [Singh, 2013]. However such separation of electrons into π and σ or valence and core do not have the sanction of theory as all electrons are indistinguishable. It is now well known that the wavefunction of a many electron system has to be anti-symmetric with respect to interchange of the coordinates of any pair of electrons, and so we seek wavefunctions satisfying this requirement in a self-consistent field procedure. When the function is sought to be represented as a single Slater determinant of occupied spin-orbitals we have the Hartree-Fock method, which is the starting point for many more refined calculation methods. In the present chapter we shall give an account of this method and others that seek to remove its shortcomings.

A typical molecular system consists of several nuclei and several electrons interacting via the coulomb interaction.

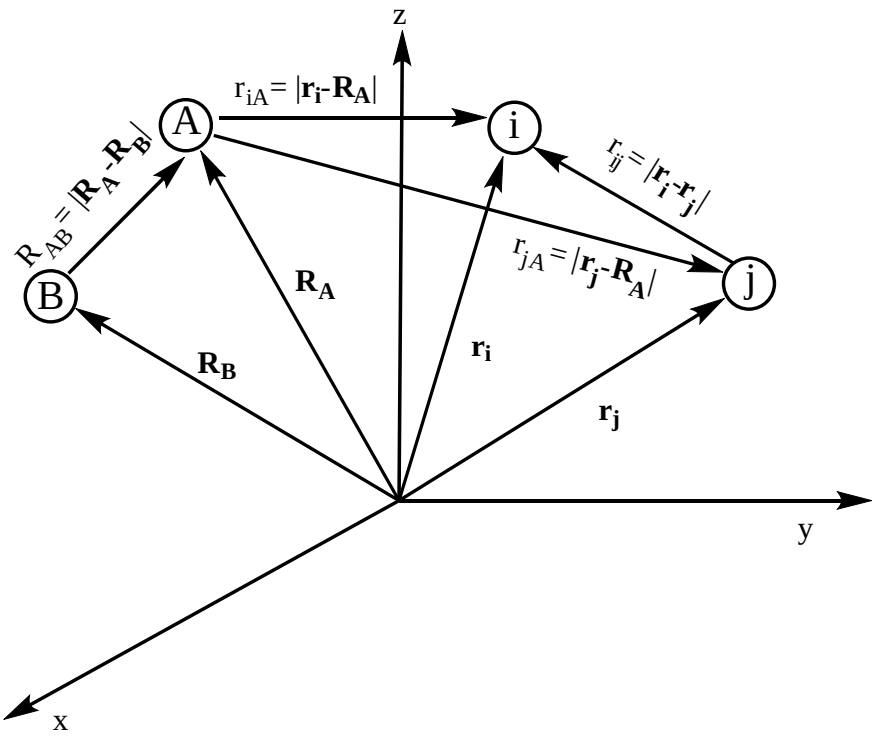

Figure 2.1: A molecular coordinate system, i, j are electrons and A, B are nuclei

The non-relativistic time-independent Schrödinger equation for a system consisting of N_e electrons and N_n nuclei may be written as,

$$H\Psi = E\Psi \tag{2.1}$$

Here, Ψ and E are the wavefunction and the energy of the system, respectively, and H is the Hamiltonian operator which can be expressed as,

$$H = -\sum_{i=1}^{N_e} \frac{1}{2}\nabla_i^2 - \sum_{A=1}^{N_n} \frac{1}{2M_A}\nabla_A^2 - \sum_{i=1}^{N_e}\sum_{A=1}^{N_n} \frac{Z_A}{r_{iA}} + \sum_{i=1}^{N_e}\sum_{j>i}^{N_e} \frac{1}{r_{ij}} + \sum_{A=1}^{N_n}\sum_{B>A}^{N_n} \frac{Z_A Z_B}{R_{AB}} \tag{2.2}$$

Where, M_A, Z_A and R_A are the mass, atomic number and position of nucleus A respectively. In equation (2.2), the first and second terms are the kinetic energies of the electrons and nuclei, respectively. The third term represents the (attractive) Coulomb interaction between nuclei and electrons. The fourth and fifth terms represents the (repulsive) Coulomb interaction between electrons and between nuclei, respectively. The above equation is written in atomic units, so that Planck's constant (ħ), the mass of electron (m_e) and electronic charge (e) are taken to be unity, and the energies are in hartrees.

2.2 THE BORN-OPPENHEIMER APPROXIMATION

The Born-Oppenheimer Approximation is invariably used in dealing with molecules to separate electronic and nuclear motions. It is based on the fact that the nuclei are much heavier than the electrons, so that the electrons can respond almost instantaneously to any change in the nuclear positions. Hence, to a good approximation, one can consider the electrons in a molecule to be moving in the field of fixed nuclei. This approximation helps to separate the Schrödinger equation into two parts, one for the nuclei and other for the electrons. Within this approximation, the second term in equation (2.2), i.e., the kinetic energy of the nuclei, can be neglected and last term, the repulsion between the nuclei, can be taken as constant while dealing with the electronic problems. The electronic equation contains all the terms involving electron coordinates, including the terms due to attractive forces between the nuclei and the electrons and those due to repulsive forces among electrons. The 'Electronic' Schrodinger equation may be written as,

$$H_{el}\Psi_{el} = E_{el}\Psi_{el} \tag{2.3}$$

Where H_{el} is called the electronic Hamiltonian and may be written as,

$$H_{el} = -\sum_{i=1}^{N_e}\frac{1}{2}\nabla_i^2 - \sum_{i=1}^{N_e}\sum_{A=1}^{N_n}\frac{Z_A}{r_{iA}} + \sum_{i=1}^{N_e}\sum_{j>i}^{N_e}\frac{1}{r_{ij}} \tag{2. 4}$$

The electronic wavefunction and energy depend parametrically on the (fixed) nuclear coordinates:

$$\Psi_{el} = \Psi_{el}(r,R) \tag{2. 5a}$$

$$E_{el} = E_{el}(R) \tag{2. 5b}$$

The total energy for fixed nuclei includes the constant nuclear repulsion,

$$E_{total}(R) = E_{el}(R) + \sum_{A=1}^{N_n}\sum_{B>A}^{N_n}\frac{Z_A Z_B}{R_{AB}} \tag{2. 6}$$

This quantity, which is a function of nuclear coordinates, serves as a potential energy for the problem of nuclear motion (vibrations, rotations, translations etc.). Its geometrical representation is what we term as the potential energy surface.

2.3 POTENTIAL ENERGY SURFACE

The Schrodinger equation for nuclear motion can be solved under the same assumption as used to formulate the electronic problem. As the electron moves much faster than the nuclei, it is a reasonable approximation in (2.2) to replace the electronic coordinates by their average values, averaged over the electronic wave function. This generates a nuclear Hamiltonian for the motion of the nuclei in the average field of the electrons, given in equation 2.7.

$$\begin{aligned} H_{nucl} &= -\sum_{A=1}^{N_n}\frac{1}{2M_A}\nabla_A^2 + \left\langle -\sum_{i=1}^{Ne}\frac{1}{2}\nabla_i^2 - \sum_{i=1}^{N_e}\sum_{A=1}^{N_n}\frac{Z_A}{r_{iA}} + \sum_{i=1}^{N_e}\sum_{j>i}^{N_e}\frac{1}{r_{ij}}\right\rangle + \sum_{A=1}^{N_n}\sum_{B>A}^{N_n}\frac{Z_A Z_B}{R_{AB}} \\ &= -\sum_{A=1}^{N_n}\frac{1}{2M_A}\nabla_A^2 + E_{el}(R) + \sum_{A=1}^{N_n}\sum_{B>A}^{N_n}\frac{Z_A Z_B}{R_{AB}} \\ &= -\sum_{A=1}^{N_n}\frac{1}{2M_A}\nabla_A^2 + E_{total}(R) \end{aligned} \qquad 2.7$$

The nuclear motions, for which $E_{total}(R)$ forms a potential energy function, can be separated into translational and vibrational-rotational motions [Sathyamurthy and Joseph 1984]. Translations involve motion of the center of mass (COM) of the system, while the relative coordinates of the particles remains unaffected, and involve three degree of freedom: Center of mass motion is represented by the motion of a free particle in three dimensions. Rotational and vibrational motions can also be separated from each other, and the rotational degree of freedom also does not involve variation of E_{total}. However vibrational motions which involve change in internuclear distances and angles do affect E_{total}, and so the potential energy surface is essentially dependent on vibrational degree of freedom. Hence the PES is a hypersurface in a 3N−5 dimensional space (3N−4 for linear molecules), one of the dimensions corresponds to energy and each of the others to a vibrational degree of freedom. In the case of a diatomic molecule, this reduces to a potential energy curve, as shown in Figure 2.2.

On this potential energy curve the potential energy is a minimum at a certain internuclear distance, called the equilibrium internuclear distance. If the nuclei come very close together, they repel each other and E_{total} shoots up, and as **r** goes to infinity, the molecule dissociates, the asymptote of the curve corresponding to its dissociation energy.

Several types of stationary points may exist on the PES: minima (local and global) and saddle point of various orders, and possibly local maxima. There is however no global maximum, as the energy has singularities corresponding to configurations in which two nuclei come too close together.

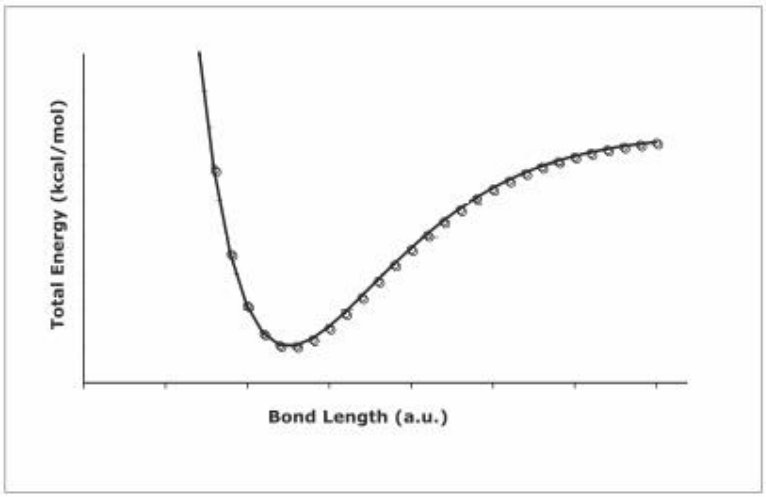

Figure 2.2: Schematic illustration of a potential energy curve for a diatomic molecule

A stable structure occurs at a minimum, and transition states at saddle points of first order on the surfaces, and this is what makes the PES important from the chemist's standpoint.

For A function of one variable, the stationary points can be characterized as minima or maxima based on the sign of the second derivative. In the case of multidimensional potential energy surface, the vector with first partial derivatives as components is called the gradient, and a vanishing gradient characterizes a stationary point. Physically if all components of the force ($\equiv -\nabla V$) are zero, then the atoms of the molecule feel no net force, i.e. they are in equilibrium.

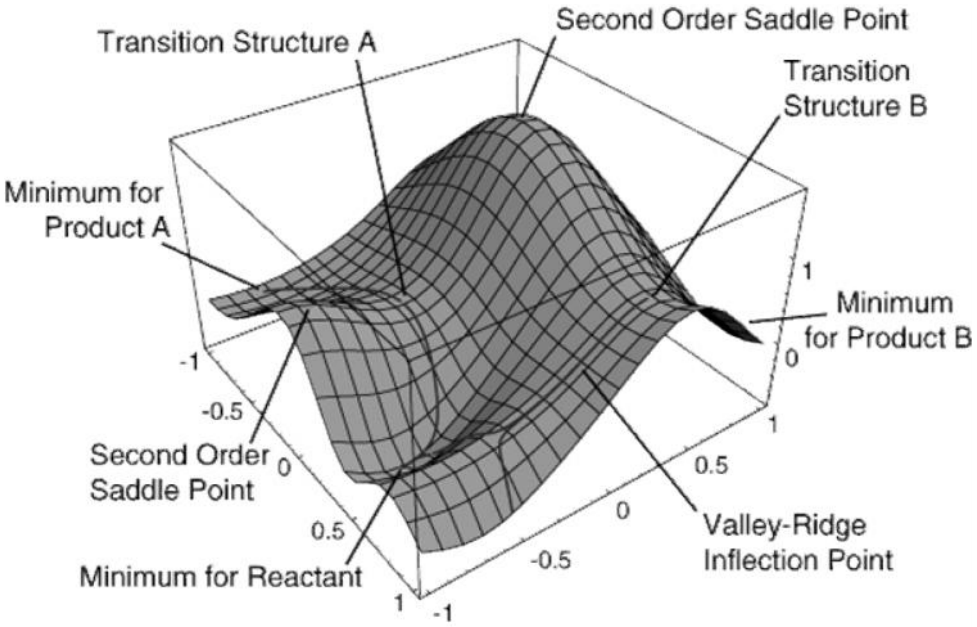

Figure 2.3: Three-dimensional cross-section of a multidimensional potential energy hyper surface [http://www.chem.wayne.edu/~hbs/chm6440/PES.html]

The second partial derivatives form a matrix called the Hessian or force constant matrix. The stationary points are characterized by the Hessian: If all eigen values of the Hessian are positive, it is a local minimum of the multidimensional potential energy surface. If all are negative, the point is a local maximum. A point with one negative eigen value is a first order saddle point and represents a minimum from all directions except one, with respect to which it is maximum. First order saddle points therefore represent transition states in chemical reactions.

2.4 ANTISYMMETRY OR PAULI EXCLUSION PRINCIPLE

The electronic Hamiltonian in equation (2.3) depends only on the spatial coordinates of the electrons. To completely describe an electron it is necessary to specify its spin. To incorporate the spin, two spin functions α(ω), and β(ω), corresponding to spin up and down respectively, are introduced. These functions are orthonormal, i.e.,

$$\langle \sim | \sim \rangle = \langle \quad | \quad \rangle = 1 \qquad (2.8)$$

and $$\langle \sim | \quad \rangle = \langle \quad | \sim \rangle = 0 \qquad (2.9)$$

here an electron is described not only by the three spatial coordinates but also by one spin coordinate. These four coordinates collectively are represented as X,. where X= (x,y,z,ω)

The wavefunction for an N electron system can be written as $\Phi(X_1, X_2, X_3, \ldots X_N)$. Because the Hamiltonian operator does not involve spin, making the wavefunction depend on spin does not make any difference by itself. What does is the fact that electrons are Fermions, and as such are goverened by the antisymmetry principle: A many electron wavefunction must be antisymmetric with respect to the interchange of the coordinates (both space and spin) of any two electrons. i.e.

$$\Phi(X_1, X_2, X_3 \ldots\ldots X_i \ldots\ldots X_j \ldots\ldots X_N) = -\Phi(X_1, X_2, X_3 \ldots\ldots X_j \ldots\ldots X_i \ldots\ldots X_N) \qquad (2.10)$$

The antisymmetry requirement leads to the Pauli Exclusion Principle.

2.5 THE HARTREE METHOD

In the Hartree method a wavefunction Ψ is sought to be expressed as the product of wavefunctions of each particle.

This form of wavefunction would be exact if the Hamiltonian was the sum of one particle operators and the particles themselves were distinguishable. Since interelectronic interaction exists, an iterative scheme is used to successively improve approximate starting functions, till at some stage the difference between current and previous function becomes sufficiently small - this is called the self-consistent field method. However indistinguishablity of electrons imposes the antisymmetry requirement on the wavefunctions, and this cannot be satisfied by the simple Hartree product functions.

2.6 SLATER DETERMINANTS

The simplest form of many-electron function to satisfy the antisymmetry principle is the Slater determinant. For an N-electron system the Slater determinant may be written as,

$$\Psi(X_1, X_2, \ldots\ldots\ldots\ldots X_N) = \frac{1}{\sqrt{N!}} \begin{vmatrix} \cdot_i(X_1) & \cdot_j(X_1) & \ldots\ldots & \cdot_k(X_1) \\ \cdot_i(X_2) & \cdot_j(X_2) & \ldots\ldots & \cdot_k(X_2) \\ .. & .. & \ldots\ldots & .. \\ .. & .. & \ldots\ldots & .. \\ .. & .. & \ldots\ldots & .. \\ \cdot_i(X_N) & \cdot_j(X_N) & \ldots\ldots & \cdot_k(X_N) \end{vmatrix} \qquad (2.11)$$

The factor $\frac{1}{\sqrt{N!}}$ ensures normalization of the determinant, which contains N! terms. Antisymmetry is satisfied as interchange of two rows (corresponding to two specific electrons) changes the sign of the determinant.

2.7 THE HARTREE-FOCK (HF) METHOD

In the HF method, a wavefunction of the Slater determinant form is sought, with the electron-electron repulsion treated in an average way. Each electron is considered to be moving in the field of the fixed nuclei and average field of the other N-1 electrons. The spin orbitals (a product of a spatial orbital and a spin function) that give the best N-electron determinantal wavefunction are found by minimizing the expectation value of energy with respect to variations in the spin-orbitals, subject to requirements of orthonormality.

The application of this procedure leads to the Hartree-Fock equation for the individual spinorbitals. The Hartree-Fock equation for spinorbital $\psi_a(1)$ is

$$f_1\psi_a(1) = E_a\,\psi_a(1) \tag{2.12}$$

where E_a is the orbital energy of the spinorbital and f_1 is the Fock operator.

$$f_1 = h_1 + \sum_u \{J_u(1) - K_u(1)\} \tag{2.13}$$

h_1 is the core Hamiltonian for the electron 1, and J_u and K_u are the Coulomb and exchange operator respectively, and can be defined as follows:

$$J_u(1)\cdot_a(1) = \left\{\int \cdot_u^*(2)\left(\frac{1}{r_{12}}\right)\cdot_u(2)dX_2\right\}\cdot_a(1) \tag{2.14}$$

$$K_u(1)\cdot_a(1) = \left\{\int \cdot_u^*(2)\left(\frac{1}{r_{12}}\right)\cdot_a(2)dX_2\right\}\cdot_u(1) \tag{2.15}$$

The Coulomb and exchange operators are defined in terms of spinorbitals rather than in terms of spatial wavefunctions. The Coulomb operator takes into account the Coulombic repulsion between electrons, and the exchange operator represents the modification of this energy that can be ascribed to the effects of spin correlation. It follows that the sum in equation (2.13) represents the average potential energy of electron 1 due to the presence of the other N-1 electrons.

Each spin orbitals must be obtained by solving an equation of the form of equation (2.12) with the corresponding Fock operator f_i. However, because f_i depends on the

spinorbitals of all the other N-1 electrons, it appears that to set up the HF equation, one must know the solutions beforehand. This apparent paradox is handled by adopting an iterative type of solution, and stopping when the solution is self-consistent. In self-consistent procedure, a trial set of spinorbitals is constructed and used to formulate the Fock operator, and then the HF equations are solved to obtain a new set of spinorbitals which are used to construct a revised Fock operator, and so on. The cycle of calculation and reformation is repeated until a chosen convergence criterion is satisfied. The total energy of the system however is not the sum of the one-electron energies as the Hartree-Fock scheme involves double counting of the electron-electron interactions.

2.8 RESTRICTED AND UNRESTRICTED HF MODELS

In a closed system or a fully filled orbital system, each spatial orbital is occupied by two electrons with opposite spins, whereas in an open-shell system there are partially filled spatial orbitals containing only one electron. If the number of electrons present in the system is odd, it will be always an open-shell system. In a closed-shell system, the orbitals can be grouped in pairs with the same spatial dependence and orbital energy but with opposite spins (spin functions α and β). The setting up of the HF model by imposing the double occupancy principle is called the Restricted Hartree-Fock (RHF) model. For an open-shell system, orbital pairing does not occur in any level of computation. There are two possibilities for extending HF calculations to open-shell systems:

1. Strictly presuming that orbital pairing does not occur in any level. Each spinorbital is allowed to have its own spatial part. This type of modeling is known as Unrestricted Hartree-Fock (UHF) method.

2. The RHF procedure is extended to spatial orbitals other than the orbitals which are singly occupied. Modeling of this type is known as restricted open shell Hartree-Fock modeling (ROHF).

2.9 ROOTHAAN-HALL EQUATIONS

The Hartree-Fock method attempts to construct appropriate one electron ψ_i orbital functions and find their optimum forms using variational theory. This is reasonably straight forward in atoms because the spherical symmetry of the system allows us to use the angular part of the hydrogen wavefunction without changes and thus only the radial part of

the wavefunction must be varied. This reduces the complexity of the problem. Unfortunately, the same method is inconceivable for molecules and requires modification. In 1951, C.C.J. Roothaan and G.G Hall independently suggested using a known set of basis functions with which to expand the spinorbitals [Roothaan, 1951; Hall, 1951]. Roothaan-Hall equations are obtained by applying the variational principle and using one electron functions expressed as linear combination of atomic orbitals (LCAOs) in the HF equation. Roothaan-Hall equations apply to closed-shell molecules or atoms where all molecular orbitals or atomic orbitals are doubly occupied. With a suitable set of basis functions, the orbitals can be represented as:

$$\phi_i = \sum c_{ij}\,\chi_j \tag{2.16}$$

Where χ_j is a basis function.

Using one electron functions of this form, the HF equation takes the form known as Roothaan-Hall equations (2.17)

$$\sum_{\nu} F_{\mu\nu} C_{\nu i} = \varepsilon_i \sum_{\nu} S_{\mu\nu} C_{\nu i} \tag{2.17}$$

and can be expressed in matrix form as

$$\mathbf{FC} = \mathbf{SCE} \tag{2.18}$$

The elements of $\overline{S}$ are called overlap integrals:

$$S_{ij} = \int \chi_i^*(1)\,\chi_j(1)\,d\tau_1 \tag{2.19}$$

And the Fock matrix elements F_{ij} are

$$F_{ij} = \int \chi_i^*(1)\,f_1\,\chi_j(1)\,d\tau_1 \tag{2.20}$$

Where f_1 is given by (2.13)

The matrix C contains the coefficients of expansion of the MO's in terms of the chosen basis; the column indices corresponds to MO's and the row indices to the basis functions. As **F** = **F(C)** its solution involves the familiar iterative process where we start with an approximate **C** and generate a first approximation to **F**, then obtain an (improved) **C** by solving **FC** = **SCF** and so on till self consistency is reached to within the desired tolerance limits.

2.10 BASIS SETS

Since the relevant Hilbert space is infinite dimensional, an infinite number of basis functions are needed to expand the molecular orbitals. A very considerable effort has gone into choosing finite sets of basis functions such that the MO's are adequately representable in terms of them. Minimization of computation time without too great a loss of accuracy has been the goal of all such efforts. Early calculations used basis functions centered on each atom which were of the form $r_A^{n-1}e^{-,r_A}$ (radial part only). Where r_A is the distance from centre A, and ¸ is an exponent and n is the principal quantum number. These functions were called Slater Type functions or STF's. The exponents used in early work were given by Slater's rule [Slater, 1930] and later authors determined optimum exponents from calculations on atoms [Clementi and Raimondi, 1963; Clementi et al., 1967]

More accurate calculations used two STF's with different (optimized) ¸ values corresponding to each AO; these then gave double zeta (DZ) basis sets. Evaluation of multicentre integrals, especially over two-electron operators was quite difficult over STF's. This led Boys [Boys, 1950] to propose the use of Gaussian type orbitals or GTF's. This makes the evaluation of integrals easy since the product of two Gaussians centered at two points A and B is a Gaussian centered at a point C on the line AB.

However Gaussian functions have the wrong cusp behavior at r = 0, and to get results comparable to those obtained with a modest slater type basis one needed to use a large number of Gaussian basis functions. A via media was found in the use of contracted Gaussian basis sets, where a number of primitive Gaussians with different exponents are linearly combined with fixed coefficients to give basis functions. The SCF procedure varies coefficients for functions of this type, while the 'inner' contraction coefficients are untouched.

A Cartesian Gaussian centered on atom *A* can be represented as:

$$G_{i,j,k} = Nx_A^i y_A^j z_A^k e^{-\sim r_A^2} \qquad (2.21)$$

where *i*, *j*, and *k* are nonnegative integers, α is a positive orbital exponent, x_a, y_a, z_a are Cartesian coordinates with the origin at *A*, and *N* is the Cartesian Gaussian normalization constant. This constant is given by the expression:

$$N = \left(\frac{2\sim}{\circledR}\right)^{3/4}\left[\frac{(8\sim)^{i+j+k}\, i!\, j!k!}{(2i)!(2j)!(2k)!}\right]^{1/2} \qquad (2.22)$$

when $i = 0$, $j = 0$, $k = 0$ and $i + j + k = 0$, then the Gaussian type function (GTF) is known as an *s*-type function; when $i + j + k = 1$, as a *p*-type function , when $i + j + k = 2$, it is a *d*-type function, and so on.

2.10.1 TYPES OF BASIS SETS

2.10.1.1 Minimal Basis Sets

In a minimal basis set one basis function is selected for every atomic orbital that is required to describe the free atom. All the orbitals in a given shell are taken into consideration. The most commonly used minimal basis sets are the STO-*n*G sets devised by John Pople and his group. It involves a linear combination of "*n*" GTOs fitted to each STO. The individual GTOs are called primitive orbitals, while the linear combinations are called contracted functions. The STO-3G basis set is a minimal basis set, in which each basis function is a contraction of three primitive Gaussians. The exponents and expansion coefficients for the primitives are obtained from a least squares fit to STOs. STO-3G basis sets are available for the elements H-Xe. They are commonly not used in serious work, but they provide a rapid way of obtaining a "quick and dirty" look at a molecule.

2.10.1.2 Double Zeta and Split Valence Basis Sets

A double-zeta (DZ) basis set uses two functions where the minimal basis set had only one function. In double-zeta basis sets each atomic orbital function is represented by two basis functions, each basis function typically being a contraction of a small set of primitives. The D95 basis set of Dunning and coworkers are DZ type basis sets which uses 9 s-type primitive Gaussians to describe the 1s and 2s atomic orbital [Dunning and Hay, 1976]. Split valence (SV) basis sets were introduced by Pople and coworkers in late 1970s. An SV basis set is single zeta for the inner shell orbitals and double zeta for valence shell. A triple zeta (TZ) basis set uses three basis functions instead of one. The smallest SV basis set is the 3-21G set, which uses three primitive expansion of inner core orbitals and represents each valence orbital by two basis functions, one function being a contraction of two Gaussians and the other function being just a single Gaussian.

2.10.1.3 Polarized Basis Sets

Polarized basis sets improve the representation of molecular orbital by adding functions with angular momentum higher than is required for the description of each atom of the ground state. For example, polarized basis sets add *d* functions for carbon atoms and *f* functions for transition metals and in some cases add *p* functions for hydrogen atoms. The 6-31G(d,p) set or 6-31G** set is a polarized basis set which uses *p* functions on the hydrogen atoms and *d* functions on first row atoms over and above the 6-31G set. It is possible to use polarization functions of still higher angular momenta too.

2.11 CONFIGURATION INTERACTION

In Hartree-Fock method the effect of N-1 electrons on an electron of interest is treated in an average way, i.e. HF method does not take into account electron correlation. The HF method yields a finite set of spin orbitals when a finite basis set expansion is used. In general, a basis with M members results in 2M different spin orbitals. Out of 2M spin orbitals it takes n lowest energy orbitals and remaining 2M-n are virtual orbitals. Therefore we can form Hartree-Fock wavefunction Φ_0, which can be denoted as

$$\Phi_0 = \left| \text{¤}_1 \text{¤}_2 \ldots\ldots \text{¤}_a \text{¤}_b \ldots\ldots\ldots \text{¤}_n \right| \tag{2.23}$$

Where Φ_a and Φ_b are among the n occupied spinorbitals for the HF ground state.

A singly excited determinant corresponds to one for which a single electron in occupied spin orbital Φ_a has been promoted to a virtual spinorbital Φ_p

$$\Phi_0^p = \left| \text{¤}_1 \text{¤}_2 \ldots\ldots \text{¤}_p \text{¤}_b \ldots\ldots\ldots \text{¤}_n \right| \tag{2.24}$$

A doubly excited determinant is one in which two electron have been promoted, one from Φ_a to Φ_p and another from Φ_b to Φ_q

$$\Phi_{ab}^{pq} = \left| \text{¤}_1 \text{¤}_2 \ldots\ldots \text{¤}_p \text{¤}_q \ldots\ldots\ldots \text{¤}_n \right| \tag{2.25}$$

In a similar manner multiply excited determinants can be formed. Each of the determinants, or a linear combination of a small number of them constructed so as to have the correct electronic symmetry, is called a configuration state function (CSF).

The exact ground state and excited state wavefunctions can be expressed as linear combination of all possible n-electron Slater determinants arising from a complete set of

spin orbitals [Lowdin, 2007]. The exact electronic wavefunction ψ for any state of the system can be expressed as:

$$\cdot = C_0 ¤_0 + \sum_{a,p} C_a^p ¤_a^p + \sum_{\substack{a<b \\ p<q}} C_{ab}^{pq} ¤_{ab}^{pq} + \sum_{\substack{a<b<c \\ p<q<r}} C_{abc}^{pqr} ¤_{abc}^{pqr} + \ldots\ldots \tag{2.26}$$

where the C's are expansion coefficients and a given excited determinant appears only once in the summation. An *ab-initio* method in which the wavefunction is expressed as a linear combination of determinants is termed a Configuration Interaction (CI) method.

The energy associated with the exact ground state wavefunction of the form of equation 2.26 is the exact nonrelativistic ground state energy. The difference between this exact energy and the HF limit is called the correlation energy. Configuration interaction takes into account the electron correlation missed out in the Hartree-Fock method.

But even with a small number of electrons and relatively small number of basis set functions, the total number of determinants can be extremely large. Therefore, the expansion in equation 2.26 must almost always be truncated. Nonetheless, although the calculation is limited to a finite set of spin orbitals and only a fraction of all possible determinants, CI is a popular method for the calculation of accurate molecular wavefunctions. Even with a small number of CSFs it can correct for one of the deficiencies that stem from the use of only doubly occupied orbitals in the restricted HF method, the incorrect behavior at the dissociation limit of a molecule. A calculation in which the incorrect behavior of the HF wavefunction upon dissociation is corrected accounts for an important part of the correlation energy called nondynamic correlation or structural correlation. On the other hand, dynamic correlation accounts for the error in the HF wavefunction at short interatomic distances.

In CI calculation, the ground or excited state wavefunction, ψ, for state *s* is represented as a linear combination of N-electron Slater determinants. Equation 2.26 can be written in simpler form as:

$$\cdot_s = \sum_{J=1}^{L} C_{Js} \Phi_J \tag{2.27}$$

where the sum is over a number L of determinants Φ_J with expansion coefficients C_{Js} for the states.

2.12 MULTICONFIGURATION AND PERTURBATION METHODS

2.12.1 MULTI-CONFIGURATION SELF-CONSISTENT FIELD

The Multi-Configuration Self-Consistent Field (MCSCF) method can be considered as a CI where not only are the coefficients of the determinants optimized by the variational principle, but the MOs used for constructing the determinants are also optimized. The MCSCF optimization is iterative like the SCF procedure (if the "number of configurations" is only one, it reduces to HF). Since the number of MCSCF iterations required for achieving convergence tends to increase with the number of configurations included, the size of MCSCF wave functions that can be treated is somewhat smaller than for CI methods.

When deriving the HF equations only the variation of the energy with respect to an orbital variation was required to be zero, which is equivalent to the first derivatives of the energy with respect to the MO expansion coefficients being equal to zero. The HF equations can be solved by an iterative SCF method. There is, however, no guarantee that the solution found by the SCF procedure is a minimum of the energy as a function of the MO coefficients. In order to ensure that a minimum has been found, the matrix of second derivatives of the energy with respect to the MO coefficients can be calculated and diagonalized, with a minimum having only positive eigenvalues. This is rarely checked for SCF wave functions; in the large majority of cases the SCF procedure converges to a minimum without problems. MCSCF wave functions, on the other hand, are much harder to converge, and much more prone to converge on solutions that are not minima. MCSCF wave function optimizations are therefore normally carried out by expanding the energy to second order in the variational parameters (orbital and configurational coefficients) and using Newton–Raphson-based methods to force convergence to a minimum.

MCSCF methods can be considered as an extension of single-determinant methods to give a qualitatively correct description. MCSCF methods are mainly used for generating a qualitatively correct wave function, i.e. recovering the "static" part of the correlation. The major problem with MCSCF methods is selecting which configurations are necessary to include for the property of interest. One of the most popular approaches is the Complete Active Space Self-Consistent Field (CASSCF) method (also called Full Optimized Reaction Space (FORS)). Here the selection of configurations is done by partitioning the

MOs into active and inactive spaces. The active MOs will typically be some of the highest occupied and some of the lowest unoccupied MOs from an RHF calculation. The inactive MOs have either 2 or 0 electrons, i.e. always either doubly occupied or empty. Within the active MOs a full CI is performed and all the proper symmetry-adapted configurations are included in the MCSCF optimization. Which MOs to include in the active space, must be decided manually by considering the problem at hand and the computational expense. If several points on the potential energy surface are desired, the MCSCF active space should include all those orbitals that change significantly, or for which the electron correlation is expected to change. A common notation is [n,m]-CASSCF, which indicates that n electrons are distributed in all possible ways in m orbitals. As for any full CI expansion, the CASSCF becomes unmanageably large even for quite small active spaces. A variation of the CASSCF procedure is the Restricted Active Space Self-Consistent Field (RASSCF) method. Here the active MOs are divided into three sections, RAS1, RAS2 and RAS3, each having restrictions on the occupation numbers (excitations) allowed. A typical model consists of the configurations in the RAS2 space being generated by a full CI (analogously to CASSCF), or perhaps limited to SDTQ excitations. The RAS1 space consists of MOs that are doubly occupied in the HF reference determinant, and the RAS3 space consists of MOs that are empty in the HF. Configurations additional to those from the RAS2 space are generated by allowing for example a maximum of two electrons to be excited from the RAS1 and maximum of two electrons to be excited to the RAS3 space. In essence, a typical RASSCF procedure thus generates configurations by a combination of a full CI in a small number of MOs (RAS2) and a CISD in a somewhat larger MO space (RAS1and RAS3).

The full CI expansion within the active space severely restricts the number of orbitals and electrons that can be treated by CASSCF methods. Table 2.1 shows how many singlet CSFs are generated for an [n,n]-CASSCF wave function without reductions arising from symmetry

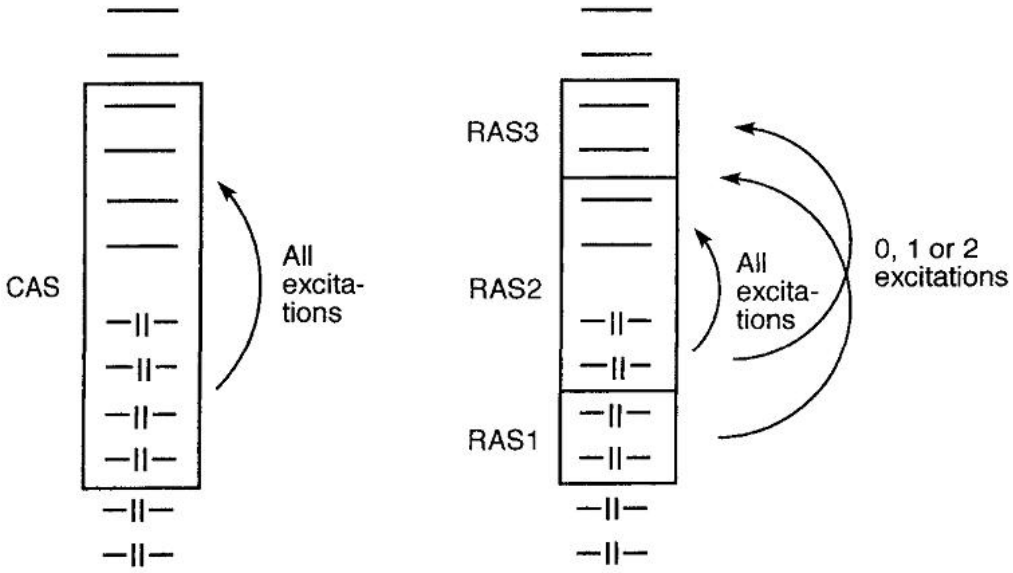

Figure 2.4: Illustration of CAS and RAS partitions

.

Table 2.1: Number of configurations generated in an [n,n]-CASSCF wave function

N	Number of CSFs
2	3
4	20
6	175
8	1764
10	19404
12	226512
14	2760615

The factorial increase in the number of CSFs (Configurational state functions) effectively limits the active space for CASSCF wave functions to fewer than 10–12 electrons/orbitals. Selecting the "important" orbitals to correlate therefore becomes very important. The goal of MCSCF methods is usually not to recover a large fraction of the total correlation energy, but rather to recover all the changes that occur in the correlation energy for the given process. Selecting the active space for an MCSCF calculation requires some insight into the problem. There are a few rules of thumb that may be of help in selecting a proper set of orbitals for the active space:

(1) For each occupied orbital, there will typically be one corresponding virtual orbital. This leads naturally to [n,m]-CASSCF wave functions where n and m are identical or nearly so.

(2) Including all the valence orbitals, i.e. the space spanned by a minimum basis set, leads to a wave function that can correctly describe all dissociation pathways. Unfortunately, a full valence CASSCF wave function rapidly becomes unmanageably large for realistic-sized systems.

(3) The orbital energies from an RHF calculation may be used for selecting the important orbitals. The highest occupied and lowest unoccupied are usually the most important orbitals to include in the active space. This can be partly justified by the formula for the second-order perturbation energy correction, the smaller the orbital energy difference, the larger contribution to the correlation energy. Using RHF orbital energies for selecting the active space may be problematic in two situations.The first is when extended basis sets are used, where there will be many virtual orbitals with low energies, and the exact order is more or less accidental. Furthermore, RHF virtual orbitals basically describe electron attachment and are therefore not particularly well suited for describing electron correlation. An inspection of the form of the orbitals may reveal which to choose: they should be the ones that resemble the occupied orbitals in terms of basis function contribution. The second problem is more fundamental. If the real wave function has significant multi-configurational character, then the RHF may be qualitatively wrong, and selecting the active orbitals based on a qualitatively wrong wave function may lead to erroneous results. The problem is that we wish to include the important orbitals for describing the multi determinant nature, but these are not known until the final wave function is known.

(4) An attempt to overcome this self-referencing problem is to use natural orbitals. The natural orbitals are those that diagonalize the density matrix, and the eigenvalues are the occupation numbers. Orbitals with occupation numbers significantly different from 0 or 2 (for a closed shell system) are usually those that are the most important to include in the active space. An RHF wave function will have occupation numbers of exactly 0 or 2, and some electron correlation must be included to obtain orbitals with non-integer occupation numbers. This may for example be done by running a preliminary MP2 or CISD calculation prior to the MCSCF. Alternatively, a UHF (when different from RHF) type

wave function may also be used. The total UHF density, which is the sum of the α and β density matrices, will also provide fractional occupation numbers since UHF includes some electron correlation. The procedure may still fail. If the underlying RHF wave function is poor, the MP2 correction may also give poor results, and selecting the active MCSCF orbitals based on MP2 occupation number may again lead to erroneous results. In practice, however, selecting active orbitals based on, for example, MP2 occupation numbers appears to be quite efficient, and better than using RHF orbital energies.

In a CASSCF type wave function the CI coefficients do not have the same significance as for a single-reference CI based on HF orbitals. In a full CI (as in the active space of the CASSCF), the orbitals may be rotated among themselves without affecting the total wave function. A rotation of the orbitals, however, influences the magnitude of the coefficients in front of each CSF. While the HF coefficient in a single-reference CISD gives some indication of the "multi-reference" nature of the wave function, this is not the case for a CASSCF wave function, where the corresponding CI coefficient is arbitrary. It should be noted that CASSCF methods inherently tend to give an unbalanced description, since all the electron correlation recovered is in the active space,with none in the inactive space, or between the active and inactive electrons. This is not a problem if all the valence electrons are included in the active space, but this is only possible for small systems. If only part of the valence electrons is included in the active space, the CASSCF method tends to overestimate the importance of "biradical" structures.

2.12.2 MULTI-REFERENCE CONfiGURATION INTERACTION

The CI methods described so far consider only CSFs generated by exciting electrons from a single determinant. This corresponds to having an HF type wave function as the reference. However, an MCSCF wave function may also be chosen as the reference. In that case, a CISD involves excitations of one or two electrons out of all the determinants that enter the MCSCF, defining the Multi-Reference Configuration Interaction (MRCI) method. Compared with the single-reference CISD, the number of configurations is increased by a factor roughly equal to the number of configurations included in the MCSCF. Large-scale MRCI wave functions (many configurations in the MCSCF) can generate very accurate wave functions, but are also computationally very intensive. Since MRCI methods truncate the CI expansion, they are not size extensive.Even truncating the

(MR) CI expansion at the singles and doubles level frequently generates more configurations than can be handled readily. A further truncation is sometimes performed by selecting only those configurations that have an "interaction" with the reference configuration(s) above a selected threshold,where the "interaction" is evaluated by second-order perturbation theory. Such state-selected CI (or MCSCF) methods all involve a preset cutoff below which configurations are neglected. This may cause problems for comparing energies of different geometries, since the potential energy surface may become discontinuous, i.e. at some point the importance of a given configuration drops below the threshold, and the contribution suddenly disappears.

2.12.3 MØLLER-PLESSET MANY-BODY PERTURBATION THEORY

Configuration interaction calculations provide a systematic approach for going beyond the Hartree-Fock level, by including determinants that are successively singly excited, doubly excited, triply excited and so on, from a reference configuration. One important feature of the method is that it is variational, but one disadvantage is its lack of size-consistency. Perturbation theory provides an alternative systematic approach for finding the correlation energy. Perturbation theory calculations are size consistent but they are not variational, i.e. it does not in general give energies that are upper bound to the exact energy.

The application of perturbation theory to a system composed of many interacting particles is called many-body perturbation theory (MBPT). Our aim is to find the correlation energy for the ground state, so it is required to take the zero-order hamiltonian as the sum of the Fock operators of the Hartree-Fock method. This choice of Hamiltonian was first made by C. Møller and M.S. Plesset and hence the procedure is called Møller-Plesset Perturbation Theory (MPPT).

In Møller-Plesset perturbation theory, the zero order Hamiltonian $H^{(0)}$ is given by the sum of one electron Fock operators :

$$H^{(0)} = \sum_{i=1}^{n} f_i \qquad (2.28)$$

The HF ground state wavefunction Φ_0 is an eigenfunction of H_{HF} with an eigenvalue $E^{(0)}$ given by the sum of the orbital energies of all the occupied spin orbitals.

The perturbation $H^{(1)}$ is given by

$$H^{(1)} = H - \sum_{i=1}^{n} f_i \tag{2.29}$$

where, H is the electronic Hamiltonian. The HF energy E_{HF} associated with the ground state HF wavefunction Φ_0 is the expectation value

$$E_{HF} = \langle \Phi_0 \mid H \mid \Phi_0 \rangle \tag{2.30}$$

or

$$E_{HF} = \langle \Phi_0 \mid H_{HF} + H^{(1)} \mid \Phi_0 \rangle \tag{2.31}$$

$$E^{(0)} = \langle \Phi_0 \mid H_{HF} \mid \Phi_0 \rangle \tag{2.32}$$

and

$$E^{(1)} = \langle \Phi_0 \mid H^{(1)} \mid \Phi_0 \rangle \tag{2.33}$$

Hence $E_{HF} = E^{(0)} + E^{(1)}$

Therefore, the first correction to the ground state energy is given by second order perturbation theory as

$$E^{(2)} = \sum_{J \neq 0} \frac{\langle \Phi_J \mid H^{(1)} \mid \Phi_0 \rangle \langle \Phi_0 \mid H^{(1)} \mid \Phi_J \rangle}{E^{(0)} - E_J} \tag{2.34}$$

$$\langle \Phi_J \mid H_{HF} \mid \Phi_0 \rangle = 0 \tag{2.35}$$

Because Φ_0 is an eigenfunction of the H_{HF}, the spin orbitals and hence the determinants, are orthogonal.

2.13 COUPLED CLUSTER (CC) METHOD

One of the most popular alternative ab initio methods for computing molecular energies including substantial amounts of correlation energy and concomitantly for computing wavefunctions of higher accuracy is the coupled cluster method. The method was originally developed for work in nuclear physics [Coester and Kummel, 1960] and was adapted to use in molecular structure work by Cizek, Paldus, Sinanoglu, Nesbet, Bartlett and other [Paldus et al, 1972; Neset, 1968; Sinanoglu, 1962; Bartlett, 1989]. The coupled cluster method attemts to build correlation into the SCF single determinantal function by systematically adding 2-particle, 3-particle etc. ‘cluster functions’ to groups of 2, 3, etc.

orbitals used in building up the Slater determinant. 1-particle cluster fuctions are also used to account for the change in the orbital basis necessitated by the introduction of cluster fuctions. The form of the cluster expansion wave functions is best determed by writing them as operator products in the second quantization formalism. Letting Φ_0 stand for the single determinant built of orbitals $¤_i, ¤_j, ...etc.,$

$$\Phi_0 = \left| ¤_i, ¤_j, ... \right\rangle \tag{2.36}$$

we wish to construct the exact function Φ

We attempt to find the cluster functions f_{ij} as two-particle functions that incorporate the correlation between electrons in $¤_i$ and $¤_j$ by replacing their 'product' $¤_i$ by

$$¤_i.¤_j + f_{ij} \tag{2.37}$$

Thereby converting the single determinant function into a combination of them.

We define

$$f_{ij}(\vec{X}_1, \vec{X}_2) = \frac{1}{2}\sum_{a,b} t_{ij}^{ab} \left\{ ¤_a(x_1)¤_b(x_2) - ¤_b(x_1)¤_a(x_2) \right\} \tag{2.38}$$

Where a, b run over the virtual orbital space and x_1, x_2 represent the spatial and spin oordinates of electrons 1 and 2 respectively.

An operator that replaces $¤_i.¤_j$ by f_{ij} can be shown to be

$$\hat{t}_{ij} = \frac{1}{2}\sum_{a,b} t_{ij}^{ab} a^{\dagger} b^{\dagger} ji \tag{2.39}$$

$a^{\dagger}, b^{\dagger}$ are creation operator and *j*, *i* are annihilation operator. The coefficient satisfy the relationwith, $t_{ij}^{ab} = -t_{ij}^{ba}, t_{ij}^{ab} = -t_{ji}^{ab}$

Products of cluster functions may be produced by successive application of cluster operators:

$$\hat{t}_{ij}\, \hat{t}_{kl} \left| ijkl \right\rangle = \left| f_{ij}\, f_{kl} \right\rangle \tag{2.40}$$

The one particle operator may be defined

$$\hat{t}_i = \sum_a t_i^a a^{\dagger} i \tag{2.41}$$

The interaction equation reduces to

$$\Phi = \left\{1 + \sum_i \hat{t}_i + \frac{1}{2}\sum_{ij} \hat{t}_i \hat{t}_j + \frac{1}{6}\sum_{ijk} \hat{t}_i \hat{t}_j \hat{t}_k + ... + \frac{1}{2}\sum_{ij} \hat{t}_{ij} + \frac{1}{2}\sum_{ijk} \hat{t}_{ij} \hat{t}_k + \frac{1}{4}\sum_{ijkl} \hat{t}_{ij} \hat{t}_k \hat{t}_l + \frac{1}{8}\sum_{ijkl} \hat{t}_{ij} \hat{t}_{kl} + ...\right\}$$

(2.42)

Further defining

$$\hat{T}_1 = \sum_i \hat{t}_i \tag{2.43}$$

$$\hat{T}_2 = \sum_{ij} \hat{t}_{ij} \quad \text{etc.} \tag{2.44}$$

The expansion may be seen to become

$$\Phi = (1 + \hat{T}_1 + \frac{1}{\lfloor 2} \hat{T}_1^2 + \frac{1}{\lfloor 3} \hat{T}_1^3 + ... + \hat{T}_2 + \hat{T}_2 \hat{T}_1 + ...)\Phi_0 \tag{2.45}$$

Since $\hat{T}_1$ and $\hat{T}_2$ commute, it may me written in exponential form as

$$\Phi = e^{T_1 + T_2}\Phi_0 \tag{2.46}$$

Including higher clusters also and defining

$$\hat{T} = \hat{T}_1 + \hat{T}_2 + \hat{T}_3 + ... \tag{2.47}$$

The relation

$$\Phi = e^{\hat{T}}\Phi_0 \tag{2.48}$$

builds up the exact wave function from the reference wave function

Restricting ourselves to

$$\hat{T} = \hat{T}_1 + \hat{T}_2 \tag{2.49}$$

alone gives as the CCSD (Coupled Cluster Singles and Doubles) method

With $\hat{T} = \hat{T}_1 + \hat{T}_2 + \hat{T}_3$ one obtains the coupled cluster singles doubles and triples (CCSDT) method [Noga and Bartlett, 1987]. CCSDT calculations gives very good estimate for correlation energies but are very demanding computationally and are only feasible for small molecules with small basis sets. Several approximate forms of CCSDT have been developed. The most widely used method is CCSD(T). CCD, CCSD, CCSD(T) and CCSDT methods are size consistent but not variational. Analytical gradients are available for these methods.

2.14 QUADRATIC CONFIGURATION INTERACTION (QCI) METHOD

Pople and coworkers developed the nonvariational QCI method which is intermediate between the CC and CI methods [Pople et al., 1987] The QCI methods exists in the size-consistent forms QCISD, which is an approximation to CCSD and QCISD(T) and is similar to CCSD+T(CCSD). QCISD(T) has given excellent results for correlation energies in many calculations. CCSD(T) and QCISD(T) methods appear to be the most accurate, yet computationally tractable. Calculations at some systems indicates that CCSD(T) is applicable for a wider range of problems than QCISD(T) [Raghavachari and Anderson, 1996]. These two methods require similar amounts of computer time and give very accurate molecular geometries and vibrational frequencies in addition to good energies.

2.15 SEMIEMPIRICAL SCF-MO METHODS

In the days when computational power was limited, *ab initio* methods could only be used with very small molecules. Several approximate methods using only valence electrons were tried out, but the first such methods using SCF formalism were proposed by Pople and co-workers [Seeger and Pople, 1976]. These methods neglected small integrals by selective application of zero differential overlap or ZDO approximations, and were named the Complete Neglect of Differential Overlap, intermediate neglect of differential overlap and the Neglect of Diatomic Differential Overlap methods (CNDO, INDO and NDDO). They were designed to mimic the results of *ab initio* minimal basis HF calculations and used a 'valence only' slater type basis. The only integrals calculated were the overlap integrals, and the other quantities were estimated from spectroscopic results. The School of Dewar [Bingham et al., 1975] sought to reproduce thermochemical results from their variants of INDO and NDDO and the result was the MINDO and MNDO schemes, where the M stood for 'modified'. Another member of the semiempirical family was the PRDDO (Partial Retention of Diatomic Differential Overlap) method of Halgren and Lipscomb (1972), devised to reproduce electrostatic potentials. A variety of semiempirical schemes to suit particular objectives has been developed by several authors and has been reviewed by Hasanein and Evans (1996). Currently popular among these are the AM1 and PM3 methods of Dewar and coworkers [Dewar et al., 1978; Stewart, 1989].

2.16 DENSITY FUNCTIONAL THEORY

Hartree-Fock method treats electron-electron interactions only in an averaged fashion, and the essentially correlated nature of the electronic motion is mostly unaccounted for. Correlation between like spins is accounted for by the exchange integrals, but that between electrons of unlike spin is not. This leads to the Hartree-Fock energy being higher than the exact (non-relativistic) energy. The usual ways of improving on the HF energy such as configuration interaction, higher order MBPT calculations etc. are costly for systems of even moderate size.

This scenario makes the alternative provided by Density Functional Theory (DFT) very attractive [Gadre and Bendale 1983]. DFT has its historical origins in the Thomas-Fermi statistical model of the atom and its logical foundations were laid by the theorems of Hohenberg and Kohn. For a system of many electrons in its ground (time independent) state, these authors established a correspondence between the electron density $°(\vec{r})$ and the external potential $V(\vec{r})$ [Hohenber and Kohn, 1964].

Further they expressed the energy of the system as a functional of the density, and demonstrated that the correct density minimizes this functional in the variational sense. The expression for the energy functional is,

$$E[\rho] = T[\rho] + V_{ext}[\rho] + U[\rho] \qquad (2.50)$$

Where T[ρ] is the kinetic energy functional, $V_{ext}[°] = \int °\hat{V}(\vec{r})d^2$ is the potential energy functional and U[ρ] gives the energy of the electron-electron interactions [Parr et al.1979], and includes the classical terms,

$$\int \frac{°(1)°(2)}{r_{12}} dr_1 dr_2 \qquad (2.51)$$

and the exchange-correlation energy, which include the 'rest and remainder' terms including the correlation and exchange corrections to the classical energy, a correction for electron's self-interaction included in 2.51 and all other defects. The difficulty, however is that generally there is no way of calculating the kinetic energy part without going into an orbital model. Kohn and Sham therefore introduced a Hartree-Fock like self consistent field scheme. Defining density ρ(r) as

$$°(\vec{r}) = \sum_{i=1}^{N} \left| ¤_i^{k-s}(\vec{r}) \right|^2 \qquad (2.52)$$

They derived a set of equations satisfied by the $¤_i^{k-s}$ or Kohn-Sham orbitals by a variational method:

$$\left[-\frac{1}{2}\nabla_i^2 + \hat{V}_{eff}(\vec{r})\right]¤_i^{k-s}(\vec{r}) = £_i ¤_i^{k-s}(\vec{r}) \tag{2.53}$$

The $\hat{V}_{eff}$ appearing herein has the form

$$\hat{V}_{eff}(\vec{r}) = \hat{V}_{ext}(\vec{r}) + \hat{U}_{el}(\vec{r}) + \hat{V}_{xc}(\vec{r}) \tag{2.54}$$

where $\hat{U}_{el}(\vec{r}) = \int \frac{°(r')}{|r-r'|} d\vec{r}'$ and $\hat{V}_{xc}(\vec{r}) = \frac{¢E_{xc}(\vec{r})}{8°}$ is called the exchange-correlation potential. Starting from an initial set of K-S orbitals, this enables us to calculate an initial density from 2.52 and improved set of K-S orbitals from 2.53 and hence a new improved $°(\vec{r})$ and so on. Once self-consistency is achieved the total energy of the system can be calculated from 2.50.

While the method has been in use by solid state theorists for long, till the 90's the method was not considered accurate enough for molecular calculations. Early work used the local density approximation for the exchange-correlation functional:

$$E_{xc}[°] = \int V_{xc}(°)°(\vec{r}) d^3\vec{r} \tag{2.55}$$

Generalized Gradient approximations involve the gradient of the density (also at $\vec{r}$) also. Other refinements involve the use of terms involving the density, its gradient, and the laplacian. Several forms of the exchange-correlation functional have appeared in the literature, but currently the most popular one seems to be the B3LYP functional, which is a combination of Becke's three-parameter exchange functional [Beck, 1993; 1996] and Lee, Yang and Parr's correlation functional [Lee et al., 1988] which are both gradient corrected. The functional is given by equation (2.56).

$$E_{xc}^{B3LYP} = E_{xc}^{LDA} + a_0(E_x^{HF} - E_x^{LDA}) + a_x(E_x^{GGA} - E_x^{LDA}) + a_c(E_c^{GGA} - E_c^{LDA}) \tag{2.56}$$

Where E_x^{HF} is the Hartree-Fock exact exchange functional, $a_0 = 0.20$, $a_x = 0.72$ and $a_c = 0.81$ are the three empirical parameters determined by fitting the predicted values to a

set of atomization energies, ionization potentials, proton affinities, and total atomic energies, E_x^{GGA} and E_c^{GGA} are generalized gradient approximations: the Becke 88 exchange functional [Beck, 1988] and the correlation functional of Lee, Yang and Parr [Lee et al., 1988] and E_c^{LDA} is the local-density approximation to the correlation functional [Vosko et al., 1980].

2.7 REFERENCES

Bartlett R J (**1989**) "Coupled-cluster approach to molecular structure and spectra: A step toward predictive quantum chemistry" *J. Phys. Chem.* **93**: 1697-1708.

Becke A D (**1988**)"Density-functional exchange-energy approximation with correct asymptotic behavior" *Phys. Rev. A* **38**: 3098-3100.

Becke A D (**1993**) "Density-functional thermo-chemistry. III. The role of exact exchange" *J. Chem. Phys*. **98**: 5648-5652.

Becke A D (**1996**) "Density-functional thermochemistry. IV. A new dynamical correlation functional and implications for exact-exchange mixing" *J. Chem. Phys.* **104**: 1040-1046.

Bingham R C, Dewar M J S and Lo D H (**1975**) "Ground States of Molecules. XXV. MINDO/3. Improved version of the MINDO semi empirical SCF-MO method" *J. Am. Chem. Soc*. **97**: 1285-1293.

Boys S F (**1950**) "Electronic wave functions. I. A general method of calculation for the stationary states of any molecular system" *Proc. Roy. Soc. Lond. Math. Phys. Sci.* **200**: 542-554.

Clementi E and Raimondi D L (**1963**) "Atomic screening constants from SCF functions" *J. Chem. Phys.* **38**: 2686-2689.

Clementi E, Raimondi D L and Reinhardt W P (1967) "Atomic screening constants from SCF functions. II. Atoms with 37 to 86 Electrons" *J. Chem. Phys.* 47: 1300-1307.

Coester F and Kummel H (**1960**) "Short-range correlations in nuclear wave functions" *Nuclear Physics* **17**: 477-485.

Dewar M J S, McKee M L and Rzepa H S (**1978**) "MNDO Parameters for Third Period Elements" *J. Am. Chem. Soc.* **100**: 3607-3607.

Dunning Jr T H and Hay P J (**1976**) "In Modern Theoretical Chemistry" ed. Schaefer H F Vol. 3, New York: Plenum: 1-28.

Gadre S R and R D Bendale (**1983**) “On representation of electron-electron repulsion energies by simple one-electron functional” J. Chern. Phys. **78:** 996-999.

Halgren T A and Lipscomb W N (**1972**) "Approximations to self-consistent field molecular wave functions" *Proc. Nat. Acad. Sci. USA* **69**: 652-656.

Hall G G (**1951**) "The molecular orbital theory of chemical valency. VIII. A method of calculating ionization potentials" *Proc. Roy. Soc. A* **205**: 541-552.

Hasanein A A and Evans M W (**1996**) "Computational methods in quantum chemistry", Vol. 2. World Scientific Publishing Co: Singapore 1-246.

Hohenberg P and Kohn W (**1964**) "Inhomogeneous electron gas" *Phys. Rev*. **136**: B864-B871.

Lee C, Yang W and Parr R G (**1988**)"Development of the Colle-Salvetti correlation-energy formula into a functional of the electron density" *Phys. Rev. B* **37**: 785-789.

Löwdin P O (2007) "Correlation problem in many-electron quantum mechanics I. Review of different approaches and discussion of some current ideas" *Adv. Chem. Phys.* John Wiley & Sons, Inc.: 207-322.

Nesbet R K (**1968**) "Atomic Bethe-Goldstone Equations. III. Correlation energies of ground states of Be, B, C, N, O, F, and Ne" *Phys. Rev.* **175:** 2-9.

Noga J and Bartlett R J (**1987**) "The full CCSDT model for molecular electronic structure" *J. Chem. Phys.* **86**: 7041-7050.

Paldus J, Cizek J and Shavitt I (**1972**) "Correlation Problems in Atomic and Molecular Systems. IV. Extended coupled-pair many-electron theory and its application to the BH_3 molecule" *Phys. Rev. A* **5**: 50-67.

Parr R G, Gadre S R and Bartolotti L J (**1979**) “Local density functional theory of atoms and molecules” Proc. Nat. Acad. Sci. (U.S.A.) **76**: 2522-2526.

Pople J A, Head-Gordon M and Raghavachari K (**1987**) "Quadratic configuration interaction. A general technique for determining electron correlation energies" *J. Chem. Phys.* **87**: 5968-5975.

Raghavachari K and Anderson J B (**1996**) "Electron correlation effects in molecules" *J. Phys. Chem.* **100**: 12960-12973.

Roothaan C C J (**1951**) "New developments in molecular orbital theory" *Rev. Mod. Phys.* **23**: 69-89.

Sathyamurthy N and Joseph T (**1984**) "Potential energy surface and molecular reaction dynamics" J. Chem. Educ. **61**: 968-971.

Seeger R and Pople J A (**1976**) "Self-consistent molecular orbital methods. XVI. Numerically Stable direct energy minimization procedures for solution of Hartree-Fock Equations" *J. Chem. Phys.* **65**: 265-271.

Sinanoglu O (**1962**) "Many-Electron Theory of Atoms and Molecules. I. Shells, Electron Pairs vs Many-Electron Correlations" *J. Chem. Phys.* **36**: 706-717.

Singh S P (**2013**). "Theoretical studies of hydroboration and allied reactions" Unpublished doctoral thesis, Department of Chemistry, IIT Roorkee, Roorkee, India.

Slater J C (**1930**) "Atomic shielding constants" *Phys. Rev.* **36**: 57-64.

Stewart J J P (**1989**) "Optimization of parameters for semi empirical methods-I" *J. Com. Chem.* **10**: 209-220 .

Vosko S H, Wilk L and Nusair M (**1980**)"Accurate spin-dependent electron liquid correlation energies for local spin density calculations: A critical analysis" *Can. J. Phys*. **58**: 1200-1211.

3 Ring Opening Metathesis by Tungsten Catalyst

3.1 INTRODUCTION

As novel catalysts containing transition metals have become more tolerant of functionality and more available, the ring opening olefin metathesis reaction has assumed to take part in an increasingly significant role in organic synthesis. Many of the applications to date have been ring opening metathesis (ROM) of cyclic olefins [Miege et al., 2010; Mathers et al., 2009; Schneider et al., 1997]. Tungsten carbene complexes such as W(NAr)(CHR)(OR')$_2$ (R = t-Bu, R'= t-Bu or –$CMe_2(CF_3)$ and NAr = N-2,6-C_6H_3-i-Pr_2) effectively catalyze the ring opening metathesis (ROM) of alkenes to yield ring opened compounds [Schrock et al., 1988]. The catalytic ring opening metathesis (ROM) generates a new metal-alkylidene complex that can take part in a subsequent metathesis step in living ring opening metathesis polymerization (ROMP) [Dounis et al., 1995; Schrock, 2011], and tandem ring opening-cross metathesis (ROCM) [Ibrahem et al., 2012] or ring opening-ring closing metathesis (RO-RCM) [Zuercher et al., 1996]. Cyclic olefins react irreversibly with a metal alkylidene to give a new ring opened alkylidene as a product.

The ring opening metathesis proceeds through the well accepted Chauvin mechanism [Herisson and Chauvin, 1971], which involves a metallacyclobutane (MCB) as an intermediate. The mechanistic scheme of ring opening metathesis reaction, based on the Chauvin mechanism, is shown in scheme 3.1. This process is thermodynamically controlled and the requisite driving force for the reaction is the release of strain associated with the cyclic olefins. Various cyclic olefins undergo ring opening metathesis polymerization to give a range of macromolecules. Norbornene, Norbornadiene,7-Oxanorbornadiene and their derivatives are cyclic monomers that have been used [Schrock, 2011; Haigh et al.,2004; Bazan et al., 1991].

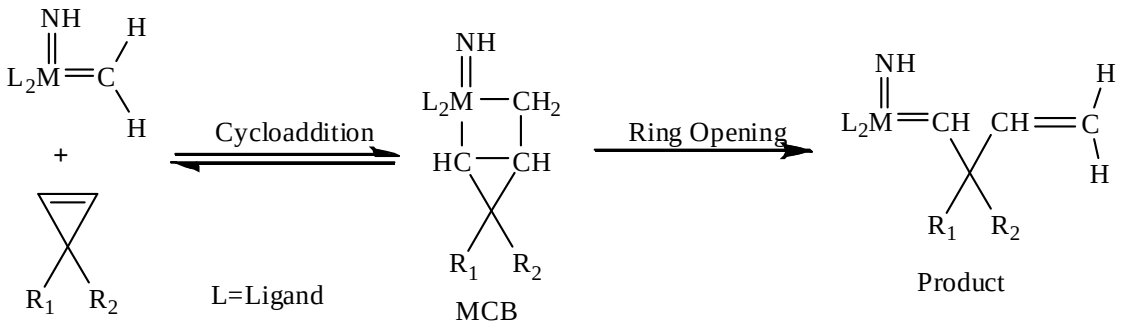

Scheme 3.1: Mechanism of ring opening of 3,3-disubstituted cyclopropene via Metathesis

The ring opening metathesis polymerization of monocyclic olefins is more difficult than normal olefin metathesis as the strained rings cannot be reformed by ring closing metathesis (RCM) [Grela, 2008]. Cyclopropenes [Flook et al., 2010] and cyclobutenes [Charvet and Novak, 2001] are the only monocyclic olefins that have been polymerized successfully in living fashion by means of ring opening metathesis polymerization. However, lack of monocyclic substrates appropriate for 'living' ROMP has limited the scope of this field [Grubbs, 2003]. Among unsaturated cyclic olefins, cyclopropene is the simplest olefin that has a triangular structure. Cyclopropene and its derivatives have being the subject of both theoretical and experimental studies [Liu et al., 2012; Zhu et al., 2011; Carter and Framton, 1964]. Since unsubstituted and some monosubstituted cyclopropenes are reported to be unstable at room temperature [Closs et al., 1963; Wiberg and Bartely, 1960] 3, 3-disubstituted cyclopropene derivatives appear to be interesting monocyclic olefins for the polymerization because of their ready availability and highly strained ring structure, (cyclopropene ring strain energy is ≈55 kcal/mol) [Khoury, 2004]. The first report of cyclopropene polymerization in a living manner via ROMP was made by Singh et al. [2006]. In recent years several reports on ROMP of 3, 3-disubstituted cyclopropenes with molybdenum alkylidene complexes of the type $Mo(NAr)(CHR')(OR)_2$ and ruthenium catalysts have appeared [Flook et al., 2010; Binder, 2009].

In recent years computational modeling is routinely used as a potential tool in the elucidation of the reaction mechanism [Tia and Adei, 2011; Suresh and Koga, 2004; Fomine et al., 2003] and in the prediction of the reactivity of many challenging olefins [Fomine et al., 2006; Fomine and Tlenkopatchev, 2007]. Various theoretical aspects of reactions involving cyclic olefins have been studied [Martinez et al., 2012; Song et al., 2010; Wu and Peng, 2003]. However, no attention has been paid to the ring opening metathesis of the highly strained monocyclic cyclopropene moiety. To the best of our knowledge, theoretical studies of ROM of cyclopropene with tungsten alkylidene have not been reported to date. The objective of the present study is to model ring opening of cyclopropene via metathesis with Schrock's tungsten catalyst. Systematic computational studies of the ring opening metathesis are performed on 3, 3-dimethyl cyclopropene (DMCP) with the model catalyst $W(NH)(CH2)(OCH_3)_2$ which is expected to reasonable model to the actual catalysts that have been used experimentally. The current study is aimed at a elucidation of the mechanistic details on the ring opening of 3, 3-dimethyl cyclopropene via metathesis.

3.2 COMPUTATIONAL DETAILS

The geometries of all stationary structures involved including reactants, products, intermediates and transition state were optimized using the hybrid B3LYP functional as implemented in Gaussian 09 (revision A.02) [Frisch et al., 2009]. The B3LYP functional is a combination of Becke's three-parameter hybrid exchange functional [Beck, 1993] with the Lee-Yang-Parr non-local correlation functional [Lee et al., 1988]. As relativistic effects are significant in the case of tungsten the LANL2DZ basis set was used, which includes Hay-Wadt effective core potential (ECP) [Hay and Wadt, 1985] plus double-zeta basis set for tungsten and Dunning-Huzinaga valence double-zeta set (D95V) for the first row atoms C, O and for hydrogen. Previous work [Guan et al., 2008, Handzlik, 2003; Tlenkopatchev and Fomine, 2001] has shown that B3LYP/LANL2DZ is a reasonable combination to study olefin metathesis reactions catalyzed by tungsten and molybdenum based alkylidene complexes. The ultrafine grid, which is a pruned (99,590) grid, was used during the computations. Harmonic vibrational frequencies were calculated for each optimized structure to ensure that the stationary points identified on the potential energy surface correspond to either a minimum (zero imaginary frequencies) or a transition state (one imaginary frequency). The transition structures were additionally verified by intrinsic reaction coordinate (IRC) calculations [Gonzalae and Schlegel, 1989; 1990].

3.3 RESULTS AND DISCUSSION

The reaction of 3,3-dimethyl cyclopropene (**2**) with the tungsten alkylidene $W(NH)(CH_2)(OCH_3)_2$ (**1**) may occur on two likely faces (COO/CNO) of the catalyst as shown in Figure 3.1. On the CNO face, cyclopropene may approach in syn or anti orientation as shown in Figure 3. 2. In syn approach the substituted carbon of the cyclopropene is closer to the NH group of the catalyst and farther in anti approach. The geometrical parameters of optimized reactants are collected in Table 3.1. The computed total electronic energies, enthalpies (at 298K), and free energies of the reactants, transition structures, intermediates and products involved in the reaction are collected in Table 3.2 while in Table 3.3 relative energies are given.

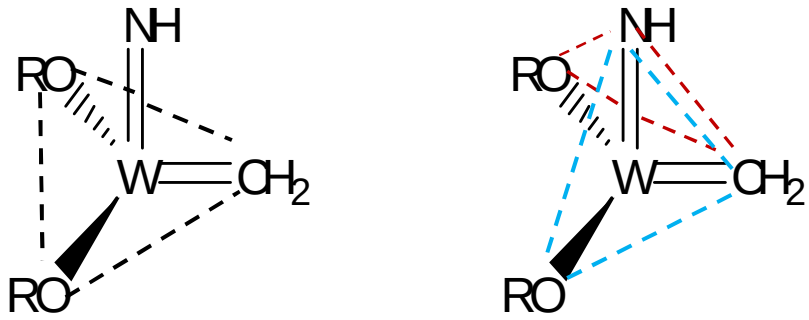

Figure 3.1: COO and CNO faces of the $W(NH)(CH_2)(OCH_3)_2$ catalyst

Table 3.1: Selected geometrical parameters[a] of the optimized tungsten catalyst model $W(NH)(CH_2)(OCH_3)_2$ (**1**) and 3,3-dimethyl cyclopropene (**2**)

[a]

Parameter	**1**	Parameter	**2**
W-C1	1.912	C_4-C_6	1.323
W-O1	1.889	C_4-C_5	1.544
W-O2	1.889	C_6-C_5	1.544
W-N1	1.751	C_5-C_4-C_6	64.638
N-W-C1	102.0	C_4-C_6-C_5	64.638
C1-W-O1	107.113	C_4-C_5-C_6	50.725
C1-W-O2	107.113	C_7-C_5-C_8	113.239
W-O1-C3	149.533		
W-O2-C2	149.533		
O1-W-O2	108.137		

Bond lengths are given in Å and angles in degrees

Table 3.2: Calculated total electronic energies (E_e), enthalpy (H) and Gibbs free energies (in hartree) for the transition structures (TS) ,Trigonal bipyramidal (TBP), Square pyramidal (SP) and ring opening metathesis product of 3,3-dimethyl cyclopropene with $W(NH)(CH_2)(OCH_3)_2$

CNO FACE			**syn orientation**	
	Structure	E_e	H	G
1.	Reactants	-588.0099847	-587.75626	-587.842855
2.	Cycloaddition TS	-587.9964824	-587.741648	-587.806161
3.	TBP Intermediate	-588.0701689	-587.810068	-587.871389
4.	SP Intermediate	-588.0764467	-587.81677	-587.88038
5.	Ring Opening TS	-588.05902	-587.801024	-587.862087
6.	syn Product	-588.0984666	-587.839156	-587.905857
			anti orientation	
7.	Cycloaddition TS	-587.9936051	-587.738731	-587.802662
8.	TBP Intermediate	-588.0680069	-587.807915	-587.868299
9.	SP Intermediate	-588.0773095	-587.817754	-587.880745
10.	Ring Opening TS	-588.0565862	-587.798212	-587.858168
11.	anti Product	-588.0969192	-587.837089	-587.903637
COO FACE				
12.	Cycloaddition TS	-587.9791255	-587.724676	-587.787523
13.	TBP Intermediate	-588.0517616	-587.792196	-587.852338

Table 3.3: Calculated Relative Energies (ΔE_e, in kcal mol^{-1}), enthalpies (ΔH_{298}, in kcal mol^{-1}) and free energies (ΔG_{298}, in kcal mol^{-1}) for the transition structures (TS), Trigonal bipyramidal (TBP), Square pyramidal (SP) and ring opening metathesis product of 3, 3-dimethyl cyclopropene with $W(NH)(CH_2)(OCH_3)_2$.

CNO FACE		**syn**			**anti**		
S.No	Structure	ΔE_e	ΔH	ΔG	ΔE_e	ΔH	ΔG
1.	Reactants	0	0	0	0	0	0
2.	Cycloaddition TS	8.47	9.17	23.03	10.28	11.0	25.22
3.	TBP Intermediate	-37.77	-33.76	-17.91	-36.41	-32.41	-15.97
4.	SP Intermediate	-41.71	-37.97	-23.55	-42.25	-38.59	-23.78
5.	Ring Opening TS	-30.77	-28.09	-12.07	-29.24	-26.32	-9.61
	Ring Opening TS*	10.94	9.88	11.48	13.01	12.26	14.17
6.	Product	-55.52	-52.02	-39.53	-54.55	-50.72	-38.14
COO FACE							
7.	Cycloaddition TS	19.36	19.82	34.72			
8.	TBP Intermediate	-26.22	-22.55	-5.95			

***Energy relative to the most stable syn & anti SP intermediate

3.3.1 CYCLOADDITION STEP

3.3.1.1Transition Structure on CNO Face

The structures of the model catalyst (**1**) and of 3, 3-dimethyl cyclopropene (**2**) along with their syn and anti relative orientations on the CNO face are shown in Figure 3. 2. In syn orientation the substituted carbon of the cyclopropene directed toward the NH group and away from it in anti orientation. Each orientation leads to a pseudo-trigonal bipyramidal (TBP) transition structure with the NH and one of the alkoxy (OR) groups occupying the axial positions, and a four centered ring is formed in the equatorial plane, as in the structures of the TBP tungstacyclobutane intermediates determined by X-ray crystal structure analysis [Feldman et al., 1990]. In Figure 3.3, SCTS and ACTS represent the optimized geometry of the syn and anti trigonal bipyramidal transition structures of the cycloaddition step respectively. The selected geometrical parameters of these structures are given in Table 3.4.

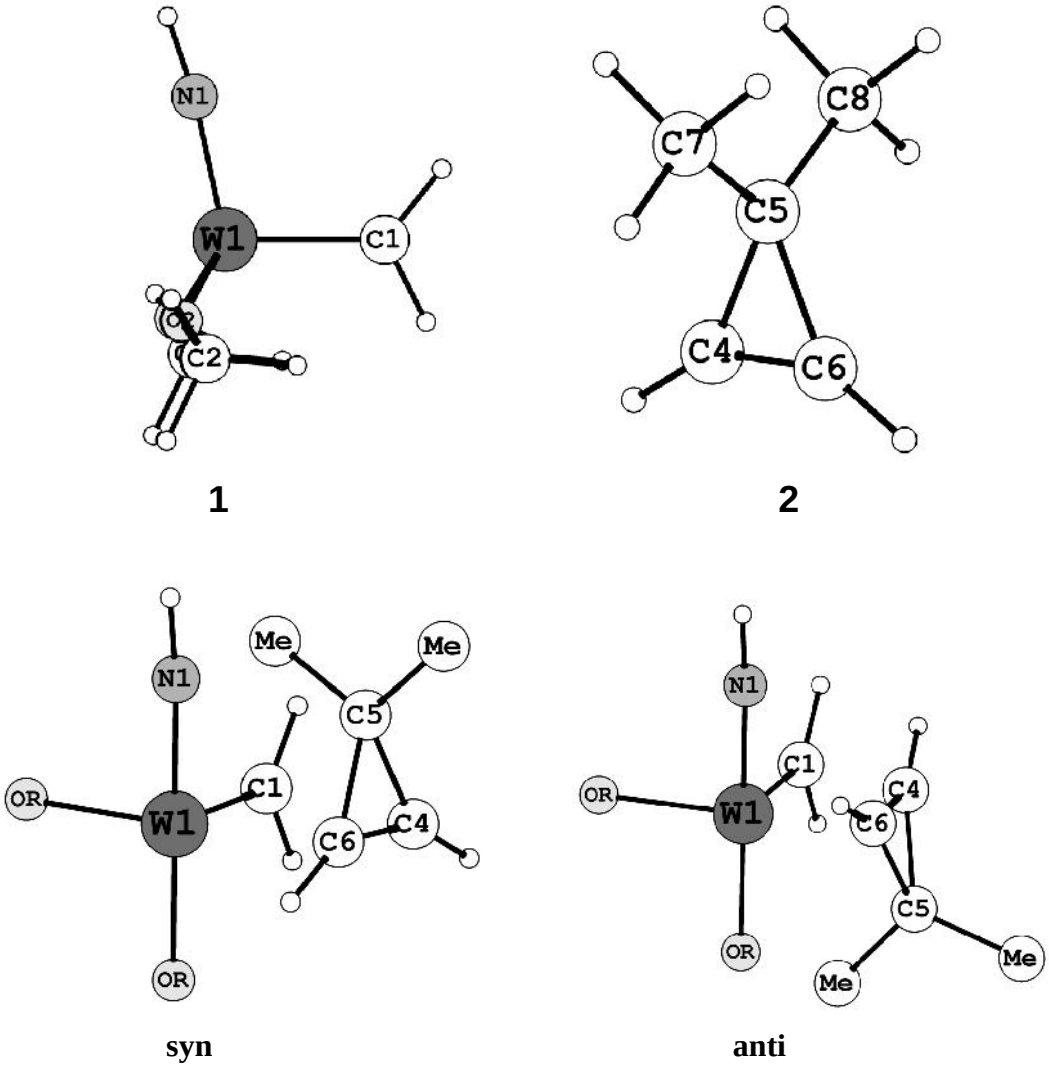

Figure 3.2: syn and anti orientations of 3, 3-dimethyl cyclopropene (**2**) at the CNO face of the model tungsten catalyst $W(NH)(CH_2)(OCH_3)_2$ (**1**)

In both syn and anti transition structures the alkylidene bonds (W-C1) have been slightly elongated while a new bond (W-C6) is seen forming between tungsten and cyclopropene carbon. The newly forming (W-C6) bonds are about 2.86 Å and 2.70Å in length in SCTS and ACTS respectively (entry 5 in Table 3.4). The shorter bond length in ACTS suggests a slightly later transition state for the anti addition. The angle C1-W-O1 is about 103-105˚ and the C6-W-O1 angle is nearly 152˚. The alkylidene carbon centers are essentially planar, while there are large distortions from planarity in the reacting C4-C6 double bond carbon centers. This is due to the steric repulsion of the C5 center of the cyclopropene with the NH group in syn transition structure and the axial alkoxy (-OCH_3) group in anti transition structures.

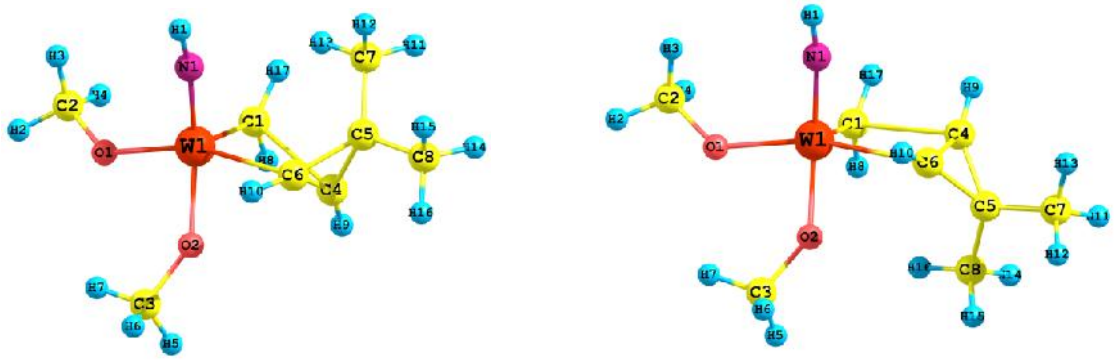

SCTS **ACTS**

Figure 3.3: Optimized transition state structures of 3,3-dimethyl cyclopropene reaction on the CNO Face of $W(NH)(CH_2)(OCH_3)_2$ catalyst

IRC calculations have been performed and confirm that the transitions structure SCTS and ACTS does fall on the path between the reactants and the corresponding TBP intermediate. IRC plots for both the transition structures are shown in Figure 3.4. The IRC shows the transition structure (SCTS & ACTS) moving downhill towards their tungstacyclobutane (STBP & ATBP) on one side and the reactants on other. Frequency calculations have also been performed and a single imaginary frequency is found for each transition structure as shown in Table 3.5.

The computed activation enthalpy for syn addition of cyclopropene with $W(NH)(CH_2)(OCH_3)_2$ is 9.17 kcal/mol and about 11.0 kcal/mol for anti addition (see entry 2 in Table 3.3). The experimental activation enthalpy for the formation of metallacyclobutane intermediate from norbornadiene is reported to be about 6.6 kcal/mol for the reaction of $W(NAr)(CH\text{-}t\text{-}Bu)(O\text{-}t\text{-}Bu)_2$ with 2,3-bis (trifluoromethyl) norbornadiene (NBDF6) [Bazan et al., 1990]. The increased activation enthalpy for cyclopropene is presumably due to the high ring strain of cyclopropene. The transition structure for syn addition (SCTS) is more stable than that for anti addition (ACTS) by about 1.83 kcal/mol. The pervious experimental studies [Oskam and Schrock, 1993] and theoretical calculations of 2,3-norbornadiene with molybdenum alkylidene have also shown a similar preference for syn addition over anti addition [Wu and Peng, 1997].

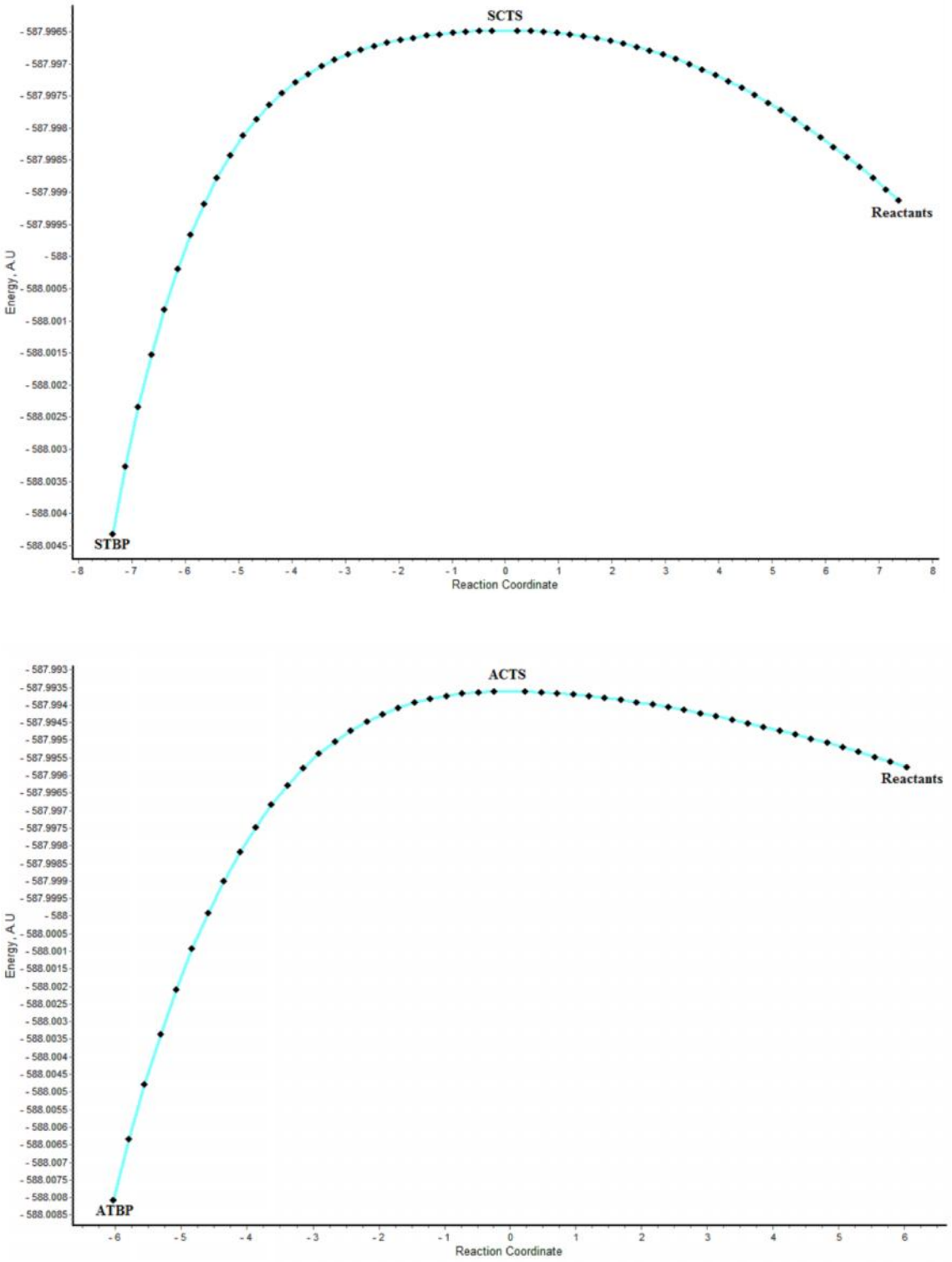

Figure 3.4: IRC plots for the syn and anti cycloaddition transition structures at the CNO face

Table 3.4: Optimized structural parameters (bond lengths in Á and angles in degree) for the transition structures (TS),Trigonal bipyramidal (TBP), Square pyramidal (SP) and ring opening metathesis product (ROP) of 3,3-dimethyl cyclopropene with $W(NH)(CH_2)(OCH_3)_2$

S. No.	Parameters	**SYN**					**ANTI**				
		SCTS	STBP	SSP	SRTS	SROP	ACTS	ATBP	ASP	ARTS	AROP
1.	W-N	1.769	1.778	1.747	1.771	1.753	1.771	1.778	1.749	1.767	1.751
2.	W-O1	1.923	1.942	1.893	1.915	1.895	1.935	1.956	1.889	1.935	1.893
3.	W-O2	1.920	1.950	1.892	1.927	1.894	1.921	1.946	1.890	1.938	1.891
4.	W-C1	1.922	2.170	2.207	2.686	-	1.927	2.180	2.211	2.814	-
5.	W-C6	2.864	2.048	2.144	1.958	1.912	2.697	2.042	2.152	1.956	1.927
6.	C1-C4	3.184	1.520	1.523	1.387	1.349	2.998	1.514	1.524	1.378	1.350
7.	C4-C6	1.336	1.677	1.579	2.155	-	1.345	1.692	1.551	2.179	-
8.	N-W-O1	102.1	93.3	113.1	104.8	115.6	98.961	92.7	113.6	99.3	115.4
9.	N-W-O2	140.0	169.9	112.1	134.8	115.2	154.3	163.2	113.6	133.8	115.3
10.	N-W-C1	102.3	91.1	103.0	79.5	-	102.1	96.8	98.8	103.5	-
11.	O1-W-O2	88.0	81.5	99.0	87.0	108.2	85.176	79.8	100.1	85.3	108.2
12.	C1-W-O1	103.1	143.3	138.5	170.2	-	104.6	147.5	140.4	154.7	-
13.	C1-W-O2	113.0	88.0	85.0	83.9	-	110.1	82.4	86.1	71.0	-
14.	C6-W-O1	152.5	134.6	84.8	107.7	106.9	151.6	129.5	86.2	106.7	108.6
15.	C6-W-O2	74.0	90.6	137.7	113.8	106.4	77.0	98.8	139.2	118.7	107.5
16.	W-O1-C2	131.1	133.6	154.8	131.3	148.8	129.3	131.6	152.0	127.5	152.0

17.	W-O2-C3	142.0	142.3	156.2	139.9	147.6	142.2	141.1	155.3	134.4	150.3
18.	C1-W-C6	102.9	80.1	66.4	80.2	-	102.2	79.9	65.6	77.4	-
19.	W-C1-C4	64.5	80.4	95.5	76.1	-	66.3	80.8	96.1	77.2	-
20.	C1-C4-C6	106.6	116.2	100.4	116.8	-	107.2	115.6	100.5	116.8	-
21.	W-C6-C4	79.3	80.9	96.3	82.3	-	81.9	81.3	97.7	86.8	-
22.	N-W-C6	80.5	99.1	104.6	104.3	103.7	84.2	97.5	100.0	103.7	101.0

Table 3.5: Imaginary frequencies (in cm^{-1}) of the first-order saddle points suggested in the ring opening metathesis mechanism of 3,3-dimethyl cyclopropene with $W(NH)(CH_2)(OCH_3)_2$ catalyst

S.No.	**Transition Structure**	**Frequency**
1.	SCTS	44.12*i*
2.	ACTS	78.07*i*
3.	COO_TS	152.44*i*
4.	SRTS	102.35*i*
5.	ARTS	115.41*i*

3.3.1.2 Transition Structure on COO Face

Figure 3.5 shows the transition structure and trigonal bipyramidal intermediate for the addition of cyclopropene to the COO face of $W(NH)(CH_2)(OCH_3)_2$ catalyst. The trigonal bipyramidal transition structure and intermediate found in this case are denoted as COO_TS and COO_TBP respectively. COO_TS also has a distorted trigonal bipyramidal geometry but two alkoxy ($-OCH_3$) groups occupy axial positions and the NH group occupies an equatorial position which is different from the structures SCTS and ACTS of the CNO Face. The geometrical parameters of COO face transition structure and TBP intermediate are collected in Table 3.6.

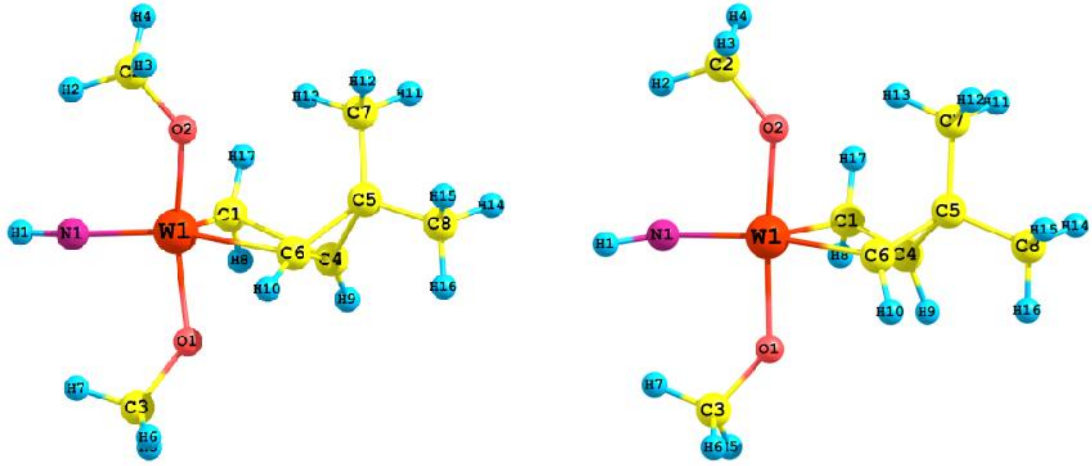

COO_TS **COO_TBP**

Figure 3.5: Optimized transition structure and trigonal bipyramidal intermediates of cyclopropene reaction on the COO Face of $W(NH)(CH_2)(OCH_3)_2$ catalyst

The metal carbene bond (W-C1) has been lengthened about .03Å while on the other side a new bond (W-C6) formation is observed in COO face transition structure (COO_TS). The bond angle C1-W-N and C6-W-N are about 116˚ and 143˚ respectively. The angle (O1-W-O2) between both axial methoxy groups is 153˚. The four membered tungstacyclobutane ring (W-C1-C4-C6) in this structure is similar to the one obtained at CNO face but the bond angle C1-W-C6 is significantly smaller by about 3-4˚ (see in Table 3.4 and Table 3.6) which shows that the COO face transition structure is more strained as compared to the CNO face transition structures.

IRC calculation has been performed and confirms that the investigated structure (COO_TS) is the first order saddle point which shows the TBP formation from the

reactants. Frequency calculations have been performed for the structures at the COO face. Only one imaginary frequency observed for the transition structure while all frequencies were found positive for the intermediate (COO_TBP). The IRC plot is shown in Figure 3.6.

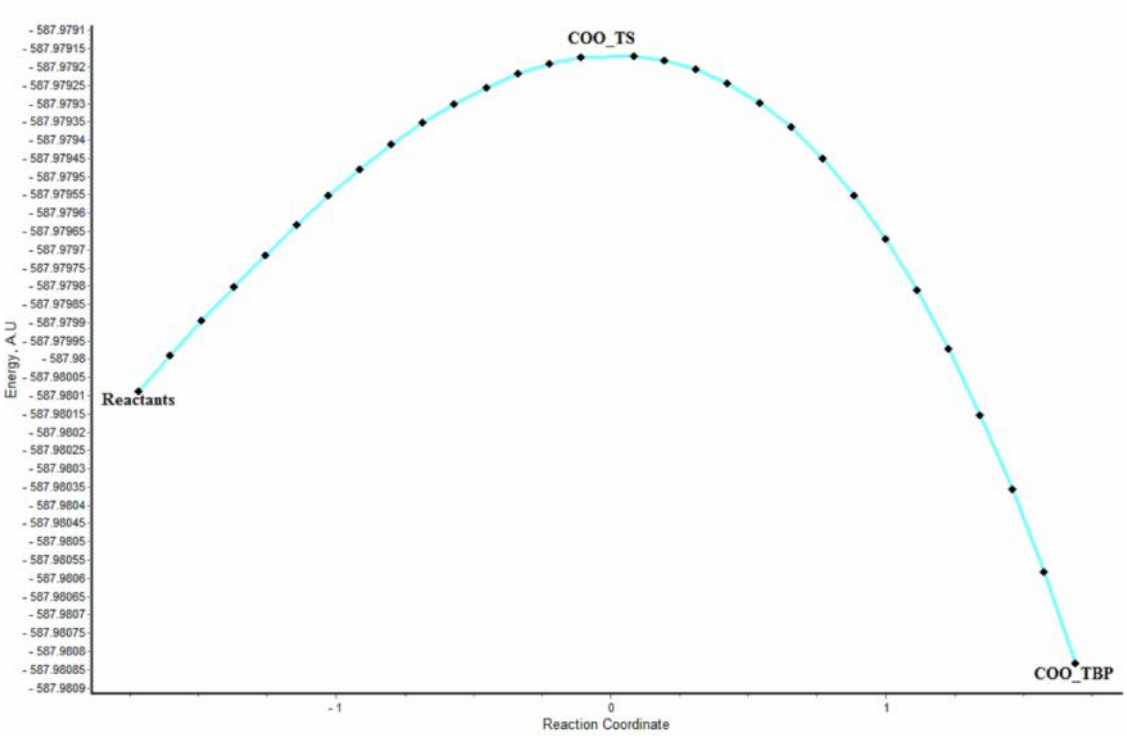

Figure 3.6: IRC plot for the transition structure at the COO face

The calculated activation enthalpies for cyclopropene addition at the COO face is about 19.82 kcal/mol, see table 3.3, entry 7. The activation enthalpy barrier for the reaction at CNO face is lower than at the COO face by about 10.89 and 9.08 kcal/mol respectively (see entry 2 for syn/anti CNO & 7 for COO in Table 3.3). The free energy values (see Table 3.3) also support this CNO face preference. In the COO face transition structure (COO_TS), steric repulsion between one of the axial methoxy group (-OCH_3) and methyl groups of cyclopropene is larger whereas this steric repulsion is smaller between NH group and methyl groups of cyclopropene in transition structure (SCTS & ACTS) at CNO face.

The larger steric repulsion increases the destabilization of the structure at COO face. Thus the TBP intermediate formed through COO_TS is less stable as compared to the TBP formed at the CNO face by about 12-14 kcal/mol. Hence we conclude that ring opening of 3,3-dimethyl cyclopropene takes place preferentially on the CNO face. Consequently, in subsequent stages we restrict our studies to the reaction at the CNO face alone.

Table 3.6: Optimized structural parameters (bond lengths in Å and angles in degree) for the transition structures (TS), Trigonal bipyramidal (TBP), of the 3,3-dimethyl cyclopropene with of $W(NH)(CH_2)(OCH_3)_2$ catalyst (**1**) On the COO Face

Parameter	COO_TS	COO_TBP
W-N	1.789	1.793
W-C1	1.951	2.15
W-C6	2.586	2.13
C1-C4	2.806	1.52
C4-C6	1.362	1.670
N-W-O1	94.87	91.76
N-W-O2	95.79	93.47
C1-W-N	116.6	125.4
C6-W-N	143.6	155.7
O1-W-O2	153.54	169.8
C1-W-O1	98.11	93.18
C1-W-O2	98.61	90.90
C6-W-O1	75.09	82.20
C6-W-O2	82.01	89.48
C1-W-C6	99.54	78.59
W-C1-C4	67.95	82.39
C1-C4-C6	108.59	116.1
W-C6-C4	82.06	79.8

3.3.1.3 TBP and SP Metallacyclobutane Intermediates

syn and anti tungstacyclobutane intermediates with trigonal bipyramidal (TBP) geometry are formed via corresponding transition states SCTS and ACTS. These intermediates are represented as STBP and ATBP and can possibly convert to square pyramidal (SP) intermediate SSP and ASP respectively, shown in Figure 3.7. The trigonal bipyramidal tungstacyclobutane intermediate (COO_TBP) of the COO face is also shown in Figure 3. 5 and its geometry is not further discussed here because of the unfavorable energetics. However geometrical details of COO_TBP are given in Table 3.6. Further discussion in this section concentrates on the CNO face alone.

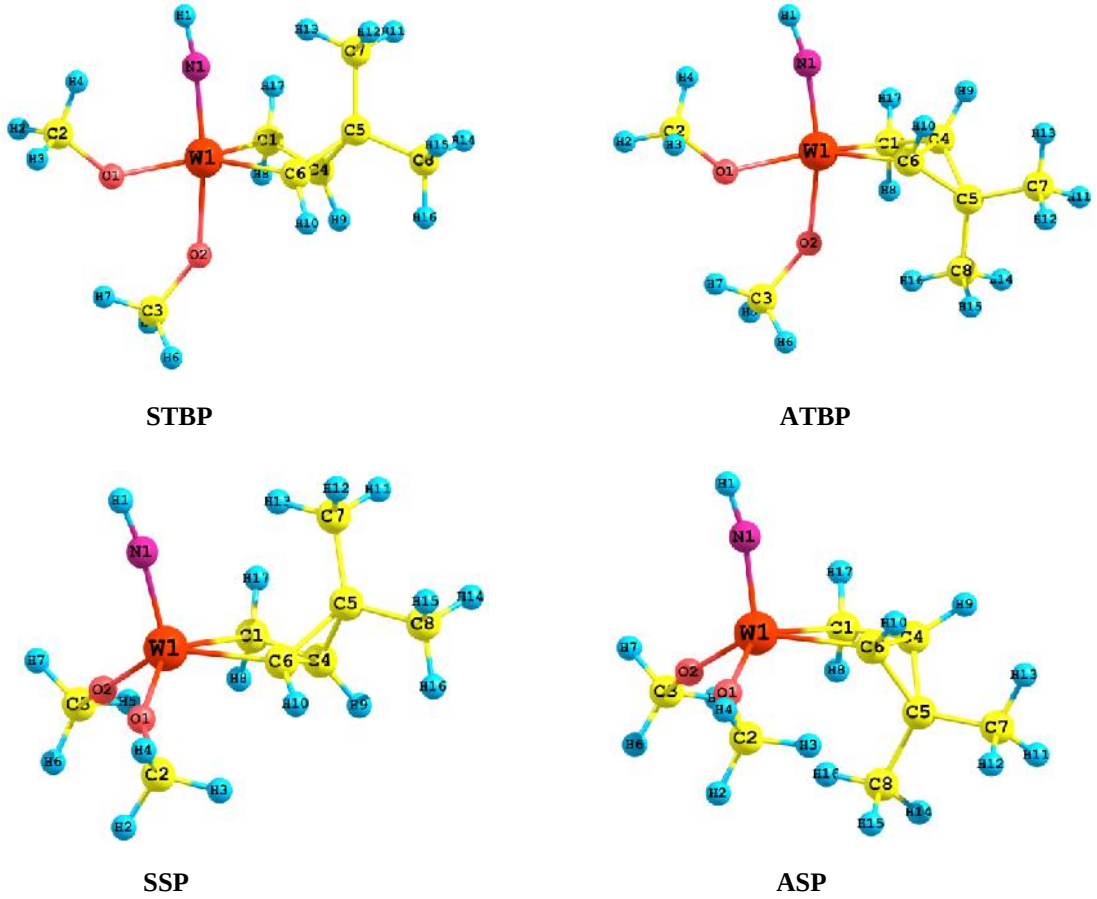

Figure 3.7: Optimized structures of trigonal bipyramidal and square pyramidal intermediates of cyclopropene reaction on the CNO face of $W(NH)(CH_2)(OCH_3)_2$ catalyst

The geometries of each structure are similar to the previously obtained X-ray crystal structures of similar compounds [Feldman et al., 1990] and theoretically computed structures in case of reaction of other cyclic olefins with molybdenum model catalyst [Wu and Peng, 1997]. The trigonal bipyramidal intermediates can also possibly rearrange by a Berry-type pseudo-rotation to the square pyramidal geometry [Floga and Ziegler, 1993; Wu and Peng, 1997]. However we were unable to characterize the corresponding transition structures.

In the TBP structures, the C4-C6 bonds of metallacyclobutane ring (W-C1-C4-C6) are unusually long, about 1.68-1.69 Å while the other C1-C4 bonds are normal (1.52Å). The newly forming bonds (W-C6) are about 2.1Å which is significantly shorter than observed in transition structures. On the other hand metal-carbene carbon bond (W-C1) has elongated (2.2Å). In square pyramidal tungstacyclobutane ring the C4-C6 and C1-C4 bonds are both shorter (in range of 1.52-1.58Å) as compared to the TBP intermediates, which is similar to the trend seen in earlier theoretical studies [Floga and Ziegler, 1993]. In general the calculated bond lengths are somewhat longer than those found for X-ray structures. The geometrical requirement in the core tungstacyclobutane part of the TBP structures causes significant strain in the cyclopropene ring (C4-C5-C6), thus making the C4-C6 bonds much longer. These very long bonds in STBP and ATBP indicate that they are very weak and thus easily breakable. The difference between the TBP and SP intermediates is due to the different core rings present [Feldman et al., 1990], the W-C1-C4, W-C6-C4 and C1-W-C6 are about 79-80˚ and C1-C4-C6 are about 116˚ while in the SP intermediates , the W-C6-C4, C1-W-C6 and C1-C4-C6 are about 79-80˚ and C1-W-C6 angles are about 66˚ (see entry 18-21 in Table 3.4).

The calculated enthalpies for the tungstacyclobutane of the reaction show that the syn and anti square pyramidal intermediates (SSP & ASP) are more stable than the corresponding syn and anti trigonal bipyramidal (STBP &ATBP) intermediates. The SSP and ASP intermediates are calculated to be more stable by 4.21kcal/mol and 6.18kcal/mol respectively than the STBP and ATBP intermediates. STBP is more stable than ATBP by 1.35kcal/mol, while ASP is about 0.62kcal/mol more stable than SSP intermediate. Smaller energy difference (4.21 kcal/mol) between STBP and SSP intermediates suggests that the rearrangement of syn oriented trigonal bipyramidal to syn square pyramidal form is easier than in the case of the anti orientation.

3.3.2 RING OPENING STEP

3.3.2.1 Transition Structures

As in the case of the cycloaddition step, the transition states (TS) for ring opening step are also in trigonal bipyramidal geometry with the NH group and one of the alkoxy ($–OCH_3$) groups occupying the axial positions but are much more twisted. We were unable to find the transition structure that connects the SP intermediates and products, and it seems that SP tungstacyclobutane cannot decompose directly to the tungsten alkylidene (W=C) center and olefin, while avoiding the TBP intermediate [Handzlik and Ogonowski, 2002]. The ring opening transition structures corresponding to syn and anti tungstacyclobutane are shown in Figure 3.8 and denoted as SRTS and ARTS respectively.

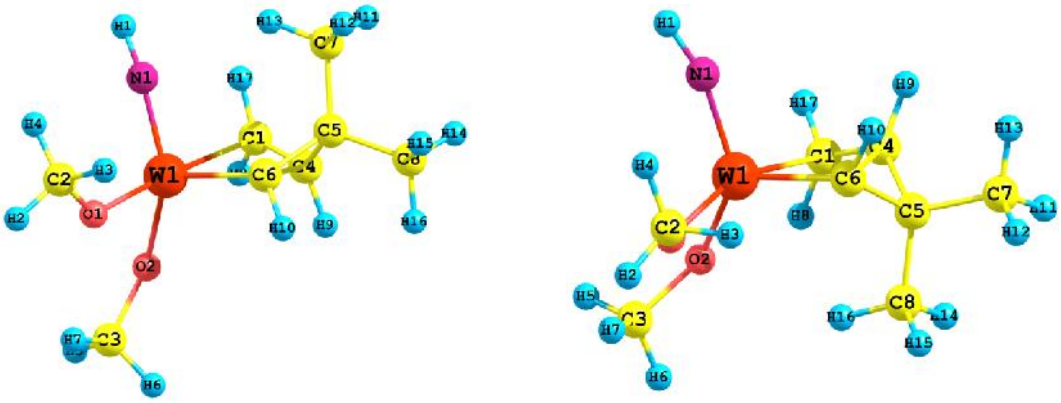

SRTS **ARTS**

Figure 3.8: Optimized syn and anti transition structures of the ring opening step

The IRC plots of these transition structures shown in Figure. 3.9 confirm that transition structures SRTS and ARTS do fall on the reaction path of the ring opening of TBP intermediates into their respective ring opening products. The IRC plots show the SRTS and ARTS moving downhill towards the corresponding STBP & ATBP on one side and the products (SROP & AROP) the other. Frequency calculations have been performed on all stationary structures and one imaginary frequency is found for SRTS and ARTS and all positive frequencies are observed for the stable species (SRTS and ARTS).

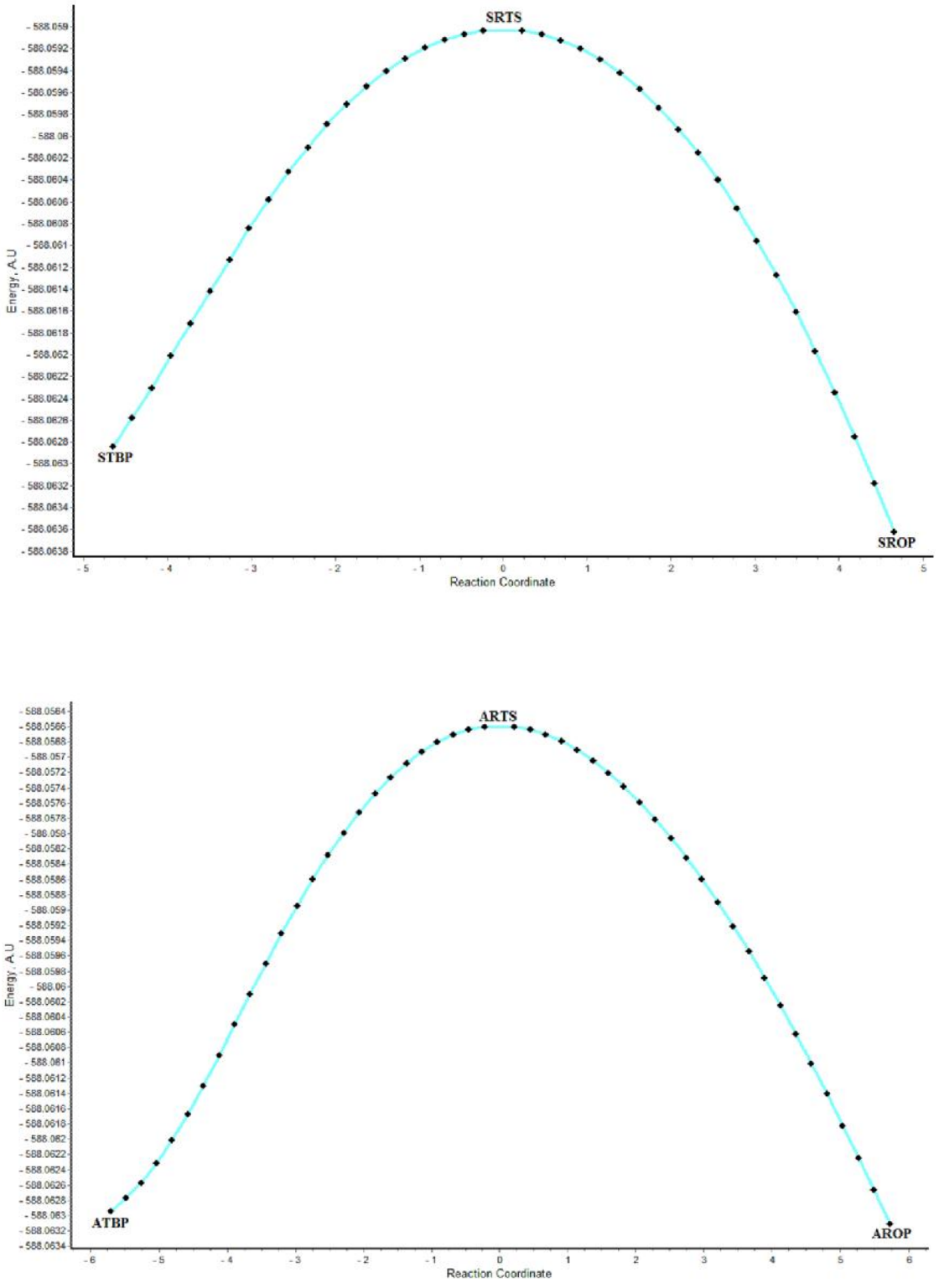

Figure 3.9: IRC plots for the syn and anti ring opening transition structures at the CNO face

In ring opening transition structures, the C1-W-O1 angles are increased to 170˚ in SRTS and 155˚ in ARTS, while on the other hand C6-W-O1 angles have decreased in comparison to cycloaddition transition structures (see entry 14, Table 3.4). On comparison with TBP intermediates, the breaking W-C1 and C4-C6 bonds have been lengthened about 0.52 & 0.48 Å in SRTS and 0.73 & 0.49 Å in ARTS, whereas forming C1=C4 bonds are 0.13 Å and W=C6 bonds are also significantly shorter [see entry 5, Table 3.4] in both structures. Consequently the calculated ring opening transition structures reflect the earlier prediction that the C4-C6 bonds in the TBP intermediates can be easily broken. This is also reflected in the computed energies, the SRTS and ARTS barriers are higher than their analogous STBP and ATBP by about 7 kcal/mol., while relative to the corresponding SP intermediates the calculated activation barriers are notably higher at about 10.94 and 13.01 kcal/mol respectively (see entry 5, Table 3.3). The activation enthalpy for syn ring opening is lower by 2.38 kcal/mol than anti ring opening. The ring opening barriers are much higher than those found for the cycloaddition step leading us to predict that the ring opening step is the rate determining step of the ring opening via metathesis of 3, 3-dimethyl cyclopropene with tungsten catalyst. This is in agreement with the general trend found by experiments that tungstacyclobutane intermediates appear to break up more slowly than their molybdenum counterparts [Schrock and Hoveyda, 2003].

3.3.2.2 Ring Opening Products

The optimized structures of the syn and anti alkylidenes formed by ring opening of the tungstacyclobutane intermediates are shown in Figure 3.10. These syn and anti ring opening products (new alkylidenes) are named as SROP and AROP respectively. In both SROP and AROP two new bonds W=C6 and C1=C4 have been formed with length 1.91Å and 1.35 Å respectively, while W=C1 and C4=C6 bonds have entirely broken (see entry 4-7, Table 3.4). The basic structures of these ring opening products are in agreement with previous experimental results on similar metal alkylidenes [Schrock et al., 1990].

The enthalpies of the new formed alkylidene (SROP & AROP) demonstrate that the ring opening of the cyclopropene moiety is an exothermic process whether the reaction proceeds through syn or anti orientations. The calculated enthalpies for syn and anti products are -52.02 kcal/mol and -50.72 kcal/mol respectively. The syn product is stabler than the anti product by1.30 kcal/mol. The calculated free energy also favored the syn path (see Table 3.3). The overall kinetic profile of the ring opening metathesis reactions of cyclopropene at the CNO face of the catalyst $W(NH)(CH_2)(OCH_3)_2$ is illustrated in

Figure 3.11. For the cycloaddition intermediates, the most stable structures of the tungstacyclobutane are used.

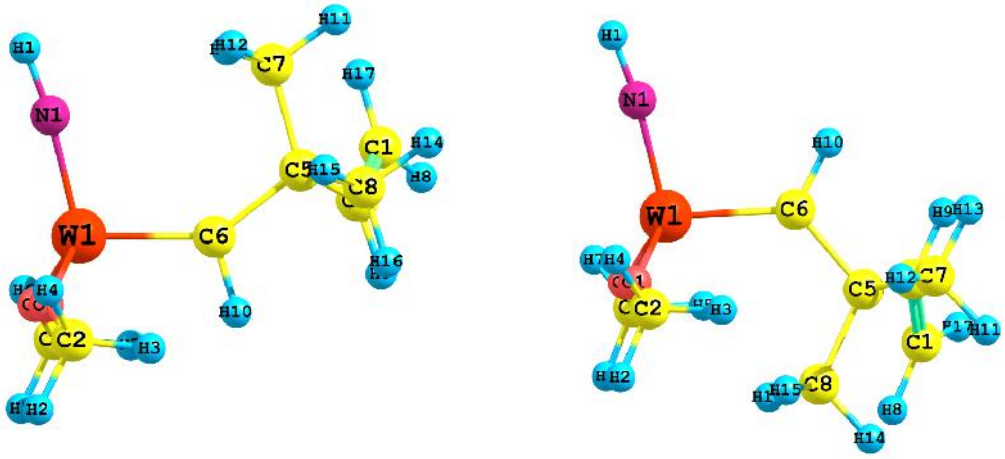

SROP **AROP**

Figure 3.10: Optimized syn and anti ring opening products of the cyclopropene reaction on the CNO face of the $W(NH)(CH_2)(OCH_3)_2$ catalyst

The ring opened products SROP and AROP act as metal alkylidene $W(NH)(CHR)(OCH_3)_2$ (where R=Propagating chain) for the propagation step of the polymerization reaction. The 3,3-dimethyl cyclopropene may react in syn and anti manner with both alkylidenes to yield the actual products of the metathesis reaction. Depending on the cyclopropene approach to the propagating alkylidene (SROP or AROP) stereochemically cis or trans macromolecules may be formed as ultimate products of metathesis reaction.

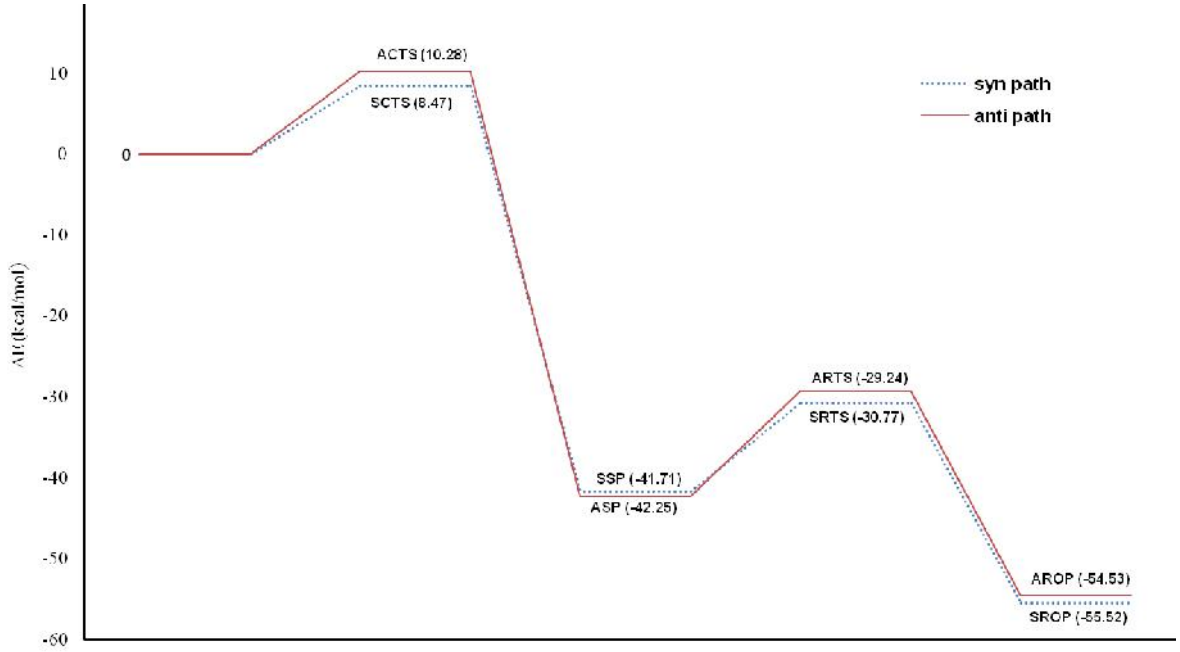

Figure 3.11: Energy diagram of the ring opening reaction of 3,3-dimethyl cyclopropene at the CNO face of the $W(NH)(CH_2)(OCH_3)_2$ catalyst. The relative energies ΔE (kcal/mol) are obtained relative to the energy of the reactants

3.4 CONCLUSIONS

In the present work, the ring opening by metathesis of highly strained 3, 3-dimethyl cyclopropene with tungsten catalyst of the type $W(NH)(CH_2)(OCH_3)_2$ has been studied. The reaction proceeds through two distorted trigonal bipyramidal transition structures. The transition structures of ring opening step are more twisted than those for the cycloaddition step. There is a significant preference for addition of cyclopropene to the CNO face of the catalyst over the COO face. Since the barrier for the cycloaddition step is lower than that for the ring opening step, we predict that the ring opening step is the rate determining step for the ROM of cyclopropene with the tungsten catalyst. The approach of cyclopropene to the $W(NH)(CH_2)(OCH_3)_2$ with syn orientation is favorable for the ring opening and the resulting syn product is more stable than the anti product by 1.3 kcal/mol. However the differences in the stability of syn and anti products is not very high and kinetically the syn path is preferred over the anti path of ring opening metathesis of highly strained cyclopropene with tungsten catalyst.

It is well-known that steric effects are important to the reactivity of these syn and anti alkylidene catalysts as well as to the stability of the tungstacyclobutane intermediates and the stereochemistry of the out coming polymers. Further investigations of ROMP of cyclopropene derivatives with molybdenum alkylidene are in next chapter.

3.5 REFERENCES

Bazan G C , Khosravi E, Schrock , Feast W J, Gibson V C, O'Regan M B, Thomas J K and Davis W M (**1990**) "Living ring-opening metathesis polymerization of 2,3-difunctionalized norbornadienes by Mo(CH-tert-Bu)(N-2,6-C_6H_3-iso-Pr_2)(O-tert-Bu)$_2$" *J. Am. Chem. Soc.* **112**: 8378-8387.

Bazan G C, Oskam J H, Cho H N, Park L Y and Schrock R R (**1991**) "Living ring-openingmetathesis polymerization of 2,3-difunctionalized 7-oxanorbornenes and 7-Oxanorbornadienes by Mo(CHCMe$_2$R)(N-2,6-C_6H_3-iso-Pr_2)(O-tert-Bu)$_2$ and Mo(CHCMe$_2$R)(N-2,6-C_6H_3-iso-Pr_2)(OCMe$_2$CF$_3$)$_2$" *J. Am. Chem. Soc.* **113**: 6899-6907.

Becke A D (**1993**) "Density-functional thermochemistry .3. the role of exact exchange" *J. Chem. Phys.* **98**: 5648-5652.

Binder W H, Pulamagatta B, Kir O, Kurzhals S, Barqawi H and Tanner S (**2009**) "Monitoring Block-Copolymer Crossover-Chemistry in ROMP: Catalyst Evaluation via Mass-Spectrometry (MALDI)" *Macromolecules* **42**: 9457-9466.

Carter F L and Frampton V L (**1964**) "Review of the Chemistry of Cyclopropene Compounds" *Chemical Reviews* **64**: 497-525.

Charvet R and Novak B M (**2001**) "New functional monomers for well-controlled ROMP polymerizations" *Macromolecules* **34**: 7680-7685.

Closs G L, Closs L E and Boll W A (**1963**) "The base-induced pyrolysis of tosylhydrazones of α,β-unsaturated aldehydes and ketones. A convenient synthesis of some alkylcyclopropenes" *J. Am. Chem. Soc.* **85**: 3796-3800.

Dounis P, Feast W J and Kenwright A M (**1995)** "Ring opening metathesis polymerization of monocyclic alkenes using molybdenum and tungsten alkylidene (Schrock-type) initiators and ^{13}C nuclear magnetic resonance studies of the resulting polyalkenamers" *Polymer* **36**: 2181-2196.

Feldman J, Davis W M, Thomas J K and Schrock R R (**1990**) "Preparation and reactivity of tungsten(VI) metallacyclobutane complexes-square pyramids versus trigonal bipyramids" *Organometallics* **9**: 2535-2548.

Flook M M, Gerber L C H, Debelouchina G T and Schrock R R (**2010**) "Z-selective and syndioselective ring-opening metathesis polymerization (romp) initiated by monoaryloxidepyrrolide (MAP) Catalysts" *Macromolecules* **43**: 7515-7522.

Folga E and Ziegler T (**1993**) "Density functional-study on molybdacyclobutane and its role in olefin metathesis" *Organometallics* **12**: 325-337.

Fomine S and Tlenkopatchev M A (**2007**) "Ring-opening of cyclohexene via metathesis by ruthenium carbene complexes-A computational study**"** *Organometallics* **26**: 4491-4497.

Fomine S, Ortega J V and Tlenkopatchev M A (**2006**) "Difluoroethylene as a chain transfer agent during ring-opening metathesis polymerization (ROMP) of norbornene by a ruthenium alkylidene complex: A computational study" *J. Organomet. Chem.* **691**: 3343-3348.

Fomine S, Vargas S M and Tlenkopatchev M A (**2003**) "Molecular modeling of ruthenium alkylidene mediated olefin metathesis reactions: DFT study of reaction pathways" *Organometallics* **22**: 93-99.

Frisch M J, et al (**2009**) Gaussian09, Revision A.02, Gaussian, Inc.,Wallingford CT.

Gonzalez C and Schlegel H B (**1989**) "An improved algorithm for reaction-path following" *J. Chem. Phys.* **90**: 2154-2161.

Gonzalez C and Schlegel H B, (**1990**) "Reaction path following in mass-weighted internal coordinates" *J. Phys. Chem.* **94**: 5523-5527.

Grela K (**2008**) "The joy and challenge of small rings metathesis" *Angew. Chem. Int. Ed.* **47**: 5504-5507.

Grubbs R H (**2003**) "Handbook of Metathesis" 1st Edn. Wiley-VCH, New York, Vol.1.

Guan J, Yang G, Zhou D, Zhang W, Liu X and Bao X H X (**2008**) "Formation of Mo-carbene active sites in Mo/Beta zeolite catalysts with different olefins: Theoretical exploration of possible reaction pathways and substituent effects" *Catal Commun.* **9**: 2213-2216.

Haigh D M, Kenwright A M and Khosravi E (**2004**) "Ring opening metathesis polymerisations of norbornene and norbornadiene derivatives containing oxygen: a study on the regeneration of Grubbs catalyst" *Tetrahedron* **60**: 7217-7224.

Handzlik J (**2003**) "Theoretical study of propene metathesis proceeding on monomeric Mo centers of molybdena-alumina catalysts" *J. Catal.* **220**: 23-34.

Handzlik J and Ogonowski J (**2002**) "DFT study of ethene metathesis proceeding on monomeric Mo^{VI} centres of MoO_3/Al_2O_3 catalyst the role of the molybdacyclobutane intermediate" *J. Mol. Catal. A: Chem.* **184**: 371-377.

Hay P J and Wadt W R (**1985**) "Ab initio effective core potentials for molecular calculations. Potentials for K to Au including the outermost core orbitals" *J. Chem. Phys.* **82**: 299-310.

Herisson J L and Chauvin Y (**1971**) "Catalyse de transformation des oléfines par les complexes du tungstène. II. Télomérisation des oléfines cycliques en présence d'oléfines acycliques" *Makromol. Chem.* **141**: 161-176.

Khoury P R, Goddard J D and Tam W (**2004**) "Ring strain energies: substituted rings, norbornanes, norbornenes and norbornadienes" *Tetrahedron* **60**: 8103-8112.

Lee C T, Yang W T and Parr R G (**1988**) "Development of the colle-salvetti correlation-energy formula into a functional of the electron-density" *Phys. Rev. B* **37**: 785-789.

Liu Y, Zhang D, and Bi S (**2012**) "Theoretical insight into $PtCl_2$-catalyzed isomerization of cyclopropenes to allenes" *Organometallics* **3**: 4769-4778.

Martinez H, Miró P, Charbonneau P, Hillmyer M A and Cramer C J (**2012**) "Selectivity in ring-opening metathesis polymerization of Z-cyclooctenes catalyzed by a second-generation Grubbs catalyst" *ACS Catal.* **2**: 2547-2556.

Mathers R T, Damodaran K, Rendos M G and Lavrich M C (**2009**) "Functional hyperbranched polymers using ring-opening metathesis polymerization of dicyclopentadiene with monoterpenes" *Macromolecules* **42**: 1512-1518.

Miege F, Meyer C and Cossy J (**2010**) "Ring-rearrangement metathesis of cyclopropenes: Synthesis of heterocycles" *Org. Lett.* **12**:248-251.

Oskam J H and Schrock R R (**1993**) "Rotational isomers of Mo(VI) alkylidene complexes and cis-trans polymer structure-investigations in ring-opening metathesis polymerization" *J. Am. Chem. Soc.* **115**:11831-11845.

Schneider M F, Lucas N, Velder J and Blechert S (**1997**) "Selective ring-opening olefin metathesis of functionalized monosubstituted olefins" *Angew. Chem. Int. Ed. Engl.* **36**: 257-259.

Schrock R R and Hoveyda A H (**2003**) "Molybdenum and Tungsten Imido Alkylidene Complexes as Efficient Olefin-Metathesis Catalysts" *Angew. Chem. Int. Ed*. **42**: 4592-4633.

Schrock R R, DePue R T, Feldman J, Schaverien C J, Dewan J C and Liu A H (**1988**) "Preparation and reactivity of several alkylidene complexes of the type W(CHR')(N-2,6-C_6H_3-i-Pr_2)$(OR)_2$, and related tungstacyclobutane complexes. Controlling metathesis activity through the choice of alkoxide ligand" *J. Am. Chem. Soc.* **110**: 1423-1435.

Schrock R R, DePue R T, Feldman J, Yap K B, Yang D C, Davis W M, Park L, DiMare M, Schofield M, Anhaus J, Walborsky E, Evitt E, Kruger C and Betz P (**1990**) "Further studies of imido alkylidene complexes of tungsten,well-characterized olefin metathesis catalysts with controllable activity" *Organometallics* **9**: 2262-2275.

Schrock RR (**2011**) "Synthesis of stereoregular ROMP polymers using molybdenum and tungsten imido alkylidene initiators" *Dalton. Trans*. **40**: 7484-7495.

Singh R, Czekelius C and Schrock R R (**2006**) "Living ring-opening metathesis polymerization of cyclopropenes" *Macromolecules* **39**: 1316-1317.

Song A, Lee J C, Parker K A and Sampson N S (**2010**) "Scope of the ring-opening metathesis polymerization (ROMP) reaction of 1-substituted cyclobutenes" *J. Am. Chem. Soc.* **132**: 10513-10520.

Suresh C H and Koga N (**2004**) "Orbital interactions in the ruthenium olefin metathesis catalysts" *Organometallics* **23**: 76-80

Tia R and Adei E (**2011**) "Computational studies of the mechanistic aspects of olefin metathesis reactions involving metal oxo-alkylidene complexes" *Comp. Theor. Chem.* **971**: 8–18.

Tlenkopatchev M and Fomine S (**2001**) "Molecular modeling of the olefin metathesis by tungsten (0) carbene complexes" *J. Organomet. Chem.* **630**: 157-168.

Wiberg K B and Bartley W J (**1960**) "Cyclopropene. V. Some Reactions of Cyclopropene" *J. Am. Chem. Soc.* **82**: 6375-6380.

Wu Y D and Peng Z H (**1997**) "Theoretical Studies on Alkene Addition to Molybdenum Alkylidenes" *J. Am. Chem. Soc.* **119**: 8043-8049.

Wu Y D and Peng Z H (**2003**) "Theoretical studies on the ring-opening metathesis reaction of norbornadiene with molybdenum alkylidenes" *Inorg. Chim. Acta.* **345**: 241-245.

Yu M, Ibrahem I, Hasegawa M, Schrock R R and Hoveyda A H (**2012**) "Enol ethers as substrates for efficient Z- and enantioselective ring-opening/cross-metathesis reactions promoted by stereogenic-at-Mo complexes: Utility in chemical synthesis and mechanistic attributes" *J. Am. Chem. Soc.* **134**: 2788-2799.

Zhu Z B, Wei Y and Shi M (**2011**) "Recent developments of cyclopropene chemistry" *Chem. Soc. Rev.* **40**: 5534-5563.

Zuercher W J, Hashimoto M and Grubbs R H (**1996**) "Tandem ring opening-ring closing metathesis of cyclic olefins" *J. Am. Chem. Soc.* **118**: 6634-6640.

4 Molybdenum Catalyzed Ring Opening Metathesis Polymerization

4.1 INTRODUCTION

The ring opening metathesis polymerization (ROMP) and acyclic diene metathesis (ADMET) are the most powerful metathetic methods for the preparation of polymers with unique properties [Ivin and Mol, 1997; Grubbs, 2003]. ROMP in particular produces polymers and copolymers with high molecular weights and low dispersity [Bielawski and Grubbs, 2007; Schrock, 1990] In ROMP the release of ring strain energy, associated with cyclic olefins, is the driving force to compensate for the entropy of polymerization [Hejl et al., 2005; walker et al., 2009]. Ring opening metathesis polymerization is successful for many cyclic olefins possessing different functional groups.[Bazan et al.,1991; Khosravi et al., 2000; Biagini et al., 1998] This functional group tolerance allows for the synthesis of a wide range of both experimentally interesting and industrially significant polymers. Strained cycloalkene monomers are best suited for ROMP because secondary reactions of relatively unstrained C=C bonds in the resulting polymer thereby can be minimized and the polymerizations can be living (a living polymerization is one in which the propagating species does not decompose on the time scale of the polymerization).

The mechanistic scheme of ROMP, based on the widely accepted the Chauvin mechanism [Herisson and Chauvin, 1971], is shown in Scheme 4.1. The ring opening metathesis polymerization begins with cycloaddition to form a metallacyclobutane intermediate (MCB). This intermediate subsequently undergoes a retro-[2+2] cycloreversion that leads to the formation of a new metal alkylidene. Due to the incorporated monomer the resulting metal alkylidene has increased in size, however its reactivity towards cyclic alkenes is comparable to that of the initiator. Hence, similar steps are repeated during the propagation stage until polymerization ceases. Although every step is reversible, the equilibrium is driven to the polymer product by the overall thermodynamics of the metathesis polymerization [Bielawski and Grubbs2007; Hejl et al. 2005; Walker et al.2009].

In the last 25 years “well-defined” metathesis catalysts, useful for ring opening olefin metathesis (ROMP), have been prepared, largely imido alkylidene catalysts based on molybdenum (Mo) or tungsten (W) in the highest possible oxidation state [Schrock, 2001; 2002; Schrock and Hoveyda, 2003; Schrock et al., 1990] or catalysts that contain ruthenium (Ru) [Vougioukalakis and Grubbs, 2010].

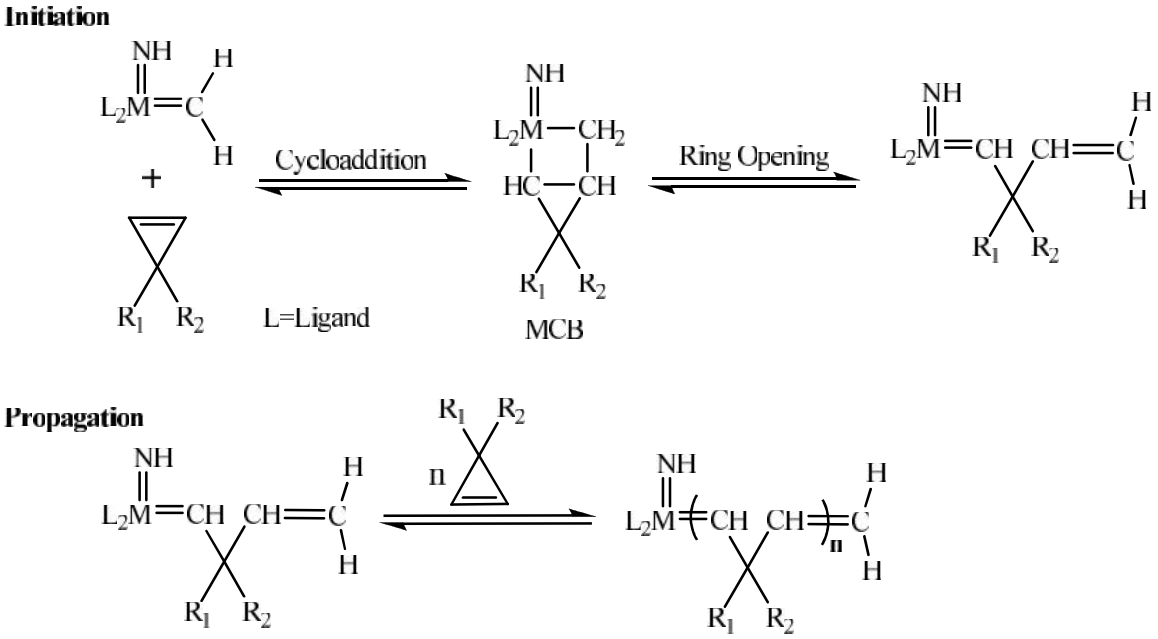

Scheme 4.1: A general mechanism to a typical ROMP reaction

The structures of the "Well-defined catalysts" are well known and their reactivities and selectivities can be altered in a knowledgeable manner through ligand design. Well defined olefin metathesis catalysts allow ring opening metathesis polymerization to be controlled and used for a diversity of purposes [Buchmeiser, 2000; Bielawski and Grubbs, 2007; Smith et al., 2007**].** Polymer-supported versions of well-defined metathesis catalysts have also been explored [Buchmeiser, 2009**]**. The molybdenum [Schrock, 2009] and ruthenium [Monsaert et al., 2009] catalysts open vast opportunities to metathesize olefins; but the great efficiency of Schrock's molybdenum complexes (Figure 4.1) of the type $Mo(NAr)(CHR')(OR")_2$ (Ar = 2,6-i-$Pr_2C_6H_3$, R = t-Bu, R"=t-Bu, $C(CF_3)_2Me$) make them more useful among these [Schrock, 2009; Kress and Blechert, 2012]. Molybdenum based catalysts were found to polymerize a range of cyclic olefins with varying degrees of ring strain and functionality [Schrock et al., 1988; Dounis and Feast, 1996]. Cyclopentene was polymerized with controllable molecular weights and narrow polydispersities (PDI < 1.1) using Mo-catalyst [Trzaska et al., 2000].

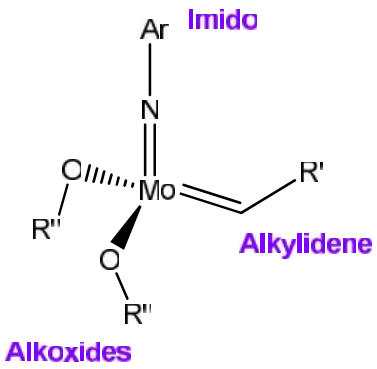

Figure 4.1: Molybdenum imido alkylidene complex of the type $Mo(NAr)(CHR')(OR'')_2$

Cycloalkenes are recognized as versatile monomers, which can be easily polymerized in the presence of a metal alkylidene to form ring-opened poly(cycloolefin)s [Hayano et al., 2006].The ring opening metathesis polymerization of olefins having small ring is more challenging than general olefin metathesis as the strained rings cannot be reformed by ring closing metathesis (RCM) [Grela, 2008]. Three-, four-, and eight-, and higher-membered monocyclic olefins are good prospects for living ROMP. However, paucity of monocyclic substrates suitable for 'living' ROMP has limited the scope of this field [Ivin and Mol, 1997; Grubbs, 2003]. Cyclopropenes have been widely used as substrates for a broad range of transition metal catalyzed reactions [Rubin et al., 2007; Marek et al., 2007; Li, 2011; Miege et al., 2011; Fang et al., 2012]; however their polymerization in living fashion by means of olefin metathesis with molybdenum catalyst has only been investigated since 2006 [Singh et al., 2006]. 3, 3-disubstituted cyclopropenes are quite appropriate for insertion polymerizations because they do not have any β-hydrogen which could affect chain transfer reactions potentially leading to low molecular weight polymers [Rush et al., 1997]. In recent years many experimental reports on molybdenum and ruthenium catalyzed ring opening metathesis polymerization of 3, 3-disubstituted cyclopropenes have appeared [Singh et al., 2006, Singh and Schrock, 2008; Binder et al., 2008; Flook et al., 2010].

In the last decade many reports on experimental [Perrot and Novak, 1996; Gibson et al., 1997; Singh and Schrock, 2008; Flook et al., 2010] and theoretical [Song etal., 2010;

Martinez et al., 2012; Wu and Peng, 2003] investigations on the ring opening metathesis polymerization (ROMP) have appeared. However they are chiefly focused on bicyclic and polycyclic or low strain olefins. Cyclopropene appears to be an interesting monocyclic monomer for the polymerization because of its ready availability and highly strained ring structure, (the ring strain energy of cyclopropene is ≈55 kcal/mol) [Bingham et al., 1975; Schleyer et al., 1970]. The objective of the present study is to model ring opening metathesis polymerization (ROMP) reaction of cyclopropene with Schrock's molybdenum catalyst. Systematic DFT studies of the whole catalytic cycle are performed on 3,3-dimethyl cyclopropene (DMCP) with the model catalyst $Mo(NH)(CH_2)(OCH_3)_2$ which reasonably represents to the Schrock catalyst [Schrock, 2009]. To the best of our knowledge, theoretical studies of molybdenum catalyzed ring opening metathesis polymerization of cyclopropene have not been reported. In this chapter we describe the mechanistic details of the molybdenum catalyzed ROMP of 3,3-dimethyl cyclopropene.

4.2 COMPUTATIONAL DETAILS

Gaussian 09 [Frisch et al., 2009] was used to fully optimize all the structures presented in this chapter using the B3LYP level of density functional theory (DFT) [Lee et al., 1988; Miehlich et al., 1989; Beck, 1993]. The effective-core potential with a double-ζ valence basis set (LANL2DZ) [Hay and Wadt, 1985a; 1985b] was selected to describe Mo and the D95V basis set was used for other atoms. The ultrafine pruned (99,590) grid was used throughout the calculations in this chapter. Frequency calculations were carried out at the same level of theory as those for the structural optimization. Intrinsic reaction coordinate (IRC) [Fukui, 1970; 1981] calculations were used to confirm the connectivity between transition structures and minima.

4.3 RESULTS AND DISCUSSION

Optimized structure of the model catalyst **1**(in Figure 4.2) was compared with experimental [Bazan et al., 1990; 1991] and previous theoretical calculations [Cundari, 1992; Floga 1993; Wu and Peng, 1997] on similar complexes. The geometry of the model catalyst used agrees well in essential features with earlier results on similar complexes and therefore we expect it to give an adequate representation of the molybdenum containing structures in the reaction with cyclopropene. The optimized geometry of the reactants (molybdenum catalyst and 3,3-disubstituted cyclopropene) are shown in Figure in 4.2 and their geometrical parameters are collected in Table 4.1.

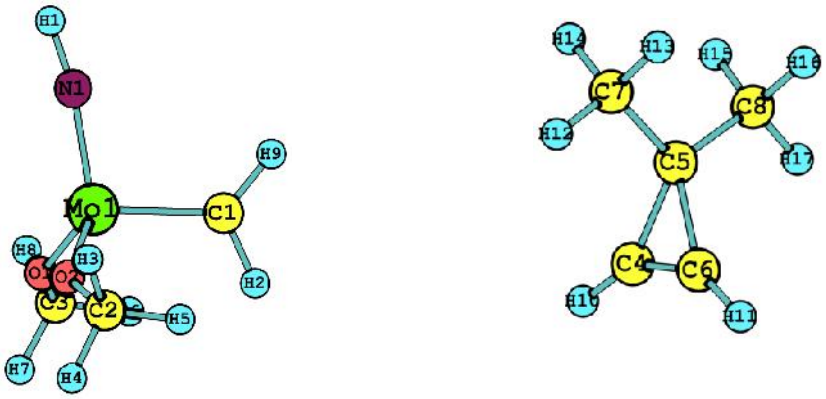

1 **DMCP**

Figure 4.2: Optimized geometries of the Model catalyst Mo(NH)(CH_2)(OCH_3)$_2$ and 3,3-dimethyl cyclopropene

The reaction may take place at two possible faces, the CNO face or the COO face, of the molybdenum catalyst similar to the tungsten catalyst as shown in Figure 3.1 in previous chapter. In each case the cyclopropene moiety may be oriented syn or anti to the NH group of the catalyst. The substituted carbon of cyclopropene is closer to the NH group in the syn orientation and farther in the anti orientation. The two orientations in the case of the CNO face of Mo(NH)(CH_2)(OCH_3)$_2$ are shown in Figure 4.3.

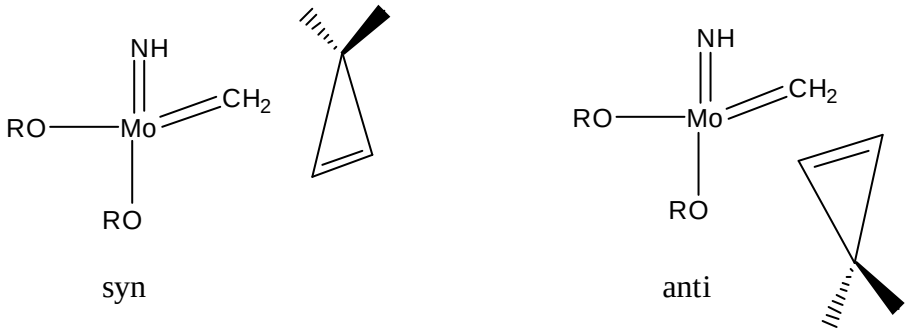

Figure 4.3 syn and anti orientation of 3, 3-dimethyl cyclopropene with the CNO face of Mo(NH)(CH_2)(OCH_3)$_2$ catalyst

Table 4.1: Selected optimized geometrical parameters[a] of the tungsten catalyst model $Mo(NH)(CH_2)(OCH_3)_2$ (**1**) and 3,3-dimethyl cyclopropene (**2**)

Parameter	**1**	Parameter	**2**
$Mo\text{-}C_1$	1.905	$C_4\text{-}C_6$	1.323
$Mo\text{-}O_1$	1.905	$C_4\text{-}C_5$	1.544
$Mo\text{-}O_2$	1.905	$C_6\text{-}C_5$	1.544
$Mo\text{-}N_1$	1.745	$C_4\text{-}H_{10}$	1.079
$N\text{-}M\text{-}C_1$	101.3	$C_6\text{-}H_{11}$	1.079
$Mo\text{-}C_1\text{-}H_9$	128.084	$C_5\text{-}C_4\text{-}C_6$	64.638
$Mo\text{-}C_1\text{-}H_2$	116.444	$C_4\text{-}C_6\text{-}C_5$	64.638
$Mo\text{-}N_1\text{-}H_1$	170.479	$C_4\text{-}C_5\text{-}C_6$	50.725
$C_1\text{-}Mo\text{-}O_1$	106.180	$C_7\text{-}C_5\text{-}C_8$	113.239
$C_1\text{-}Mo\text{-}O_2$	106.180		
$Mo\text{-}O_1\text{-}C_3$	145.829		
$Mo\text{-}O_2\text{-}C_2$	145.829		
$O_1\text{-}Mo\text{-}O_2$	110.071		

[a]Bond lengths are given in Å and angles in degrees

In the previous chapter (3) it had been found that the CNO face of the transition metal catalyst $W(NH)(CH_2)(OMe)_2$ is more favorable than the COO face for attack by the cyclopropene moiety. We reinvestigated the face preference in the case of the Molybdenum catalyst $Mo(NH)(CH_2)(OCH_3)_2$. Our results again support to the CNO face preference for the addition of DMCP. We conclude that there is no significant effect on the face preference of the catalyst by the change in the transition metal. The energy barrier for the reaction at the CNO face is lower by about 13.92kcal/mol in comparison with the COO face, as seen from entries 2 and 7 in Table 4.3. The enthalpies and free energies also show a similar trend. Therefore in the subsequent stages of the reaction we restrict our studies to the CNO face of the molybdenum catalyst. In Table 4.2 the calculated total electronic energies, enthalpies (at 298K) and Gibbs free energies (at 298K) of the reactants, transition structures, intermediates and products of the initiation step are provided.

Table 4.2: Calculated total electronic energies (E_e), enthalpy (H) and Gibbs free energies (in hartree) for the transition structures (TS) ,Trigonal bipyramidal (TBP), Square pyramidal (SP) and ring opening products of 3,3-dimethyl cyclopropene with $Mo(NH)(CH_2)(OCH_3)_2$.

CNO FACE		**syn orientation**		
	Structure	E_e	H	G
1.	Reactants	-587.674759	-587.421771	-587.507902
2.	STS1	-587.662593	-587.408285	-587.470496
3.	TBPI	-587.728597	-587.469399	-587.529982
4.	SPI	-587.734737	-587.47565	-587.538291
5.	STS2	-587.725230	-587.46764	-587.527626
6.	SPr	-587.766291	-587.507587	-587.573766
		anti orientation		
7.	ATS1	-587.65926	-587.405001	-587.46735
8.	TBPI	-587.7282903	-587.46924	-587.529223
9.	SPI	-587.7359373	-587.476937	-587.540273
10.	ATS2	-587.7272598	-587.469474	-587.528015
11.	APr	-587.7634504	-587.504341	-587.570747
COO FACE				
12.	Cycloaddition TS	-587.640410	-587.386733	-587.448748
13.	TBP Intermediate	-587.708653	-587.44998	-587.510183

Table 4.3: Calculated Relative Energies (ΔE_e, in kcal mol^{-1}), enthalpies (ΔH_{298}, in kcal mol^{-1}) and free energies (ΔG_{298}, in kcal mol^{-1}) for the transition structures (TS), Trigonal bipyramidal (TBP), Square pyramidal (SP) and ring opening products of 3,3-dimethyl cyclopropene with $Mo(NH)(CH_2)(OCH_3)_2$.

CNO FACE		**syn orientation**		
	Structure	ΔE_e	ΔH	ΔG
1.	Reactants	0	0	0
2.	STS1	7.63	8.46	23.47
3.	TBPI	-33.78	-29.89	-13.86
4.	SP I	-37.64	-33.81	-19.07
5.	STS2	-31.67	-28.78	-12.38
	STS2*	5.97	5.03	6.69
6.	SPr	-57.44	-53.85	-41.33
		anti orientation		
7.	ATS1	9.73	10.52	25.45
8.	TBPI	-33.59	-29.79	-13.38
9.	SPI	-38.39	-34.62	-20.31
10.	ATS2	-32.94	-29.93	-12.62
	ATS2*	5.45	4.68	7.69
11.	APr	-55.65	-51.81	-39.44
COO FACE				
12.	Cycloaddition TS	21.55	21.99	37.12
13.	TBP Intermediate	-21.27	-17.70	-1.43

*Energy relative to the most stable corresponding syn & anti SP intermediate

4.3.1 INITIATION

Ring opening metathesis polymerization is initiated with the 2+2 cycloaddition of the cyclopropene moiety to the molybdenum catalyst and followed by the ring opening step which formed a new alkylidene capable to propagate the polymerization of cyclopropene.

4.3.1.1 Cycloaddition Step

In the cycloaddition reaction, 3,3-dimethyl cyclopropene molecule **2** attacks the CNO face of molybdenum methylidene **1** in either syn or anti orientation as indicated in Figure 4. 3. Distorted trigonal bipyramidal transition structures are formed in both syn and anti orientations, in these one of the OCH_3 groups and the NH group occupy axial positions and the metallacyclobutane ring assumes a four centered non planar distorted rectangular shape. These optimized transition structures are shown in Figure 4.4. The syn and anti transition structures are denoted as STS1 and ATS1 respectively. The geometrical parameters of these structures are collected in Table 4.4.

Intrinsic reaction coordinate (IRC) calculations confirm that the transition structures STS1 and ATS1 do fall on the reaction path of cycloaddition. Figure 4.5 show IRC plots for both transition structures. IRC shows the STS1 and ATS1 moving downhill towards their respective molybdacyclobutane intermediate on one side and the reactants on other. Frequency calculations have also been performed and an imaginary frequency is found for each STS1 and ATS1 as shown in Table 4.5.

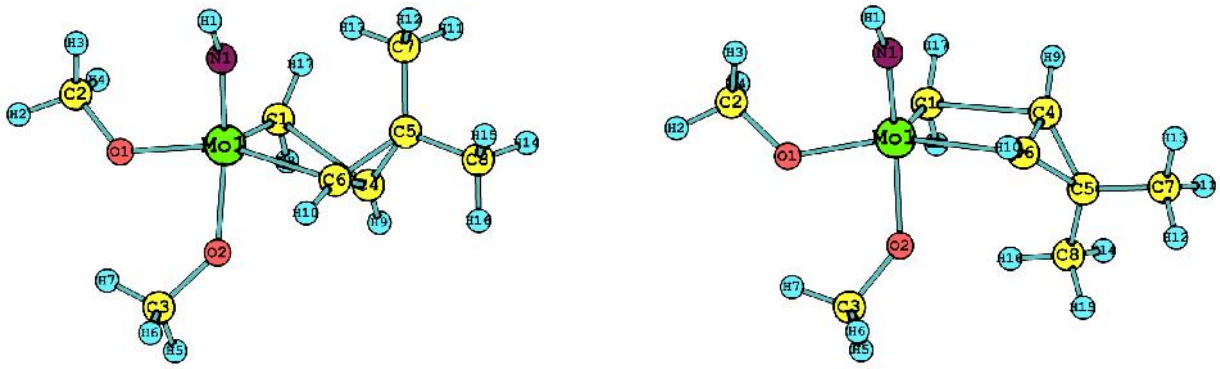

STS1 ATS1

Figure 4.4: Optimized geometries of the transition structure of syn and anti cycloaddition of 3, 3-dimethyl cyclopropene with Mo catalyst

In both syn and anti transition structures, there is significant Mo-C_6 bond formation. On the other hand the Mo-C_1 bond of the catalyst is slightly elongated. The newly forming bond (Mo-C_6) has a length of 2.6 Å whereas the Mo-C_1 bond is slightly elongated to 1.93Å from 1.91Å. The C_4-C_6 bond also lengthened (1.36Å) .The C_1-Mo-O_1 angle is about 106º in these geometries but the C_6-Mo-O_1 is larger 152-154º. The N-Mo-O_2 angle is 144-147º. The four membered ring formed by the Mo-C_1-C_6-C_4 moiety is farther from planarity in STS1 than in ATS1, probably due to the net effect of the steric repulsion between the methyl on C_5 and the NH group in STS1 and that between the methyl on the C_5 and the axial OCH_3 group in ATS1.

The calculated activation enthalpies for the cycloaddition stage are 8.46 kcal/mol in the syn (STS1) and 10.52 kcal/mol in the anti addition (ATS1) as seen in Table 4.3 entry 2. The activation enthalpies for the formation of metallacyclobutane intermediate from norbornadiene from earlier theoretical calculations are 9.5 kcal/mol and 10.5 kcal/mol respectively [Wu and Peng, 2003]. In the norbornadiene case the syn transition structure is reported to be stabler than the anti transition structure by approximate by 1 kcal/mol, whereas in the cyclopropene case we find a somewhat higher stabilization of the syn structure by about 2 kcal/mol relative to the anti. It must be noted however that the model catalyst in both cases have less bulky groups as against in the experimentally used catalyst Mo(NAr)(CHR)(OR')$_2$ in which R = CMe_2Ph, t-Bu R'= $C(CF_3)_2Me$ and Ar = 2,6-diisopropylphenyl [Singh et al., 2006]. Oskam and Schrock (1993) as well as Wu and Peng (2003) have also supported syn addition.

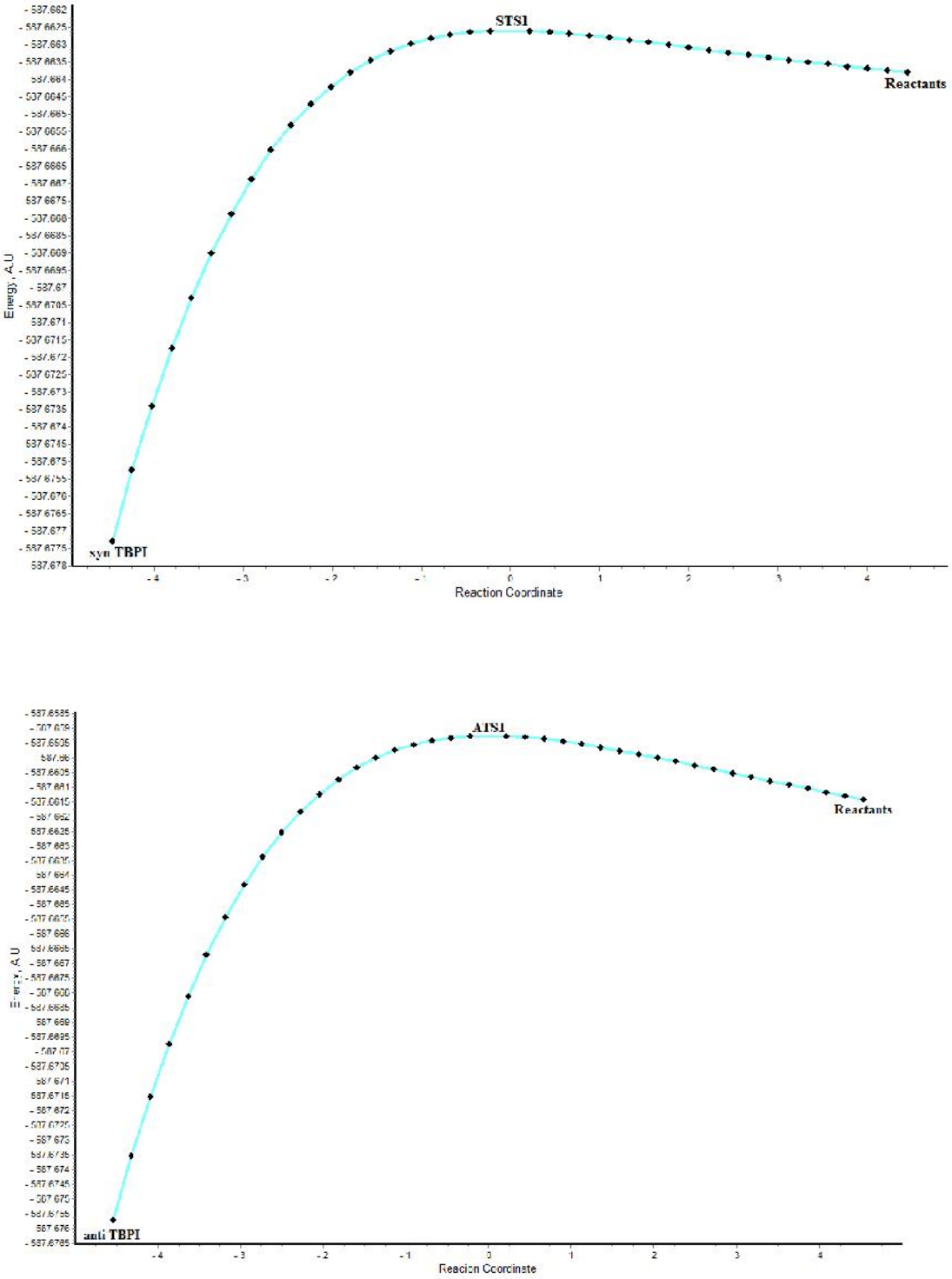

Figure 4.5: IRC plots for the syn and anti transition structures of the cycloaddition step

Table 4.4: Optimized structural parameters (bond lengths in Á and angles in degree) for the transition structures (TS),Trigonal bipyramidal (TBP), Square pyramidal (SP) and ring opened product of initiation step of ROMP reaction of 3,3-dimethyl cyclopropene with $Mo(NH)(CH_2)(OCH_3)_2$

S. No.	Parameters	**SYN**					**ANTI**				
		STS1	TBPI	SPI	STS2	SPr	ATS1	TBPI	SPI	ATS2	APr
1.	Mo-N	1.767	1.774	1.741	1.769	1.747	1.770	1.773	1.743	1.768	1.745
2.	$Mo-O_1$	1.957	1.962	1.907	1.953	1.912	1.966	1.977	1.903	1.965	1.911
3.	$Mo-O_2$	1.945	1.956	1.908	1.950	1.911	1.936	1.965	1.905	1.962	1.910
4.	Mo-C1	1.928	2.210	2.220	2.442	-	1.927	2.256	2.228	2.536	-
5.	$Mo-C_6$	2.556	2.030	2.164	1.980	1.907	2.555	2.016	2.164	1.972	1.922
6.	C_1-C_4	2.752	1.495	1.514	1.419	1.350	2.744	1.469	1.517	1.399	1.350
7.	C_4-C_6	1.357	1.713	1.566	1.972	-	1.357	1.780	1.539	2.045	-
8.	$N-Mo-O_1$	98.5	93.0	113.6	98.84	115.5	96.0	92.8	113.4	96.5	115.7
9.	$N-Mo-O_2$	144.8	163.1	111.8	144.8	115.5	147.0	153.3	113.8	139.6	115.0
10.	$N-Mo-C_1$	101.9	89.4	103.1	84.34	-	102.0	97.2	97.5	100.0	-
11.	O_1-Mo-O_2	84.3	81.6	102.8	83.43	110.2	83.0	79.98	103.8	82.5	110.3
12.	C_1-Mo-O_1	105.8	147.7	136.2	161.9	-	106.2	152.3	139.5	157.1	-
13.	C_1-Mo-O_2	111.2	86.9	83.8	83.86	-	110.0	79.56	85.2	74.6	-
14.	C_6-Mo-O_1	152.1	130.6	84.01	115.3	105.7	153.7	123.1	84.6	111.6	107.6
15.	C_6-Mo-O_2	75.4	94.7	138.1	107.5	105.6	80.8	104.6	137.5	114.6	106.6
16.	$Mo-O_1-C_2$	127.0	130.4	148.7	127.5	144.3	126.5	126.8	149.0	124.3	149.2

17.	Mo-O_2-C_3	136.2	139.4	153.3	137.0	144.4	137.8	136.7	153.0	133.1	146.5
18.	C_1-Mo-C_6	99.3	80.2	64.98	80.85	-	98.8	80.17	64.4	78.0	-
19.	Mo-C_1-C_4	67.5	79.57	96.8	78.63	-	68.7	80.37	96.8	79.7	-
20.	C_1-C_4-C_6	108.9	116.8	99.78	115.9	-	108.5	115.8	99.94	115.1	-
21.	Mo-C_6-C_4	80.5	80.6	97.47	81.18	-	82.0	81.24	98.82	83.3	-
22.	N-Mo-C_6	87.8	100.8	102.3	103.2	103.0	86.6	100.8	99.7	103.3	100.3
23.	Mo-C_1-C_6-C_4	155.3	159.81	169.87	157.6		-162.46	-161.4	-177.8	-163.1	

Table 4.5: Imaginary frequencies (in cm^{-1}) of the transition structures found in the initiation step of (ROMP) of 3,3-dimethyl cyclopropene with $Mo(NH)(CH_2)(OCH_3)_2$ catalyst

S.No.	**Transition Structure**	**Frequency**
1.	STS1	107.79*i*
2.	ATS1	123.91*i*
3	STS2	97.54*i*
4.	ATS2	115.41*i*

The molybdacyclobutane intermediates are formed, with distorted trigonal bipyramidal geometry, via their corresponding transition structures (STS1 &ATS1). These intermediates are in pseudo-TBP geometry and can rearrange by a Berry-type pseudorotation to a square –pyramidal structures [Feldman et al., 1989]. The syn/anti molybdacyclobutane intermediates in trigonal bipyramidal and square pyramidal geometry are denoted as TBPI and SPI respectively and shown in Figure 4.6.

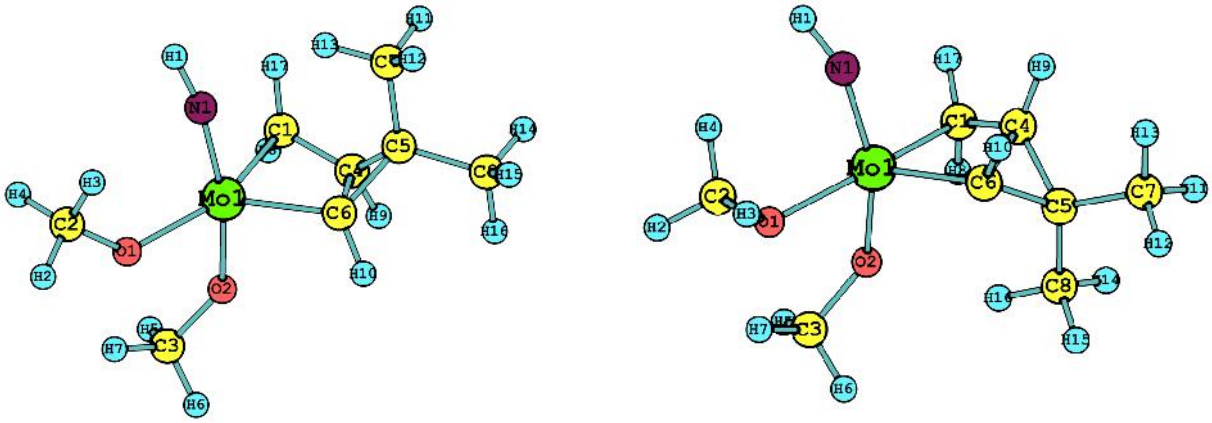

syn TBPI anti TBPI

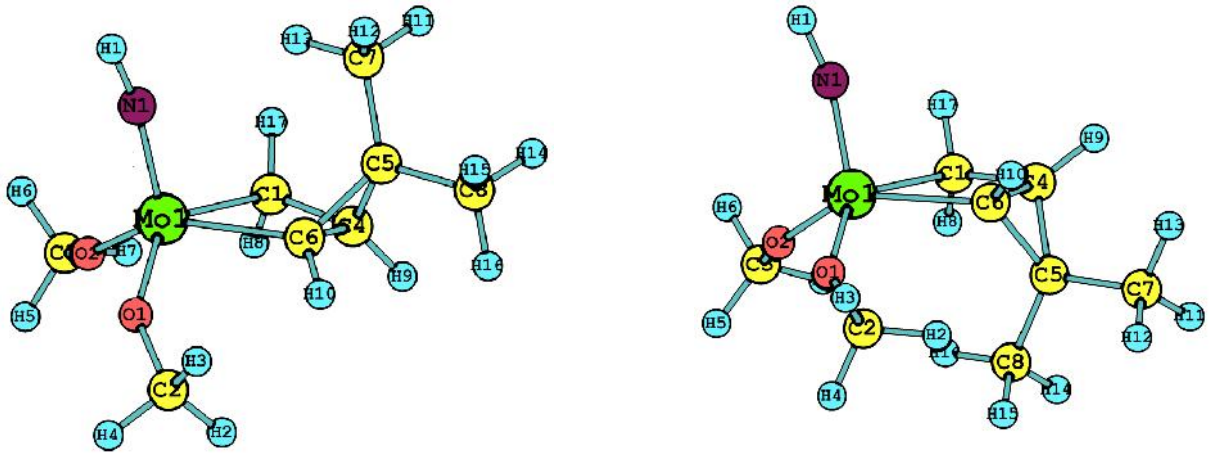

syn SPI anti SPI

Figure 4.6: Optimized geometries of syn/anti trigonal bipyramidal and square pyramidal intermediates of 3, 3-dimethyl cyclopropene with Mo catalyst

The TBP intermediates have a four centered molybdacyclobutane (Mo-C_1-C_4-C_6) ring, which is somewhat different from that of the SP structure. In TBP molybdacyclobutane ring the C_1-Mo-C_6 and Mo-C-C angles are about 80º, the C_1-C_4-C_6 angles are about 116º while in SP ring these angles are 65º & 97º and 100º respectively. The bond length (C_4-C_6) of molybdacyclobutane ring is unusually large (1.71-1.78Å). This bizarre increase is due to significant ring strain in the fused ring. In SP intermediates, it has values in the more usual range of 1.54-1.57Å. The Mo-C_6 and C_1-C_4 distances have become shorter as compared to the corresponding syn and anti transition structures and show the formation of two new bonds. The Mo-C_6 bond length is about 2.0Å in TBPI and notably higher (2.2Å) in SPI. The other new bond C_1-C_4 is somewhat shorter in TBPI than SPI. There is only 0.01-0.02 difference between the Mo-C_1 length in TBP and SP intermediates. The structure of the ring of the metallacyclobutane of the SPI is consistent with the X-ray crystal structures of the isolated molybdacyclobutane [Bazan et al.,1991] and with the results of previous theoretical calculations on the reaction of ethene and norbornadiene with $Mo(NH)(CH_2)(OCH_3)_2$ [Wu and Peng, 2003; 1997].

The syn TBP intermediate is about 0.10 kcal/mol stabler than the anti TBP intermediate. But in case of SP intermediates the stability order is reversed i.e. the anti intermediate is about 0.81 kcal/mol more stable than the syn intermediate. We ascribe it to the fact that the axial OCH_3 group has become equatorial so that the repulsion between axial OCH_3 and C_5 centre ceases to be significant but in syn SPI the repulsion between NH group and the C_5 centre remains. For both the syn and anti cases the SP intermediates are calculated to be lower in energy than the corresponding TBP Intermediates; the syn SP by about 3.86 kcal/mol and anti SP by about 4.80 kcal/mol. These trends are similar to earlier findings for the reactions of ethene [Wu and Peng, 1997] and norbornadiene [Wu and Peng, 2003] with same model catalyst, though the stabilization of the SPI is numerically smaller in our case.

4.3.1.2 Ring Opening Step

Attempts were made to find a direct pathway for conversion of the stable SP intermediate to the ring opened product but failed. However we were able to find a transition state for the opening of the ring in TBP isomer that goes over to the ring opened product on one side and to TBPI on the other. These optimized transition structures are shown in Figure 4.7 and labeled as STS2 and ATS2 respectively for the syn and anti cases.

IRC plots of syn and anti transition structures of ring opening step are shown in Figure 4.8 and it confirm that the transition structures STS2 and ATS2 connect to the trigonal bipyramidal intermediate (STBP & ATBP) and their corresponding ring opened products (SPr & Apr). An imaginary frequency (given in Table 4.5) was obtained for each transition structure by frequency calculations.

As expected the lengths of the breaking Mo-C_1 and C_4-C_6 bonds are longer in STS2 and ATS2 in comparison with corresponding TBP Intermediates, about 0.23Å & 0.26Å and about 0.28Å & 0.27Å respectively. The forming bond Mo-C_6 and C_1-C_4 are slightly shortened by about 0.05Å & 0.08Å in STS2 and 0.04Å & 0.07Å in ATS2. The ring opening transition structures are also in pseudo-TBP geometry, similar to the cycloaddition transition structures. Compared with the cycloaddition transition structures (STS1 and ATS1), the C_1-Mo-O_1 angles are larger (162º & 157º) while C_6-Mo-O_1 angles are smaller (115º & 112º) in ring opening transition structures (STS2 and ATS2) respectively (see in Table 4.4)

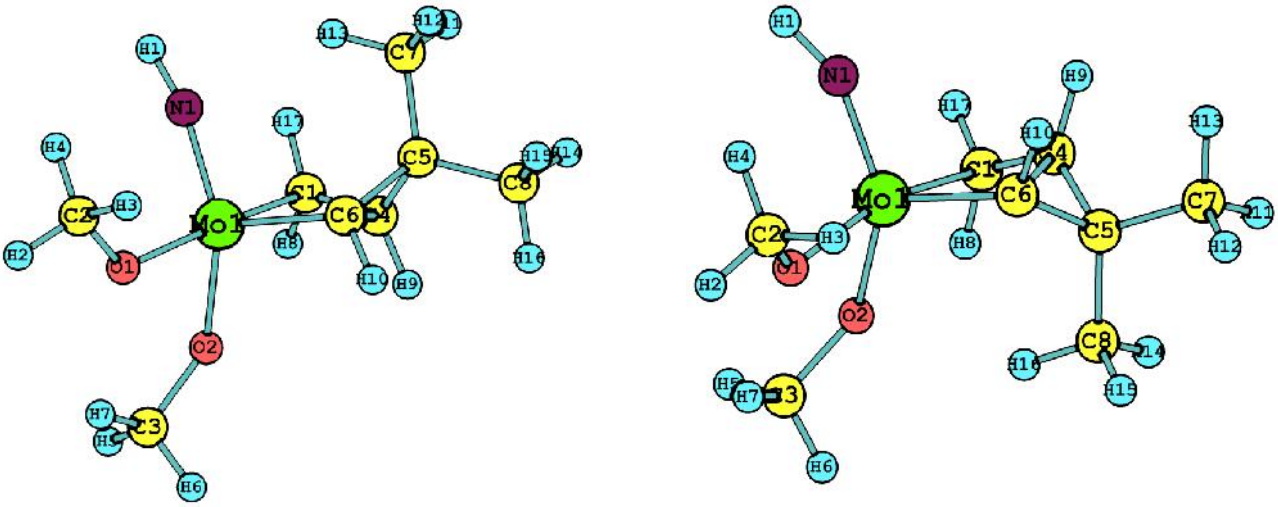

STS2 ATS2

Figure 4.7: Optimized geometries of the ring opening transition structures (STS2 and ATS2) of the 3,3-dimethyl cyclopropene with Mo catalyst.

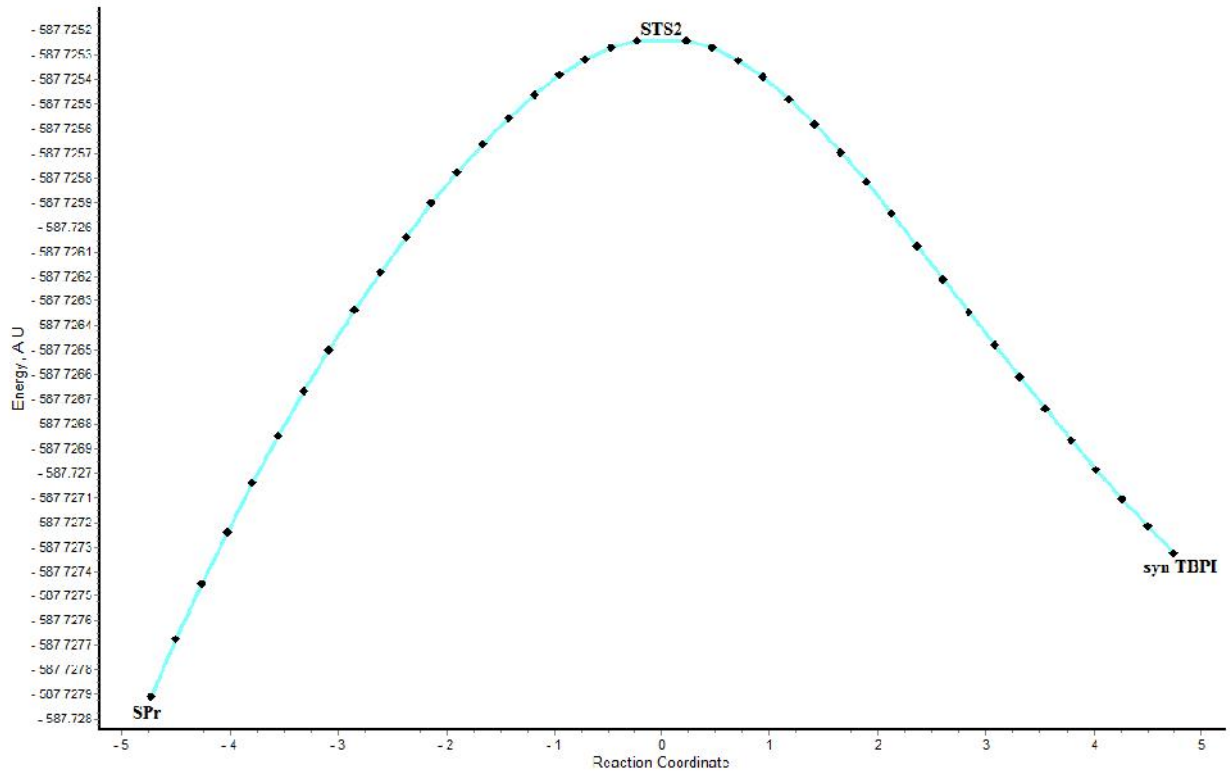

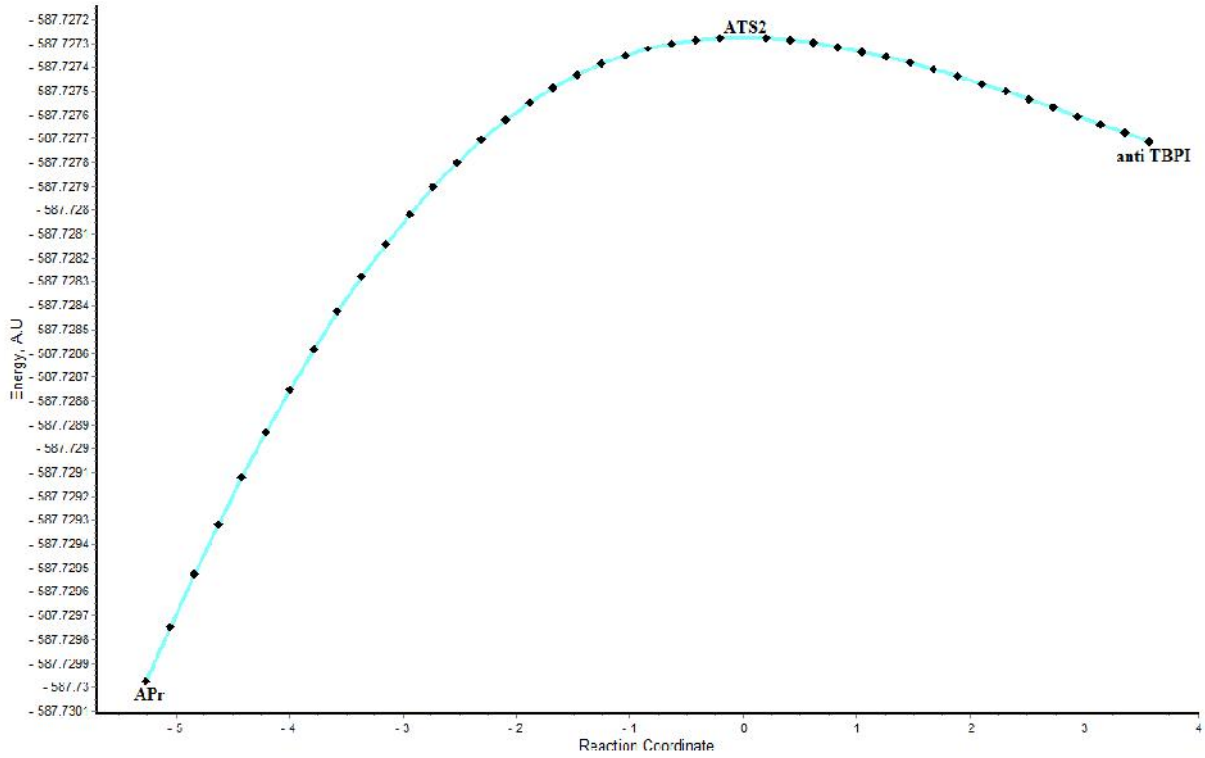

Figure 4.8: IRC plots for the syn and anti transition structures of the ring opening step

It has been predicted earlier [Wu and Peng, 2003] that the fused C_4-C_6 bonds in the molybdacyclobutane ring of the TBP intermediates can be very easily broken. The calculated transition structures (STS2 & ATS2) support this prediction. The transition structures are higher in energy than the TBP intermediates by only about 2.11 and 0.65 kcal/mol for the syn and anti cases respectively. Relative to the most stable intermediate (SPI), the calculated activation enthalpies for ring opening STS2 and ATS2 are about 5.03 and 4.68 kcal/mol respectively (See Table 4.3, entries 5). In terms of product stability, both energy and enthalpy are lower for the product formed via the anti transition structure (ATS2); however the computed free energy favors the product formed via the syn transition structure (STS2). The trend seen in our calculations are parallel to the findings of earlier work on the norbornadiene system, however our calculations on cyclopropene give lower energy barriers for ring opening for the cyclopropene case, probably on account of the higher strain on the ring system. The energy barriers for ring opening steps are significantly lower than that for cycloaddition steps, leading us to predict that the cycloaddition step is the slower; and consequently the rate determining step of the ring opening metathesis of 3, 3-dimethyl cyclopropene with molybdenum catalyst. This is in contrast with the case of the tungsten catalyst reported in the previous chapter, but in agreement with the general trend found by experiments that molybdacyclobutane intermediates appear to break up more readily than their tungsten counterparts [Schrock and Hoveyda 2003]. In case of tungsten (in Chapter 3) ring opening activation enthalpies are higher by about 4.85 kcal/mol and 8.58 kcal/mol for syn and anti paths respectively. The lower activation barriers of cycloaddition and ring opening step with molybdenum catalyst suggest that the metathesis of cyclopropene initiate more easily as compared to tungsten catalyst.

The optimized structures of the products of the ring opening metathesis reaction of 3, 3- dimethyl cyclopropene with $Mo(NH)(CH_2)(OCH_3)_2$ are shown in Figure 4.9. The syn and anti ring opened product denoted as SPr and APr respectively. In both the syn and anti products, the rings (C_4-C_5-C_6) of the 3, 3-dimethyl cyclopropene have been opened. Two new bonds, one metal alkylidene (Mo-C_6) and one carbon -carbon bond (C_1-C_4) has been formed. The Mo-C_1 and C_4-C_6 bonds have completely broken (see in Table 4.4) These findings and the products structure are consistent with the previous experimental [Bazan et al., 1990] studies on the syn and anti Mo(NH)(CHMe)(OR') catalyst and the theoretically [Wu and Peng, 2003] reported products from the reaction with norbornadiene .The newly formed Mo-C_6 bond has a length of 1.907Å while the other newly formed double bond

(C_1-C_4)length is 1.350Å (see in Table 4.4). Respectively, these lengths are comparable with the Mo-C_1 bond length in the starting model catalyst and the double bond (C_4-C_6) of the cyclopropene moiety.

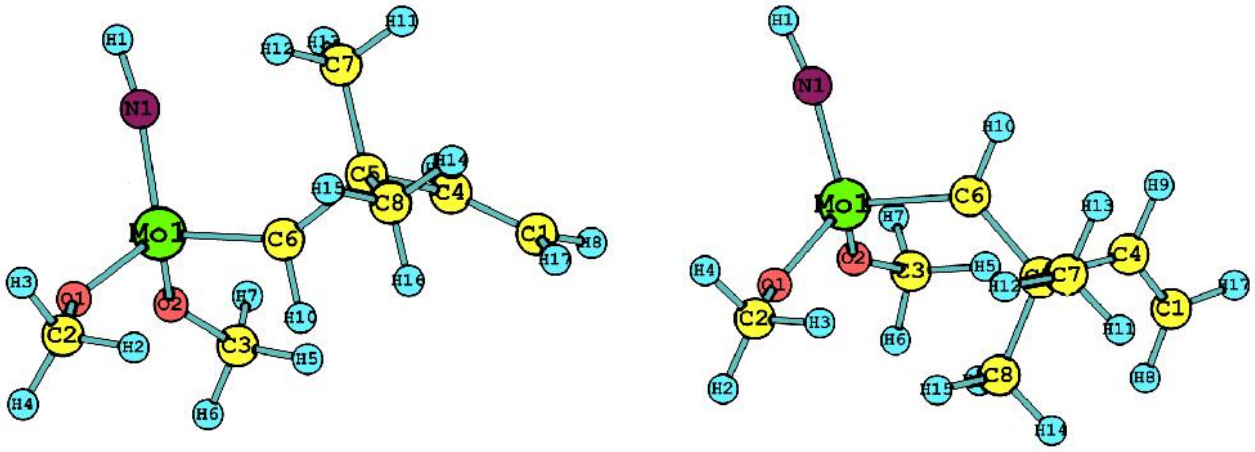

SPr APr

Figure 4.9: Optimized geometries of the ring opening syn (SPr) and anti (APr) products of the 3,3-dimethyl cyclopropene with Mo catalyst

Overall, the formation of the ring opening products either syn or anti is an exothermic process. The enthalpies of the syn and anti products are -53.85 kcal/mol and -51.81 kcal/mol respectively. Relative to the reactants SPr is more stable than APr by 2.04 kcal/mol, due to larger steric hindrance of the methyl groups in anti products. Gibbs free energy (see Table 4.3 Entry 6) also favors the syn product.

4.3.2 PROPAGATION

The newly formed alkylidene (SPr or APr) can proceed to the propagation step of ROMP of 3,3 dimethyl cyclopropene following the same sequence of steps as earlier. As the cycloaddition step is the rate determining step of the initiation stage, the stereochemical outcome of ROMP can be discussed based on the transition structures for cycloaddition intermediates.

4.3.2.1 Cycloaddition step

In investigating the reaction of syn and anti $Mo(NH)(CHR)(OCH_3)_2$ (where R=Propagating chain) alkylidene with DMCP, the activation barriers are calculated in both cases. Cyclopropene reacts in syn and anti manner with both syn (SPr) and anti (APr) alkylidene. Thus four transition structures are possible for the cycloaddition step in the propagation stage. Two transition structures are obtained with syn and anti addition of cyclopropene to syn alkylidene and two with anti alkylidene. The transition structures have similar geometry to that found in the cycloaddition reaction of the initiation step and the geometries of these structures are not further discussed here. The two transition structures with syn alkylidene (syn-syn **PTS1**, syn-anti **PTS2**) and two with anti-alkylidene (anti-syn **PTS3**, anti-anti **PTS4**) are shown in Figure 4.10.

The calculated total electronic energy (E_e), enthalpy (H), and Gibbs energy of these transition structures are provided in Table 4.6 whereas relative energies, enthalpies and free energies are shown in Table 4.7. Frequency calculations performed for the all transition structures of the cycloaddition step propagation and imaginary frequencies associated with these structures are given in Table 4.8. All transition structures of the confirmed by the IRC calculations. IRC plots for the transition structures with syn alkylidene (PTS1& PTS2) are shown in Figure 4.11 while for anti alkylidene in Figure 4.12. The optimized geometrical parameters are collected in Table 4.9.

The transition structures with syn cyclopropene PTS1and PTS3 are more stable than those with anti cyclopropene PTS2 and PTS4 respectively (see in Table 4.7). The transition structure syn-anti (PTS2) is the least stable ones. The transition structure (PTS3) has the lowest barrier path for the reaction. These findings suggest that cyclopropene approaches the molybdenum-alkylidene catalyst preferentially in the syn manner. Our results are in good agreement with the hypothesis proposed by Schrock and Oskam [Oskam and Schrock 1993], wherein propagation proceeds preferentially through syn approach of cyclopropene to anti molybdenum alkylidene. Thus we conclude that the steric hindrance of the R group of molybdenum catalyst $Mo(NH)(CHR))OCH_3)_2$ plays an important role in stereochemical outcomes of the ROMP of cyclopropene. ROMP of cyclopropene proceeds via syn approach whether reaction takes place through syn or anti $Mo(NH)(CHR))OCH_3)_2$ catalyst. Since, the anti alkylidene (PTS3) is more reactive than syn alkylidene (PTS1); it results in the preferential formation of all trans polymer from the ROMP of cyclopropene, in good agreement with experimental results [Singh and Schrock 2008].

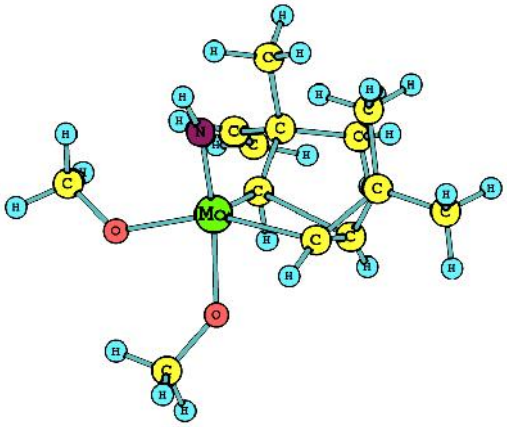

syn-syn (PTS1)

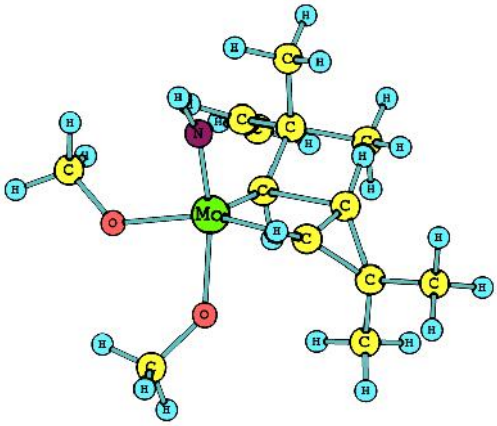

syn-anti (PTS2)

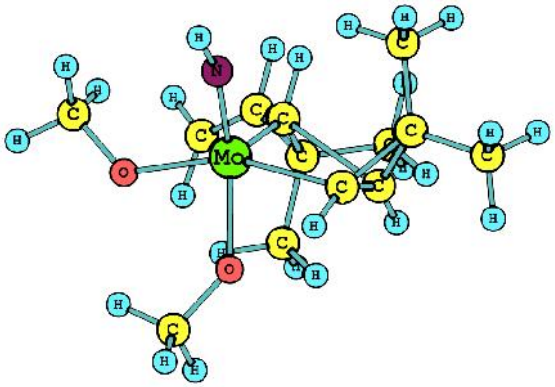

anti-syn (PTS3)

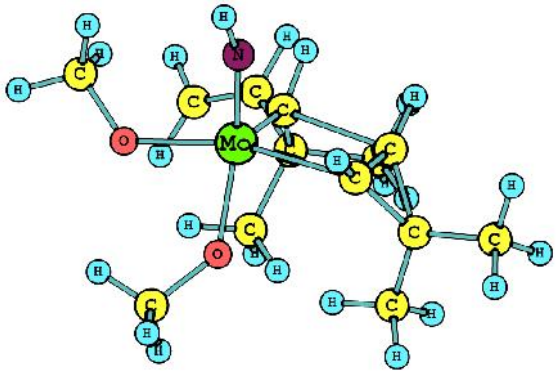

anti-anti (PTS4)

Figure 4.10: Optimized transition structures of cycloaddition reactions of 3,3-dimethyl cyclopropene with syn and anti alkylidene of molybdenum catalyst

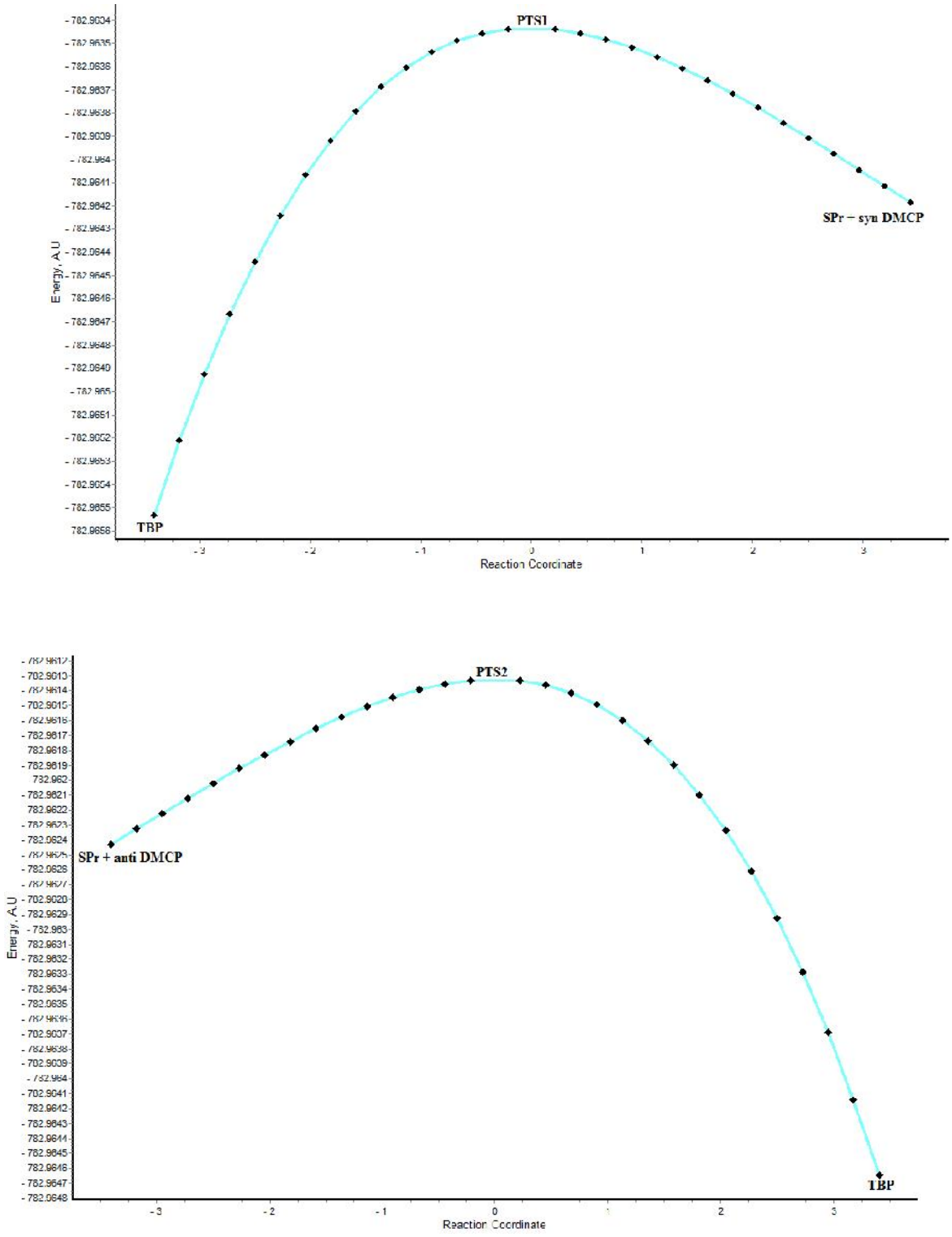

Figure 4.11: IRC plots for the transition structures of propagation step proceeding through syn alkylidene (SPr) and syn/anti DMCP

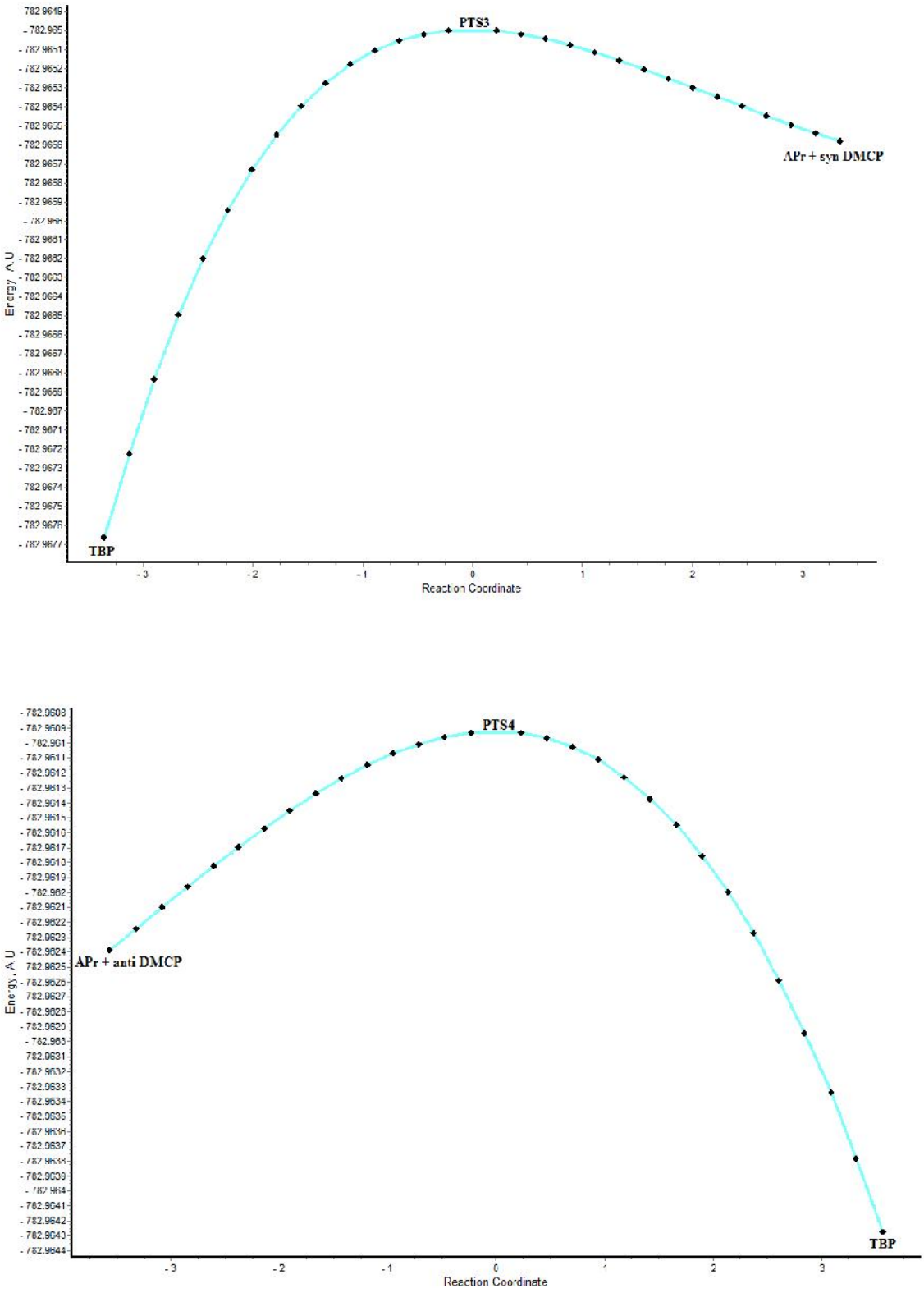

Figure 4.12: IRC plots for the transition structures of propagation step proceeding through anti alkylidene (APr) and syn/anti DMCP

Table 4.6: Calculated total electronic energies (in kcal/mol), enthalpies (ΔH_{298}, in kcal/mol) and Gibbs energies (ΔG_{298} in kcal/mol) of the transition states (TSs) of cycloaddition reaction of 3,3 dimethyl cyclopropene with $Mo(NH)(CHR)(OCH_3)_2$ in propagation step

S.No.	Structure	E_e	H	G
1.	syn-syn (PTS1)	-782.9634343	-782.584174	-782.661823
2.	syn-anti (PTS2)	-782.9613159	-782.582236	-782.659700
3.	anti-syn (PTS3)	-782.9649718	-782.585642	-782.662193
4.	anti-anti (PTS4)	-782.9609018	-782.581478	-782.658095

Table 4.7: Calculated relative[a] electronic energies (in kcal/mol), enthalpies (ΔH_{298}, in kcal/mol) and Gibbs energies (ΔG_{298} in kcal/mol) of the transition states (TSs) of cycloaddition reaction of 3,3 dimethyl cyclopropene with syn and anti alkylidene (SPr & APr) in propagation step

S.No.	Structure	ΔE_e	ΔH	ΔG
1.	syn-syn (PTS1)	9.05	10.01	25.06
2.	syn-anti (PTS2)	10.38	11.23	26.39
3.	anti-syn (PTS3)	6.31	7.05	22.93
4.	anti-anti (PTS4)	8.86	9.67	25.50

[a]Relative to the SPr/APr + DMCP

Table 4.8: Imaginary frequencies (in cm^{-1}) of the transition structures found in the propagation step of ROMP of 3,3-dimethyl cyclopropene with syn and anti alkylidene (SPr & APr)

S.No.	**Transition Structure**	**Frequency**
1.	syn-syn (PTS1)	78.29*i*
2.	syn-anti (PTS2)	95.67*i*
3	anti-syn (PTS3)	80.49*i*
4.	anti-anti (PTS4)	101.59*i*

Table 4.9: Optimized geometrical parameters (bond lengths in Å and angles in degree) of the transition structures (TS) investigated for the propagation step of ROMP reaction of 3,3-dimethyl cyclopropene with syn and anti alkylidene (SPr & APr)

S.No.	Parameter	PTS1	PTS2	PTS3	PTS4
1.	Mo-N	1.768	1.769	1.768	1.770
2.	Mo-O_1	1.949	1.940	1.950	1.940
3.	Mo-O_2	1.969	1.974	1.965	1.974
4.	Mo-C_1	1.936	1.936	1.950	1.952
5.	Mo-C_6	2.58	2.573	2.540	2.535
6.	C_1-C_4	2.884	2.861	2.806	2.769
7.	C_4-C_6	1.354	1.354	1.359	1.362
8.	N-Mo-O_1	147.1	148.0	141.8	144.5
9.	N-Mo-O_2	96.77	95.36	98.86	96.07
10.	N-Mo-C_1	103.96	103.8	101.3	101.1
11.	O_1-Mo-O_2	83.52	82.80	83.76	82.36
12.	C_1-Mo-O_1	107.8	107.43	115.3	113.80
13.	C_1-Mo-O_2	104.4	105.5	103.4	103.2
14.	C_6-Mo-O_1	73.75	80.20	75.06	82.56
15.	C_6-Mo-O_2	147.82	150.6	151.9	154.3
16.	Mo-O_1-C_2	136.55	137.7	135.5	137.2
17.	Mo-O_2-C_3	127.87	128.0	126.4	125.7
18.	C_1-Mo-C_6	104.04	102.3	102.3	101.9
19.	Mo-C_1-C_4	64.74	65.73	64.47	66.18
20.	C_1-C_4-C_6	110.13	108.6	110.3	111.4
21.	Mo-C_6-C_4	80.10	81.10	78.85	80.23
22.	N-Mo-C_6	90.60	86.78	87.08	84.43

4.4 CONCLUSIONS

In this chapter, we have presented results of computational studies on the molybdenum catalyzed ring opening metathesis polymerization reaction of 3,3-dimethyl cyclopropene. The 3, 3-dimethyl cyclopropene reacts with the catalyst at the CNO face rather than the COO face during the metathesis process. The enthalpy change for the cycloaddition to form trigonal bipyramidal molybdacyclobutane at the CNO face is 12.19 kcal/mol lower than for the COO face.

Out of the two likely orientations (as shown in Fig 2) of the 3, 3-dimethyl cyclopropene with the present model catalyst, the syn orientation gives a lower barrier path for the formation of molybdacyclobutane intermediates. However there is no large difference in the stability of the syn and anti products of this step. Kinetically we conclude that the syn orientation of the 3, 3-dimethyl cyclopropene is preferred over the anti orientation to precede the ring opening metathesis reaction of cyclopropene. The cycloaddition step is the rate determining step, as the activation barriers for ring opening are lower. The ring opening metathesis polymerization reaction either in syn or anti orientation is very exothermic with respect to the reactants. Thermodynamically the syn ring opened product is stabler by 2.04 kcal/mol. The ring opened products (new alkylidene) propagate the polymerization of the DMCP. It is found that syn addition of cyclopropene moiety to the anti alkylidene of Mo-catalyst is more favorable, resulting in all trans polymers. We have characterized an exhaustive set of intermediates, transition states and products in the ring opening metathesis polymerization reaction of 3, 3-dimethyl cyclopropene with molybdenum catalyst as well as stereochemical outcomes of ROMP reaction.

4.5 REFERENCES

Bazan G C , Khosravi E, Schrock , Feast W J, Gibson V C, O'Regan M B, Thomas J K and Davis W M (**1990**) "Living ring-opening metathesis polymerization of 2,3-difunctionalized norbornadienes by Mo(CH-tert-Bu)(N-2,6-C_6H_3-iso-Pr_2)(O-tert-Bu)$_2$" *J. Am. Chem. Soc.* **112**: 8378-8387.

Bazan G C, Oskam J H, Cho H N, Park L Y and Schrock R R (**1991**) "Living ring-openingmetathesis polymerization of 2,3-difunctionalized 7-oxanorbornenes and 7-Oxanorbornadienes by Mo(CHCMe$_2$R)(N-2,6-C_6H_3-iso-Pr_2)(O-tert-Bu)$_2$ and Mo(CHCMe$_2$R)(N-2,6-C_6H_3-iso-Pr_2)(OCMe$_2$CF$_3$)$_2$"*J. Am. Chem. Soc.* **113**: 6899-6907.

Bazan G C, Schrock R R, Cho H N and Gibson V C (**1991**) "Polymerization of functionalized norbornenes employing Mo(CH-t-Bu)(NAr)(O-t-Bu)$_2$ as the initiator" *Macromolecules* **24**: 4495-4502.

Becke A D (**1993**) "Density-functional thermochemistry .3. The role of exact exchange" *J. Chem. Phys.* **98**: 5648-5652.

Biagini S C G, Coles M P, Gibson V C, Giles M R, Marshall E L and North M (**1998**) "Living ring-opening metathesis polymerisation of amino ester functionalised norbornenes" *Polymer* **39**: 1007-1014.

Bielawski C W and Grubbs R H (**2007**) "Living ring-opening metathesis polymerization" *Prog. Polym. Sci.* **32**: 1-29.

Binder W H, Kurzhals S, Pulamagatta B, Decker U, Pawar G M, Wang D, Kuhnel C and Buchmeiser M R (**2008**) "Homologous Poly(isobutylene)s: Poly(isobutylene)/High-Density Poly(ethylene) Hybrid Polymers" *Macromolecules* **41**: 8405-8412.

Binder W H, Pulamagatta B, Kir O, Kurzhals S, Barqawi H and Tanner S(**2009**) "Monitoring block-copolymer crossover-chemistry in ROMP: catalyst evaluation via mass-spectrometry (MALDI)" *Macromolecules* **42**: 9457-9466.

Bingham R C, Dewar M J S and Lo D H (**1975**) "Ground-states of molecules .26. MINDO-3 calculations for hydrocarbons" *J. Am. Chem. Soc.* **97**: 1294-1301.

Buchmeiser M R (**2000**) "Homogeneous Metathesis Polymerization by Well-Defined Group VI and Group VIII Transition-Metal Alkylidenes: Fundamentals and Applications in the Preparation of Advanced Materials" *Chem. Rev.***100**: 1565-1604.

Dounis P and Feast W J (**1996**) "A route to low polydispersity linear and star polyethylenes via ring-opening metathesis polymerization" *Polymer* **37**: 2547-2554.

Fang R, Yang L and Wang Q (**2012**) "DFT study on the mechanism of $PtCl_2$-catalyzed rearrangement of cyclopropenes to allenes" *Organometallics* **31**: 4020-4030.

Feldman J, Davis W M and Schrock R R (**1989**) "Trigonal-bipyramidal and square-pyramidal tungstacyclobutane intermediates are both present in systems in which olefins are metathesized by complexes of the type W(CHR')(N-2,6-C_6H_3-iso-Pr_2)$(OR)_2$" *Organometallics* **8**: 2266-2268.

Flook M M, Gerber L C H, Debelouchina G T and Schrock R R (**2010**) "Z-Selective and Syndioselective Ring-Opening Metathesis Polymerization (ROMP) Initiated by Monoaryloxidepyrrolide (MAP) Catalysts" *Macromolecules* **43**: 7515-7522.

Frisch M J, et al. (**2009**) Gaussian 09, revision A.02; Gaussian, Inc.:Wallingford, CT.

Fukui K J (**1970**) "A Formulation of the Reaction Coordinate" *Phys. Chem.* **74**: 4161-4163.

Fukui K (**1981**) "The path of chemical reactions - The IRC approach" *Acc. Chem. Res.* **14**:363-375.

Gibson V C, Marshall E L, North M, Robson D A and Williams P J (**1997**) "Thymine functionalised polymers via living ring-opening metathesis polymerization" *Chem. Commun.* 1095-1097.

Grubbs R H (**2003**) "Handbook of Metathesis" first ed., Wiley-VCH, New York, Vol.1.

Hay P J and Wadt W R (**1985**) "Ab initio effective core potentials for molecular calculations. Potentials for K to Au including the outermost core orbitals" *J. Chem. Phys.* **82**: 299-310.

Hayano S, Takeyama Y, Tsunogae Y and Igarashi I (**2006**) "Hydrogenated ring-opened poly(*endo*-dicyclopentadiene)s made via stereoselective ROMP catalyzed by tungsten complexes: Crystalline tactic polymers and amorphous atactic polymer" *Macromolecules* **39**: 4663-4670.

Hejl A, Sherman O A and Grubbs R H (**2005**) "Ring-Opening Metathesis Polymerization of Functionalized Low-Strain Monomers with Ruthenium-Based Catalysts" *Macromolecules* **38**: 7214-7218.

Herisson J L and Y Chauvin (**1971**) "Catalyse de transformation des oléfines par les complexes du tungstène. II. Télomérisation des oléfines cycliques en présence d'oléfines acycliques" *Makromol. Chem*. **141**: 161-176.

Ivin K J and Mol J C (**1997**) "Olefin Metathesis and Metathesis Polymerization" Academic Press, San Diego.

K Grela (**2008**) "The joy and challenge of small rings metathesis" *Angew. Chem. Int. Ed.* **47**: 5504-5507.

Khosravi E, Feast W J, Al-Hajaji A A and Leejarkpai T (**2000**) "ROMP of n-alkyl norbornene dicarboxyimides: from classical to well-defined initiators, an overview" *J. Mol. Catal. A: Chem.***160**: 1-11.

Kress S and Blechert S (**2012**) "Asymmetric catalysts for stereocontrolled olefin metathesis reactions" *Chem. Soc. Rev*. **41**: 4389-4408.

Lee C, Yang W and Parr R G (**1988**) " Development of the colle-salvetti correlation-energy formula into a functional of the electron-density" *Phys. Rev. B* **37**: 785-789.

Li J, Sun C, Demerzhan S and Lee D (**2011**) "Metal-catalyzed rearrangement of cyclopropenes to allenes" *J. Am. Chem. Soc.* **133**: 12964-12967.

Buchmeiser M R (**2009**) "Ruthenium-based olefin metathesis catalysts bearing *N*-heterocyclic carbene ligands" *Chem. Rev*. **109**: 3708-3742.

Marek I, Simman S and Masarwa A (**2007**) "Enantiomerically enriched cyclopropene derivatives: versatile building blocks in asymmetric synthesis" *Angew. Chem.,Int. Ed.* **46**: 7364-7376.

Martinez H, Miro P, Charbonneau P, Hillmyer M A and Cramer C J (**2012**) "Selectivity in ring-opening metathesis polymerization of Z-cyclooctenes catalyzed by a second-generation grubbs catalyst" *ACS Catal.* **2**: 2547-2556.

Miege F, Meyer C and Cossy J (**2011**) "When cyclopropenes meet gold catalysts" *Beilstein J. Org. Chem.***7**: 717-734.

Miehlich B, Savin A, Stoll H and Preuss H (**1989**) "Results obtained with the correlation energy density functional of becke and lee, yang and parr" *Chem. Phys. Lett.* **157**: 200-206.

Monsaert S, Vila A L, Drozdzak R, Voort P V D and Verpoort F (**2009**) "Latent olefin metathesis catalysts" *Chem. Soc. Rev.* **38**: 3360-3372.

Oskam J H and Schrock R R (**1993**) "Rotational isomers of Mo(VI) alkylidene complexes and cis-trans polymer structure-investigations in ring-opening metathesis polymerization" *J. Am. Chem. Soc.* **115**: 11831-11845

Perrott M G and Novak B M (**1996**) "Living ring-opening metathesis polymerizations of 3,4-disubstituted cyclobutenes and synthesis of polybutadienes with protic functionalities" *Macromolecules* **29**: 1817-1823.

Rubin M, Rubina M and Gevorgyan V (**2007**) "Transition Metal Chemistry of Cyclopropenes and Cyclopropanes" *Chem. Rev*. **107**: 3117-3179.

Rush S, Reinmuth A and Risse W (**1997**) "Palladium (II)-catalyzed olefin addition polymerizations of 3,3-dialkyl-substituted cyclopropenes" *Macromolecules* **30**: 7375-7385.

Schleyer P v R, Williams J E and Blanchard K R (**1970**) "Evaluation of strain in hydrocarbons - strain in adamantane and its origin" *J. Am. Chem. Soc*. **92**: 2377-2386.

Schrok R R (**1990**) "Living ring-opening metathesis polymerization catalyzed by well-characterized transition-metal alkylidene complexes" *Acc. Chem. Res*. **23**: 158-165.

Schrock R R (**2001**) "Transition metal-carbon multiple bonds*" J. Chem. Soc., Dalton Trans.* 2541-2550.

Schrock R R (**2002**) "High oxidation state multiple metal-carbon bonds" *Chem. Rev.* **102**: 145-179.

Schrock R R (**2009**) "Recent advances in high oxidation state Mo and W imido alkylidene chemistry" *Chem. Rev.* **109**: 3211-3226.

Schrock R R and Hoveyda A H (**2003**) "Molybdenum and tungsten imido alkylidene complexes as efficient olefin-metathesis catalysts" *Angew. Chem. Int. Ed*. **42**: 4592-4633.

Schrock R R, Krouse S A, Knoll K, Feldman J, Murdzek J S and Yang D C (**1988**) "Controlled ring-opening metathesis polymerization by molybdenum and tungsten alkylidene complexes" *J. Mol. Catal.* **46**: 243-253.

Schrock R R, Murdzek J S, Bazan G C, Robbins J, DiMare M, and O'Regan M (**1990**) "Synthesis of molybdenum imido alkylidene complexes and some reactions involving acyclic olefins" *J . Am. Chem. Soc*. **112**: 3875-3886.

Singh R and Schrock R R (**2008**) "Stereospecific ring-opening metathesis polymerization of 3-methyl-3-phenylcylopropene by molybdenum alkylidene initiators" *Macromolecules* **41**: 2990-2993.

Singh R, Czekelius C and Schrock R R (**2006**) "Living ring-opening metathesis polymerization of cyclopropenes" *Macromolecules* **39**: 1316-1317.

Smith D, Pentzer E B and Nguyen S T (**2007**) "Bioactive and therapeutic ROMP polymers" *Polym. Rev*.**47**: 419-459.

Song A, Lee J C, Parker K A and Sampson N S (**2010**) "Scope of the ring-opening metathesis polymerization (ROMP) reaction of 1-substituted cyclobutenes" *J. Am. Chem. Soc*. **132**: 10513-10520.

Trzaska S T, Lee L B W and Register R A (**2000**) 'Synthesis of narrow distribution 'perfect' polyethylene and its block copolymers by polymerization of cyclopentene" *Macromolecules* **33**: 9215-9221.

Vougioukalakis G C and Grubbs R H (**2010**) "Ruthenium-Based Heterocyclic Carbene-Coordinated Olefin Metathesis Catalysts" *Chem. Rev*.**110**: 1746-1787.

Wadt W R and Hay P J (**1985**) "Ab Initio effective core potentials for molecular calculations.Potentials for main group elements Na to Bi" *J. Chem. Phys*. **82**: 284-298.

Walker R, Conrad R M and Grubbs R H (**2009**) "The Living ROMP of *trans*-cyclooctene" *Macromolecules* **42**: 599-605.

Wu Y D and Peng Z H (**1997**) "Theoretical Studies on Alkene Addition to Molybdenum Alkylidenes" *J. Am. Chem. Soc*. **119**: 8043-8049.

Wu Y D and Peng Z H (**2003**) "Theoretical studies on the ring-opening metathesis reaction of norbornadiene with molybdenum alkylidenes" *Inorg. Chim. Acta* **345**: 241-245.

5 Stereochemistry and Effect of Substituents

5.1 INTRODUCTION

Recently theoretical studies on the ring opening metathesis (ROM) and ring opening metathesis polymerization (ROMP) of 3,3-dimethyl cyclopropene were reported [Meena and Thankachan, 2013; 2014]. This was the only instrumental report of the ROMP of symmetrical disubstituted cyclopropene. If the substituents on 3-position of the cyclopropene are different then stereoselectivity becomes more severe in the ring opening of the 3,3-disubstituted cyclopropenes (DSCP). Stereoselectivity of asymmetric cyclopropenes derivatives have been attracted the interest of theoretical study [Xidos et al., 2001].

Ring opening metathesis of cycloalkene is the key step in ring opening-cross metathesis (ROCM) and ring opening metathesis polymerization (ROMP). Theoretical studies of the stereochemistry of the ring opening process can be of use to gain deeper insights into ROCM and ROMP reactions [Lin et al., 2013]. In this chapter we present our computational studies on the stereochemistry of $Mo(NH)(CH_2)(OCH_3)_2$ catalyst mediated ROM of 3-methyl-3-phenylcyclopropene (MPCP) and effect of substituents on ring opening of cyclopropene. The phenyl group was substituted by NH_2, OH, CN and CF_3 groups to study the substituent effect on syn ring opening of cyclopropene. Optimized geometries of all disubstituted cyclopropenes, 3-methyl-3-phenylcyclopropene, 3-amino-3-methylcyclopropene (AMCP), 3-hydroxyl-3-methylcyclopropene (HMCP), 3-cyanide-3-methylecyclopropene (CMCP), and 3-methyl-3-trifluoromethylcyclopropene (MTCP), used in this chapter are shown in Figure 5.1.

5.2 COMPUTATIONAL DETAILS

All the DFT computations reported here have been performed with the Gaussian 09 [Frisch et al. 2009] suite of programs using the nonlocal hybrid three-parameter exchange functional of Becke [Becke 1993]denoted as B3LYP. Earlier studies reveal that B3LYP is a reliable method for calculations on reactions of olefins [Gaytri and Sastry, 2009, Mishra and Sathyamurthy 2005]. LANL2DZ basis set (the Hay-Wadt effective core plus double-zeta basis) is used for molybdenum and Dunning-Huzinaga valence double-zeta basis set (D95V) for other non-transition elements. Computation of the harmonic vibrational frequencies has been carried out to determine the nature of each critical point. All the minima were verified to have all positive frequencies and the transition state to have only one imaginary frequency.

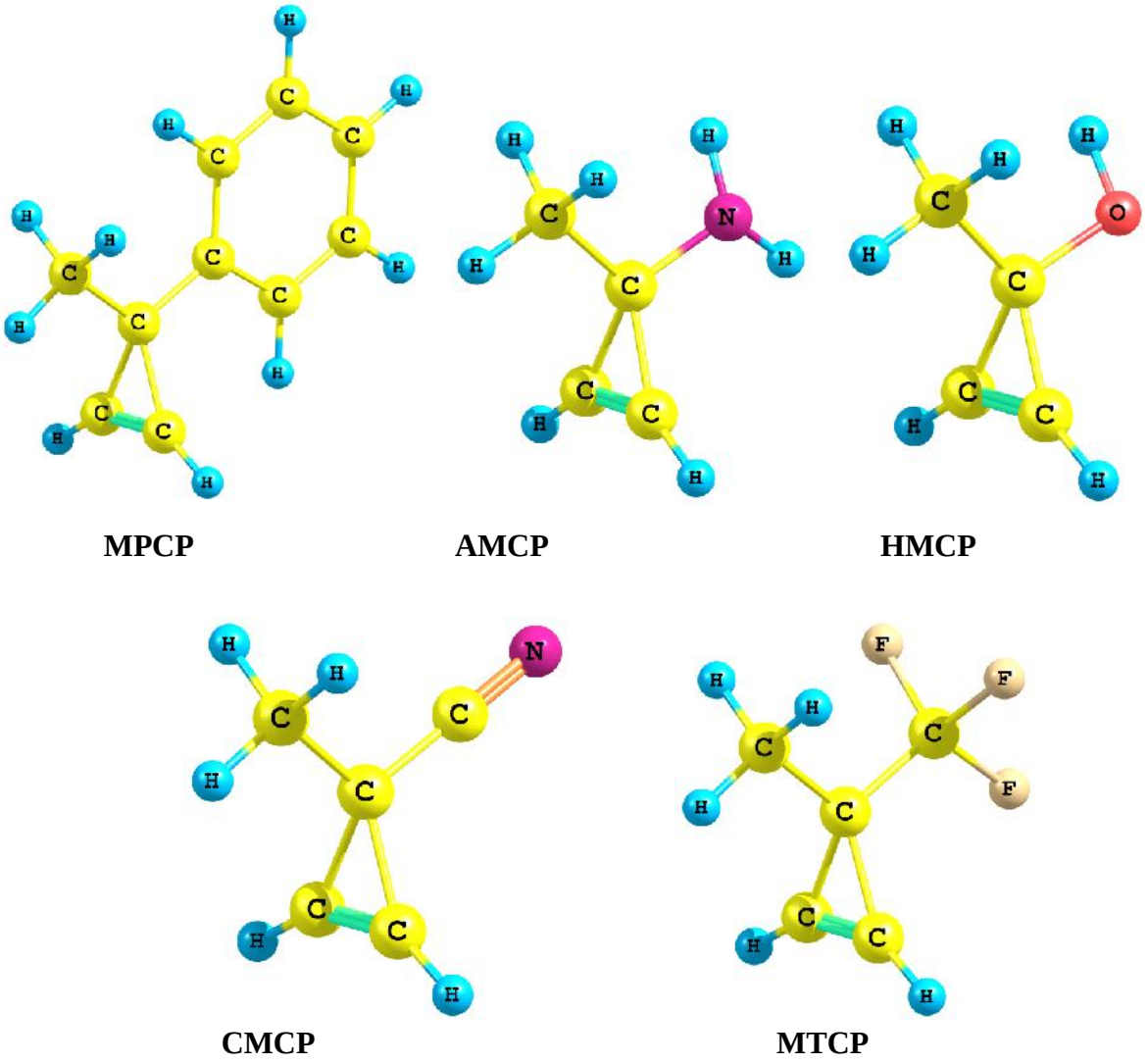

Figure 5.1: Optimized geometries of the 3,3-disubstituted cyclopropenes

5.3 RESULTS AND DISCUSSION

There are two faces of the disubstituted cyclopropenes at which the reaction with the molybdenum catalyst may occurs namely the "methyl face" and the "X face" (where X= Ph, NH_2, OH, CN and CF_3), as shown in Figure 5.2. We began our studies by examining the stereochemistry including possible conformational changes during the ring opening of 3-methyl-3-phenylcyclopropene (MPCP) [Rubin and Gevorgyan 2004]. In this case (MPCP), both syn and anti orientations of the cyclopropene at the CNO face (as discussed in Chapter 4) of the molybdenum catalyst are considered whereas in investigating effect of substituents only the reaction in the preferred syn orientation is considered for remaining (NH_2, OH, CN and CF_3) cases.

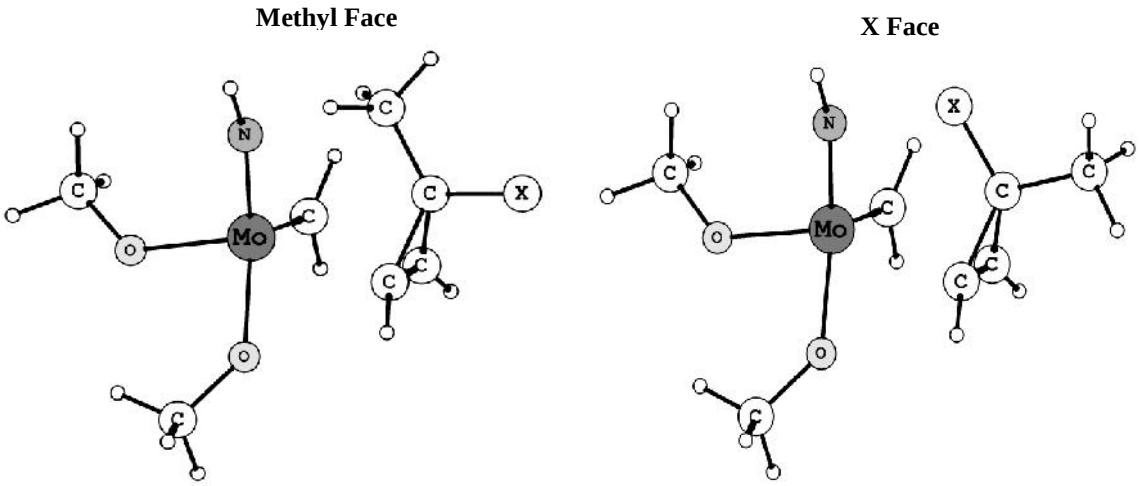

Figure 5.2: Showing two reacting faces of 3,3-disubstituted cyclopropenes in syn orientation at the CNO face of molybdenum catalyst

5.3.1 STEREOCHEMISTRY OF ROM OF MPCP

Two types of approach namely syn and anti of cyclopropene to the CNO face of molybdenum catalyst are investigated. 3-methyl-3-phenylcyclopropene may react along two faces the "methyl face" and the "phenyl face" (as shown in Figure 5.2). Each face has two orientations that are syn and anti with respect to NH group of the molybdenum catalyst. Thus there are total four stereochemical orientations in which ring opening may possibly occur. The four possible transition structures of cycloaddition are shown in Figure 5.3. Due to steric hindrance "phenyl face" is considered less likely to be involved and initialization will be slower as compared to the "methyl face". This view is also supported by our calculated activation barriers. In both cases syn/anti, energy barriers are higher (see in Table 5.2) with the "phenyl face". The calculated activation barriers for syn /anti cycloaddition are 9.81kcal/mol and 13.06 kcal/mol respectively. When initialization proceed through the "methyl face" the activation barrier of cycloaddition is lower than phenyl face by about 1.90 kcal/mol in syn case and by about 3.03 kcal/mol in anti. For steric reasons it is proposed that the C=C face in MPCP that adds to the M=C bonds is the more accessible "methyl face". Our results are supported by the experimental report on stereochemistry of ring opening metathesis polymerization of 3-methyl-3-phenylcyclopropene with molybdenum catalyst [Flook et al., 2010]. Accordingly, we decided to use the sterically less encumbered "methyl face" for further studies.

Methyl Face

Phenyl Face

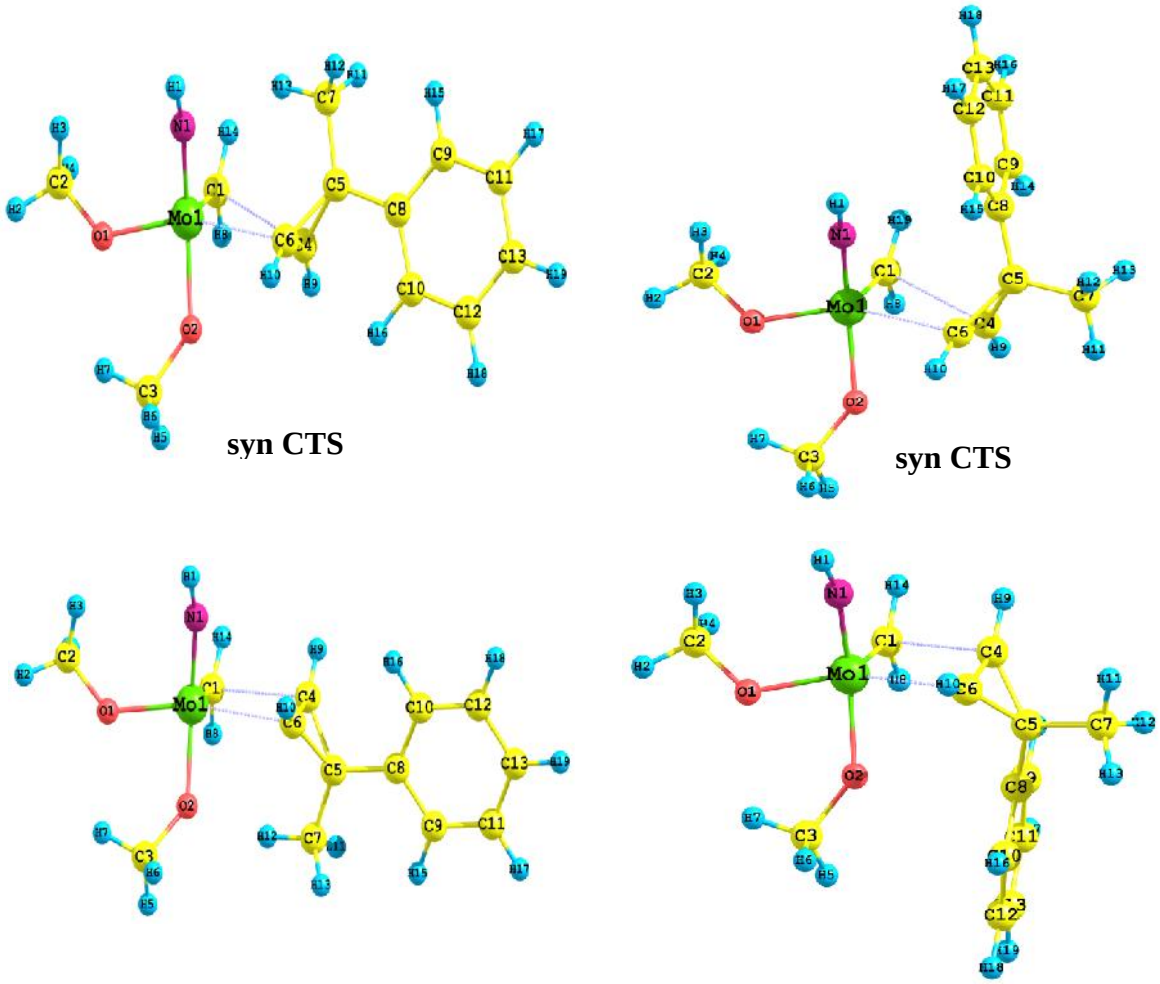

Figure 5.3: Geometries of the transition structures with 'methyl face' and 'phenyl face' of syn and anti oriented 3-methyle-3-phenylcyclopropene

syn and anti transition structures (syn CTS & anti CTS) of the methyl face formed distorted trigonalbipyramidal (TBP) metallacyclobutane intermediates that possibly rearrange towards geometrically more stable square pyramidal (SP) intermediates. Stereochemically all structures, excepting cycloaddition transition structures, are investigated in two isomeric forms namely perpendicular and parallel isomers. In perpendicular isomers, the phenyl ring is vertical to the core ring (Mo-C1-C4-C6) of the metallacyclobutane and phenyl ring is horizontal in case of parallel isomers.

The calculated total electronic energies (in hartree) for structures (including isomers) found in the path of ring opening of MPCP through methyl and phenyl face are provided in Table 5.1 and relative energies (in kcal/mol) are shown in Table 5.2. In case of perpendicular and parallel isomers, relative energies of stabler conformers are calculated. Table 5.3 provides the relative energies of most stable species among the possible conformational structures in the path of syn and anti ring opening metathesis. The basic features of the calculated structures are similar to previous calculations on the 3,3-dimethylcyclopropene with $Mo(NH)(CH_2)(OCH_3)_2$ alkylidenes [Meena and Thankachan, 2013] apart from conformations due to phenyl ring. Thus, we are not going into details about the geometries of structures found in the path of ring opening of MPCP. Optimized geometrical parameters of the structures (most stable isomer) involved in the path of ring opening of MPCP are collected in Table 5.4 and Table 5.5 shows parameters of the only syn and anti cycloaddition transition structures with phenyl face.

The perpendicular and parallel conformational isomers of syn TBP (A &B) and syn SP (C & D) intermediates are shown in Figure 5.4 and in Figure 5.5 anti TBP (A&B) and anti SP (C&D) intermediates isomers are presented. The calculated energies of the parallel isomer (TBP_B &SP_D) of syn TBP and SP are lower than their corresponding perpendicular syn isomers (TBP_A & SP_C) respectively because net steric hindrance of phenyl ring is less in parallel isomers.

Table 5.1: Calculated total electronic energies (in hartree) of reactants (catalyst and MPCP), cycloaddition (CTS) and ring opening (RTS) transition structures , intermediates (TBP & SP) and products involved in ring opening metathesis reaction of 3-methyl-3-phenylcyclopropene

Catalyst +MPCP	(-392.4631882) +(-386.9193331) = -779.3825213					
Structure	**syn**			**anti**		
	Methyl Face		Phenyl Face	Methyl Face		Phenyl Face
	Perpendicular	Parallel		Perpendicular	Parallel	
CTS	-779.3699171	-	-779.3668849	-779.3665264	-	-779.361705
TBP	-779.4308542 (A)	-779.4335203 (B)		-779.4301461(A)	-779.4331816(B)	
SP	-779.4398789 (C)	-779.4403179(D)		-779.4420452 (C)	-779.4409566 (D)	
RTS	-779.4255192 (A)	-779.4301213 (B)		-779.4278068 (A)	-779.432080 (B)	
Pr	-779.4646256 (A)	-779.4683848[a] (C)		-779.4630792 (A)	-779.4666831[b] (B)	
	-779.4665544(B)	-779.4650967 (D)		-	-779.4653857 (C)	

a,b = most stable isomer of syn and anti products respectively

Table 5.2: Calculated relative electronic energies (in kcal/mol) of species involved in ring opening metathesis reaction of 3-methyle-3-phenylcyclopropene (MPCP) with molybdenum catalyst $Mo(NH)(CH_2)(OCH_3)_2$

Structure	**syn**			**anti**		
Reactants	0.0			0.0		
	Methyl Face		Phenyl Face	Methyl Face		Phenyl Face
	Perpendicular	Parallel		Perpendicular	Parallel	
CTS	7.909	-	9.812	10.037	-	13.062
TBP	-30.329 (A)	-32.002 (B)		-29.885 (A)	-31.790 (B)	
SP	-35.992 (C)	-36.268 (D)		-37.352 (C)	-36.669 (D)	
RTS	9.011*(A)	6.398* (B)		8.935* (A)	5.570* (B)	
Pr	-51.521(B)	-53.880 (C)		-50.551(A)	-52.812(B)	

*Energy relative to the corresponding more stable isomeric SP intermediate.

Table 5.3: Most stable stereochemical species (conformers) of ring opening of syn/anti MPCP through 'methyl face'

Path Species	**syn**	**anti**
CTS	7.909	10.037
TBP	-32.002 (B)	-31.790 (B)
SP	-36.268 (D)	-37.352 (C)
RTS	6.398[c] (B)	6.253[c] (B)
Pr	-53.880 (C)	-52.812 (B)

c = energy relative to the most stable isomer of syn and anti SP intermediate

Table 5.4 & 5.5: Selected geometrical parameters (bond lengths in Á and angles in degree) of optimized structures (only most stable corresponding isomer) investigated in the path of stereoselective ring opening of syn/anti 3-methyl-3-phenylcyclopropene

Table 5.4: Methyl face structures

Parameters	**syn**					**anti**				
	CTS	CTBP	CSP	RTS	Pr	CTS	CTBP	CSP	RTS	Pr
Mo-C1	1.928	2.210	2.220	2.440	-	1.928	2.253	2.229	2.543	-
C1-C4	2.750	1.495	1.514	1.420	1.348	2.741	1.470	1.517	1.397	1.349
C4-C6	1.353	1.710	1.561	1.965	-	1.353	1.771	1.524	2.044	-
Mo-C6	2.556	2.032	2.167	1.982	1.907	2.561	2.018	2.167	1.973	1.924
Mo-C1-C4	67.50	79.56	96.67	78.56	-	68.73	80.19	96.69	79.59	-
C1-C4-C6	109.2	116.9	100.0	116.1	-	109.2	116.0	100.2	115.3	-
C4-C6-Mo	80.46	80.67	97.37	81.18	-	81.74	81.24	99.02	83.36	-
C6-Mo-C1	99.28	80.09	64.94	80.76	-	98.76	80.04	64.08	79.74	-
C1-Mo-O1	105.7	147.6	135.8	161.9	-	106.0	152.1	139.2	157.2	-
O1-Mo-C6	152.1	130.8	84.0	115.3	-	154.1	123.6	84.43	111.4	-
N-Mo-O2	144.7	163.4	111.7	144.4	114.9	147.1	153.7	113.3	139.0	116.3

Table 5.5: Phenyl face cycloaddition transition structural parameters

Parameters	**syn** CTS	**anti** CTS
Mo-C1	1.926	1.930
C1-C4	2.860	2.749
C4-C6	1.350	1.357
Mo-C6	2.617	2.545
Mo-C1-C4	66.47	68.58
C1-C4-C6	109.5	108.7
C4-C6-Mo	80.41	82.05
C6-Mo-C1	101.6	98.93
C1-Mo-O1	104.5	105.25
O1-Mo-C6	151.4	154.0
N-Mo-O2	144.4	144.9

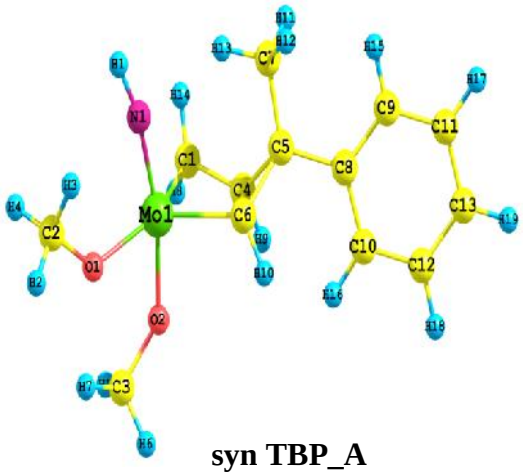

syn TBP_A

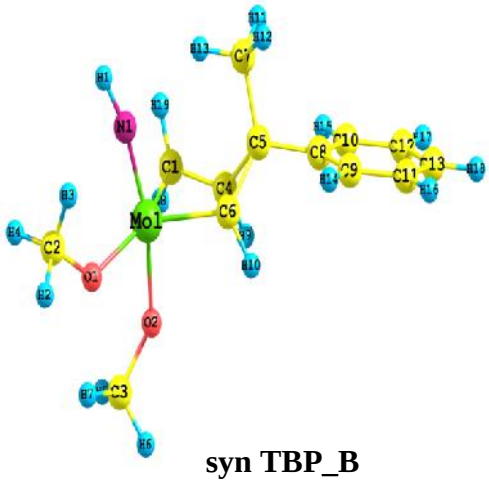

syn TBP_B

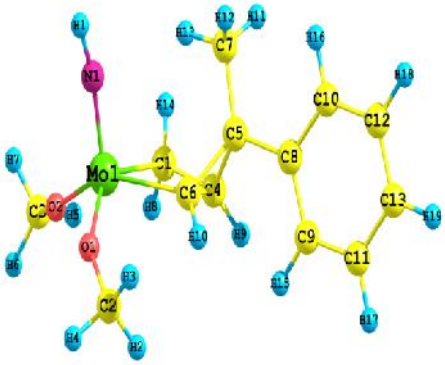

syn SP_C

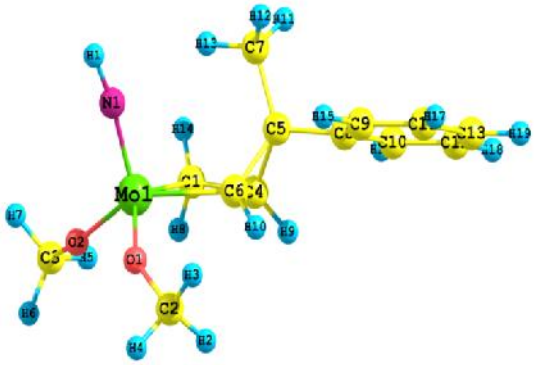

syn SP_D

Figure 5.4: Optimized geometries of the perpendicular (A & C) and parallel (B & D) syn trigonal bipyramidal and square pyramidal intermediates respectively

The perpendicular (TBP_A) and parallel (TBP_B) conformers of TBP intermediate differ in energy by about 1.67 kcal/mol in syn case and 1.91 kcal/mol in anti case. But the difference is lower for conformers of SP intermediates (SP_C &SP_D). In syn case, conformers (syn SP_C & syn SP_D) have energy difference only about 0.28 kcal/mol and 0.69 kcal/mol for conformers (anti SP_C & anti SP_D) of anti SP intermediate. In both syn and anti cases, lower energy differences between SP conformers show that the perpendicular and parallel conformers can interconvert into each other more easily as compared to conformers of TBP intermediates.

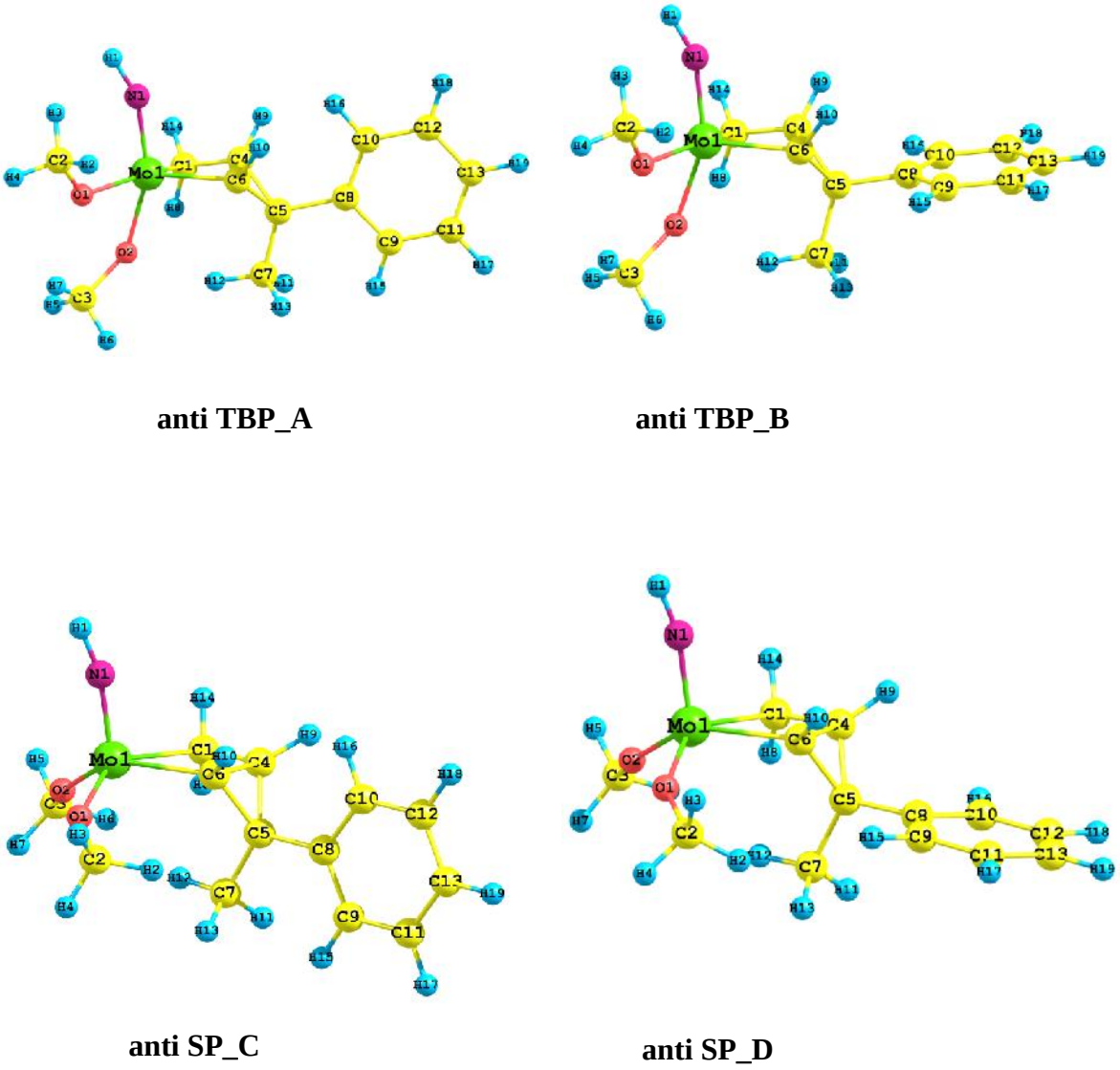

Figure 5.5: Optimized geometries of the perpendicular (A & C) and parallel (B & D) anti trigonal bipyramidal and square pyramidal intermediates respectively

The metallacyclobutane intermediates lead towards the ring opening transition structures (RTS) in distorted TBP geometries, as shown in Figure 5.6. As was expected, the stabler conformer (parallel) of syn and anti TBP transformed into stabler ring opening transition structures (syn/anti RTS_B) having energy barriers about 6.4 kcal/mol and 5.6 kcal/mol respectively. The perpendicular conformers syn/anti (RTS_B) are higher than the corresponding parallel conformer syn/anti (RTS_A) by about 2.6 kcal/mol and 3.4 kcal/mol respectively. We conclude that the ring opening of metallacyclobutane intermediates of reaction of 3-methyl-3-phenylcyclopropene with molybdenum catalyst stereochemically

proceeds with the parallel conformers whether the reaction goes through syn or anti orientation.

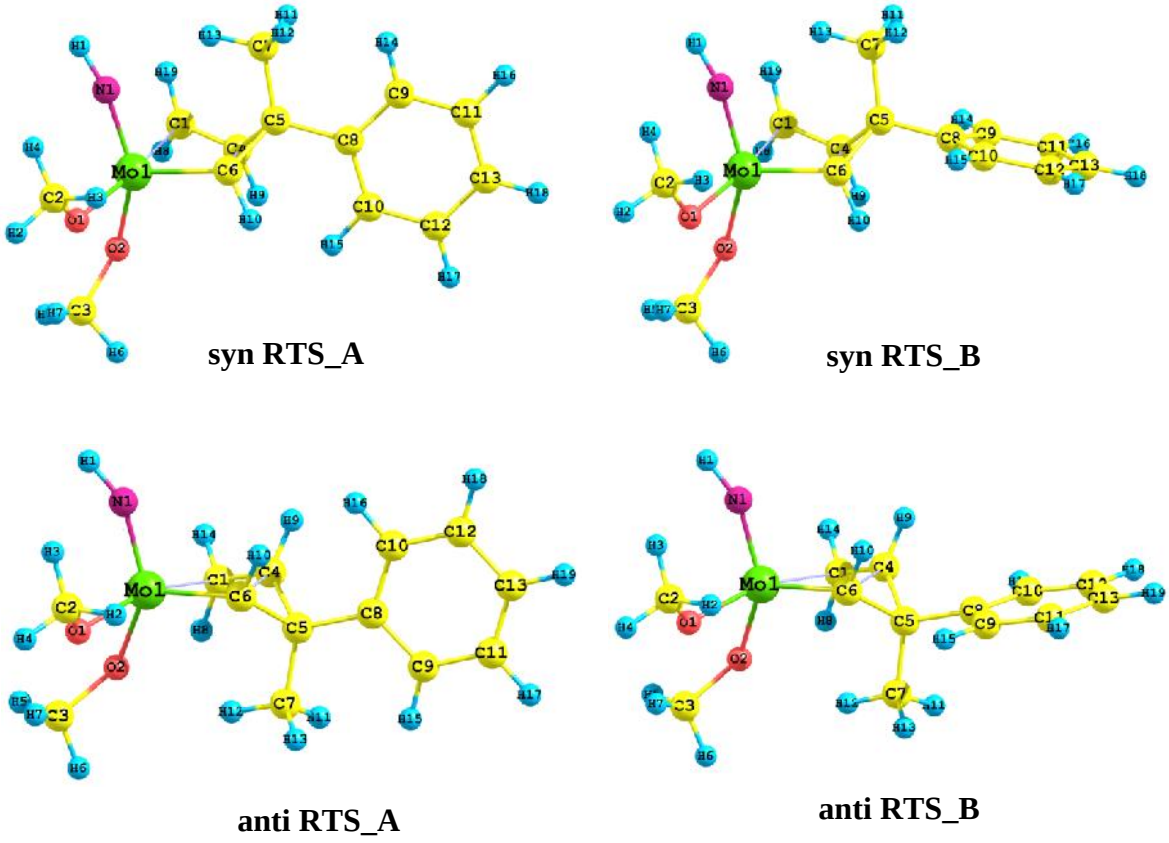

Figure 5.6: Optimized geometries of conformers of ring opening transition structure of syn and anti molybdacyclobutane intermediate of stereochemical ring opening of MPCP

The parallel conformers (RTS_B) of syn and anti RTS lead to the formation of ring opened products (Pr). These products may be present in different conformational isomers. In Figure 5.7, optimized geometries of conformers of syn products are shown and conformers of anti products are presented in Figure 5.8. The product conformers B and C are stabler than A and D conformers due to less steric oriented (parallel) phenyl ring. Among the four possible conformers of syn ring opening product, Pr_C is the most stable (see in Table 5.1)

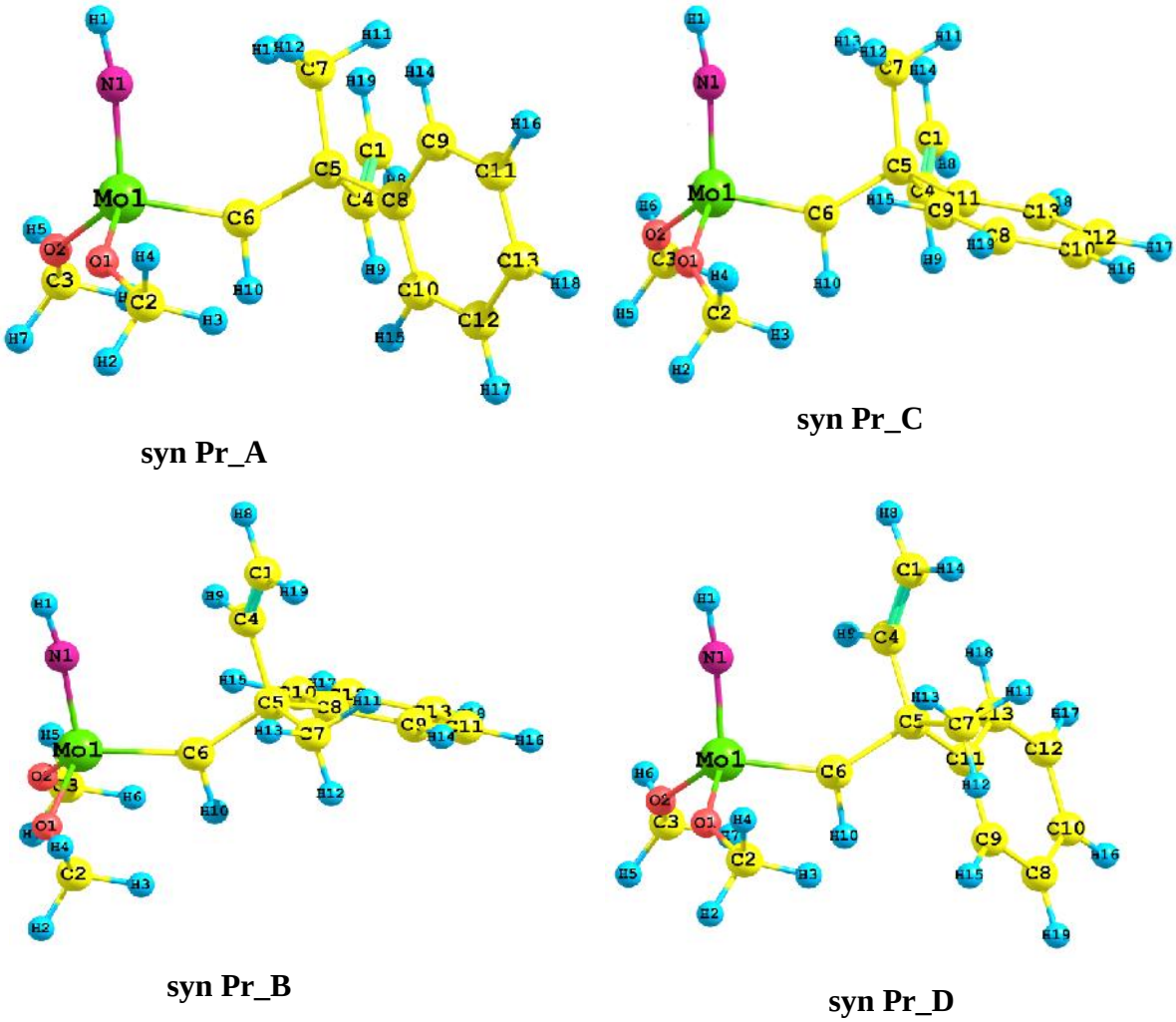

Figure 5.7: Optimized geometries of the isomeric structures of syn ring opening product of 3-methyl-3-phenylcyclopropene

In case of the anti product there may be three conformers (Pr_A, B, C) and Pr_B is the stabler conformer (see in Table 5.1). The syn product (Pr_C) is preferential isomeric product over anti product (Pr_B) by about 1.07 kcal/mol. Over all stereochemically preferred conformational species investigated for ring opening metathesis of 3-methyl-3-phenylcyclopropene with molybdenum catalyst are given in Table 5.3. We concluded that the $Mo(NH)(CH_2)(OCH_3)_2$ mediated ring opening reaction of 3-methyl-3-phenylcyclopropene involved conformational isomers. In both syn/anti ring opening, the parallel conformers are the most stable species during the formation of new alkylidenes as ring opened products.

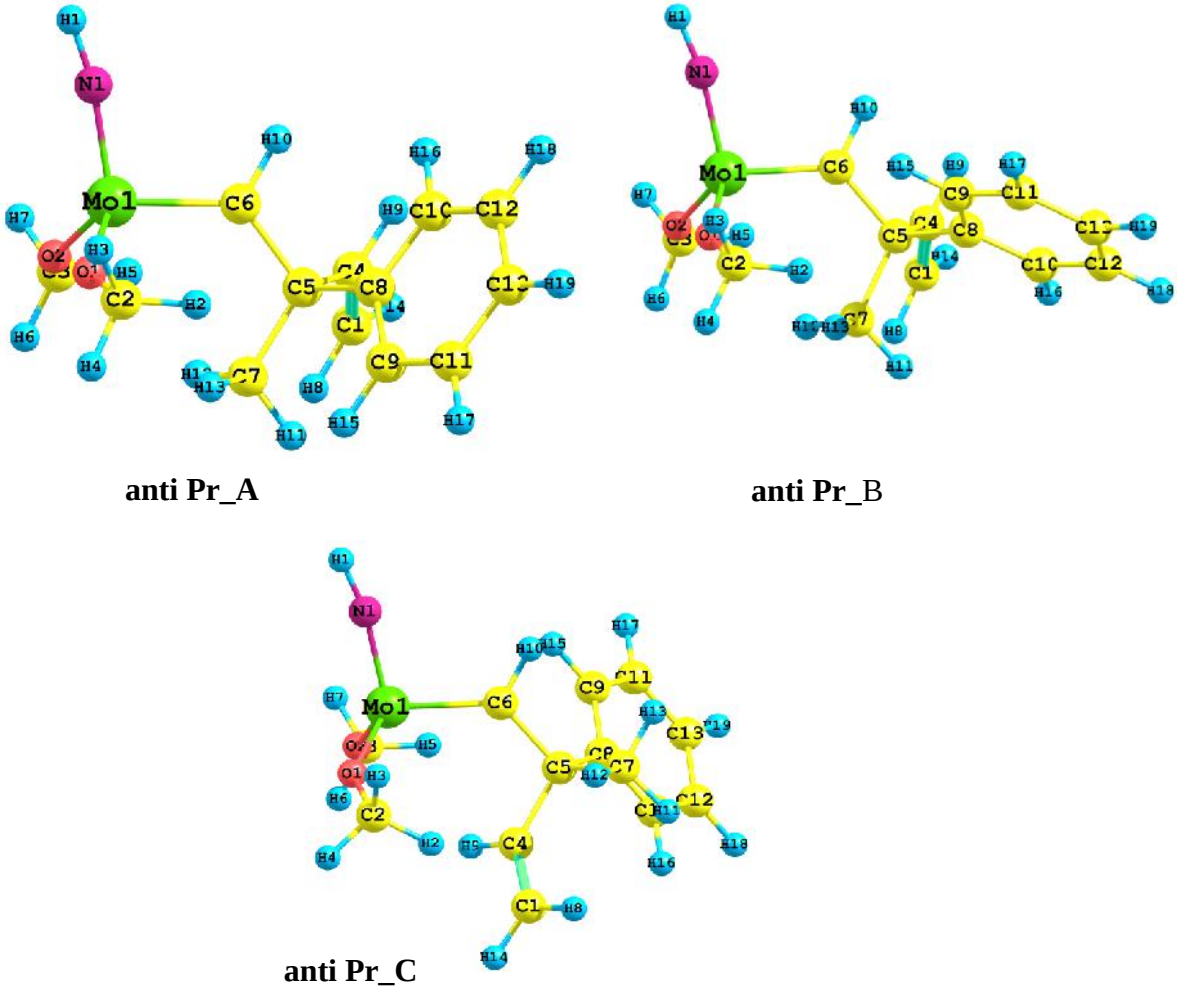

Figure 5.8: Optimized geometries of the conformers of anti ring opening product of 3-methyl-3-phenylcyclopropene

5.3.2 EFFECT OF SUBSTITUENTS ON RING OPENING OF CYCLOPROPENE

This section deals with the effect of variations in one part of a disubstituted cyclopropene on the ring opening metathesis of cyclopropene. Considering syn orientation of cyclopropene, optimization led to two transition structures. In one case (Methyl face) the methyl group is closer to the CNO face and is farther in the other case when reaction takes place with 'X' face (X=NH_2, OH, CN and CF_3).

5.3.2.1 Cycloaddition Transition Structures

Disubstituted cyclopropenes AMCP, HMCP, CMCP and MTCP react with molybdenum catalyst at the methyl face and the NH_2, OH, CN and CF_3 face respectively and formed cycloaddition transition structures (CTS) with pseudo trigonal bipyramidal geometry. These structures are shown in Figures 5.9, 5.10, 5.11 and 5.12 respectively. In

cycloaddition transition structures formed at the methyl face it is seen that the breaking Mo-C1 bond lengths are smaller in NH_2 and OH substituted cyclopropene while larger in cyclopropenes having CN and CF_3 groups. The C4-C6 bond length is found to be larger in NH_2 & OH substituted cyclopropene and shorter in CN & CF_3 bearing cyclopropenes (see in Table 5.8-5.11). The slightly shorter length of forming bond C1-C4 (2.69Å) and Mo-C6 (2.55Å) in methyl face transition structure of MTCP shows that this is slightly later transition state among four structures investigated with methyl face. The lower bond angle C6-Mo-C1 (97.9º) of transition structure of MTCP decreases its stability due to higher strain in core ring (C6-Mo-C1-C4).

In case of 'X' face transition structures (CTS), the Mo-C1 bond length is the least (1.921Å) for HMCP. The MTCP transition structure is later CTS as found in case of methyl face. Comparable to the methyl face CTS of MTCP the bond length of C1-C4 and Mo-C6 are slightly shorter as compared to CTS of cyclopropenes containing NH_2, OH and CN groups. The bond angle C6-Mo-C1 is not significantly different in these transition structures as was found in case of the reaction at the methyl face and in 'X' face transition structures it is about 99-100º. The calculated total electronic energies (in hartree) of these transition structures are given in Table 5.6 and relative energies (in kcal/mol) are shown in Table 5.7. Selected optimized geometrical parameters of CTS of AMCP, HMCP, CMCP and MTCP are collected in Table 5.8, 5.9, 5.10 and 5.11 respectively.

The calculated activation barrier, by methyl face, for the cycloaddition of AMCP with molybdenum catalyst is lower (6.8 kcal/mol) as compared to the addition of HMCP, CMCP and MTCP. For the addition of MTCP, the calculated barrier is the considerably higher (9.66 kcal/mol). The decreasing order of negative inductive effect (-I) of groups is -CF_3 > -CN > -OH > -NH_2.The lower activation energy of AMCP correlates with lower negative inductive (-I) effect of the NH_2 group while the CF_3 group that has the most negative inductive effect has the highest activation barrier. The CTS of HMCP and CMCP have activation barriers about 7.4 kcal/mol and 9.1 kcal/mol respectively.

When the cycloaddition of AMCP, HMCP, CMCP and MTCP occurs by their NH_2, OH, CN and CF_3 faces the activation energy is found to be lowest for the CTS of HMCP and MTCP has again highest activation energy similar to the case of the methyl face. The calculated activation energies of cycloaddition transition structures (CTS) by NH_2, OH, CN and CF_3 faces are 6.67 kcal/mol, 2.74 kcal/mol, 8.37 kcal/mol, and 12.75 kcal/mol respectively. In HMCP, OH group has lower negative inductive effect as compared to CN

and CF3 group of CMCP and MTCP. Thus provide the lowest activation barrier (2.74kcal/mol) path for the ring opening metathesis of HMCP. For AMCP and HMCP, a deviation is observed in order of activation energies than that found in case of methyl face. In case of addition of HMCP by OH face, a strong hydrogen bonding between OH group and NH group lowers the activation energy to the cycloaddition of HMCP with molybdenum catalyst while this hydrogen bonding is weaker between NH and NH_2 groups in case of AMCP.

The increasing order of activation energies of CTS formed through the methyl face of disubstituted cyclopropenes is AMCP < HMCP < CMCP < MTCP while by 'X' face this order is HMCP < AMCP < CMCP < MTCP (see in Table 5.7). Three disubstituted cyclopropenes AMCP, HMCP and CMCP have lower activation barriers when they react through their corresponding NH_2, OH and CN face as compared to reaction through methyl face while MTCP has higher activation barrier through its CF_3 face probably because of lone pair-lone pair repulsion between NH of catalyst and CF_3 of cyclopropene. Steric hindrance is also greater between CF_3 group and NH group as compared to between methyl and NH group in transition structure of MTCP with molybdenum catalyst.

5.3.2.2 Metallacyclobutane Intermediates

The corresponding trigonal bipyramidal (TBP) and square pyramidal (SP) intermediates of CTS of AMCP, HMCP, CMCP and MTCP are shown in Figure 5.9, 5.10, 5.11 and 5.12 respectively. The basic differences in geometries of TBP and their corresponding SP intermediates of all disubstituted cyclopropenes are similar to the previous reports on molybdenum and tungsten catalyzed ring opening metathesis of 3,3-dimethyl cyclopropene [Meena and Thanakchan, 2013; 2014] and their comparative geometrical parameters are not discussed here. Optimized geometrical parameters of these structures are given in Table 5.8, 5.9, 5.10 and 5.11. The geometry of methyl face intermediates formed by CTS of AMCP, HMCP, CMCP and MTCP are very much like their 'X' face intermediates.

In case of AMCP, HMCP and CMCP their respective NH_2, OH and CN faces formed stabler TBP/SP intermediates than their methyl face while in MTCP, CF_3 face formed more reactive TBP/SP intermediates than its methyl face. The energy difference between stabler TBP and SP intermediates of NH_2 face in AMCP is 3.76 kcal/mol, and 4.09kcal/mol for OH face in HMCP and 8.71 kcal/mol for CN face of CMCP. For MTCP,

methyl face TBP and SP intermediates are stabler and have energy difference by about 8.81 kcal/mol and 9.9 kcal/mol for CF_3 face intermediates. The methyl face SP intermediates are higher in energy than their corresponding NH_2, OH and CN face SP intermediates in AMCP, HMCP and CMCP by 2.2 kcal/mol, 5.88 kcal/mol and 1.59 kcal/mol respectively. In contrast methyl face SP intermediate of MTCP is lower than CF_3 face by about 3.8 kcal/mol. As was expected from the cycloaddition transition structure at the OH face, the SP intermediate of HMCP is the most stable among the all SP intermediates of disubstituted cyclopropenes and the least stable SP intermediate is at the CF_3 face.

CH_3 Face

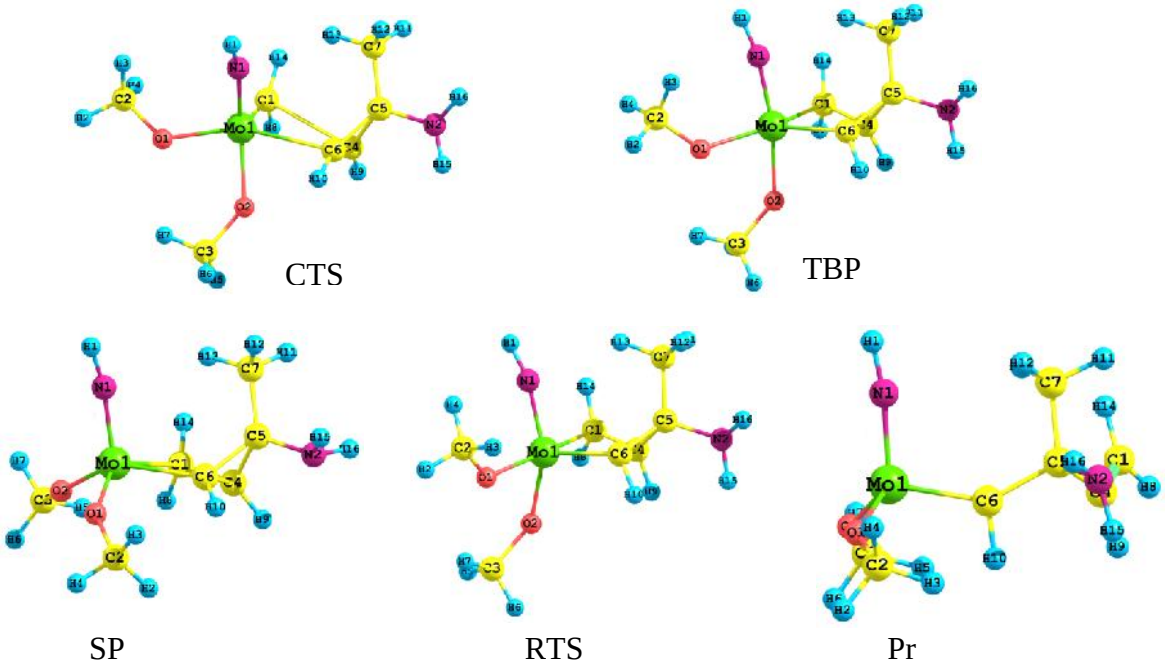

NH_2 Face

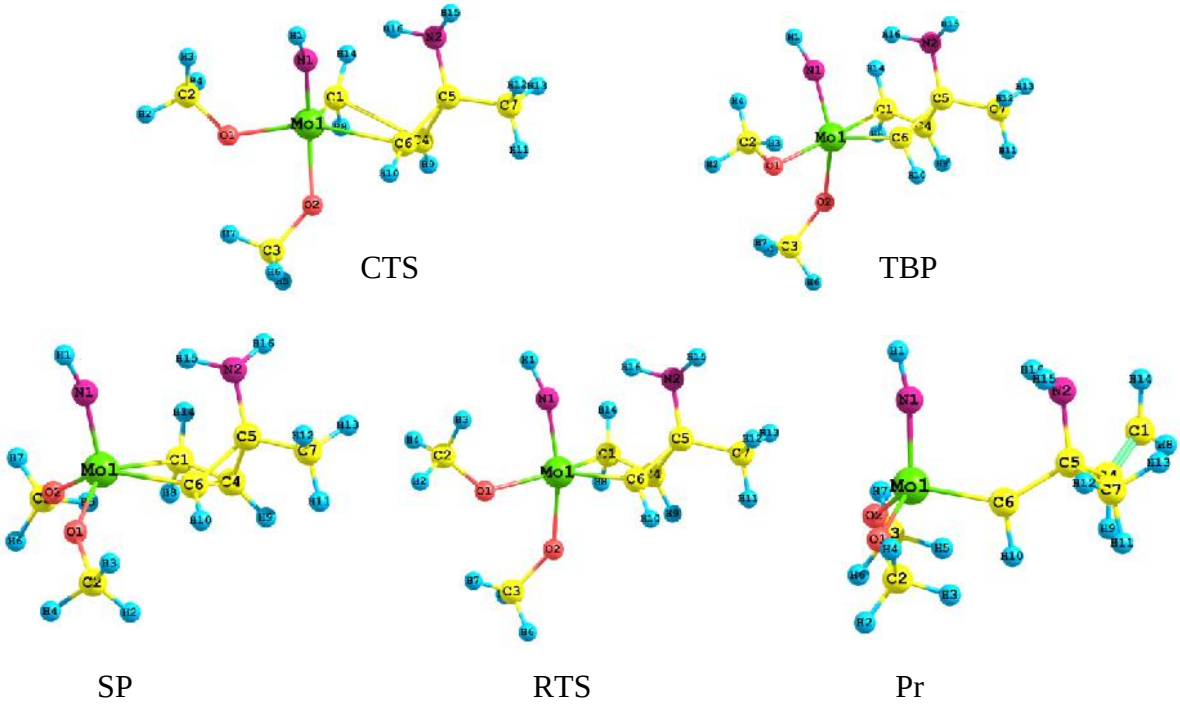

Figure 5.9: Optimized structures involved in ring opening of amino substituted methyl cyclopropene (AMCP)

CH_3 Face

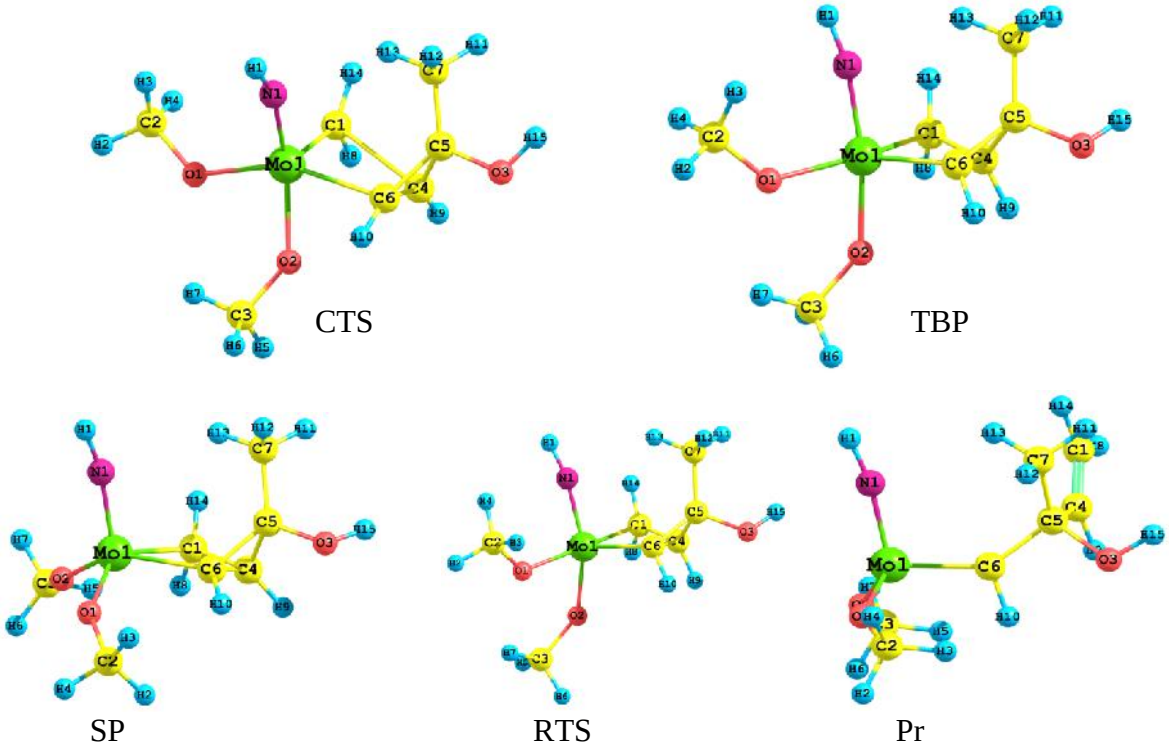

OH Face

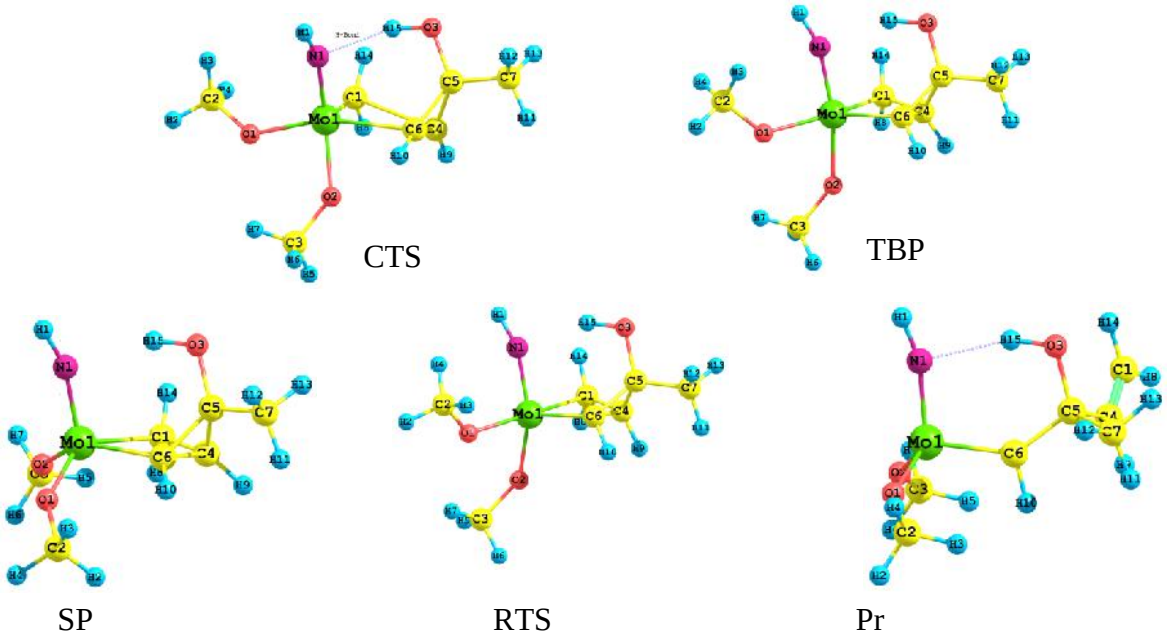

Figure 5.10: Optimized structures involved in ring opening of hydroxyl substituted methyl cyclopropene (HMCP)

CH_3 Face

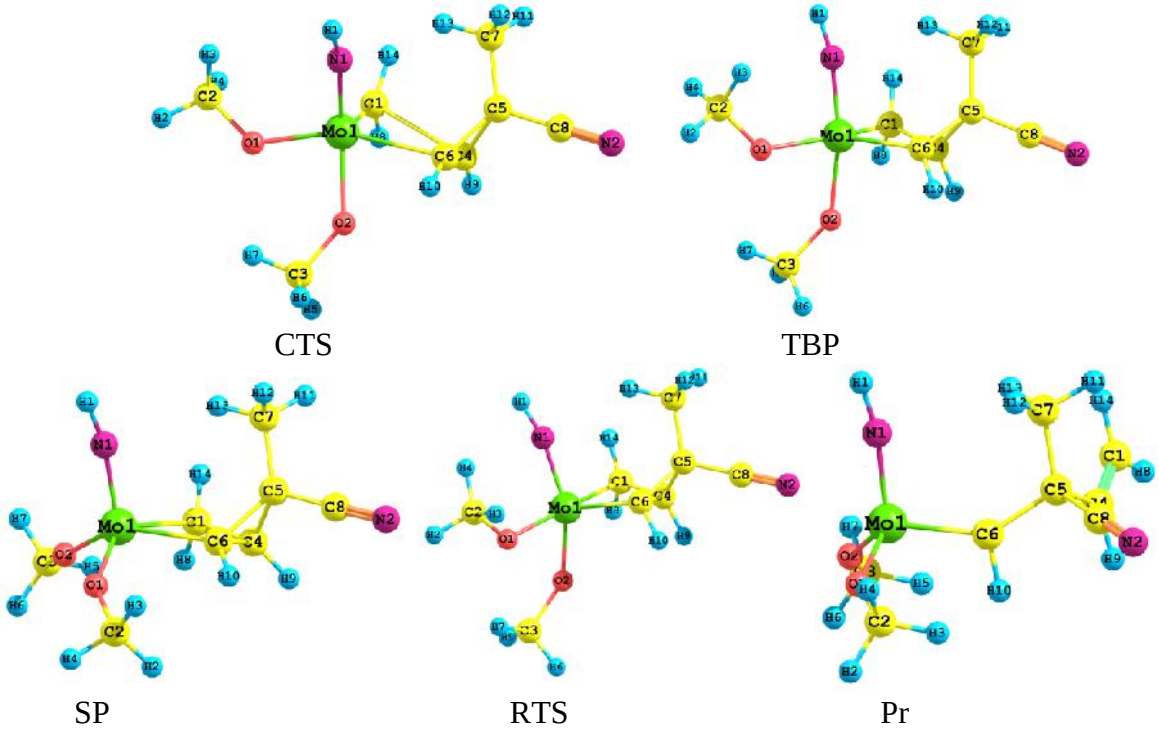

CN Face

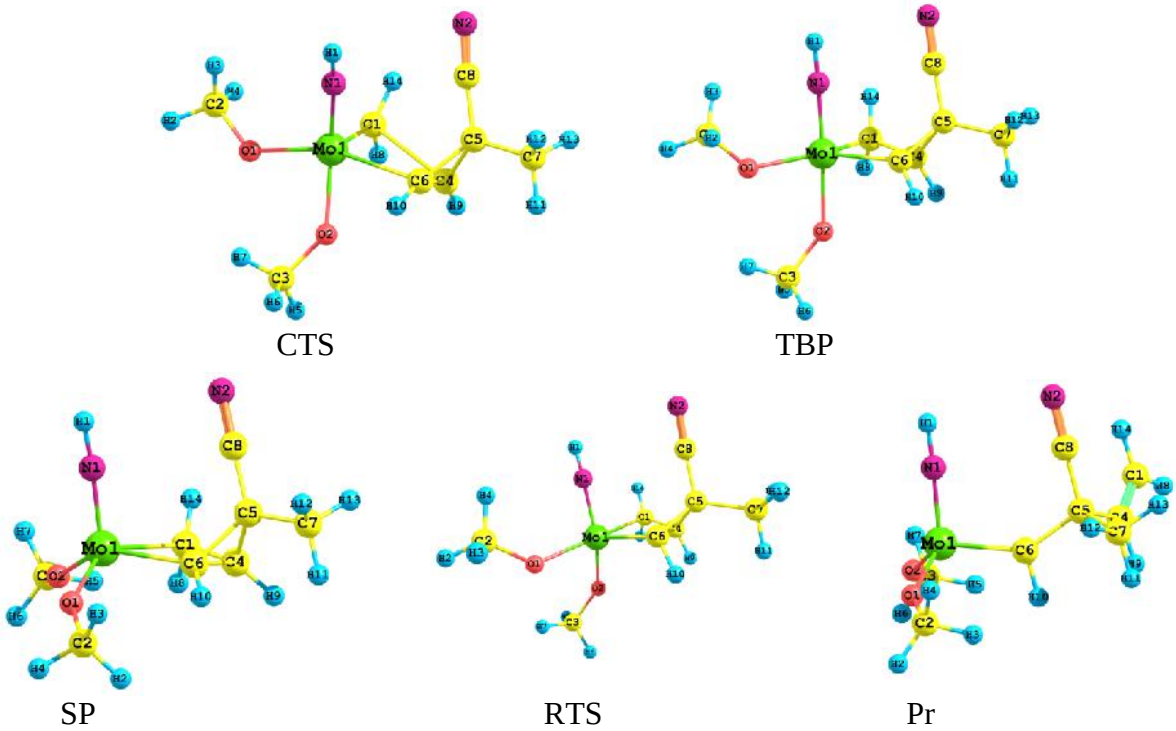

Figure 5.11: Optimized structures involved in ring opening of cyanide substituted methyl cyclopropene (CMCP)

CH_3 Face

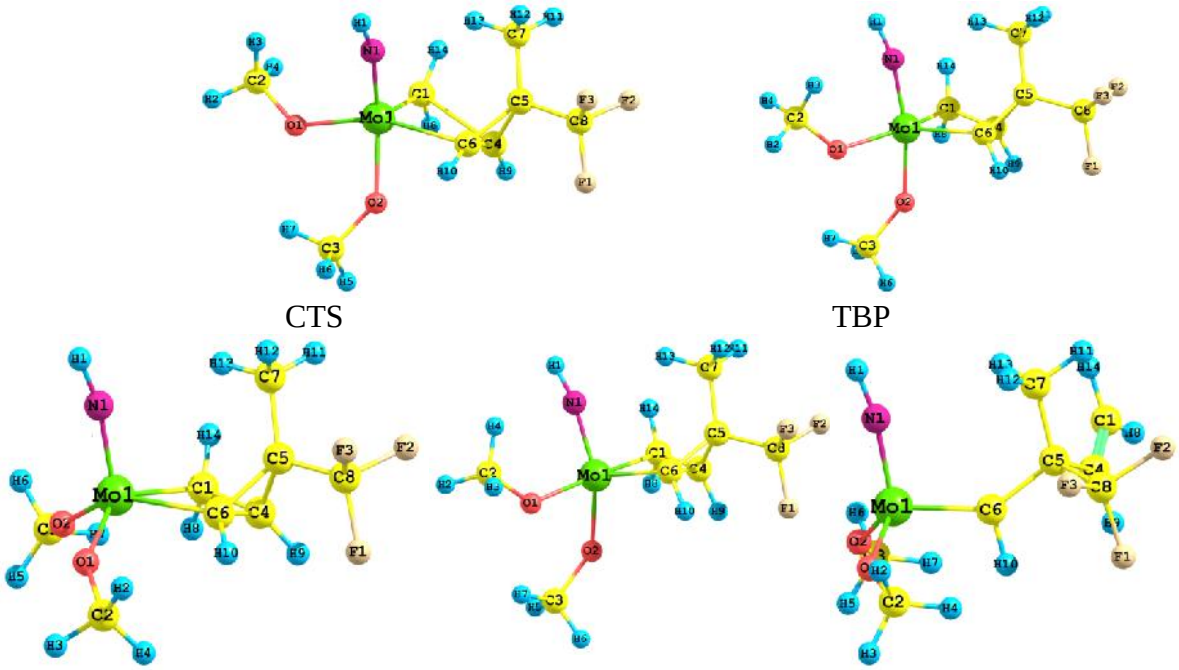

CTS TBP

SP TBP Pr

CF_3 Face

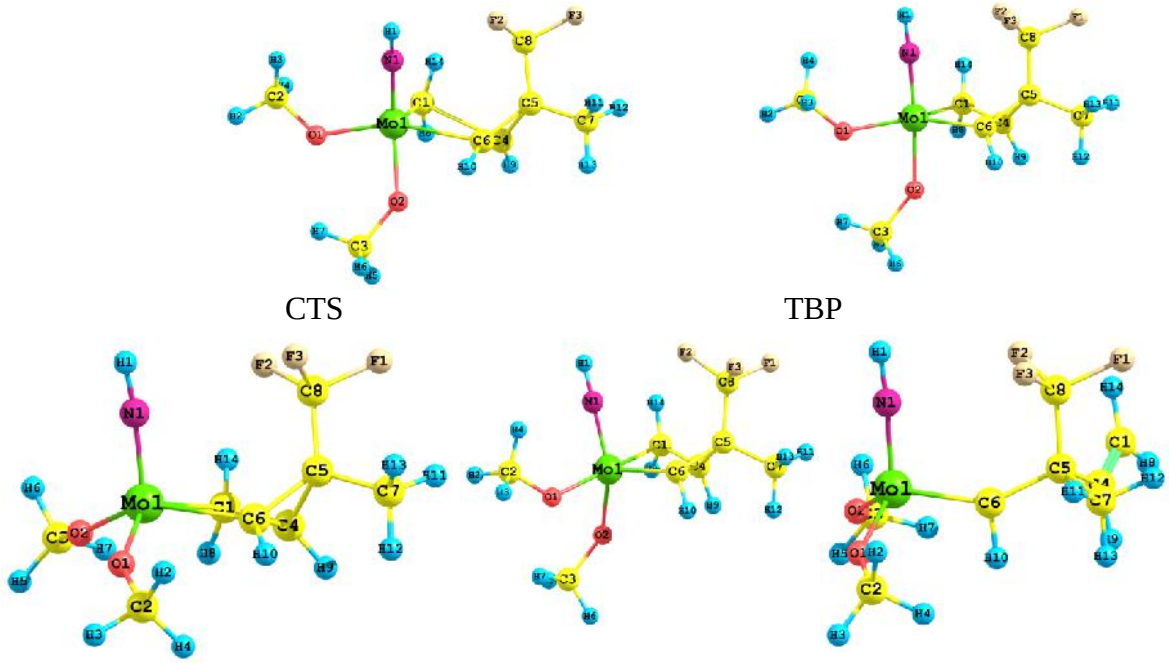

CTS TBP

SP RTS Pr

Figure 5.12: Optimized structures involved in ring opening of cyanide substituted methyl cyclopropene (MTCP)

Table 5.6: Calculated total electronic energies (in hartree) for the transition structures of cycloaddition (CTS) & ring opening (RTS) ,Trigonal bipyramidal (TBP), Square pyramidal (SP), and ring opening product (Pr)of reaction of $Mo(NH)(CH_2)(OCH_3)_2$ with disubstituted cyclopropene (derived by substituting phenyl group of the MPCP)

Structure	AMCP		HMCP		CMCP		MTCP	
Reactants	-603.7090598		-623.5791081		-640.5843359		-885.4228679	
	CH_3 Face	**NH_2 Face**	**CH_3 Face**	**OH Face**	**CH_3 Face**	**CN Face**	**CH_3 Face**	**CF_3 Face**
CTS	-603.6982240	-603.6984241	-623.5672518	-623.5747463	-640.5697957	-640.5709978	-885.4074783	-885.4025432
TBP	-603.7600334	-603.7636361	-623.6298018	-623.6386431	-640.6322567	-640.6356505	-885.4708460	-885.4629936
SP	-603.7661306	-603.769635	-623.6357806	-623.6451554	-640.6469974	-640.6495272	-885.4848821	-885.4788181
RTS	-603.7563770	-603.7601315	-623.6272445	-623.6349777	-640.6277851	-640.6295763	-885.4671839	-885.4598403
Pr	-603.7956728	-603.8007608	-623.6701069	-623.6761145	-640.6706987	-640.6737456	-885.5109649	-885.5055504

Table 5.7: Calculated relative energies (in kcal/mol) for the transition structures (TS) ,Trigonal bipyramidal (TBP), Square pyramidal (SP) and ring opening metathesis product of reaction of $Mo(NH)(CH_2)(OCH_3)_2$ with disubstituted cyclopropene (derived by substituting phenyl group of the MPCP)

Structure	AMCP		HMCP		CMCP		MTCP	
	CH_3 Face	**NH_2 Face**	**CH_3 Face**	**OH Face**	**CH_3 Face**	**CN Face**	**CH_3 Face**	**CF_3 Face**
CTS	6.800	6.674	7.440	2.737	9.124	8.370	9.657	12.754
TBP	-31.986	-34.247	-31.811	-37.359	-30.071	-32.200	-30.107	-25.180
SP	-35.812	-38.012	-35.563	-41.445	-39.321	-40.908	-38.915	-35.110
RTS	6.120*	5.963*	5.357*	6.387*	12.056*	12.520	11.106*	11.909
Pr	-54.350	-57.543	-57.103	-60.872	-54.193	-56.105	-55.282	-51.884

*Energy calculated relative to the corresponding most stable SP intermediate

Table 5.8: Selected geometrical parameters (bond lengths in Å and angles in degree) of optimized structures investigated in the path of ring opening of 3-amino-3-methylcyclopropene (AMCP)

Parameters	**CH_3 face**					**NH_2 face**				
	CTS	TBP	SP	RTS	Pr	CTS	TBP	SP	RTS	Pr
Mo-C1	1.923	2.201	2.221	2.454	-	1.925	2.206	2.217	2.464	-
C1-C4	2.851	1.496	1.513	1.414	1.347	2.771	1.494	1.511	1.413	1.347
C4-C6	1.362	1.720	1.563	2.0	-	1.362	1.720	1.569	1.998	-
Mo-C6	2.622	2.035	2.162	1.977	1.910	2.580	2.023	2.165	1.969	1.904
Mo-C1-C4	66.71	79.37	96.62	78.45	-	67.40	79.62	96.87	78.45	-
C1-C4-C6	108.8	117.0	99.88	115.9	-	109.8	116.8	99.78	116.3	-
C4-C6-Mo	80.03	79.87	97.46	80.69	-	79.92	80.59	97.22	81.3	-
C6-Mo-C1	100.94	80.67	64.97	81.35	-	100.0	80.64	65.04	81.3	-
C1-Mo-O1	104.1	146.2	135.3	161.6	-	105.4	147.0	135.2	161.8	-
O1-Mo-C6	152.3	131.7	83.97	115.5	-	152.2	131.1	84.16	115.6	-
N-Mo-O2	143.2	164.6	113.9	146.0	115.5	145.0	163.0	113.8	145.9	115.7

Table 5.9: Selected geometrical parameters (bond lengths in Å and angles in degree) of optimized structures investigated in the path of ring opening of 3-hydroxyl-3-methylcyclopropene (HMCP)

Parameters	**CH_3 face**					**OH face**				
	CTS	TBP	SP	RTS	Pr	CTS	TBP	SP	RTS	Pr
Mo-C1	1.927	2.211	2.223	2.429	-	1.921	2.197	2.216	2.467	-
C1-C4	2.764	1.493	1.513	1.421	1.349	2.829	1.50	1.512	1.413	1.346
C4-C6	1.364	1.728	1.570	1.971	-	1.359	1.710	1.571	2.002	-
Mo-C6	2.569	2.033	2.164	1.983	1.905	2.631	2.029	2.162	1.968	1.907
Mo-C1-C4	67.74	79.63	96.84	78.67	-	67.37	79.92	97.66	78.86	-
C1-C4-C6	109.2	117.0	99.80	116.2	-	109.5	116.7	99.22	116.0	-
C4-C6-Mo	80.61	80.22	97.47	80.79	-	79.86	80.72	98.03	81.62	-
C6-Mo-C1	99.63	80.60	65.03	81.28	-	100.3	80.56	64.85	81.28	-
C1-Mo-O1	105.4	146.5	135.5	160.3	-	104.3	145.9	135.4	161.6	-
O1-Mo-C6	152.3	131.6	83.92	117.1	-	153.6	132.7	84.75	116.3	-
N-Mo-O2	144.9	164.3	113.7	147.9	115.4	143.1	164.2	114.1	147.9	115.2

Table 5.10: Geometrical parameters (bond lengths in Å and angles in degree) of optimized structures investigated in the path of ring opening of 3-cyanide-3-methylcyclopropene (CMCP)

Parameters	**CH_3 face**					**CN face**				
	CTS	TBP	SP	RTS	Pr	CTS	TBP	SP	RTS	Pr
Mo-C1	1.932	2.192	2.221	2.429	-	1.929	2.172	2.225	2.450	-
C1-C4	2.717	1.506	1.515	1.420	1.346	2.819	1.514	1.515	1.415	1.346
C4-C6	1.351	1.672	1.544	1.960	-	1.343	1.655	1.542	1.987	-
Mo-C6	2.561	2.046	2.175	1.987	1.910	2.628	2.059	2.178	1.981	1.912
Mo-C1-C4	67.89	79.69	96.58	78.69	-	66.97	80.14	96.86	78.67	-
C1-C4-C6	110.2	117.2	100.4	116.1	-	110.3	117.5	100.4	116.2	-
C4-C6-Mo	79.81	80.82	97.57	80.97	-	79.39	80.74	97.92	81.01	-
C6-Mo-C1	98.40	79.59	64.62	80.80	-	99.90	79.63	64.44	81.12	-
C1-Mo-O1	105.8	145.3	135.6	161.8	-	104.5	139.3	137.1	161.3	-
O1-Mo-C6	152.9	133.5	83.81	115.7	-	153.5	139.9	84.10	116.4	-
N-Mo-O2	144.2	165.9	113.5	144.8	115.4	143.0	175.0	114.2	147.6	116.1

Table 5.11: Geometrical parameters (bond lengths in Å and angles in degree) of structures found in the path of ring opening of 3-methyl-3-trifluoromethylcyclopropene (MTCP)

Parameters	**CH_3 face**					**CF_3 face**				
	CTS	TBP	SP	RTS	Pr	CTS	TBP	SP	RTS	Pr
Mo-C1	1.933	2.198	2.222	2.433	-	1.933	2.172	2.220	2.375	-
C1-C4	2.689	1.502	1.514	1.419	1.346	2.744	1.517	1.517	1.434	1.347
C4-C6	1.353	1.685	1.549	1.970	-	1.355	1.665	1.556	1.927	-
Mo-C6	2.550	2.043	2.174	1.985	1.908	2.542	2.059	2.180	1.998	1.913
Mo-C1-C4	68.22	79.71	96.40	78.73	-	67.70	80.51	97.18	79.92	-
C1-C4-C6	110.4	117.2	100.6	115.9	-	109.2	116.9	99.94	114.2	-
C4-C6-Mo	79.79	80.75	97.24	80.86	-	81.18	80.94	97.63	81.02	-
C6-Mo-C1	97.94	79.76	64.82	80.83	-	99.42	79.71	64.66	80.27	-
C1-Mo-O1	106.2	145.6	135.7	162.2	-	106.0	139.0	133.9	161.4	-
O1-Mo-C6	153.0	133.1	83.78	115.0	-	151.9	139.8	84.09	116.2	-
N-Mo-O2	144.7	165.2	111.5	144.6	115.4	144.7	175.2	111.3	145.1	115.1

5.3.2.3 Ring Opening Transition Structures of Intermediates

The intermediates of methyl face and NH_2, OH, CN, CF_3 faces of AMCP, HMCP, CMCP and MTCP respectively produced ring opening transition structures (RTS) in pseudo-TBP geometry with the NH group and one of the alkoxy (-OCH_3) groups taking the axial position. The corresponding ring opening transition structures of AMCP, HMCP, CMCP and MTCP are shown in Figure 5.9, 5.10, 5.11 and 5.12 respectively.

Compared with the methyl face RTS, the breaking Mo-C1 bond length is little larger in RTS of NH_2, OH, CN faces and smaller in RTS of CF_3 face (See in Table 5.8-5.11). This suggest that the Mo-C1 bond easily broken when reaction proceed through NH_2, OH, CN faces in AMCP, HMCP, CMCP and through methyl face in case of MTCP. The other breaking bond (C4-C6) is longer in the methyl face RTS of AMCP and MTCP while it is smaller in RTS of HMCP and CMCP as compared to NH_2, OH, CN and CF_3 faces. In ring opening transition structures of methyl face of disubstituted cyclopropenes, except MTCP, new forming bonds C1-C4 and Mo-C6 are greater and indicate that they are weaker bond than those formed in RTS of NH_2, OH, CN face. For MTCP case, in RTS of methyl face C1-C4 and Mo-C6 bond lengths are smaller than CF3 face.

Methyl face ring opening processes of AMCP and HMCP intermediates have activation energy about 6.1 kcal/mol and 5.36 kcal/mol respectively. These activation barriers are lower than their corresponding CTS. For CMCP and MTCP the ring opening activation barrier is higher (see in Table 5.7) by about 2.9 kcal/mol and 1.45 kcal/mol than their relevant CTS and it is in contrast to the AMCP and HMCP moieties for those ring opening process is found lower by about 0.68 kcal/mol and 2.08 kcal/mol respectively.

When ring opening of intermediates occurs by NH_2, OH, CN and CF_3 faces, RTS of NH_2 and CF_3 face is lower than their cycloaddition transition structures (CTS) and observed higher for OH and CN face. Activation energy differences between RTS and CTS of NH_2 and CF_3 face is smaller by about 0.71 kcal/mol and 0.85 kcal/mol respectively but higher for OH and CN faces by about 3.65 kcal/mol and 4.15 kcal/mol correspondingly. The lowest ring opening activation barrier is calculated for the NH_2 face (about 5.96 kcal/mol) and the highest for the CN face (about12.52 kcal/mol). OH face has activation barrier of about 6.39 kcal/mol and 11.91 kcal/mol for RTS of CF_3 face. The calculated relative energies (in kcal/mol) are given in Table 5.7.

Our calculated activation energies at methyl face of disubstituted cyclopropenes shows that cycloaddition is kinetically the rate determining step for ROM of AMCP and HMCP while for CMCP and MTCP rate determining step is the ring opening of intermediates. When ROM occurs through OH and CF_3 face in HMCP and MTCP the rate determining step altered. Ring opening step become rate determining for HMCP and cycloaddition step for MTCP. The rate determining step remains the same for AMCP and CMCP whether ROM reaction proceeds through methyl face or NH2 and CN face respectively.

5.3.2.4 Ring Opening Products

The basic features of the ring opening products investigated are similar to previous findings on the syn $Mo(NH)(CH_2)(OCH_3)_2$ alkylidene. Thus we are not elaborating about the geometries of these structures. The optimized structures of methyl face and NH_2, OH, CN and CF_3 products are shown in Figure 5.9, 5.10, 5.11 and 5.12 respectively and their geometrical parameters are given in Table 5.8, 5.9, 5.10 and 5.11. Calculated relative electronic energies (in kcal/mol) are given in Table 5.7.

The NH_2, OH, and CN faces of corresponding AMCP, HMCP and CMCP formed kinetically stabler products than their methyl face. The methyl face products are higher by about 3.2 kcal/mol, 3.77 kcal/mol and 1.9 kcal/mol respectively. In methyl face products, the net steric hindrance between NH and CH_3 is more than that between NH & NH_2 or OH or CN in products formed by the NH_2, OH and CN faces respectively. As discussed in earlier section, the hydrogen bonding between NH group of catalyst and NH_2 or OH also lowers the energies of product of AMCP and HMCP. In case of MTCP, the methyl face product is stabler than CF_3 face product by about 3.40 kcal/mol. In case of the product at CF_3 face it may be that lone pair-lone pair repulsion between NH and CF_3 groups make it unstable as compared to methyl face product. Out of the all products of AMCP, HMCP, CMCP, and MTCP the ring opening product formed by OH face of HMCP is the most stable product. The strong hydrogen bonding (O-H---N) most likely give extra stability to product.

5.4 CONCLUSIONS

The ring opening reaction of asymmetric 3-methyl-3phenylcyclopropene with $Mo(NH)(CH_2)(OCH_3)_2$ catalyst occurs preferably in syn orientation and proceeds through the less sterically demanding methyl face and the phenyl face is instrumental in reaction of ROM. Parallel and perpendicular conformers are involved in the reaction and parallel conformers, having phenyl ring horizontal, are stabler isomers.

Substituent effect on ring opening of cyclopropene was also investigated using 3-amino-3-methylcyclopropene (AMCP), 3-hydroxyl-3-methylcyclopropene (HMCP), 3-cyanide-3-methylecyclopropene (CMCP), and 3-methyl-3-trifluoromethylecyclopropene (MTCP). The methyl face is preferred for the ring opening metathesis reaction in MTCP but not for AMCP, HMCP and CMCP, thus their respective NH_2, OH and CN faces are preferred for ROM reaction. Among the all investigated disubstituted cyclopropenes, the OH face of the HMCP is found to be the most favorable for the ring opening metathesis of cyclopropene.

5.5 REFERENCES

Becke A D (**1993**) "Density-functional thermochemistry .3. The role of exact exchange" *J. Chem. Phys*. **98**:5648-5652.

Flook M M, Gerber L C H, G T Debelouchina and Schrock R R (**2010**) "Z-Selective and Syndioselective Ring-Opening Metathesis Polymerization (ROMP) Initiated by Monoaryloxidepyrrolide (MAP) Catalysts" *Macromolecules* **43**:7515-7522.

Gayatri G and Sastry G N (**2009**) "Estimating regio and stereoselectivity in [4+2] cycloadditions of vinyl-substituted cyclic dienes with maleic anhydride" J. Phys. Chem. A **113**:12013-12021.

Lin N T, Ke Y Z, Satyanarayana K, Huang S L, Lan Y K, Yang H C, and Luh T Y (**2013**) "On the stereoselectivity of ring-opening metathesis polymerization (ROMP) of N-arylpyrrolidine-fused cyclobutenes with molybdenum-and ruthenium-alkylidene catalyst. *Macromolecules* **46**: 7173-7179.

Meena J S and Thankachan P P (**2014**) "Ring opening of monocyclic dimethyl cyclopropene via metathesis by tungsten catalyst- A computational study"*J.Chem. Sci* (In press).

Meena J S and Thankachan P P (**2013**) "Theoretical Studies of the Ring Opening Metathesis Reaction of 3, 3-Dimethyl Cyclopropene with Molybdenum Catalyst" *Comp. Theor .Chem*. **1024**:1-8.

Mishra B K and Sathyamurthy N (**2005**) "π-π Interaction in Pyridine" J. Phys. Chem. A **109**:6-8.

Rubin M and Gevorgyan V (**2004**) "Simple Large-Scale Preparation of 3,3-Disubstituted Cyclopropenes: Easy Access to Stereodefined Cyclopropylmetals via Transition Metal-Catalyzed Hydrometalation" *Synthesis* **5**:796-800.

Xidos J D, Gosse T L, Burke E D, Poirier R A and Burnell D J (**2001**) "Endo-Exo and Facial stereoselectivity in the diels-alder reactions of 3 substituted cyclopropenes with butadiene" *J. Am. Chem. Soc.* **123**: 5482-5488.

6 Tandem Ring Opening-Cross Metathesis

6.1 INTRODUCTION

Ruthenium catalyzed olefin metathesis reactions can lead to the efficient production of highly functionalized, unsaturated polymers and small molecules [Credendino et al., 2011; Randall and Snapper, 1998]. The ruthenium based Grubbs first and second generation catalysts are widely used in reactions that involve multiple metathesis transformations [Schwab et al., 1995; 1996; Scholl et al., 1999]. The combination of ring opening metathesis polymerization (ROMP) and cross metathesis (CM) reactions is used in the production of unique telechelic and multiple-block copolymers with novel properties [Chung and Chasmawala, 1992; Hillmyer et al., 1997; Maughon et al., 2000]. For the synthesis of small molecules, ring opening metathesis-ring closing metathesis (tandem ROM-RCM) allows the rapid production of multiple ring systems, as well as those in natural products [Park et al., 2013; Voigtmann and Blechert, 2000; Harrity et al., 1997, 1998; Weatherhead, 2000; Zuercher et al., 1996]. In all these types of reactions, the product of one occurrence of metathesis is directly accessible for the next, which allows the rapid generation of complexity in a single reaction [Schuster and Blechert, 2001; Naota et al., 1998].

An important variation on this theme is ring opening metathesis-cross metathesis (ROM-CM, Scheme 6.1) [Arjona, 2000; Garber, 2000; Katayama et al., 2000; La et al., 1999; 2001; Michaut, 1998; Snapper et al., 1997; Stuer et al.,1998; Tallarico et al.,1997]. In this tandem ROCM, a cycloalkene is opened and other olefins are crossed onto the newly formed termini. Ideally, the resultant olefins should be sterically or electronically orthogonal to permit subsequent elaboration in a straightforward mode. One approach to end-differentiation of olefins is shown in Scheme 6.1. After the initial ring opening metathesis (ROM) reaction, the ruthenium-bound intermediate reacts with cross partner. This method allows end differentiation in a single reaction when the cross metathesis step is faster than the ring opening of another cycloolefin. Two products are possible from this cross metathesis: the end-differentiated product (EDP) and the non end-differentiated product (NEDP). The selective synthesis of end-differentiated product is dependent on the nature of both the substrate and the catalyst.

The ruthenium alkylidene catalyst of second generation opens opportunities to metathesize selective ROCM reaction [Arjona et al., 1999; Giudici and Hoveyda, 2007; Weeresakare et al., 2004]. Electron-poor acrylates and electron-rich cycloolefins have been noted as excellent substrates for synthesis of end-differentiated products by ROCM. In

presence of ruthenium catalyst [Morgan et al., 2002]. trisubstituted cycloolefins underwent ROCM with α,β-unsaturated carbonyl compounds to generate end-differentiated dienes, in which the carbonyl segment of the cross partner was located on the less-hindered side of the diene.

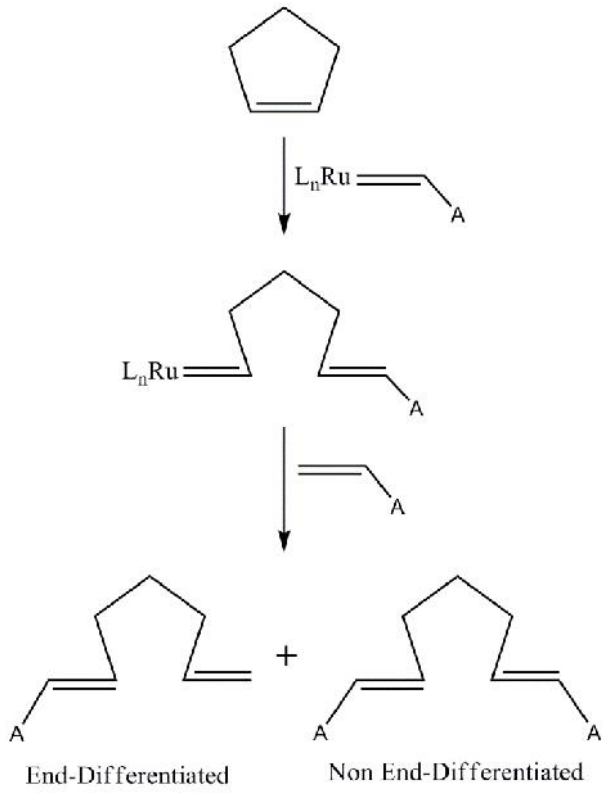

Scheme 6.1: Tandem Ring Opening Cross Metathesis

The mechanism of ruthenium alkylidene catalyzed olefin metathesis has recently been a subject of intense experimental [Ulman and Grubbs, 1998; Sanford et al., 2001a; 200b; Hinderling et al., 1998] and theoretical [Cavallo, 2002; Fomine et al., 2003; Minenkov et al., 2013; Suresh, 2006;Vyboischikov et al., 2002] investigations. However, not much attention has been paid in these studies to the peculiarities of the mechanism of ROCM of trisubstituted cycloolefins to produce end-differentiated olefins.

In this chapter, we discuss computational modeling of ruthenium mediated ROCM to obtained end-differentiated product. In particular, we exhaustively characterize stationary points on the potential energy surface for Grubbs ruthenium catalyst (G2) mediated ROCM of 1-methylcyclopentene (TCP) with methyl vinyl ketone (MVK).

1-methylcyclopentene is an ideal monomer scaffold for this purpose because it has a low tendency to form dimer. The optimized structures of TCP and MVK are given in Figure 6.1. The ruthenium alkylidene complex $(PH_3)(NHC)Cl_2Ru{=}CH_2$ (NHC = 1,3-dihydroimidazol-2-ylidene) was applied as the model catalyst. Optimized geometry of model catalyst (G2) and its dissociative species are shown in Figure 6.2. The optimized geometrical parameters of model catalyst (G2) and its dissociated active catalyst are collected in Table 6.1 and their associated energies, enthalpies and free energy are given in Table 6.2.

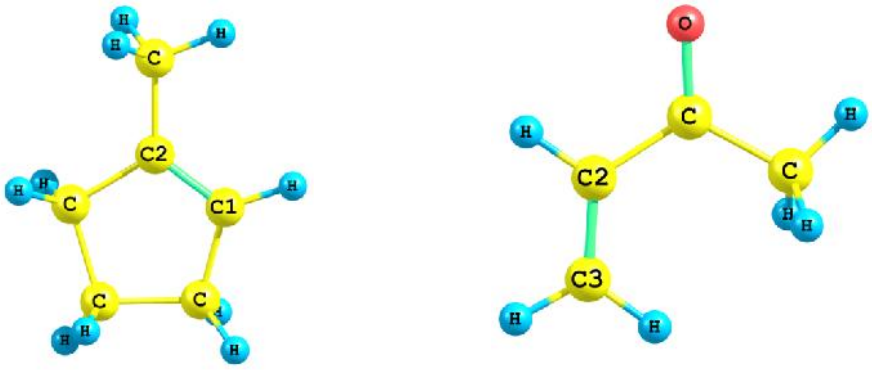

Trisubstituted Cyclopentene (**TCP**) Methyl Vinyl Ketone (**MVK**)

Figure 6.1: Optimized geometries of the olefin monomers used in ROCM reaction

 # Green bond shows double bond and some atoms are numbered for identification purpose only

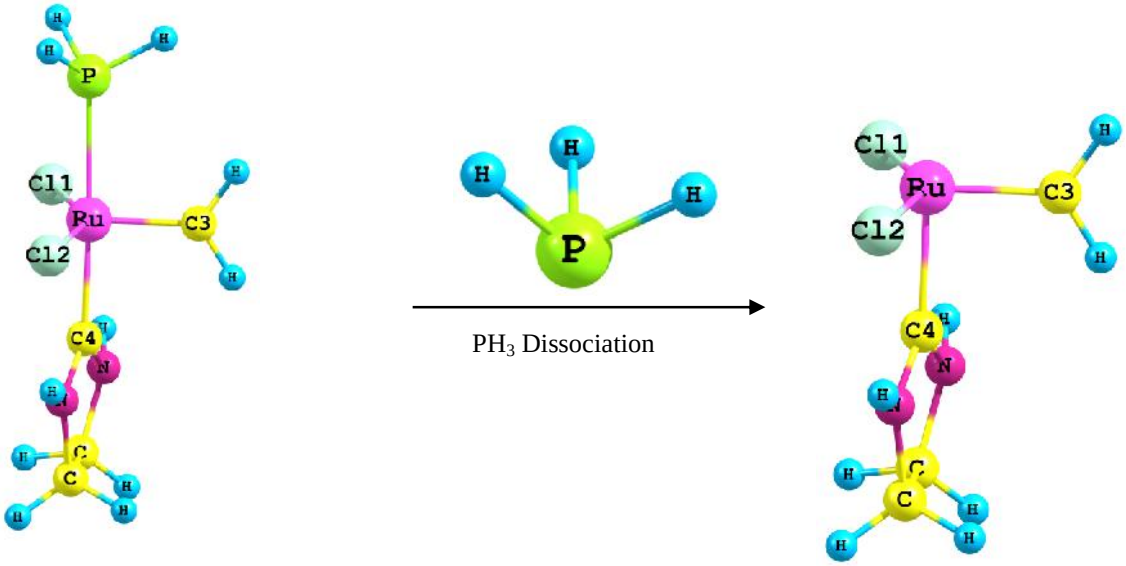

Grubbs Model Catalyst (**G2**) Active Catalyst (**AC**)

Figure 6.2: Showing optimized geometries of G2 catalyst and species formed by its dissociation

Table 6.1: Selected bond lengths (Å) and angles [degree) for model of Grubbs second generation catalyst optimized at B3LYP level.

Parameters	**G2**	**AC**
Ru-C3	1.828	1.812
Ru-C4	2.049	1.946
Ru-P	2.461	-
Ru-Cl1	2.404	2.366
Ru-Cl2	2.407	2.372
Cl1-Ru-C3	104.8	105.3
Cl2-Ru-C3	105.9	106.1
Cl1-Ru-Cl2	149.3	147.4
Cl1-Ru-C4	88.8	92.6
Cl2-Ru-C4	89.8	93.7
P-Ru-C3	92.1	-
P-Ru-C4	177.9	-
C3-Ru-C4	89.9	94.0

Table 6.2: Calculated total electronic energies, enthalpies and free energies (in hartree) of the species involved in dissociation of Grubbs (G2) catalyst at the B3LYP level and M06L functional (in parentheses)

Species	Energy (E_e)	Enthalpy (H)	Free Energy (G)
Catalyst (G2)	-1624.2291606	-1624.060678	-1624.119738
	(-1624.1622004)	(-1623.993954)	(-1624.052180)
Active Catalyst (AC)	-1281.0673741	-1280.930047	-1280.98108
	(-1281.0189868)	(-1280.882011)	(-1280.932627)
PH_3	-343.1402804	-343.112206	-343.137094
	(-343.115804)	(-343.087217)	(-343.112086)
AC1+PH_3	-1624.207654	-1624.042253	-1624.118174
	(-1624.13479)	(-1623.96228)	(-1624.044713)

It is generally accepted at present that ruthenium catalyzed olefin metathesis proceeds via dissociative mechanism based on the general Herisson-Chauvin mechanism (Scheme 6.2) which involves a metallacyclobutane intermediate. This mechanism starts with the dissociation of one phosphine ligand to form a tetracoordinated 14-electron complex known as the active catalyst (AC) of the catalytic cycle. The recent investigations [Sanford et al., 2001a; 2001b] favor the dissociative path. The tetracoordinated 14-electron intermediates (AC) were unambiguously characterized experimentally using both Grubbs type catalysts with a cationized phosphane ligand [Hinderling et al., 1998; Adlhart, 2000].

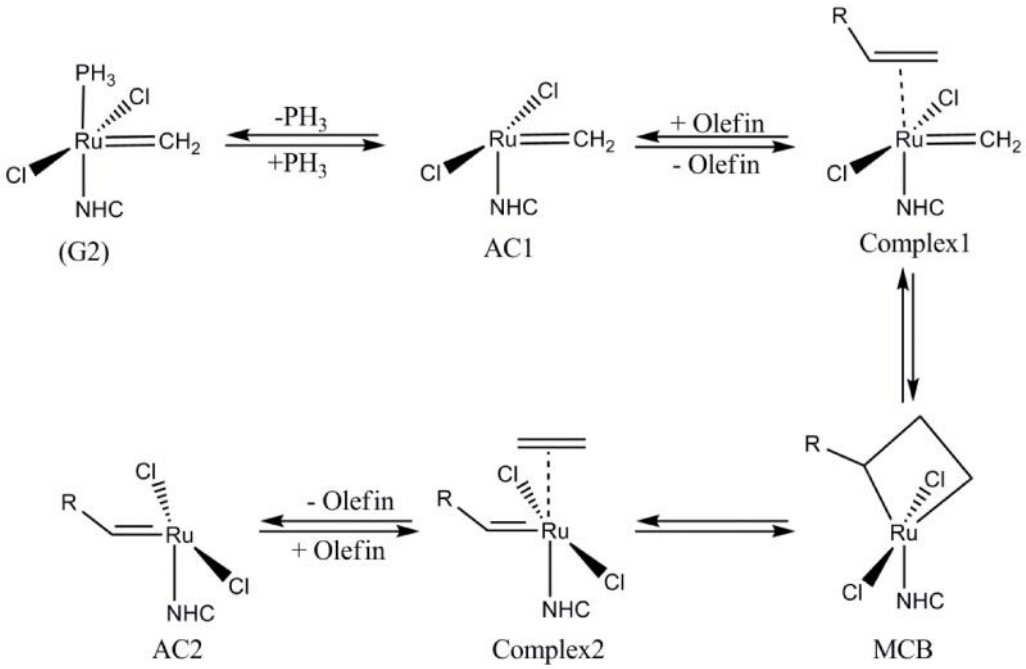

Scheme 6.2: Herisson-Chauvin Mechanism for Olefin Metathesis Catalyzed by Grubbs Ruthenium Catalyst (G2)

6.2 COMPUTATIONAL DETAILS

All structure optimizations were performed using the hybrid DFT method at the B3LYP level, a combination of Becke's three-parameter hybrid exchange functional (B3) [Becke 1993, 1996] with the Lee-Yang-Parr correlation functional [Lee et al. 1988] as implemented in Gaussian 09W [Frisch et al. 2009..]. The reliability of the B3LYP functional is well-documented in the context modeling chemical reactions [Roy and Sunoj, 2010; Patil et al., 2010].To test whether the relative stability of the structures could depend on the chosen hybrid B3LYP functional, we optimized all structures with more recent M06-L functional recommended by Zhao and Truhlar for modeling Grubbs II olefin metathesis catalysts [Zhao and Truhlar 2006]. For ruthenium, the LANL2DZ basis set was

applied. In this basis set the 28 innermost electrons of Ru have been replaced by a relativistic core potential (ECP) of Hay and Wadt [Hay and Wadt, 1985; Wadt and Hay, 1985]. All non-metal atoms (H, C, N, O, P and Cl) were treated with 6-31G (d) basis set [Hehre et al., 1986]. The stationary points were characterized by frequency calculations located as minima or transition state.

6.3 RESULTS AND DISCUSSIONS

The rate of formation of the ruthenium active catalyst (AC) upon dissociation of phosphine from model catalyst $(PH_3)(NHC)Cl_2Ru{=}CH_2$ is the same regardless of trisubstituted cyclopentene structure and will not contribute to the selectivities. The energetic of this step has been the subject of earlier calculations in both gas phase [Zhao and Truhlar, 2007; 2009] and toluene [Benitez et al., 2009; Minenkov, 2012]. Therefore, we investigate the steps following phosphine dissociation in whole catalytic cycle of ROCM to study the formation of end-differentiated product, namely (a) formation of the metallacyclobutane intermediate and (b) cycloreversion of intermediate to form product.

6.3.1 RING OPENING METATHESIS OF TCP

Trisubstituted cyclopentene molecule can attack the Ru-center of the active catalyst in two different orientations, distal and proximal as shown in Scheme 6.3. In the distal case, the methyl group connected to the carbon atom of trisubstituted cyclopentene is positioned farther from the Ru-centre and positioned closer the Ru-center in proximal case.

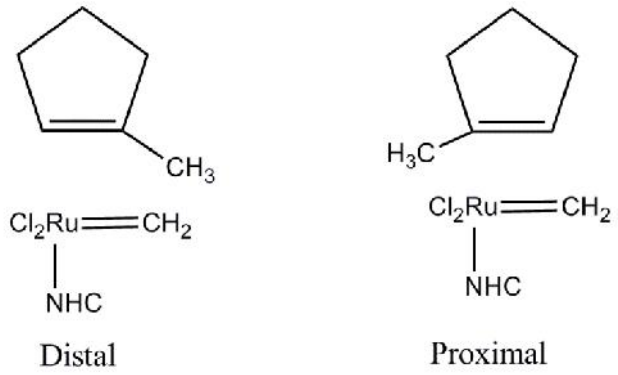

Scheme 6.3: Distal and Proximal addition of trisubstituted cyclopentene with Ru-active catalyst

6.3.1.1 Formation of the Metallacyclobutane Intermediates

The initial coordination of trisubstituted cyclopentene with active catalyst gives π - complexes in both distal and proximal cases. These complexes are formed due to interaction between the π- electrons of C1=C2 of TCP and the empty d-orbital of Ru atom [Serguei et al., 2007]. Each complex (C1) undergoes [2 + 2] cycloaddition to give the metallacyclobutane intermediate (MCB1) via a transition state TS1. The structures corresponding to potential energy minima and transition states on the reaction path of distal and proximal TCP addition to active catalyst are shown in Figure 6.3. In distal addition the forming bonds are Ru-C1 and C3-C2, whereas in case of the proximal addition of TCP, Ru-C2 and C3-C1 bonds are forming. In both cases the Ru-C3 and C1-C2 are breaking bonds. In distal complex (DC1) the bond distances of C1 and C2 with Ru- center are 2.835 Å and 3.099 Å while in proximal complex (PC1) these distancess are 2.786 Å and 2.885 Å. As compared to Ru-C2 bond length of DC1, the Ru-C1 bond length in PC1 is shorter and indicates that the proximal complex is tighter than the distal complex. Details bond lengths (Å) and angles [degree) of the geometries (at B3LYP level) of the structures presented are given in Table 6.3D, P for distal and proximal cases respectively.

In transition structures involved, a significant bond formation Ru-C1 in distal case (DTS1) and Ru-C2 in proximal case (PTS1) can be seen. The forming Ru-C1 and Ru-C2 bond distances are 2.179 Å and 2.236 Å in DTS1 and PTS1 respectively. The bond length C3-C2 and C3-C1 have also been decreased and are about 2.169Å and 2.129 Å respectively in distal and proximal transition states. The breaking bond lengths Ru-C3 and C1-C2 have also been elongated (see in Table 6.3D, P). The bond angle Cl-Ru-Cl is about 172º. The bond angle C3-Ru-C4 has been increased by about 115-117º while on other side bond angle C1-Ru-C4 and C2-Ru-C4 has been shortened in DTS1 and PTS1 respectively.

The calculated enthalpy, at B3LYP, of distal complex (DC1) is higher than that of the proximal complex (PC1) by about 1.41 kcal/mol. (see in Table 6.5). The activation barriers for distal and proximal coordination of the trisubstituted cyclopentene with Grubbs catalyst were calculated to be about 12.02 kcal/mol and 11.51 kcal/mol respectively. The greater electrostatic attraction between the carbon (C2) attached to methyl group of TCP and Ru atom of the active catalyst reduced the activation barrier for the PTS1. The total electronic energies, enthalpies, and Gibbs free energies calculated at the B3LYP and M06L level for the species found in ROM step are collected in Table 6.4. Relative energies at both levels are given in the Table 6.5.

The enthalpy, calculated using M06L functional, also predicted that the proximal complex is more stable than distal complex by about 2.22 kcal/mol. The energy barriers at this level are are 14.55 kcal/mol and 12.94 kcal/mol. respectively. With respect to the complex1, the both B3LYP and M06L functional show similar trend for the reaction. The calculated activation barriers at B3LYP and M06L showing that the proximal coordination of trisubstituted cyclopentene with the Ru-active catalyst is more easy than distal coordination.

The distal and proximal transition states convert to the corresponding metallacyclobutane intermediates (MCB1). These intermediates have a core ring (Ru-C-C-C) in which a complete bond formation has been occurred. The core ring of DMCB1 is nearly planar but it seems to be slightly puckered in PMCB1. The forming bond lengths Ru-C1 and C3-C2, in DMCB1, are shorter by about 0.197 Å and 0.594 Å respectively than those found in DTS1. As compared to PTS1, in PMCB1 the forming bond lengths Ru-C2 and C3-C1 are shorter by about 0.226 Å and 0.567 Å. The Cl-Ru-Cl angle is about 167-170º and three atoms form an axis that almost bisects the ruthenacyclobutane ring. The bond angles C3-Ru-C4 of the MCB1 is about 135-138º and close to the bond angle C1-Ru-C4 and C2-Ru-C4 (136-139º) of DMCB1 and PMCB1 respectively.

In terms of enthalpies, ruthenacyclobutane intermediate formed through the proximal coordination (PMCB1) is calculated to be more stable than the distal (DMCB1) by only 0.62 kcal/mol with B3LYP method (see energies relative to the C1 in Table 6.5) and by about 1.51 kcal/mol with M06L method. The less steric hindered transition state PTS1 provides the stabler intermediate PMCB1. Lower Gibbs free energy (in Table 6.5) also supports the ease formation of the intermediate by proximal coordination. Both intermediates have positive enthalpies and indicate that the formation of MCB1 from the C1 is an endothermic process.

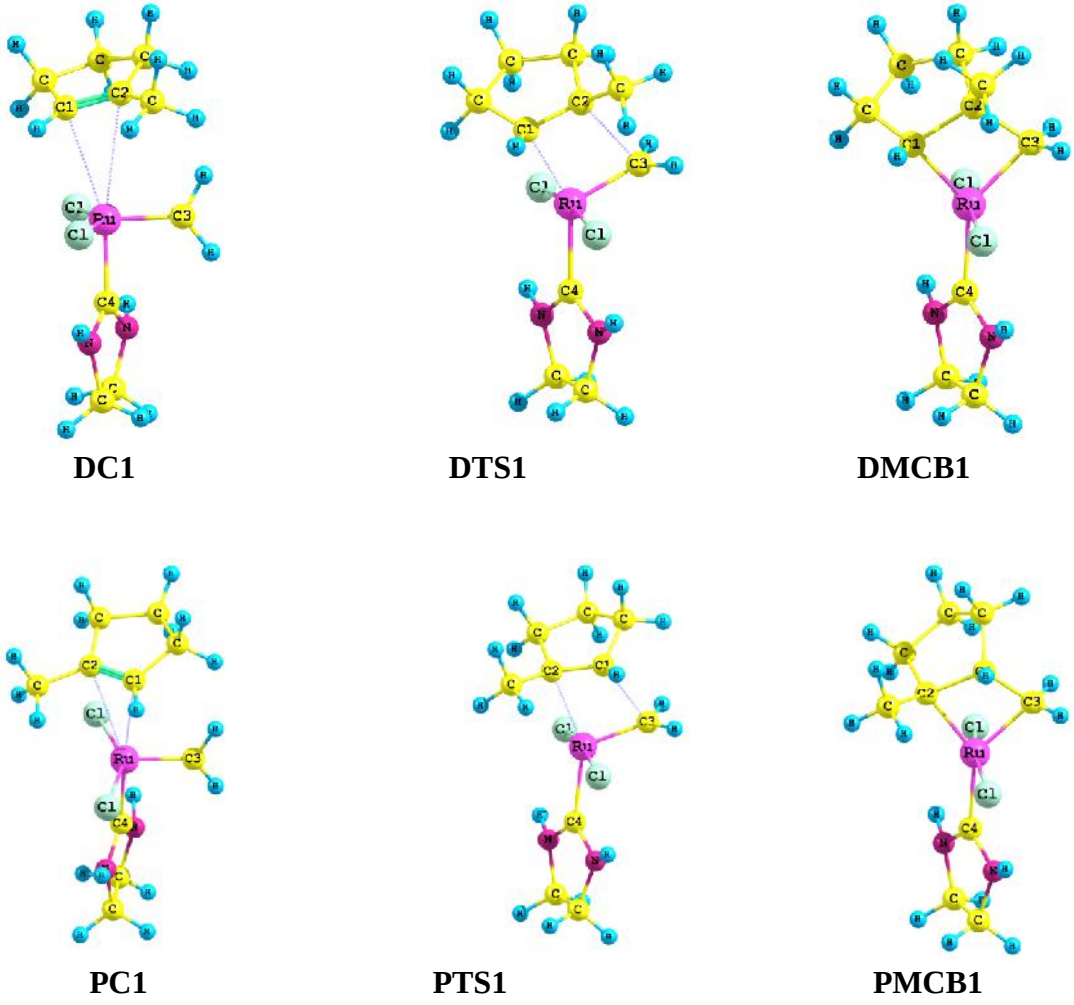

Figure 6.3: Optimized B3LYP structures for the distal and proximal cycloaddition reaction of ROM of TCP

6.3.1.2 Cycloreversion of Metallacyclobutane Intermediates

The distal and proximal intermediates of ROM undergo cycloreversion process via TS2. The rupturing of the MCB1 ring produced the ring opened product of the ROM catalytic cycle. Figure 6.4 shows the optimized structures (at B3LYP) of the species found during the cycloreversion of metallacyclobutane intermediates of ROM reaction. Optimized geometrical parameters of these structures are collected in Table 6.3D and 6.3P for distal and proximal respectively.

In the distal ring opening transition structure (DTS2) the breaking Ru-C3 and C1-C2 bonds are longer than those in the ruthenacyclobutane intermediates (MCB1) only by about 0.113 Å and 0.388 Å and in the proximal ring opening transition structure (PTS2) by about 0.088Å and 0.302 Å. The forming Ru-C1 and C3-C2 bonds are shorter by about

0.094 Å and 0.117 Å in DTS2 while in PTS2 the forming Ru-C2 and C3-C1 bonds are shorter by about 0.089 Å and 0.096 Å respectively. The bond angle C3-Ru-C4 is about 143-147º while on other hand the C1-Ru-C4 and C2-Ru-C4 bond angles are lower at about 121-125º.

The distal and proximal ring opening transition structures lead to the corresponding product formation DPr and PPr respectively. Unless otherwise noted, the product is itself a complex of the newly created double bond to the ruthenium center. The newly formed double bond C3-C2 in DPr and C3-C1 in PPr are of length (1.36 Å) which is close to normal double bond length.

Relative to the metallacyclobutane, the activation barrier (calculated at B3LYP) of DTS2 is about 2.64 kcal/mol and 1.50 kcal/mol for PTS2. The difference of activation barrier of DTS2 and PTS2 is larger (3.67 kcal/mol) at the M06L functional than B3LYP (1.14 kcal/mol) (see in Table 6.5). Ring opening transition structures DTS2 and PTS2 produced secondary and tertiary carbenes as ring opened products respectively. The relative stability of both metallacarbenes was found to be similar to the previous theoretical results on secondary and tertiary metallacarbenes [Fomine and Tlenkopatchev, 2010].

Thermodynamically, the product formed by DTS2 (secondary carbene) is more active than the product of the PTS2 (tertiary carbene) by about 2.07 kcal/mol. Relative stability difference (2.34 kcal/mol) of products at M06L level is very close to the B3LYP level. Gibbs free energies of the products predict that the ROM catalytic cycle of ROCM is exeothermic (see in Table 6.5). These newly formed products ruthenium alkylidenes will act as active catalyst (AC) for the sequence reaction cross metathesis of the ROCM.

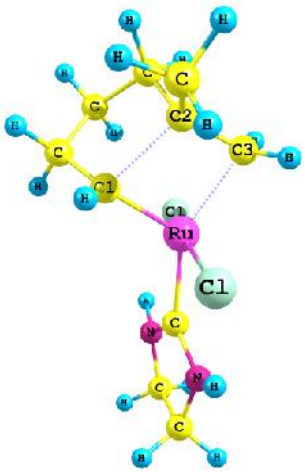

DTS2

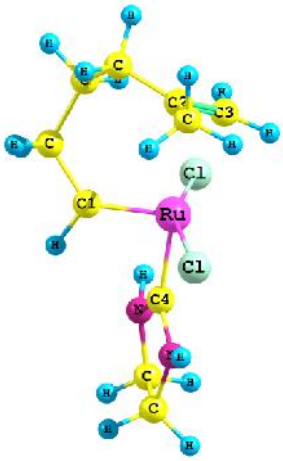

DPr

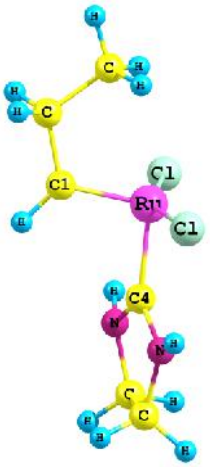

MDPr

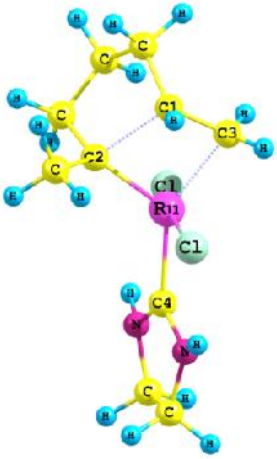

PTS2

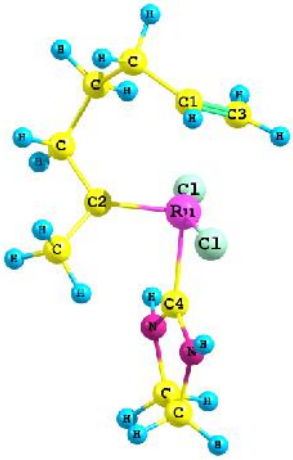

PPr

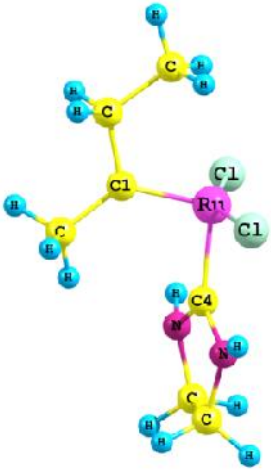

MPPr

Figure 6.4: Optimized B3LYP structures involved in the cycloreversion of distal and proximal metallacyclobutane of ROM of TCP with G2 catalyst model

Table 6.3D, P: Optimized geometrical parameters of the structures found in the reaction path of distal/proximal ring opening reaction of trisubstituted cyclopentene

Table 6.3D

Parameters	DC1	DTS1	DMCB1	DTS2	DPr
Ru-C3	1.818	1.852	1.990	2.103	2.522
C1-C2	1.354	1.438	1.635	2.023	3.281
Ru-C2	3.099	2.463	2.332	2.40	2.886
Ru-C1	2.835	2.179	1.982	1.888	1.832
C3-C2	3.351	2.169	1.575	1.458	1.357
Ru-C4	1.980	2.092	2.01	2.098	2.018
Cl-Ru-Cl	149.4	171.6	170.0	166.1	157.2
Ru-C1-C2	-	83.14	79.7	75.6	-
C1-C2-C3	-	108.03	114.0	110.0	-
C2-C3-Ru	-	75.1	80.8	82.6	-
C3-Ru-C1	-	93.7	85.4	91.8	-
C3-Ru-C4	90.6	116.9	138.1	147.0	161.2
C1-Ru-C4	162.56	149.1	136.3	121.2	89.86

Table 6.3P

Parameters	PC1	PTS1	PMCB1	PTS2	PC2
Ru-C3	1.817	1.851	1.988	2.076	2.394
C1-C2	1.356	1.436	1.647	1.949	3.00
Ru-C1	2.786	2.384	2.291	2.320	2.571
Ru-C2	2.885	2.236	2.01	1.921	1.854
C3-C1	3.269	2.129	1.562	1.466	1.362
Ru-C4	1.988	2.077	2.062	2.10	2.049
Cl-Ru-Cl	151.6	171.9	167.5	164.8	162.0
Ru-C2-C1	-	77.6	76.9	73.7	-
C2-C1-C3	-	111.4	115.3	112.8	-
C1-C3-Ru	-	73.2	79.4	79.8	-
C3-Ru-C2	-	92.8	85.5	91.1	-
C3-Ru-C4	90.1	115.2	135.6	143.8	155.0
C2-Ru-C4	158.8	151.9	138.7	124.9	90.0

Table 6.4: Calculated total electronic, enthalpies (at 298K) and free energies (in hartree) of the structures involved in ROM of trisubstituted cyclopentene (TCP) with Grubbs Second generation catalyst model at the B3LYP and M06L level (in parentheses)

Species	**Distal (D)_ROM**			**Proximal (P)_ROM**		
	Energy (E_e)	Enthalpy (H)	Free Energy (G)	Energy (E_e)	Enthalpy (H)	Free Energy (G)
TCP	-234.6481416	-234.495696	-234.532251	-234.6481416	-234.495696	-234.532251
	(-234.6027374)	(-234.450251)	(-234.486731)	(-234.6027374)	(-234.450251)	(-234.486731)
RT[a]	-1515.715516	-1515.425743	-1515.513331	-1515.715516	-1515.425743	-1515.513331
	(-1515.621723)	(-1515.332262)	(-1515.419358)	(-1515.621723)	(-1515.332262)	(-1515.419358)
C1	-1515.7213985	-1515.429158	-1515.49746	-1515.7236878	-1515.431405	-1515.499172
	(-1515.647134)	(-1515.355596)	(-1515.422578)	(-1515.6507013)	(-1515.359127)	(-1515.425294)
TS1	-1515.7022382	-1515.410277	-1515.474309	-1515.7053454	-1515.413381	-1515.476617
	(-1515.6240017)	(-1515.332944)	(-1515.397205)	(-1515.6300654)	(-1515.339179)	(-1515.402113)
MCB1	-1515.7153280	-1515.421029	-1515.48511	-1515.7187194	-1515.424265	-1515.487563
	(-1515.646310)	(-1515.352736)	(-1515.415867)	(-1515.6475727)	(-1515.353872)	(-1515.416835)
TS2	-1515.7111248	-1515.418283	-1515.482253	-1515.7163244	-1515.423201	-1515.486279
	(-1515.6352093)	(-1515.343212)	(-1515.406137)	(-1515.6422327)	(-1515.350105)	(-1515.413555)
Pr	-1515.7311406	-1515.438011	-1515.504852	-1515.7370307	-1515.443567	-1515.510171
	(-1515.6564547)	(-1515.363977)	(-1515.406137)	(-1515.6637607)	(-1515.371239)	(-1515.436622)

[a] **RT= Reactants (AC + TCP)**

Table 6.5: Calculated relative electronic energies (in kcal/mol), enthalpies and free energies (at 298K) of the reactants, complexes; transition structures (TS), Metallacyclobutanes and products of the ROM of trisubstituted cyclopentene with Grubbs Second generation catalyst model at the B3LYP and M06L level (in parentheses)

Species	**Relative to the Reactants (RT)**						**Relative to the Complex1 (C1)**					
	Distal (D)_ROM			**Proximal (P)_ROM**								
	ΔE_e	ΔH	ΔG	ΔE_e	ΔH	ΔG	**Distal (D)_ROM**			**Proximal (P)_ROM**		
RT	0	0	0	0	0	0	ΔE_e	ΔH	ΔG	ΔE_e	ΔH	ΔG
C1	-3.69	-2.14	9.96	-5.13	-3.55	8.88	0	0	0	0	0	0
	(-15.95)	(-14.64)	(-2.02)	(-18.18)	(-16.86)	(-3.73)						
TS1	8.33	9.71	24.49	6.38	7.76	23.04	12.02	11.8	14.53	11.51	11.31	14.15
	(-1.4)	(13.90)	(13.90)	(-5.24)	(-4.34)	(10.82)	(14.52)	(14.21)	(15.92)	(12.95)	(12.52)	(14.55)
MCB1	0.12	2.96	17.71	-2.01	0.93	16.17	3.81	5.10	7.75	3.12	4.48	7.28
	(-15.42)	(-12.85)	(2.19)	(-16.22)	(-13.56)	(1.58)	(0.5)	(1.79)	(4.21)	(1.96)	(3.30)	(5.31)
TS2	2.76	4.68	19.50	-0.51	1.60	16.98	6.45	6.82	9.54	4.62	5.15	8.09
	(-8.4)	(-6.87)	(8.30)	(-12.87)	(-11.20)	(3.64)	(7.48)	(7.77)	(10.32)	(5.31)	(5.66)	(7.37)
Pr	-9.80	-7.70	5.32	-13.5	-11.18	1.98	-6.11	-5.56	-4.64	-8.37	-7.63	-6.90
	(-21.79)	(-19.90)	(-6.64)	(-26.38)	(-24.46)	(-10.83)	(-5.8)	(-5.26)	(-4.62)	(-8.20)	(-7.60)	(-7.11)

6.3.2 CROSS METATHESIS OF MVK

To continuing the catalytic cycle of ROCM (Scheme 6.1), addition of methyl vinyl ketone to the newly formed Ru-alkylidenes (DPr and PPr) center must take place. Methyl vinyl ketone can coordinate to the Ru-alkylidene center in two different orientations cis and trans as shown in Scheme 6.4. The carbonyl group of MVK is oriented towards the alkylidene carbon (CHR) and opposite in trans coordination. The experimental studies [Morgan et al., 2002] have shown that the cis orientation produces the end differentiated products and only this orientation with both products of ROM is explored in the current work.

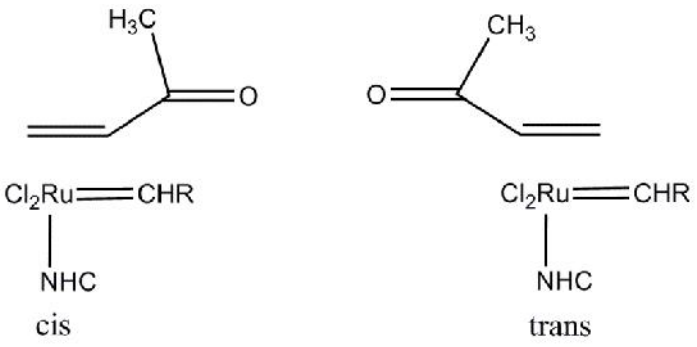

Scheme 6.4: cis and trans coordination of methyl vinyl ketone with ruthenium alkylidene

To simplify the computation, the ROM products (DPr and PPr) are modeled to obtained similar metal alkylidenes for cross metathesis. The unsaturated part -CH_2-C(CH_3)=CH_2 and -CH_2-CH=CH_2 are substituted by H in distal (DPr) and proximal (PPr) products respectively. The model of DPr is abbreviated as MDPr whereas that of PPr as MPPr. The optimized structures of these new model products are shown in Figure 6.4.

6.3.2.1 Metallacyclobutane Intermediates

Both Ru-alkylidenes MDPr and MPPr coordinate to methyl vinyl ketone in cis manner and lead to π-complexes (DC2 and PC2). After complex formation, the reaction passes through a transition structure (TS3) to form a metallacyclobutane intermediate (MCB2). Figure 6.5 show the geometries of the structures involved addition reaction of cross metathesis of methyl vinyl ketone with model products of preceding ROM reaction.

The initial bond distance of C2-C3 carbons of MVK is normal in the complex and shows a weak interaction between double bond and Ru-center. In these complexes the bond length (C2=C3) is around 1.354-1.357Å quite close to that of the double bond of MVK.

The forming bond Ru-C3 is shorter in PC2 than DC2 by about 0.097Å. Bond length of Ru-C3 is 2.59 Å in DC2 and 2.50 Å in PC2. The geometrical parameters of the structures involved in cross metathesis reaction of methyl vinyl ketone with MDPr and MPPr are collected in Table 6.6.

The complex (C2) convert into corresponding transition structure (TS3), as shown in Figure 6.5. In the transition state the π-electron density is shifted toward the alkylidene carbon (C1) to form a new carbon-carbon bond. Compared with the corresponding complex in DTS3 and PTS3, the forming Ru-C3 bond has also shortened by 0.477Å & 0.434 Å respectively and the other forming bond C1-C2 distance is 2.09 Å in DTS3 and 1.95 Å in PTS3. The breaking bonds C2-C3 and Ru-C1 have been slightly elongated (see in Table 6.6). The angles Cl-Ru-Cl are about 163-170º in these transition structures and C1-Ru-C4 angles are large (117-123º). Larger value of Cl-Ru-C4 angle indicates that the Ru=C1 bond is shifted toward the reacting double bond of MVK. Both new forming bonds Ru-C3 and C1-C2 are slightly longer in DTS3 by about 0.054 Å and 0.139 Å than those found in PTS3.

The addition transition structures transform into the corresponding four membered metallacyclobutane intermediates (MCB2). Forming and breaking bonds create a metallacyclobutane core ring (Ru-C3-C2-C1) in these structures. The Cl-Ru-Cl angles of the ring are about 165-173º. The Ru-C3-C2 and C2-C1-Ru angles are about 76-79º, and angle C3-C2-C1 is about 115-117º. The C1-Ru-C3 angles are about 85-87º. The C1-C2 bonds are unusually long, about 1.608 Å in DMCB2 & 1.658 Å in PMCB2, while the other C2-C3 bond lengths are about normal (1.57 Å). The bond lengths of Ru-C1 & Ru-C3 are 1.995 & 1.986 in DMCB2 and in PMCB2 these lengths are 2.016 & 1.987 respectively.

Calculated total electronic energies (in hartree), enthalpies (at 298 K), and Gibbs energies (at 298 K) , at B3LYP and M06L level ,of the all species investigated in cross metathesis catalytic cycle of ROCM are given in Table 6.7a (for CM with MDPr) & 6.7b (for CM with MPPr). Relative energies of these species are given in Table 6.8a and 6.8b respectively.

The addition of methyl vinyl ketone with distal alkylidene (MDPr) formed stabler π-complex (C2) as compared to that with proximal alkylidene (MPPr) (see Table 6.8a,b). The complex (DC2) with distal alkylidene is lower in energy than complex (PC2) with

proximal alkylidene by about 4.63 kcal/mol with B3LYP method. This relative stability is a little smaller (3.74 kcal/mol) with the M06L method.

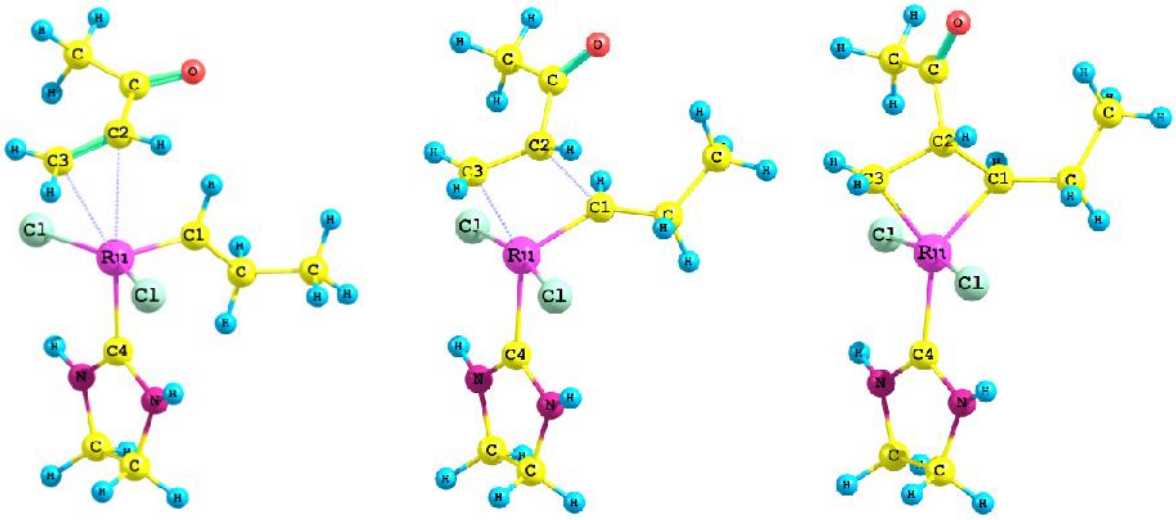

DC2 **DTS3** **DMCB2**

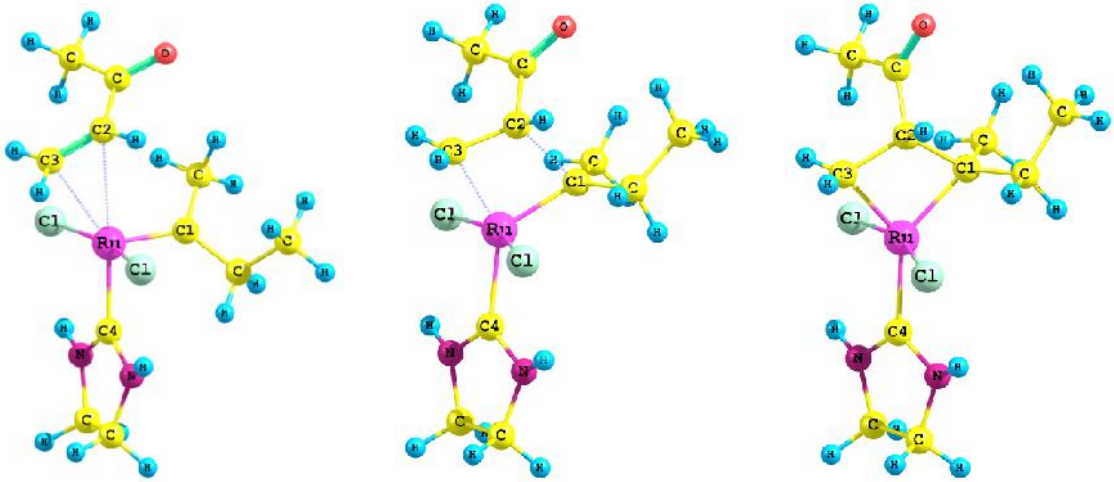

PC2 **PTS3** **PMCB2**

Figure 6.5: Optimized geometries of the addition reaction of cross metathesis of methyl vinyl ketone with MDPr and MPPr

The calculated activation barriers (at B3LYP level) for the formation of the metallacyclobutane intermediates, from complex (C2) DMCB2 and PMCB2 formed via their corresponding TS3 are 10.92 kcal/mol and 13.43 kcal/mol respectively. Kinetically the formation of the DMCB2 from the complex (C2) is easier than PMCB2 by about 2.51 kcal/mol. In Table 6.8a & 6.8b, the calculated energy of the metallacyclobutane is higher than complex (C2). Due to the absence of steric hindrance of the methyl group at the alkylidene carbon, DMCB2 is stabler than PMCB2 by about 6.02 kcal/mol at B3LYP and 5.38 kcal/mol with M06L method (see energy relative to the complex C2). Enthalpy and Gibbs free energy of B3LYP and M06L predict that the formation of the metallacyclobutane intermediates from the complex is endothermic, see in Table 6.8a & 6.8b.

6.3.2.2 Cycloreversion of Metallacyclobutane Intermediates

The decomposition of the metallacyclobutane intermediates via TS4 provide a end-differentiated π-complex (C3) which transforms into final product (DPr2 and PPr2) of the tandem ring opening cross metathesis (ROCM). The located ring opening transition structures from DMCB2 and PMCB2 are represented as DTS4 and PTS4 respectively. The ring opening transition structures, complexes and final product of this step are shown in Figure 6.6.

Compared with the metallacyclobutanes (DMCB2 and PMCB2), the C1-Ru-C4 angles have been opened up (150-152º), while C3-Ru-C4 angles are smaller at about 114º. The Cl-Ru-Cl angles are larger than those in intermediates MCB2. The breaking Ru-C1 and C2-C3 bonds are longer than presented in metallacyclobutane only by about 0.198 Å and 0.609 Å in DTS4 and by about 0.269 Å and 0.576 Å in PTS4 structure. On the other hand, the forming C1-C2 and Ru-C3 bonds are shorter by about 0.182 Å & 0.132 Å in DTS4 and 0.219 Å and 0.131 Å in PTS4 structure.

In complexes (DC3 and PC3) that are formed with the DTS4 and PTS4 respectively, the Ru-C1 and C2-C3 bonds have been completely broken although two new bonds C1=C2 and Ru=C3 have been created. Finally, the decoordination of olefin from DC3 and PC3 produces the initial active catalyst (AC) that may enter again into to the catalytic cycle of the tandem ring opening-cross metathesis (ROCM) reaction and olefin products of the DC3 and PC3 are DPr2 and PPr2 respectively.

The B3LYP calculated activation barriers for the formation of DC3 and PC3 from their corresponding metallacyclobutane, via DTS4 and PTS4, are 8.45 kcal/mol and 9.19 kcal/mol respectively. The transformation of the metallacyclobutane to the complex is an exothermic process. The complexes DC3 and PC3 are more stable than the respective MCB2 by about 2.88 kcal/mol and 7.04 kcal/mol. Relative to the initial reactants the enthalpy of the complex (C3) predicts that complex formation with MDPr is an exothermic process but an endothermic with MPPr. The calculated enthalpy of the product (PT) of the cross metathesis of methyl vinyl ketone with MDPr is lower than the product with the MPPr alkylidene by about 6.09 kcal/mol.

The activation energy, at M06L method, of the TS4 transition structures are higher than those calculated with B3LYP method but follow a similar trend. The transition state DTS4 is slightly lower than PTS4. The activation energy for these transition structures with this method are about 13.36 kcal/mol and 13.91kcal/mol respectively. Thermodynamically, the reaction product (PT) of the cross metathesis with MDPr is more stable than the MPPr by about 6.09 kcal/mol. Our calculations, at both B3LYP and M06L methods, predict a preferential formation of the product with cross metathesis of methyl vinyl ketone with MDPr alkylidene of the ROM reaction.

Because in treating of the cross metathesis the unsaturated part $-CH_2-C(CH_3)=CH_2$ and $-CH_2-CH=CH_2$ were replaced by H in distal (DPr) and proximal (PPr) products respectively, to obtain the original end-differentiated product of the ROCM, the replaced part must be added to the cross metathesis products (DPr2 and PPr2). The real (end-differentiated) products equivalent to the DPr2 and PPr2 are represented as EDPr1 and EDPr2 respectively and optimized structures are shown in Figure 6.7. In both products carbonyl group of the methyl vinyl ketone (MVK) caps the product and regenerated the initial active ruthenium methylidene complex.

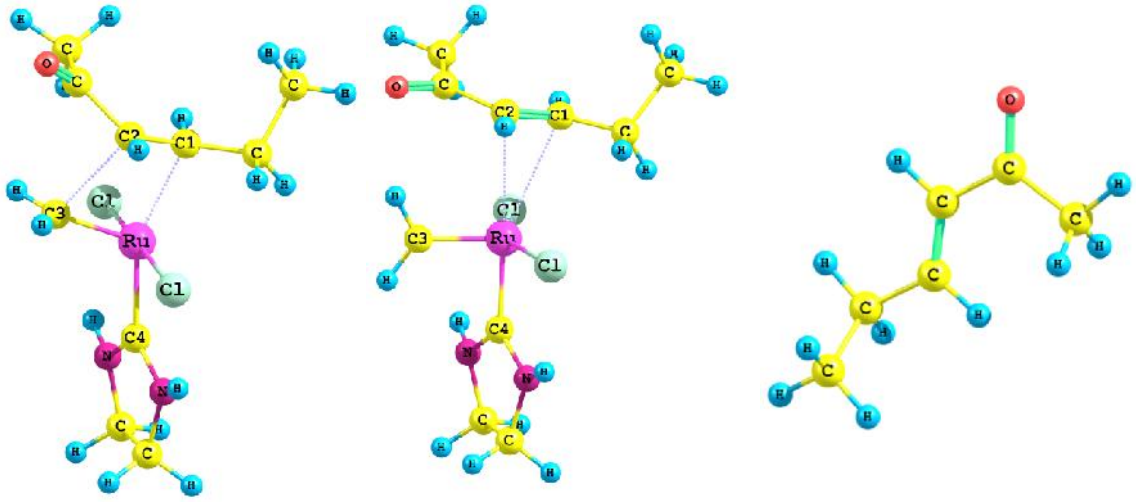

DTS4 **DC4** **DPr2**

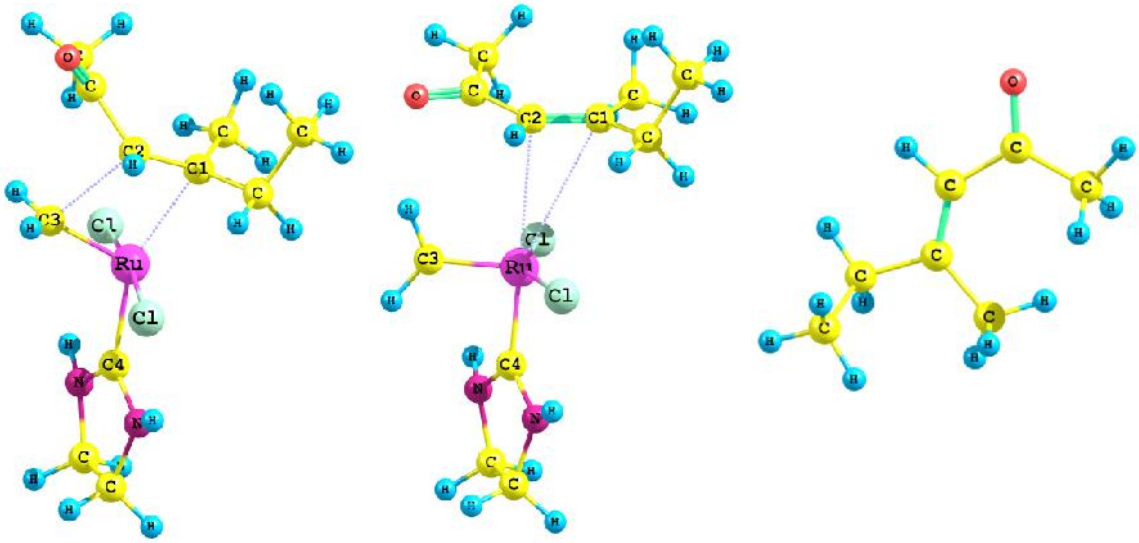

PTS4 **PC4** **PPr2**

Figure 6.6: B3LYP optimized geometries of structures investigated for cycloreversion of intermediates of cross metathesis catlytic cycle in ROCM

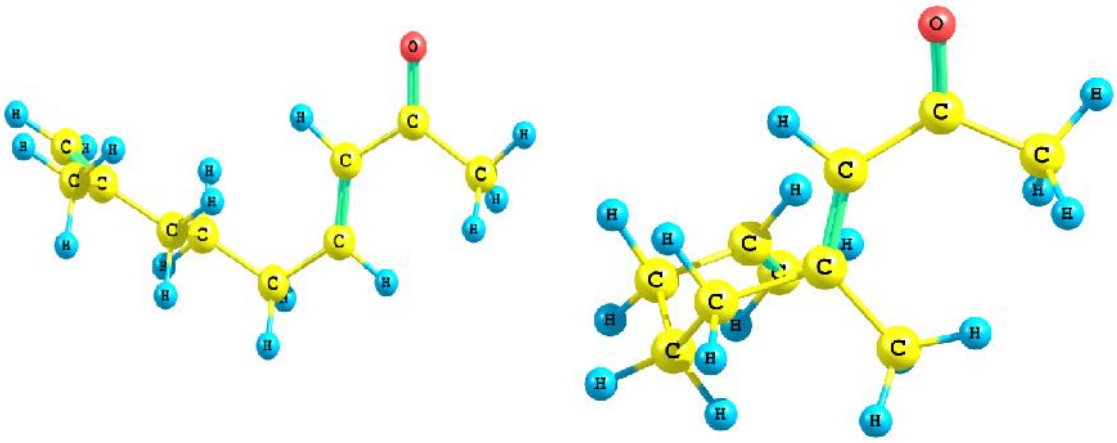

EDPr1 **EDPr2**

Figure 6.7: Optimized geometries of the original end-differentiated olefin products of tandem ROCM

Table 6.6: Optimized parameters (bond lengths in Á and angles in degree) for investigated structures in cross metathesis of MVK with model products MDPr and MPPr of ROM reaction carried out with B3LYP level

	MDPr + MVK						**MPPr + MVK**					
Parameters	DC2	DTS3	DMCB2	DTS4	DC3	DEDPr	PC2	PTS3	PMCB2	PTS4	PC3	PEDPr
Ru-C1	1.839	1.888	1.995	2.193	2.826	-	1.865	1.941	2.016	2.285	3.335	-
C2-C3	1.354	1.442	1.574	2.183	3.252	-	1.357	1.476	1.565	2.141	3.436	-
Ru-C2	2.714	2.341	2.278	2.376	2.771	-	2.747	2.307	2.284	2.389	2.986	-
Ru-C3	2.594	2.117	1.986	1.854	1.823	-	2.497	2.063	1.987	1.856	1.817	-
C1-C2	3.149	2.089	1.608	1.426	1.356	1.342	3.397	1.950	1.658	1.439	1.362	1.351
Ru-C4	2.00	2.088	2.070	2.090	1.983	-	2.018	2.087	2.068	2.083	1.963	-
Cl-Ru-Cl	155.1	170.6	173.0	174.5	152.6	-	164.3	163.3	165.4	171.6	151.1	-
Ru-C3-C2	-	79.8	78.6	71.6	-	-	-	79.4	79.1	73.0	-	-
C3-C2-C1	-	111.8	115.3	110.3	-		-	114.8	117.1	115.0	-	
C2-C1-Ru	-	71.9	77.6	78.9	-	-	-	72.7	76.2	76.1	-	-
C1-Ru-C3	-	94.5	85.0	95.0	-	-	-	92.7	86.8	94.0	-	-
C1-Ru-C4	93.6	117.4	136.8	150.2	155.3	-	93.9	123.8	135.7	152.1	156.4	-
C3-Ru-C4	152.1	148.0	137.6	114.2	90.0	-	144.4	143.5	137.6	113.9	91.6	-

Table 6.7a: Calculated total electronic energies, enthalpies and free energies (in hartree) of the reactants, Complexes, transition structures (TS), Metallacyclobutanes and products of the CM of methyl vinyl ketone with model catalyst of ROM product (MDPr) at the B3LYP and M06L level

MDPr + MVK

	B3LYP			**M06L**		
Species	Energy (E_e)	Enthalpy (H)	Free Energy (G)	Energy (E_e)	Enthalpy (H)	Free Energy (G)
MDPr	-1359.7066569	-1359.509149	-1359.567538	-1359.6473695	-1359.450316	-1359.508374
MVK	-231.2348818	-231.138180	-231.173721	-231.1993705	-231.102867	-231.138468
RT[b]	-1590.941538	-1590.647329	-1590.741259	-1590.84674	-1590.553183	-1590.646842
DC2	-1590.9496845	-1590.652704	-1590.727915	-1590.870517	-1590.574211	-1590.646562
DTS3	-1590.9322815	-1590.636086	-1590.706179	-1590.8518479	-1590.556894	-1590.627161
MCB2	-1590.9399426	-1590.641560	-1590.711861	-1590.8641618	-1590.566569	-1590.636526
DTS4	-1590.9264819	-1590.630577	-1590.701181	-1590.8428626	-1590.548240	-1590.618914
DC3	-1590.9445442	-1590.647818	-1590.722061	-1590.8645178	-1590.568675	-1590.641996
DPr2	-309.8698039	-309.713126	-309.756130	-309.8190895	-309.662523	-309.705495
AC	-1281.0673741	-1280.930047	-1280.981080	-1281.0189868	-1280.882011	-1280.932627
PT[c]	-1590.937178	-1590.643137	-1590.73721	-1590.8380763	-1590.544534	-1590.638122
EDPr1	-465.8899747	-465.638107	-465.693354			

[b]RT = MDPr + MVK [c]PT = DPr2 + AC

Table 6.7b: Calculated total electronic energies, enthalpies and free energies (in hartree) of the reactants, Complexes (C), transition structures (TS), Metallacyclobutanes and products of the CM of methyl vinyl ketone with model catalyst of ROM product (MPPr) at the B3LYP and M06L level

MPPr + MVK

	B3LYP			**M06L**		
Species	Energy (E_e)	Enthalpy (H)	Free Energy (G)	Energy (E_e)	Enthalpy (H)	Free Energy (G)
MPPr	-1399.027633	-1398.800364	-1398.862571	-1398.9647399	-1398.737918	-1398.800958
MVK	-231.2348818	-231.138180	-231.173721	-231.1993705	-231.102867	-231.138468
RT[b]	-1630.262515	-1629.938544	-1630.036292	-1630.1641104	-1629.840785	-1629.939426
PC2	-1630.2632864	-1629.936535	-1630.014147	-1630.1819191	-1629.855898	-1629.929527
PTS3	-1630.2418851	-1629.915364	-1629.986974	-1630.1622926	-1629.836832	-1629.908298
PMCB2	-1630.2439619	-1629.915907	-1629.988147	-1630.1669801	-1629.839737	-1629.912089
PTS4	-1630.2293074	-1629.903334	-1629.975977	-1630.1448089	-1629.819973	-1629.892476
PC3	-1630.2551796	-1629.928798	-1630.006822	-1630.1713085	-1629.845413	-1629.920836
PPr2	-349.1812388	-348.994627	-349.041227	-349.126636	-348.940092	-348.985796
AC	-1281.0673741	-1280.930047	-1280.981080	-1281.0189868	-1280.882011	-1280.932627
PT[c]	-1630.248613	-1629.924674	-1630.022307	-1630.1456228	-1629.822103	-1629.918423
EDPr2	-465.8830571	-465.630739	-465.685562			

[b]RT = MPPr + MVK [c]PT = PPr2 +AC

Table 6.8a: Calculated relative electronic energies, enthalpies and free energies (in kcal/mol) of the reactants, Complexes, transition structures (TS), Metallacyclobutanes and products of the CM of methyl vinyl ketone with catalyst model of ROM product at the B3LYP and M06L level

MDPr + MVK

	Relative to RT						Relative to Complex2 (DC2)					
	B3LYP			**M06L**								
Species	ΔE_e	ΔH	ΔG	ΔE_e	ΔH	ΔG	**B3LYP**			**M06L**		
RT	0	0	0	0	0	0	ΔE_e	ΔH	ΔG	ΔE_e	ΔH	ΔG
DC2	-5.11	-3.37	8.37	-14.92	-13.20	0.18	0	0	0	0	0	0
DTS3	5.809	7.06	22.01	-3.21	-2.33	12.35	10.92	10.43	13.64	11.72	10.87	12.17
DMCB2	1.002	3.62	18.45	-10.93	-8.40	6.47	6.11	6.99	10.07	3.99	4.80	6.30
DTS4	9.448	10.51	25.15	2.43	3.10	17.53	14.56	13.88	16.78	17.35	16.30	17.35
DC3	-1.89	-0.31	12.05	-11.16	-9.72	3.04	3.23	3.07	3.673	3.76	3.48	2.87
PT	2.74	2.61	2.54	5.44	5.43	5.47	7.85	5.98	-5.83	20.36	18.63	5.30

Note: ΔH and ΔG are calculated at 298 K.

Table 6.8b: Calculated relative electronic energies, enthalpies and free energies (in kcal/mol) of the reactants, Complexes, transition structures (TS), Metallacyclobutanes and products of the CM of methyl vinyl ketone with catalyst model of ROM product at the B3LYP and M06L level

MPPr + MVK

	Relative to RT						Relative to Complex2 (PC2)					
	B3LYP			**M06L**			**B3LYP**			**M06L**		
Species	ΔE_e	ΔH	ΔG	ΔE_e	ΔH	ΔG	ΔE_e	ΔH	ΔG	ΔE_e	ΔH	ΔG
RT	0	0	0	0	0	0						
PC2	-0.48	1.26	13.90	-11.18	-9.48	6.21	0	0	0	0	0	0
PTS3	12.95	14.55	30.95	1.14	2.48	19.53	13.43	13.29	17.05	12.32	11.96	13.32
PMCB2	11.64	14.21	30.21	-1.80	0.66	17.15	12.13	12.94	16.32	9.37	10.14	10.94
PTS4	20.84	22.10	37.85	12.11	13.06	29.46	21.32	20.83	23.95	23.29	22.54	23.25
PC3	4.60	6.12	18.49	-4.52	-2.90	11.67	5.09	4.86	4.60	6.66	6.58	5.45
PT	8.72	8.70	8.78	11.60	11.72	13.18	9.21	7.44	-5.12	22.78	21.21	6.97

Note: ΔH and ΔG are calculated at 298 K

6.4 CONCLUSIONS

We have investigated computationally the whole catalytic cycle of the ruthenium catalyst mediated tandem ring opening -cross metathesis reaction to obtain end-differentiated olefins. To enable a detailed study of the ROCM path a trisubstituted cyclopentene (TCP or1-methylecyclopentene) and methyl vinyl ketone (cross partner) were selected as model compounds. Both B3LYP and M06L method gave similar results for the ROCM reaction; however numeric values of relative energies of structures depend on the method chosen.

Based on the current calculations and the ruthenium catalyst model used, it can be concluded that the through ring opening metathesis of trisubstituted cyclopentene, two types of alkylidenes (DPr and PPr) are produced. In ROM reaction, the active catalyst preferentially coordinates at the substituted carbon (proximal) of double bond of trisubstituted cyclopentene. In DPr alkylidene, the methyl group of TCP is associated at the end of the alkylidene chain while in PPr alkylidene, methyl group attached at the first carbon (Ru=C) that forms a bond with Ru-center. The Distal alkylidene (DPr) is found to be active to initiate the cross metathesis catalytic cycle of ROCM more efficiently.

At the B3LYP functional, the activation energy of the addition reaction of MVK with DPr is lower than with PPr by about 2.51 kcal/mol and ring opening of intermediates is lower by about 0.74 kcal/mol respectively. The enthalpy of the ROCM product (DPr2) formed with distal alkylidene (MDPr) is significantly stabler than the product (PPr2) by proximal alkylidene (MPPr) by about 6.09 kcal/mol. The calculated Gibbs free energy also favors the formation of (DPr2 or EDPr1) product with the DPr alkylidene. Thus we conclude that ROCM reaction of Trisubstituted cycloolefins (TCP) with acroyl species (MVK) selectively produces distal end-differentiated product (EDPr1) in which methyl group attached at non-carbonyl end.

A possible pathway that describes this ROCM is detailed in Scheme 6.5. The propagating active catalyst opens the ring, placing the sterically large metal fragment away from the methyl group of trisubstituted cyclopentene. A subsequent cross metathesis with the methyl vinyl ketone caps the product and regenerates the initial active ruthenium catalyst (AC).

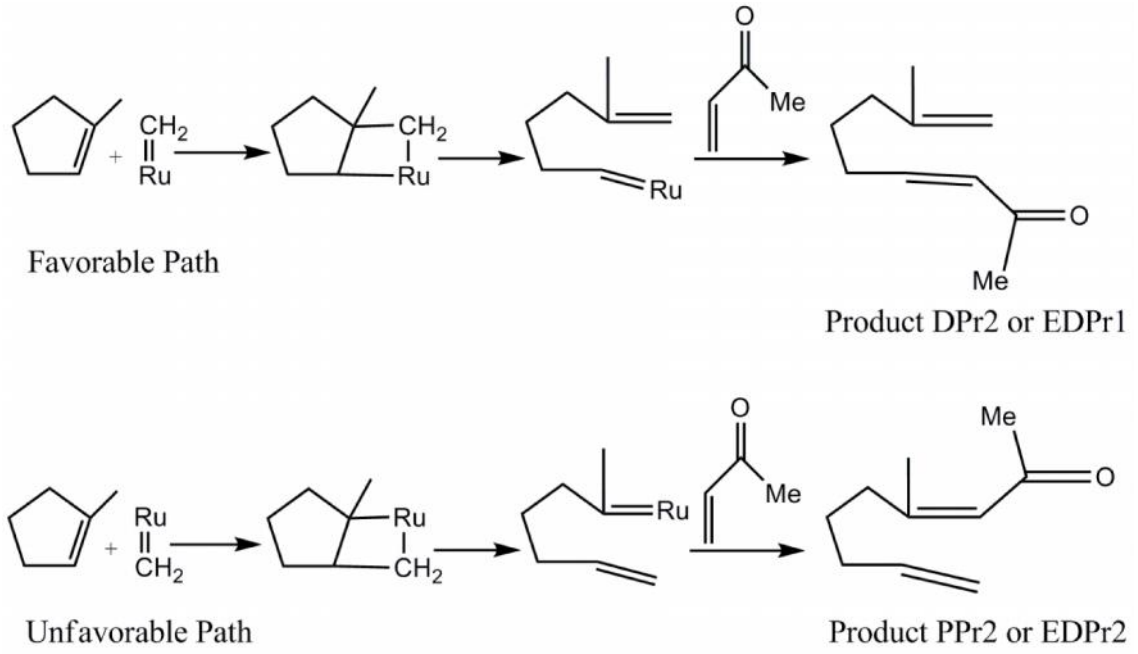

Scheme 6.5: ROCM reaction of trisubstituted cyclopentene with methyl vinyl ketone

6.5 REFERENCES

Adlhart C, Hinderling C, Baumann H and Chen P (**2000**) "Mechanistic studies of olefin metathesis by ruthenium carbene complexes using electrospray ionization tandem mass spectrometry" *J. Am.Chem. Soc.* **122**: 8204-8214.

Arjona O, Csaky A G and Plumet J (**2000**) "Regiochemical aspects in the ring opening-cross metathesis of bicyclic alkenes" *Synthesis* 857-861.

Arjona O, Csaky A G, Murcia M C and Plumet J (**1999**) "Regioselective ring-opening and cross-coupling metathesis of 2-substituted 7-oxanorbornenes. New stereoselective entry into trisubstituted tetrahydrofurans" *J. Org. Chem.* **64**: 9739-9741.

Becke A D (**1993**) "Density-functional thermochemistry .3. The role of exact exchange" *J. Chem. Phys*. **98**: 5648-5652.

Becke A D (**1996**) "Density-functional thermochemistry. IV. A new dynamical correlation functional and implications for exact-exchange mixing" *J. Chem. Phys.* **104**: 1040-1046.

Benitez D, Tkatchouk E and Goddard III W A, (**2009**) "Conformational analysis of olefin-carbene ruthenium metathesis catalysts" *Organometallics* **28**: 2643-2645.

Cavallo L J (**2002**) "Mechanism of ruthenium-catalyzed olefin metathesis reactions from a theoretical perspective" *J. Am. Chem. Soc.* **124**: 8965-8973.

Chung T C and Chasmawala M (**1992**) "Synthesis of telechelic 1,4-polybutadiene by metathesis reactions and borane monomers" *Macromolecules* **25**:5137-5144.

Credendino R, Poater A, Ragone F and Cavallo L (**2011**) "A Computational perspective of olefin metathesis catalyzed by N-heterocyclic ruthenium (pre) catalysts" *Catal. Sci. Technol.* **1**:1287-1297.

Fomine S and Tlenkopatchev M A (**2010**) "Computational modeling of renewable molecules. Ruthenium alkylidene-mediated metathesis of trialkyl-substituted olefins" *Organometallics* **29**: 1580-1587.

Fomine S, Ortega J V and Tlenkopatchev M A (**2007**) "Metathesis of halogenated olefins-A computational study of ruthenium alkylidene mediated reaction pathways" *J. Mol. Catal. A: Chem.* **263**: 121-127.

Fomine S, Vargas S M and Tlenkopatchev M A (**2003**) "Molecular modeling of ruthenium alkylidene mediated olefin metathesis reactions. DFT study of reaction pathways" *Organometallics* **22**: 93-99.

Frisch M J, et al (**2009**) Gaussian09, Revision A.02, Gaussian, Inc.,Wallingford CT.

Garber S B, Kingsbury J S, Gray B L and Hoveyda A H (**2000**) "Efficient and recyclable monomeric and dendritic Ru-based metathesis catalysts" *J. Am. Chem. Soc.* **122**: 8168-8179.

Giudici R E and Hoveyda A H (**2007**) "Directed catalytic asymmetric olefin metathesis. selectivity control by enoate and ynoate groups in Ru-catalyzed asymmetric ring-opening/cross-metathesis" *J. Am.Chem. Soc.* **129**: 3824-3825.

Harrity J P, La D S, Cefalo D R, Visser M S and Hoveyda A H (**1998**) "Chromenes through metal-catalyzed reactions of styrenyl ethers. Mechanism and utility in synthesis" *J. Am. Chem. Soc.* **120**: 2343-2351.

Harrity J P, Visser M S, Gleason J D and Hoveyda A H (**1997**) "Ru-catalyzed rearrangement of styrenyl ethers. Enantioselective synthesis of chromenes through Zr- and Ru-catalyzed processes" *J. Am. Chem. Soc.* **119**: 1488-1489.

Hay P J and Wadt W R (**1985**) "Ab initio effective core potentials for molecular calculations. Potentials for K to Au including the outermost core orbitals" *J. Chem. Phys.* **82**: 299-310.

Hehre W J, Radom L, Schleyer P v R and Pople J A (**1986**) "Ab Initio Molecular Orbital Theory" Wiley: New York.

Hillmyer M A, Nguyen S T and Grubbs R H (**1997**) "Utility of a ruthenium metathesis catalyst for the preparation of end-functionalized polybutadiene" *Macromolecules* **30**: 718-721.

Hinderling C, Adlhart C and Chen P (**1998**) "Olefin metathesis of a ruthenium carbene complex by electrospray ionization in the gas phase" *Angew. Chem. Int. Ed.* **37**: 2685-2689.

Hinderling C, Adlhart C and Chen P (**1998**) "Olefin metathesis of a ruthenium carbene complex by electrospray ionization in the gas phase"*Angew. Chem. Int. Ed.* **37**: 2685-2689.

Katayama H, Urushima H, Nishioka T, Wada C, Nagao M and Ozawa F (**2000**) "Highly selective ring-opening/cross-metathesis reactions of norbornene derivatives using selenocarbene complexes as catalysts" *Angew. Chem. Int. Ed. Engl.* **39**: 4513-4515.

La D S, Ford J G, Sattely E S, Bonitatebus P J, Schrock R R and Hoveyda A H (**1999**) "Tandem catalytic asymmetric ring-opening metathesis/cross metathesis" *J. Am. Chem. Soc.* **121**: 11603-11604.

La D S, Satteley E S, Ford J G, Schrock R R and Hoveyda A H (**2001**) "Catalytic asymmetric ring-opening metathesis/cross metathesis (AROM/CM) reactions. Mechanism and application to enantioselective synthesis of functionalized cyclopentanes" *J. Am. Chem. Soc.* **123**: 7767-7778.

Lee C, Yang W T and Parr R G (**1988**) "Development of the Colle-Salvetti correlation-energy formula into a functional of the electron density" *Phys. Rev. B* **37**: 785-789.

Maughon B R, Morita T, Bielawski C W and Grubbs R H (**2000**) "Synthesis of cross-linkable telechelic poly(butenylene)s derived from ring-opening metathesis polymerization" *Macromolecules* **33**: 1929-1935.

Michaut M, Parrain J-L and Santelli M (**1998**) "Selective ring opening cross metathesis of cyclopropenone ketal: a one step synthesis of protected divinyl ketones" *Chem. Commun.* 2567-2568.

Minenkov Y, Occhipinti G and Jensen V R (**2013**) "Complete Reaction Pathway of Ruthenium-Catalyzed Olefin Metathesis of Ethyl Vinyl Ether: Kinetics and Mechanistic Insight from DFT" *Organometallics* **32**: 2099-2111.

Minenkov Y, Occhipinti G, Heyndrickx W and Jensen V R (**2012**) "The Nature of the Barrier to Phosphane Dissociation from Grubbs Olefin Metathesis Catalysts" *Eur.J. Inorg. Chem.* **9**: 1507-1516.

Morgan J P, Morrill C, and Grubbs R H (**2002**) "Selective ring opening cross metathesis of cyclooctadiene and trisubstituted cycloolefins" *Org. Lett.* **4**: 67-70.

Morgan J P, Morrill C, and Grubbs R H (**2002**) "Selective ring opening cross metathesis of cyclooctadiene and trisubstituted cycloolefins" *Org. Lett.* **4**: 67-70.

Naota T, Takaya H and Murahashi S I (**1998**) "Ruthenium-catalyzed reactions for organic synthesis" *Chem. Rev.* **98**: 2599-2660.

Park H, Lee H K, and Choi T L (**2013**) "Tandem ring-opening/ring-closing metathesis polymerization: Relationship between monomer structure and reactivity" *J. Am. Chem. Soc.* **135**:10769-10775.

Patil M P, Sharma A K and Sunoj R B (**2010**) "Importance of the nature of R-substituents in pyrrolidine organocatalysts in asymmetric michael additions" J. Org. Chem. **75**:7310-7321.

Randall M L and Snapper M L (**1998**) "Selective olefin metatheses-new tools for the organic chemist: A review" *J. Mol. Catal. A: Chem.***133**: 29-40.

Roy D and Sunoj R B (**2010**) "Ni, Pd, or Pt catalyzed ethylene dimerization: A mechanistic description of the catalytic cycle and the active species" Org. Biomol. Chem. **8**:1040-1051.

Sanford M S, Love J A and Grubbs R H (**2001**) "Mechanism and activity of ruthenium olefin metathesis catalysts" *J. Am. Chem. Soc.* **123**: 6543-6554.

Sanford M S, Love J A and Grubbs R H (**2001**) "Mechanism and activity of ruthenium olefin metathesis catalysts" *J. Am. Chem.Soc.* **123**: 6543-6554.

Sanford M S, Ulman M and Grubbs R H (**2001**) "New insights into the mechanism of ruthenium-catalyzed olefin metathesis reactions" *J. Am. Chem. Soc.* **123**: 749-750.

Scholl M, Ding S, Lee C W and Grubbs R H (**1999**) "Synthesis and activity of a new generation of ruthenium-based olefin metathesis catalysts coordinated with 1,3-dimesityl-4,5-dihydroimidazol-2-ylidene Ligands" *Org. Lett.* **1**: 953-956.

Schuster M and Blechert S (**2001**) "Die Olefinmetathese -neue Katalysatoren vergrößern das Anwendungspotential: Synthesemethoden" *Chem. Unserer Z.* **35**: 24-29.

Schwab P, France M B, Ziller J W and Grubbs R H (**1995**) "A series of well-defined metathesis catalysts-synthesis of $[RuCl_2(=CHR')(PR_3)_2]$ and its reactions" *Angew. Chem. Int. Ed. Engl.* **34**: 2039-2041.

Schwab P, Grubbs R H and Ziller J W (**1996**) "Synthesis and applications of $RuCl_2(=CHR')$ $(PR_3)_2$: The influence of the alkylidene moiety on metathesis activity" *J. Am. Chem. Soc.* **118**: 100-110.

Snapper M L, Tallarico J A and Randall M L (**1997**) "Regio- and stereoselective ring - opening cross-metathesis. Rapid entry into functionalized bicyclo [6.3.0] ring systems" *J. Am. Chem. Soc.* **119**:1478-1479.

Stuer W, Wolf J, Werner H, Schwab P and Schulz M (**1998**) "Carbynehydridoruthenium complexes as catalysts for the selective, ring-opening metathesis of cyclopentene with methyl acrylate"*Angew. Chem. Int. Ed.Engl.* **37**:3421-3423.

Suresh C H (**2006**) "Nature of α,β-CCC agostic bonding in metallacyclobutanes" J. Organomet. Chem. **691**:5366-5374.

Tallarico J A, Randall M L and Snapper M L (**1997**) "Selectivity in ring-opening metatheses" *Tetrahedron* **53**: 16511-16520.

Ulman M and Grubbs R H (**1998**) "Relative reaction rates of olefin substrates with ruthenium(II) carbene metathesis initiators" *Organometallics* **17**:2484-2489.

Voigtmann U and Blechert S (**2000**) "Variable and stereoselective synthesis of azasugar analogues by a ruthenium-catalyzed ring rearrangement" *Org. Lett.* **2**: 3971-3974.

Vyboishchikov S F, Buhl M and Thiel W (**2002**) "Mechanism of olefin metathesis with catalysis by ruthenium carbene complexes: Density functional studies on model systems" *Chem. Eur. J.* **8**: 3962-3975.

Wadt W R and Hay P J (**1985**) "Ab Initio effective core potentials for molecular calculations.Potentials for main group elements Na to Bi" *J. Chem. Phys.* **82**: 284-298.

Weatherhead G S, Ford J G, Alexanian E J, Schrock R R and Hoveyda A H (**2000**) "Tandem catalytic asymmetric ring-opening metathesis/ring-closing metathesis" *J. Am. Chem. Soc.* **122**: 1828-1829.

Weeresakare G M, Liu Z and Rainier J D (**2004**) "highly regioselective ring-opening/cross-metathesis reactions of 2-sulfonylnorbornene derivatives" *Org. Lett.* **6**: 1625-1627.

Zhao Y and Truhlar D G (**2006**) "A new local density functional for main-group thermochemistry, transition metal bonding, thermochemical kinetics, and noncovalent interactions" *J. Chem. Phys.* **125**:194101(1-18).

Zhao Y and Truhlar D G (**2007**) "Attractive noncovalent interactions in the mechanism of grubbs second-generation Ru catalysts for olefin metathesis" *Org. Lett.* **9**: 1967-1970.

Zhao Y and Truhlar D G (**2009**) "Benchmark energetic data in a model system for Grubbs II metathesis catalysis and their use for the development, assessment, and validation of electronic structure methods" *J. Chem. Theory Comput.* **5**: 324-333.

Zuercher W J, Hashimoto M and Grubbs R H (**1996**) "Tandem ring opening-ring closing metathesis of cyclic olefins" *J. Am. Chem. Soc.* **118**: 6634-6640.

Concluding Remarks

The mechanistic pathways of three transition metal catalyzed olefin metathesis reactions have been studied using hybrid density functional theory (DFT). Based on the dual criteria of efficiency and accuracy, the DFT method was preferred for use throughout the calculations. Although calculations by density functional theory may underestimate weak interactions such as van der Waals interactions, they usually give better and more consistent descriptions of the geometries and relative energies for systems containing transition metals than either Hartree-Fock or MP2 methods.

For the chosen reactions, we have theoretically investigated the reaction pathways under the generally accepted mechanisms. The path of reaction is elucidated by determining the structures and energies of substrates, intermediates, transition states and products. The preferred directions for olefin attack to the catalysts and barrier heights have been explored computationally

Ring opening metathesis (ROM) and ring opening metathesis polymerization (ROMP) reaction of 3,3-dimethyl cyclopropene have been explored using tungsten and molybdenum alkylidenes respectively. Tandem ring opening -cross metathesis reaction is investigated using cyclopentene moiety with methyl vinyl ketone in presence of ruthenium catalyst.

In the study of tungsten and molybdenum catalyzed reactions face selectivity (CNO/COO) arises in the metathesis reaction. In our work the CNO face is found to be preferred for olefin attack. Depending on the orientation of cyclopropene with respect to NH group of W and Mo catalyst syn and anti paths have also been investigated. Two types of intermediates namely square pyramidal and trigonal bipyramidal have been characterized for reaction path of tungsten and molybdenum catalyzed reactions of 3,3-dimethyl cyclopropene. The ring opening of intermediates was the rate determining step in tungsten catalyzed ring opening metathesis of cyclopropene moiety but on using molybdenum catalyst the cycloaddition step was rate determining.

In the study of stereochemistry of ring opening of asymmetric 3-methyl-3-phenylcyclopropene, we have characterized parallel and perpendicular conformers. Effect of substituents on ring opening of cyclopropene moiety is also explored. Among all the disubstituted cyclopropenes investigated, 3-hydroxyl-3-methylcyclopropene (HMCP) formed the most stable ring opened product with its OH face.

In the study of tandem ring opening cross metathesis reaction between 1-methylcyclopropene and methyl vinyl ketone, it was found that the first step ROM reaction provide two types of active alkylidenes. We conclude that the distal alkylidene is preferred over the proximal alkylidene in cross metathesis step for production of end differentiated olefins. .Preferentially a product in which methyl group is attached to the C=C bond present on the non- carbonyl end is produced.

Future work in olefin metathesis needs to be done on solvent effects by incorporating a relevant solvent field model in the calculations. Ring closing metathesis (RCM), acyclic diene metathesis (ADMET), cross metathesis (CM) are also proposed to be studied. Study of ligand substituted catalysts to explore the influence on the energetics of the ring opening metathesis reactions of the various cyclic olefins could also be of interest.